AD-A212 935
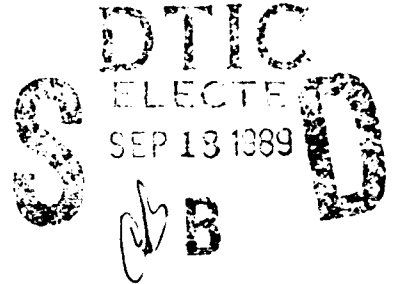
AL-TR-89-005   AD:

Final Report
for the Period
September 1987 to
January 1989

Fusion Propulsion Study

July 1989

Authors: **McDonnell Douglas Space Systems Co.**
V. E. Haloulakos   **5301 Bolsa Avenue**
                           Huntington Beach CA 92647

R. F. Bourque   **General Atomics**
                           P.O. Box 85608
                           San Diego CA 92138

F04611-87-C-0092

Approved for Public Release

Prepared for the   **Astronautics Laboratory (AFSC)**

Air Force Space Technology Center
Space Systems Division
Air Force Systems Command
Edwards Air Force Base, California 93523-5000
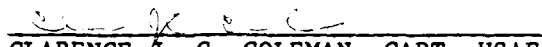
89 9 15 033

NOTICE

When U.S. Government drawings, specifications, or other data are used for any purpose other than a definitely related Government procurement operation, the fact that the Government may have formulated, furnished, or in any way supplied the said drawings, specifications, or other data, is not to be regarded by implication or otherwise, or in any way licensing the holder or any other person or corporation, or conveying any rights or permission to manufacture, use, or sell any patented invention that may be related thereto.
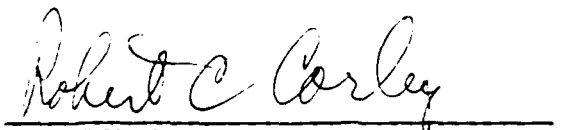
FOREWORD

This final report was submitted by McDonnell Douglas Space Systems Company on completion of contract F04611-87-C-0092 with the Astronautics Laboratory (AFSC), Edwards Air Force Base CA. The AL Project Manager was Dr Franklin B. Mead, Jr.

This report has been reviewed and is approved for release and distribution in accordance with the distribution statement on the cover and on the DD Form 1473.

FRANKLIN B. MEAD, JR.
Project Manager

CLARENCE J. C. COLEMAN, CAPT, USAF
Chief, Advanced Concepts Branch

FOR THE DIRECTOR

ROBERT C. CORLEY
Deputy Director, Astronautical Sciences
  Division

REPORT DOCUMENTATION PAGE

Form Approved
OMB No 0704-0188

1a REPORT SECURITY CLASSIFICATION Unclassified	1b RESTRICTIVE MARKINGS
2a SECURITY CLASSIFICATION AUTHORITY	3 DISTRIBUTION/AVAILABILITY OF REPORT Approved for public release:
2b DECLASSIFICATION/DOWNGRADING SCHEDULE	Distribution is unlimited
4. PERFORMING ORGANIZATION REPORT NUMBER(S)	5 MONITORING ORGANIZATION REPORT NUMBER(S) AFAL-TR-89-005

6a NAME OF PERFORMING ORGANIZATION M Donnell Douglas Space Systems Company	6b OFFICE SYMBOL (If applicable)	7a NAME OF MONITORING ORGANIZATION Astronautics Laboratory (AFSC)
6c ADDRESS (City State, and ZIP Code) 5301 Bolsa Avenue Huntington Beach CA 92647		7b ADDRESS (City, State, and ZIP Code) AL/LSVF Edwards AFB, CA 93523-5000

8a NAME OF FUNDING/SPONSORING ORGANIZATION	8b OFFICE SYMBOL (if applicable)	9 PROCUREMENT INSTRUMENT IDENTIFICATION NUMBER Contract N. F04611-87-c-0092

8c ADDRESS (City, state and ZIP Code)	10. SOURCE OF FUNDING NUMBERS			
	PROGRAM ELEMENT NO 62302F	PROJECT NO. 3058	TASK NO 00	WORK UNIT ACCESSION NO 6G

11 TITLE (include Security Classification)

Fusion Propulsion Study

12 PERSONAL AUTHOR(S)
Haloulakos, V. E., McDonnell Douglas; Bourgue, R. F., General Atomics

13a. TYPE OF REPORT Final	13b. TIME COVERED FROM 87/09 TO 89/01	14. DATE OF REPORT (Year, Month, Day) 89/07	15. PAGE COUNT 230

16 SUPPLEMENTARY NOTATION

17. COSATI CODES			18. SUBJECT TERMS (Continue on reverse if necessary and identify by block number)
FIELD	GROUP	SUB-GROUP	Propulsion, Fusion, Fusion Reactor, Mission Analysis,
21	08		Fusion Fuel, Fuel Cycles, Confinement Methods,
18	01		Orbit Transfer Vechicles

19 ABSTRACT (Continue on reverse if necessary and identify by block number)

This study explored the potential of fusion propulsion for Air Force missions. Fusion fuels and existing confinement concepts were evaluated according to elaborate criteria. Two fuels deuterium-tritium and deuterium-helium 3 (D-3He) were condidered worthy of further consideration. D-3He was selected as the most attractive for this Air Force study. The colliding translating compact torus confinement concept was evaluated in depth and found to possibly possess the low mass and compactness required. Another possible concept is inertial confinement with the propellant surrounding the target. A key issue for any long-burn concept is propellant addition without interfering with the fusion burn. This is required to increase thrust and generate an optimum specific impulse for a given mission. A reusable orbit transfer vehicle (ROTV) was identified as a mission and application where fusion propulsion can play a constructive role and is superior to both cryogenic chemical bipropellant and nuclear fission propulsion systems. Numerous technical and technological problems were identified and a development program is recommended.

20 DISTRIBUTION/AVAILABILITY OF ABSTRACT ☒ UNCLASSIFIED/UNLIMITED ☐ SAME AS RPT ☐ DTIC USERS	21. ABSTRACT SECURITY CLASSIFICATION Unclassified	
22a NAME OF RESPONSIBLE INDIVIDUAL Dr. Franklin B. Mead, Jr.	22b TELEPHONE (Include Area Code) 805/275-5540	22c OFFICE SYMBOL AL/LSVF

DD Form 1473, JUN 86 · Previous editions are obsolete. · SECURITY CLASSIFICATION OF THIS PAGE

TABLE OF CONTENTS

TABLE OF CONTENTS (cont'd)

LIST OF TABLES

LIST OF FIGURES

LIST OF ACRONYMS

ACRONYM	DEFINITION
AF PF II	Air Force Project Forecast II
CFR	Code of Federal Regulations
CT	Compact Torus
FRC	Field Reversed Configuration
GEO	Geosynchronous Earth Orbit
ICF	Inertially Confined Fusion
LEO	Low Earth Orbit
LINUS	Liner Fusion
NCOS	National Commission on Space
RFP	Reversed Field Pinch
ROTV	Reusable Orbit Transfer Vehicle
SD	Space Division
TCT	Translating Compact Torus

INTRODUCTION AND SUMMARY

The purpose of this study is to analyze and evaluate the feasibility and applicability of fusion energy to rocket propulsion for Air Force Missions. There have been concerns about whether or not it was possible to design realistic fusion devices that could be developed in a reasonable time frame with some assurance of success. However, some recent developments in a variety of technologies. e.g., fusion containment, aneutronic fuels, new materials and superconductivity, have pointed to a possible change of this situation. In fact, these developments appear to render possible the design of sufficiently small and compact fusion energy devices which are suitable for rocket propulsion applications in Air Force Missions.

GENERAL SCOPE OF STUDY

The study from its onset had as its objectives (1) to search out, define, evaluate and study fusion energy concepts and devices for rocket propulsion; (2) provide an evaluation as to its competitive standing against the alternative concepts of chemical and nuclear fission propulsion; (3) identify the most promising concepts, the problems and technology issues to be resolved; and (4) provide information as to the possible solutions to the problems and identify the technical groups that can best develop these solutions.

Accordingly, the study was divided into two phases:

Phase 1: This phase provided the technical assessment of the general problems, reviewed and identified the Air Force Mission spectrum and selected the candidate fusion fuel cycles and fusion reactor concepts which appeared promising for further study.

Phase 2: In this phase the most promising missions where fusion propulsion might offer some advantages were selected, the fusion fuel cycles and reactors were further evaluated and vehicle design mission and systems analyses were conducted. It was in this phase that the comparative trades between chemical, nuclear fission and fusion propelled vehicles were made, the pacing technology development problems in the fusion area identified, and a future development plan formulated.

1

FUSION ENERGY PRINCIPLES

Fusion energy is released when lighter element nuclei combine (fuse) to form heavier ones. Because of the increased height of the coulomb energy barrier with increasing atomic number, reactions involving the lighter elements take place more readily than those involving heavier ones. These reactions are thermonuclear, i.e., they require an input of energy to be initiated at some specified temperature and pressure conditions, ignite causing some of them, e.g., Deuterium-Tritium (D-T), to become self-sustaining. A large class of thermonuclear reactions (fuel cycles) are possible, depending on the temperature achieved and the objective. Some of the most prominent reactions are:

$$D + T \longrightarrow \alpha\ (3.52) + n\ (14.07)$$

$$D + D \begin{cases} \longrightarrow {}^3He\ (0.82) + n\ (2.45) & 50\% \\ \longrightarrow T\ (2.02) + p\ (4.03) & 50\% \end{cases}$$

$$p + {}^{11}B \longrightarrow 3\,\alpha\ (2.89\ \text{each})$$

$$D + {}^3He \longrightarrow p\ (14.68) + \alpha\ (3.67)$$

$$p + {}^6Li \longrightarrow {}^3He\ (2.3) + \alpha\ (1.43)$$
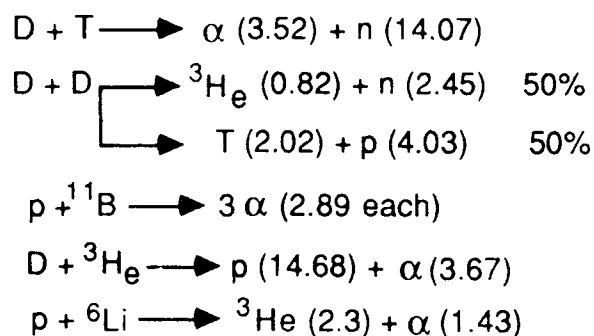
where the numbers in the parentheses represent the particle energy in MeV.

As seen from the equations, the energy released is distributed between the various reaction products. There are two aspects of the distribution of energy between charged and uncharged particles which are of importance. First, in magnetically confined thermonuclear reactors, all the neutrons would escape from the reacting system and deposit their energy in materials outside the reaction zone. In inertial confinement reactors, perhaps one-fourth of the neutron energy can be contained. But it is mainly the energy of the charged particles that is retained within the reaction region and which will be available internally to sustain thermonuclear reactions. Second, it is only the charged particles that can be used to generate electricity for the containment system directly; neutron energy is deposited as heat and therefore requires a thermal system for recovery. The charged particles will also deposit their energy directly to a propellant most readily, thus avoiding high temperature heat transfer and materials problems associated with the energy deposition in a solid and heat transfer to the propellant.

HISTORY OF FUSION PROPULSION

The exploration of rocket propulsion by fusion power has been studied off and on over the last three decades. Concepts have ranged from a pulsed fusion rocket using large inertially-confined fusion (ICF) blasts to a ramjet fusion rocket. In most of these, it was assumed that controlled energy release from fusion using advanced fuels would be feasible. Other concepts considered the possibility of a thermonuclear explosion contained within a blast chamber while the propellant was being expelled through a nozzle. Figure 1 shows a schematic of the history of nuclear pulse propulsion.

Typical of the work in the 1960's and 1970's is the work at NASA and at Aerojet-General. In the NASA scheme, a fusion reactor was assumed to supply an escaping plasma mixed with additional propellant to escape through a nozzle, thereby providing the necessary thrust. It was assumed that self-sustaining D-^{3}He or D-D fusion could be obtained either in a single- or double-ended open system or from a closed magnetic configuration. There were problems posed by the conversion of the thermal energy of the reacting plasma to an exhaust jet. These problems persist and are discussed in this report. In the Aerojet-General Study, the reacting D-^{3}He plasma was assumed to exist within a multi-polar magnetic confinement geometry. Rough estimates of rocket motor optimization showed potential for a very high specific impulse (e.g., with 25 MW in the exhaust jet, the hypothetical motor could have a specific impulse in the range 5000 to 10000 s). The resultant power-to-weight ratio for the fusion rocket motor indicated a possible improvement of an order of magnitude over the best foreseeable uranium fission-electric systems.
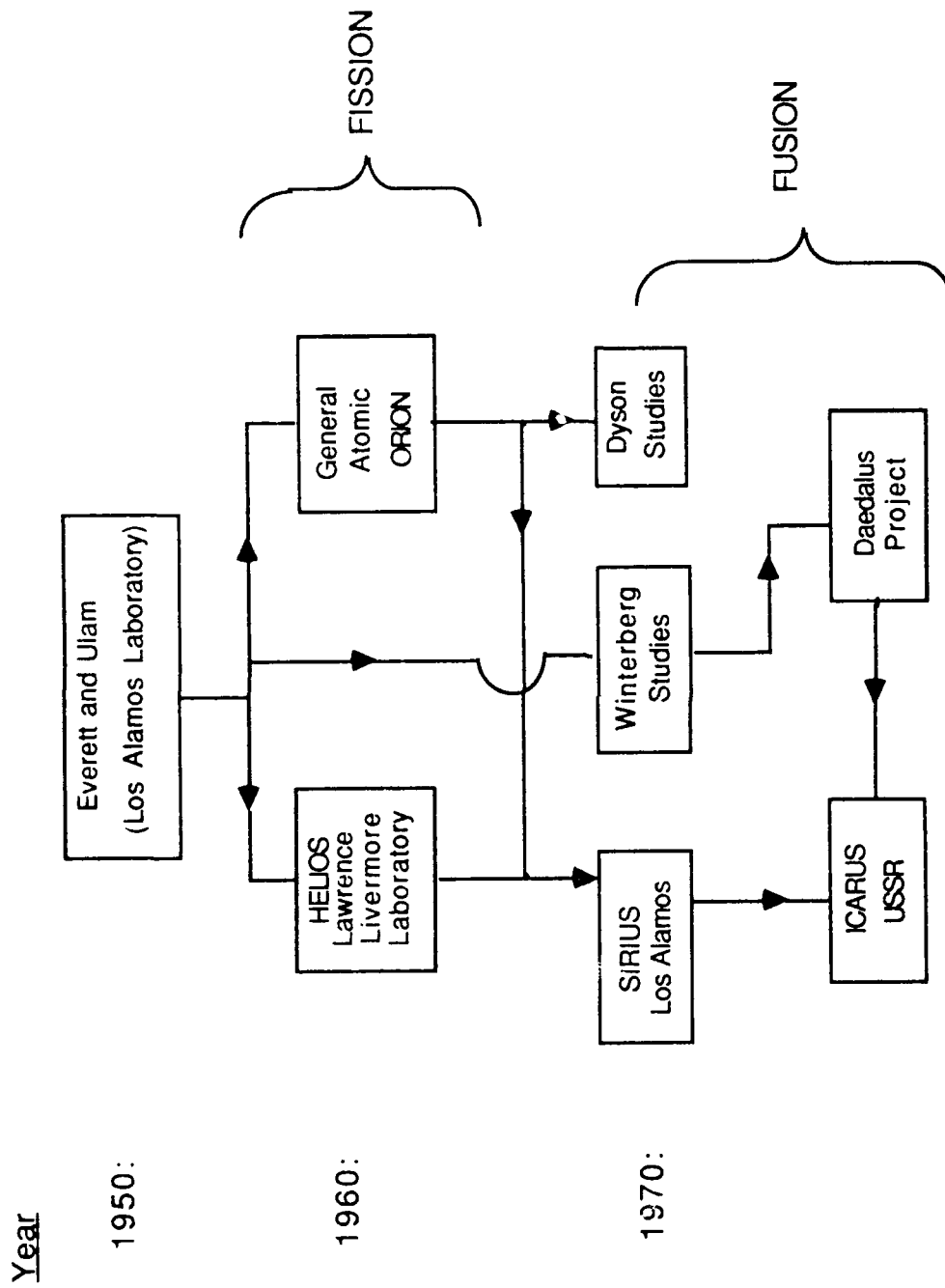
Fig. 1. Nuclear pulsed propulsion early efforts.

4

SUMMARY OF ACCOMPLISHMENTS

As mentioned above, the general goal of this study was to bring this topic of fusion propulsion up-to-date by incorporating the most recent advances in fusion research. Specific objectives were to evaluate fusion fuel and current fusion confinement concepts and, selecting one of each, perform a fairly detailed scoping analysis. Fusion fuels and concepts were evaluated based on sets of weighted criteria.

Each major topic of the study is discussed in individually dedicated sections in the following order:

1. Air Force Missions: Missions where fusion propulsion may play a constructive role are discussed, with the key question being whether fusion is suitable for near-earth and cislunar missions, or is limited to deep space activities.

2. Fusion Fuels: The many candidate fusion fuels are discussed and evaluated, their evaluation criteria including such things as power density, neutron production, temperature required, availability and radioactivity.

3. Fusion Reactors: Numerous fusion confinement concepts are evaluated with emphasis on their suitability for space propulsion. The key requirements for such an application being the mass and envelope of the power plant.

4. Translating Compact Torus (TCT): This reactor concept was selected and studied in detail because of its potential of compact size and high power density.

5. Systems/Mission Analysis: Special sections are dedicated in the studies which evaluated the various candidate systems and assessed their performance capabilities to accomplish the selected missions. A reusable orbit transfer vehicle (ROTV) is the system of choice upon which comparative trades and design studies were made for chemical c , genic, nuclear fission and fusion propulsion systems.

6. Issues, Plans and Conclusions: The numerous remaining issues, a suggested developmr t plar for continuing work on fusion propulsion, and the final conclusions of the study are presented in the final sections of this report.

Additional details on a number of topics are included in a set of appendices and a special addendum.

Fusion Fuels. All things considered, only two fusion fuels were found to be worth considering for propulsion applications: deuterium-tritium (D-T) and deuterium-helium 3 (D-^{3}He). A number of evaluation criteria were employed. The most important are (1) reaction rate for a given fuel pressure, (2) operating temperature, (3) energy per reaction, particularly charged particle energy, (4) availability, (5) neutron production, and (6) handling.

D-T rated well with regards to the first four criteria. However, it produces copious neutrons and requires handling of radioactive tritium. D-^{3}He produces far fewer neutrons and is relatively easy to handle. However, its power density is much lower and must operate at very high temperature. Ignition of D-^{3}He will be difficult in real reactors. Also, ^{3}He exists only in trace quantities on earth. Large quantities appear to exist on the moon and some studies have indicated feasibility of extracting it. Because of tritium and neutron concerns, D-^{3}He was chosen for the reactor study.

Fusion Confinement Concepts. While the tokamak has had considerable success in confining fusion-grade plasmas as presently envisioned, it is too large and heavy for space applications, at least for current Air Force missions. We therefore examined concepts that may work in space, even though little is presently known about their confinement. Most of the effort was spent exploring the colliding translating compact torus (TCT). Here, two compact tori (e.g., spheromaks) are accelerated at each other and merged. The kinetic energies prior to merging are sufficient to heat the ions to burn temperature afterwards. Merging is presumed to occur if the magnetic energy in the plasmas exceeds the kinetic energies, which it does in every case. The merged plasmas are allowed to translate into a channel whose surface has been wetted by propellant. The intense heating from the sweeping fusion reaction vaporizes the propellant, providing thrust.

The key issue in magnetic fusion propulsion turned out to be adding enough propellant to get high thrust without quenching the fusion reaction. The sweeping approach mentioned above may work, provided the sweep velocity exceeds the propellant expansion velocity. Another way is to use inertial confinement with solid or liquid propellant surrounding the target. The fusion reaction is over so quickly that the propellant has insufficient time to expand and interfere.

Another concept just touched upon in this study is direct converted fusion with propellant heated by an electrical arc. With direct energy conversion, fuels with a high fraction of energy in charged particles, like D-^{3}He, are favored. Also, the conversion hardware should be simple, giving it a mass and efficiency advantage over thermally-converted fission or fusion.

It is important not only to monitor the progress of fusion research but also to provide stimulus to pursue those confinement concepts with potential for propulsion. This would provide greater diversity in the fusion program and therefore greater probability of success.

Vehicle Design and Integration. Typical orbit transfer vehicles were defined and compared for their capabilities to perform a basic mission. The defined task was the delivery of a 36,000-kg payload from low earth orbit (LEO) to geosynchronous (GEO) or other higher orbits (X-GEO or HEO). The velocity requirements were set at 4,500 m/s and 9,000 m/s for one way and return missions, respectively.

Computer codes for vehicle/propulsion system design and integration were updated, checked out and validated against known vehicles from the SATURN-APOLLO and the NERVA programs.

In all cases, the fusion-powered vehicles are of substantially lower mass, with the optimum specific impulse range being between 1500 s and 2500 s.

Since, from the fusion reactor point of view, it is easier or more feasible to construct a 1500 s specific impulse power plant, this was the figure selected for a sample vehicle design layout discussed and shown in a special section. Additional information and vehicle design data are given in the addendum to this report.

DRIVING NEEDS AND ISSUES

The issues of propulsion and power are the main drivers in the development and deployment of space launch vehicles and the quest for exploration and utilization of space. This has been especially the case in the Air Force Space Program, from the early days of the ballistic missile programs to the present strategic sophisticated space-based payloads.

Propulsion is a technology which, though by itself may be viewed as having no intrinsic value as such, is nevertheless the main "driver" for any system application which requires the moving, deployment, and positioning of payloads.

Traditionally, chemical propulsion systems, liquid and solid, have been the "drivers and pushers" in missile and space vehicle applications.

In the area of systems applications, however, there has been a multitude of recent developments which lie beyond the capabilities of chemical propulsion and call for the development of new high energy and exotic rocket propulsion systems. The primary needs in this area stem from the new USAF and other DOD or national goals and plans which call for missions that are very costly and in many cases beyond the capabilities of the presently available or near-future propulsion systems.

The USAF Project Forecast II (AF PF II), the Strategic Defense Initiative (SDI) and the report of the National Commission on Space (NCOS) to the President have identified numerous systems and technologies that are key elements to the achievement of the national goals. Invariably, most of the missions planned involve the launching and/or delivery of payloads which are far beyond the capabilities of currently available systems. Appropriately, therefore, the development of new sophisticated systems capable of producing both high thrust and high specific impulse (e.g. $I_s > 1000$ s) have been called for.

In a study conducted by the Brookhaven National Laboratory (BNL) for the Air Force Astronautics Laboratory (AFAL)[1] numerous missions and payload deliveries were identified which are far beyond the capabilities of the Centaur G (O_2/H_2, $I_s = 452$ s) vehicle, but could be performed rather well with similar vehicles utilizing direct thermal nuclear propulsion (H_2, $I_s = 855$ s, NH_3, $I_s = 416$ s). It becomes evident then that new propulsion systems which are reliable, safe, and economical, as well as of superior performance, are required, and, since more than one alternative may exist, comparative trade studies must be conducted.

8

The framework of this study, therefore, was established from its onset that in addition to the investigation and evaluation of fusion propulsion schemes, studies are to be conducted comparing fusion and chemical systems. This is accomplished by defining the Air Force missions where such propulsion systems may be applicable, establishing the basic characteristics and selection criteria, and finally conducting comparative trade studies between the selected fusion propulsion systems and the various alternatives.

AIR FORCE MISSION REQUIREMENTS

The topic of the Air Force missions and their requirements was addressed by reviewing various applicable planning documents, visiting Air Force facilities, and interviewing certain key personnel at the Space Division (SD) and the Rand Corporation. With the sample missions defined, further review and evaluation of their requirements resulted in a list of propulsion system characteristics along with a set of pertinent evaluation criteria, upon which the evaluation and selection of fusion concepts suitable for propulsion can be conducted.

In the sections that follow, the selected missions are listed, the propulsion system characteristics are formulated, and the evaluation criteria are defined.

Candidate Missions - Most of the details and information about missions can be found in the Addendum to this report. However, a certain number of such missions and the technologies they drive are part of AF PF II where these definitions and descriptions are found. A collage of the candidate missions selected for consideration is shown in Figure 2. A summary of the AF PF II missions definitions are given below.

AF PF II Systems

Multi-Role Global Range Aircraft (PS-03)

- **Large payload weight/volume and long unrefueled range, enabled by high efficiency propulsion, in an aircraft designed for multiple missions, including transport of outsized equipment.**

9
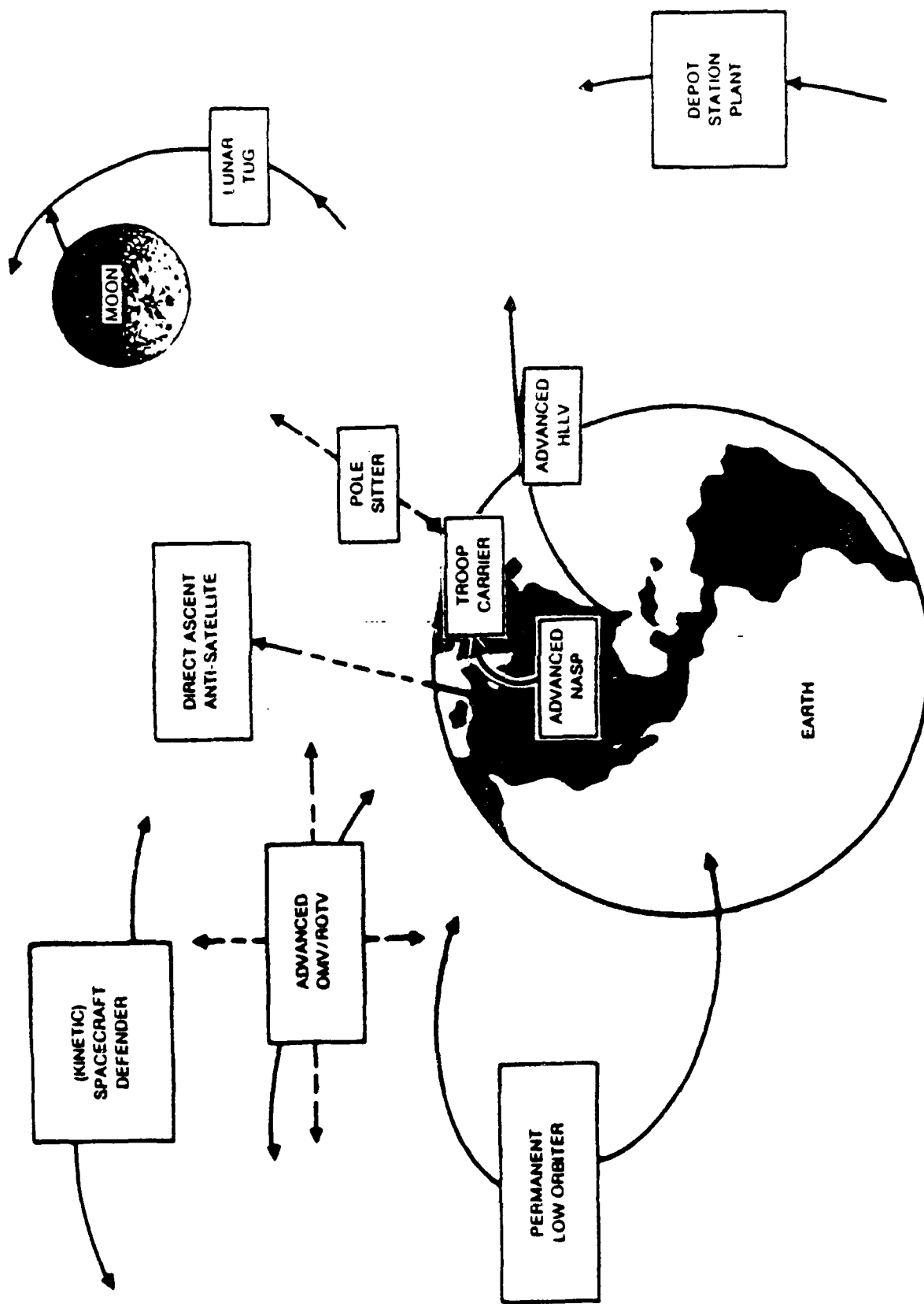
Figure 2. Air Force Mission Scenarios

10

High Altitude, Long Endurance (HALE) Unmanned Aircraft (PS-05)

- Small and large aircraft capable of operation of high altitudes for periods of days (large vehicle) to weeks (small vehicle), for continuous surveillance/targeting, communication linking, and ECM.

- HALE is a system initiative to develop a very high altitude (80 kft) unmanned vehicle capable of sustained flight for several days. This is a significant enhancement over our current "on station" capabilities and will enable the Air Force to supplement its current national resources with a more responsive, longer loiter, better resolution asset.

Aerospace Plane (PS-23)

- A family of aerospace vehicles, both earth- and space-based, which allows rapid, flexible, reliable, survivable operations to and in space.

- Hypervelocity vehicles comprise manned and unmanned vehicles that will allow rapid, low cost operations in strategic and space mission areas. Development of new propulsion engines and lightweight/strong/durable materials are required. Integrated airframe and engine designs are key to success as are leading edge cooling and cryogenic storage methods. Research and development programs incorporating focused DoD and NASA efforts and industry IR&D is the recommended programmatic approach.

Launch Systems (PS-24)

- Launch systems which use reusability and automated launch operations and refurbishment to provide low cost ($100/lb), heavy-lift (150,000-200,000 lb), responsive space launch capability.

- The objective of the Advanced Heavy Lift Space (Launch) Vehicle is to provide a new reliable and quick response capability to transfer large payloads to orbit, which will ultimately make space operations affordable and routine. Program approach: (1) to develop an economically optimized system which satisfies future transportation requirements,

(2) to develop enabling and enhancing technologies and applications as early investments keyed to specific launch vehicle need, and (3) to assure the support requirements for launch, recovery, and maintenance are affordable, which requires drastic improvements over today's capability.

Reusable Orbit Transfer Vehicle (PS-28)

- A totally reusable vehicle for transporting payloads between low earth orbit and higher (up to several time geosynchronous) orbits, enabling routine space operations, satellite retrieval, and dormant sparing.

- The objective of this program is to provide affordable access to space through routine transportation between various orbits, and on-orbit repair and reconstitution of Space Systems, which will ultimately provide a truly operational space capability in support of ground, air, and space-based forces.

Space-Based Surveillance System (PS-32)

- An infrared space surveillance system for detection, identification, tracking and cataloging of spacecraft in low earth and geosynchronous orbits in support of USAF offensive and defensive space operations.

- The objective of this development is to provide the demonstration of technology in large optics design, performance, and survivability to support the space-based space surveillance mission.

- SBSS employs long wavelength infrared and visible light sensors to detect, track, and catalog space objects from space. Current space surveillance systems are ground based with coverage limited by their geographic locations and earth horizon. SBSS, if deployed, will have the following advantages over ground based or airborne systems: wider volume of coverage, decreased time between revisit on any given target, and providing timely information in support of space operations. SBSS technologies are being pursued by Space Division and AFSC laboratories under the SDI program.

NOTE: An advanced-type propulsion system, e.g. fusion, could substantially enhance the value of this system. Further information on missions and systems is provided in the addendum to this report.

Propulsion System Characteristics - The propulsion system supplies the needed force and/or energy to meet the requirements as set by the mission. These requirements call for the delivery of a given, or the maximum possible, payload to a target point. This, of course, is to be done in an efficient and economical manner, which normally means the lowest possible expendable weight.

Present-day chemically propelled launch vehicles are burdened with propulsion systems that contain approximately 90 percent of their gross take-off mass as propellants. By way of contrast a commercial jumbo jet carries approximately 40 percent of its initial fully-loaded take-off mass as fuel. It becomes apparent, therefore, that future propulsion systems, fusion or other, must result in similar capabilities in order to render the launching, transfer, handling and deployment of the subject payloads feasible and economical.

Accordingly, the review of the subject missions resulted in propulsion systems with the following characteristics.

Thrust Levels

Three categories of thrust levels have been identified that are required to perform the missions reviewed. These thrust levels are given in Table 1. Their primary driving missions are given in the addendum.

Specific Impulse

This should be as high as possible, consistent with the specific mission and system. From the low end, it should not be below 1500 s, i.e., the plasma exhaust velocities should be in excess of 15,000 m/s, in order to offer a competitive advantage that will justify the development investment and allocations of the required resources.

13

Operating Characteristics

The candidate propulsion systems should possess the following characteristics:

Throttling: Up to 10:1

Pulsing: As rapidly as possibly

Restartability: As many as possible

Fast Start: In the order of seconds

Radiation-Free (or minimum) exhaust

Weight and Envelope: As low and compact as possible

Signature: Minimum or none detectable

Operating Life: As long as possible

Vehicle Integration Requirements

Propulsion systems must be of such geometric shapes as to allow them to be integrated into vehicles and payloads in a reasonable manner; e.g. a pancake-shaped rocket engine where the diameter is much larger than its length may not be easily designable into a vehicle. A rocket engine whose basic reactor chamber has length and diameter dimensions of the same order of magnitude can be easier integrated into a vehicle. Such an engine may then be equipped with a long nozzle to obtain high exhaust velocities and higher performance.

Table 1

TYPICAL THRUST LEVELS

THRUST RANGE

	kN	(klb)
CATEGORY 1	20 to 250	(4.5 to 56)
CATEGORY 2	2000	(450)
CATEGORY 3	10,000 TO 50,000	(2,250 TO 11,500)

Radiation and thermal soak-back effects may require the rocket engine to be mounted far away from the vehicle. This will cause feed system dynamic problems since the propellants need to be pumped over long lines. Thus, special design features are required to resolve these conflicting requirements.

In addition, the propulsion system must be compatible with the other vehicle systems and, wherever possible, capable of multiple applications. Large vehicles require all types of auxiliary propulsion such as attitude and reaction control, mid-course correction, velocity trim, etc., in addition to the main propulsion system.

Therefore, a truly advanced and versatile propulsion system, fusion or other, should also have some of the following attributes:

1. Modular Construction: A system where a basic module can be used in cluster arrangements to construct larger systems without serious effects on its reliability.

2. Capable of supplying the required energy for various operations, such as auxiliary propulsion and/or power generation.

3. Easily integrable into vehicles with large tanks that can supply the required propellant quantities for the rather large ΔV's identified in the subject missions.

4. Amenable to design features that allow ease of maintenance, accessibility and replacement of components as may be required by the long life characteristics of reusability and low life cycle cost.

Evaluation Criteria - Typical criteria with which the various concepts and systems were assessed and compared are as follows:

1. Mission Capability. The system must be able to accomplish the subject/selected mission. This includes items such as the ability of the propulsion system to provide any desired or optimum thrust profile, prescribed velocity schedules or other mission dictated constraints.

2. Engineering Feasibility and Producibility. Can the system/concept be produced in a reasonable engineering manner? Special or very stringent problems in these areas have serious impact on costs and schedules.

15

3. Extrapolation of Physics. Does the system require certain parameters, e.g. plasma beta, to exceed presently obtainable values by very much? It is important to assess the degree of extrapolation required as one looks for "revolutionary" innovations and still remain within the realm of possibility.

It was recognized from the onset that as the study progressed, the precise evaluation criteria list could be modified slightly as new knowledge was acquired. The various fusion propulsion concepts were assessed on the basis of criteria listed in Table 2. Numerical weights were assigned on each concept against the most applicable criteria. Details of this evaluation are being presented in a special section.

Table 2

EVALUATION CRITERIA

1. MISSION CAPABILITY
   - THRUST LEVEL
   - SPECIFIC IMPULSE
   - THRUST VARIABILITY AND PROFILE
     - THROTTLING
     - PULSING
   - FIRING DURATION CAPABILITY
   - RESTARTABILITY
   - SHUTDOWN CAPABILITY (e.g., AFTERHEAT)

2. WEIGHT AND SIZE CONSIDERATIONS
   - ENGINE MASS (WEIGHT)
   - THRUST-TO-MASS RATIO
   - ENGINE DIMENSIONS AND ENVELOPE
   - INTEGRATION WITH VEHICLE
     - TOTAL SYSTEM MASS
     - EASE OF PACKAGING
     - INTERACTION WITH OTHER SYSTEMS
     - VEHICLE MASS RATIOS
   - SHIELDING
   - HEAT REJECTION REQUIREMENTS

3. TECHNOLOGY STATUS
   - STATE OF DEVELOPMENT
   - UNRESOLVED PROBLEMS
   - ENGINEERING EXTRAPOLATION
   - PHYSICS EXTRAPOLATION
   - COST OF INITIAL DEVELOPMENT
   - PROBABILITY OF SUCCESSFUL RESOLUTION
   - FUEL AVAILABILITY (e.g., ^{3}He)

Table 2

EVALUATION CRITERIA

(Continued)

4. ENVIRONMENTAL CONSIDERATIONS
   - ENVIRONMENTAL REQUIREMENTS FOR SYSTEM OPERATION
   - EFFECTS ON THE ENVIRONMENT
     - RADIATION
     - EFFLUENTS/POLLUTION
   - GROUND LAUNCH OPERATIONS
   - SPACE OPERATIONS
   - MANNED SYSTEMS
   - EFFECTS ON SYSTEM COMPONENTS

5. PROPULSIVE CONCEPTS
   - TEMPERATURE EFFECTS
     - OPERATING TEMPEATURES
     - MATERIAL PROBLEMS
     - MAGNETIC FIELDS
   - SUPERCONDUCTORS
   - PLASMA CONFINEMENT
   - PLASMA STABILITY
   - STARTUP SEQUENCE
   - NEUTRON EFFECTS
   - THRUSTER IMPLEMENTATION
   - POWER/THRUST VARIATION
   - RECIRCULATING POWER

6. COMPETITIVE STANDING
   - PERFORMANCE
   - SYSTEM SIZE AND WEIGHT
   - SYSTEM OPERATION
   - MAINTENANCE REQUIREMENTS
   - LIFETIME
   - RELIABILITY & SAFETY

Table 2

EVALUATION CRITERIA

(Continued)

6. COMPETITIVE STANDING (Continued)
   - COST
     - DESIGN & DEVELOPMENT
     - PRODUCTION
     - OPERATION

7. ENGINEERING FEASIBILITY
   - PRODUCIBILITY
   - MAINTAINABILITY
   - ACCESSIBILITY
   - RELIABILITY & SAFETY
   - SPECIAL MATERIALS
   - COMPLEXITY

8. EFFECTIVENESS

9. AFFORDABILITY

10. SPECIAL BENEFITS PECULIAR TO FUSION PROPULSION

EVALUATION OF FUSION FUELS

The large number of potential fusion fuels can be quickly reduced to a handful that have reasonable potential. In this section, we examine the issue of fusion fuel selection. Considerable background for this section can be found in Appendix A.

FUSION FUELS

There are about three dozen possible fusion fuels that could be considered[2]. However, most are eliminated at once because they would produce almost no power. After such a preliminary sifting, eleven fuels emerge for further consideration. They are shown along with their reaction products and energy release in Table 3. Two of the fuels, D-T and T-^{3}He, have radioactive reactants. This is a major consideration, especially if the fuel is to be launched into orbit from earth. Seven produce either radioactive products like T or ^{14}C or produce neutrons, which can induce radioactivity in materials. The magnitudes of these products vary widely. D-T, for example, produces so many neutrons that material damage such as embrittlement is a concern. The ^{14}C from p-^{11}B, on the other hand, is nearly negligible.

Seven of the fuels produce no neutrons at all; all of their reaction products are in the form of charged particles. While neutrons carry their energy away from the reaction, charged particles remain to supply additional heating, increasing the fusion reaction rate. Neutrons tend to be quite energetic and readily penetrate materials, increasing the need for shielding. As shown in Appendix A, the fusion power per unit fuel volume is given by

$$p \, n_1 n_2 < \sigma V > E$$

where n_1 and n_2 are the number of ions per unit volume for fuels 1 and 2. For example, fuel 1 could be deuterium and fuel 2 helium-3. Some reactions, such as D-D, also produce additional fuel such as tritium and helium-3 as reaction products. These fuels can also react, boosting the power output. However, the reaction rate of these fuels in fusions per second is obviously no greater than that of the original D-D fuel. Actually, because the density of tritium and ^{3}He produced are so low, reaction rates are far less. Usually, the tritium and ^{3}He migrate out of the reacting fuel before they have a chance to react. If they are continuously recycled back to the plasma, they will eventually react. This process with D-D primary fuel is called, somewhat inappropriately, "catalyzed-D" fusion. Note that they are the only secondary reaction from the primary fuels shown in Table 3 that have any potential value.

20

EVALUATION BASED ON POWER DENSITY

Other things being equal, the more power a fusion fuel releases, the better. In Appendix A, it was shown that perhaps the best figure of merit for power density is the charged particle power density for a given fuel pressure:

$$\frac{\langle \sigma V \rangle Q^+}{T^2}$$

where $\langle \sigma V \rangle$ is the fusion reactivity, Q^+ is the charged particle energy released per fusion reaction, and T is the fuel temperature. Power density is normalized to pressure because all of the effort in fusion is to contain a given pressure.

TABLE 3
FUSION FUELS WORTH CONSIDERING

D $-$ T	$\rightarrow \alpha$ (3.52*) + $\underline{n}$ (14.07)
D $-$ D	$\rightarrow$ ^{3}He (0.82) + $\underline{n}$ (2.45)
	$\rightarrow \underline{T}$ (1.01) + p (3.02)
D-^{3}He	$\rightarrow$ p (14.68) + α (3.67) + Trace $\underline{T}$ + $\underline{n}$ From D $-$ D
p-^{11}B	$\rightarrow$ 3 α (2.89 Each) + Trace $^{14}\underline{C}$ From ^{11}B $- \alpha$
D-^{7}Be	$\rightarrow$ p (11.18) + 2α (2.8 Each)
T-^{3}He	$\rightarrow$ D (9.5) + α (4.8) ... 41%
	$\rightarrow$ p (5.4) + α (1.3) + $\underline{n}$ (5.4) ... 55%
	$\rightarrow$ p (10.1) + α (0.4) + $\underline{n}$ (1.6) ... 4%
p-^{9}Be	$\rightarrow$ D (0.3) + 2 α (0.16 Each) + Trace $\underline{n}$ From ^{9}Be $- \alpha$
	$\rightarrow \alpha$ (1.3) + ^{6}Li (0.85)
p-^{6}Li	$\rightarrow$ ^{3}He (2.3) + α (1.7)
^{3}He-^{3}He	$\rightarrow$ 2p (5.72 Each) + α (1.43)
p-^{7}Li	$\rightarrow$ 2 α (8.67 Each) + $\underline{n}$ (Endothermic)
^{3}He-^{6}Li	$\rightarrow$ p (12.39) + 2 α (2.25 Each)

*Particle Energy in MeV

$\underline{}$ **Denotes radioactive or induces radioactivity.**

As shown in Appendix A there is a temperature for each reaction at which $< \sigma V > Q^+/T^2$ is a maximum. These maximum values and their temperatures are shown in Figure 3 for the fuels listed in Table 3. Eleven fuels are shown in nine bar graphs. The height of the bars represents the maximum fusion power density for a given fusion fuel pressure. Note that only charged particle power is considered. Neutron power, unlikely to be used for thrust, is ignored. Also shown are the temperatures at which these maximum power densities occur. Lastly, those fuels that produce neutrons are also indicated.

The fuel with the greatest power density, fully 10 times greater than any other, is D-T. Not only is it the most reactive, but the temperature where power density peaks is fully one-third or less than any other fuel. It is important that D-T's disadvantages of neutron production and radioactive fuel be weighed against its much higher reactivity for the specific mission being considered. These issues are discussed in the next section.

The fuel with the next highest power density is D-^{3}He. It is 1/10 as reactive as D-T, but is two or more times as reactive as any other. Its optimum temperature is 55 keV. While this is over three times the D-T value, it is less than half that of the other fuels. As shown in Appendix B, the combination of this temperature and power density results in high photon radiation to the surroundings. This loss mechanism makes it difficult to fully utilize the charged particle power. One might conceive of introducing soot to absorb the radiation. Carbon, with its sublimation temperature[3] of around 4000 K, seems a likely choice. However, the combination of this temperature and high atomic weight would produce I_s values of 500 s or less.

Appendix B contains a detailed discussion of the photon radiation issues. Hot plasmas radiate much of their energy over a wide range of wavelengths ranging from visible to X-rays. This radiation can be a major loss mechanism, especially for fusion fuels that have low power density and require high temperatures.

There are a number of ways to enhance reactivity and reduce radiation loss. Reactivity can be enhanced by use of a non-Maxwellian energy distribution or by spin-polarization of the nuclei. See Appendix A for details. Photon radiation loss can be reduced by depressing the electron temperature. See Appendix B for details. None of these can simply be dictated. In fact they add constraints to the system that increase the difficulty. These are inherently thermal systems that gravitate toward Maxwellian distributions. Also, at the densities needed for reasonable power

Figure 3 shows that none of the other fusion fuels are of any value, at least for thermal systems. For non-thermal systems, only p-^{11}B appears to have any promise. All of the others either have negligible power density potential or must be heated to such high temperatures that, not only are radiation losses so great that ignition is impossible, but the power that must be continuously supplied to maintain the temperature far exceeds any fusion power produced.
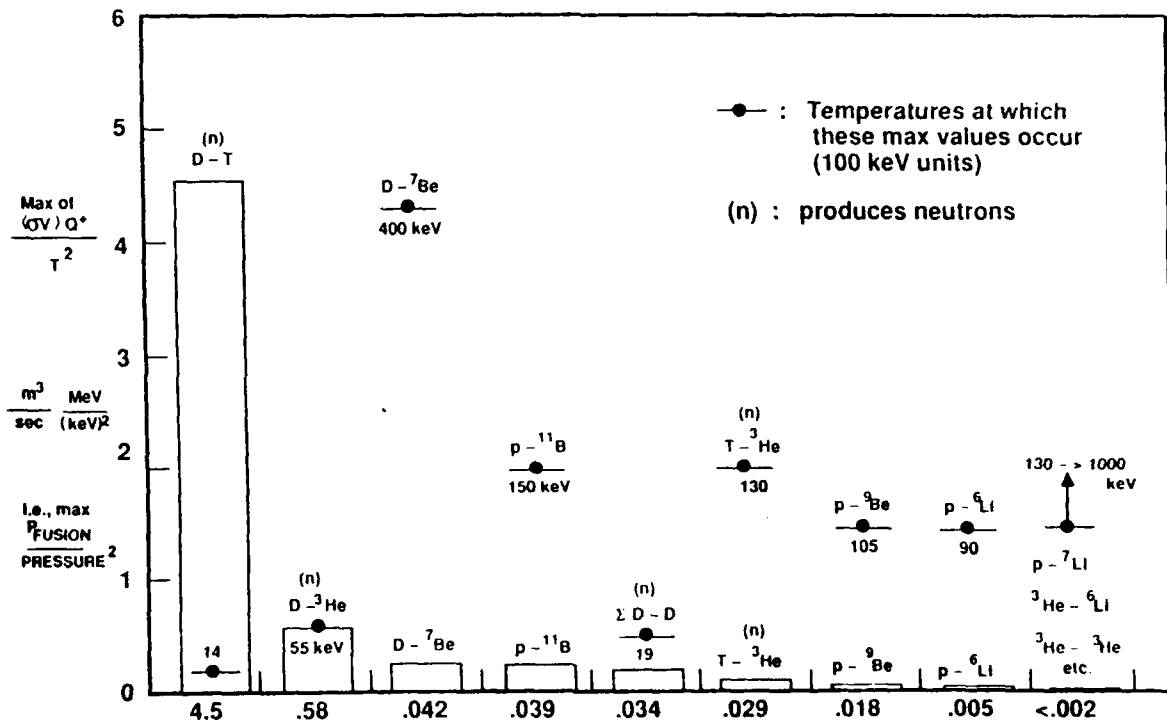
Figure 3.   Maximum values of charged particle fusion power at a given pressure. Numbers at bottom are actual values of

$$\frac{<\sigma V > Q^{+}}{T^{2}}$$

Table 4 gives a summary of the three fuels of interest. In addition to power density and temperature, neutron flux, heat rejection, and shielding must also be considered. Since 80% of the total fusion energy in D-T is in the neutrons it must either be utilized or rejected. Also, since the relative neutron flux to the first wall with D-T is 400 times that for D-^{3}He, material damage is also a concern. Finally, not mentioned in Table 4, the tritium reactant is sufficiently radioactive to warrant special handling and precautions. These issues are discussed in the next section.

TRITIUM AND NEUTRON ISSUES

Tritium. Tritium has a half-life of 12.3 years. It decays to ^{3}He by emitting beta particles (energetic electrons) with a mean energy of 5.7 keV and a maximum energy of 18.6 keV. These particles are not penetrating and are readily stopped by 0.006 mm of water. Any container holding gaseous or liquid tritium also serves as a beta shield. The specific activity of tritium is 10 Curies per gram.

TABLE 4

COMPARISON OF VIABLE FUSION FUELS

	D – T	D – ^{3}He	p – ^{11}B	Other Aneutronic
Charged particle power density (relative MW/m^3)	100	10	1	< 0.5
Operating temperature millions of °C	160	640	1740	
Relative first wall neutron flux (10^{12} n/cm^2 sec)	100	0.25	0	
Approximate shielding needed, m	1.4	0.2	0	

Tritium is perhaps the least dangerous of the radioactive substances. While chronic high level exposure is fatal, typically by reduction in bone marrow and red blood cells[5], a single high level dose of HTO* may not cause permanent damage because it flushes out of the body with a biological half-life of about 12 days. Tritium gas appears to exhibit the same behavior[6]. The major concern, however, is not HTO but the amino acid tritiated thymidine (^{3}HTdR), since it is a DNA precursor[5]. With a one-time dose, as would occur in an accident, little HTO or T_2 gas is likely to get locked up in ^{3}HTdR[6].

Since testing thus far has been to determine toxicity, no information is available on a one-time exposure followed by an antidote (e.g., drinking a lot of liquid). Some estimates can be made

---

* Hydrogen-Tritium-Oxygen = Tritiated Water

25

using the Code of Federal Regulations (CFR)[7] and EPA guidelines[8]. For one year continuous operation of a 2000 MW(th) D-T reactor, about 190 kg of tritium are required (about 0.9 m^3). At 10^4 Curies per gram, total activity is 1900 MCi. For uncontrolled areas and 40 hours per week exposure, 10CFR20 Appendix B requires air dilution to 2 x 10^{-13} Curies/cc of air. For our case, this requires an air volume of 9.2 x 10^{15} m^3. Assuming a 20 km vertical mixing zone, general population would have to remain 390 km (242 miles) away from the launch. This would require a very remote launch site such as an island or a mid-ocean platform.

The above is very conservative because it refers to continuous 40 hr/week exposure by the general population. EPA guidelines for one-time nuclear incidents[8] are shown in Table 5. A rough rule of thumb is that 1.0 milliCurie ingested and permanently retained produces 5 Rem/yr[6]. Since a one-time dose will be essentially fully purged in 1/3 year, for tritium one can use 3 milliCurie for 5 Rem. We assume that 10 minutes are required for the general population to seek shelter after a catastrophic launchpad explosion. It can be shown that, during this time, about 100 liters of air would be inhaled and absorbed. The dilution for 3 milliCuries is then 3 x 10^{-8} Ci/cc air. The total volume of air to dilute 1900 MCi is then 6.3 x10^{10} m^3. If this were a cylinder with diameter and height being equal, the cylinder diameter would be 4.3 km (2.7 miles). Based on these criteria for one-time dose, unprotected general population could be as close as 1.5 miles from the launch. Clearly, there is quite a discrepancy between the 10CFR20 and EPA guidelines. More work is needed to establish one-time tritium dose when exposure occurrence is known and an antidote immediately taken.

TABLE 5
EPA GUIDELINES FOR ONE-TIME NUCLEAR INCIDENTS
(Ref. 8)

Whole Body Dose for Airborne Material

General Population	1-5 Rem
Emergency Workers	25 Rem
Lifesaving Activities	75 Rem

This all assumes that tritium would be released during a launchpad explosion. Liquid tritium cryogenic containers can be considerably hardened and the 190 kg of tritium could be divided into many small containers. It is very unlikely that all of the containers would burst. Also, if the explosion occurred during liftoff, the tritium dose at the surface would be greatly reduced.

Tritium handling is routine in the Air Force nuclear missile program, the Canadian reactor program, and in nuclear weapons fabrication. As long as reasonable safeguards are employed, risk of exposure is small. Even catastrophic failure during launch of a tritium-bearing payload should not impact ground personnel or civilian populations providing proper care is taken (on-board personnel would have much more to worry about than tritium exposure!).

Neutrons While 80% of the fusion energy in a D-T reaction is in the form of energetic neutrons, this has been ignored in the above comparisons. It makes sense, of course, to exploit that energy. The obvious way would be to let the rocket propellant also serve as neutron shield. Not only is much of the neutron energy effectively utilized, but the first material wall would be subject to less of the damaging neutron flux. Also, heat rejection requirements would be reduced. If this is done, the ten-fold power density advantage over D-^{3}He is increased up to 50-fold if all the neutron energy is utilized. It must be emphasized, however, that to exploit such resulting high power densities, and to mitigate material damage, the propellant must be the first wall.

D-^{3}He fuel also produces some neutrons from side D-D reactions. Although fluxes are much less than D-T, wall activation and personnel protection are still of concern. In Appendix A it is shown that a 5-fold reduction in neutron production rate per unit fusion power can be obtained by running with a 15% D, 85% ^{3}He. However, fusion power is cut in half. For a given total power, the fusion fuel volume for D-^{3}He must be 20 times that for D-T, even with ignoring the neutron power from D-T. It is also shown in Appendix A that total shield volumes for D-T and D-^{3}He are roughly comparable. The D-T shield is thicker, but covers a smaller area.

With all of this in mind, it would appear that one should not rule out D-T as a fusion fuel. However, since the environmental issues are still in great flux, and considering the present concern over tritium and neutrons, D-T fuel was not further considered during the remainder of this study. Emphasis was placed on evaluation of the other candidate fusion fuels.

EVALUATION BASED ON ALL CRITERIA

In the previous section, fusion fuels were assessed only on their ability to produce power. In this section, we evaluate the fuels based on a selective set of evaluation criteria extracted from the general list given in Table 2, which is most applicable to fuels. In addition to D-^{3}He and p-^{11}B, we examine two other fuels of interest to the community: p-^{6}Li and ^{3}He-^{3}He. The selected

evaluation criteria are listed in Table 6. Each of these criteria and its use in the evaluation of the four fuels are discussed below.

TABLE 6

ALTERNATE FUEL EVALUATION CRITERIA

Criteria	Weight
High-energy exothermic reactions	10
No (or low) neutrons or gamma rays	8
Stable ignition characteristics	9
Low radiation loss	6
Reacting isotopes easily available	5
Large fusion reactivity	10
Good storage and handling	3
No radioactive secondary reaction	6
Low ignition/burn temperatures	10

Exothermic Reactions. Table 7 shows the charged particle energy for the four fuels. D-^{3}He is greatest and is given a score of 10. The others are scaled linearly. While ^{3}He-^{3}He looks pretty good here, bear in mind that this is energy per reaction and says nothing about reaction rate. The p-^{6}Li has a rather low energy output per reaction.

Low Neutrons and Gamma. Table 8 shows that D-^{3}He does produce some neutrons, as mentioned in the last section, while the other fuels do not (p-^{11}B doe produce trace amounts of ^{14}C). Also of concern are the penetrating X- and γ-rays from high temperature fusion reactions. As shown schematically in Figure 4, the fusion plasma will radiate all wavelengths up to the Maxwellian electron temperature (Te). Radiation intensity decays exponentially beyond that. Therefore, all of these high temperature fuels will radiate much of their energy. Some of this will be in the form of penetrating X- and γ-rays and therefore must be shielded.

None of these fuels therefore received high scores. Because D-^{3}He produces neutrons, it scored the worst. The p-^{6}Li scored best, followed by p-^{11}B. The ^{3}He-^{3}He is expected to radiate all of its power in the form of penetrating radiation, which would therefore require considerable shielding.

28

$$\frac{dE}{dT}$$

0   1.0

T/Te Plasma
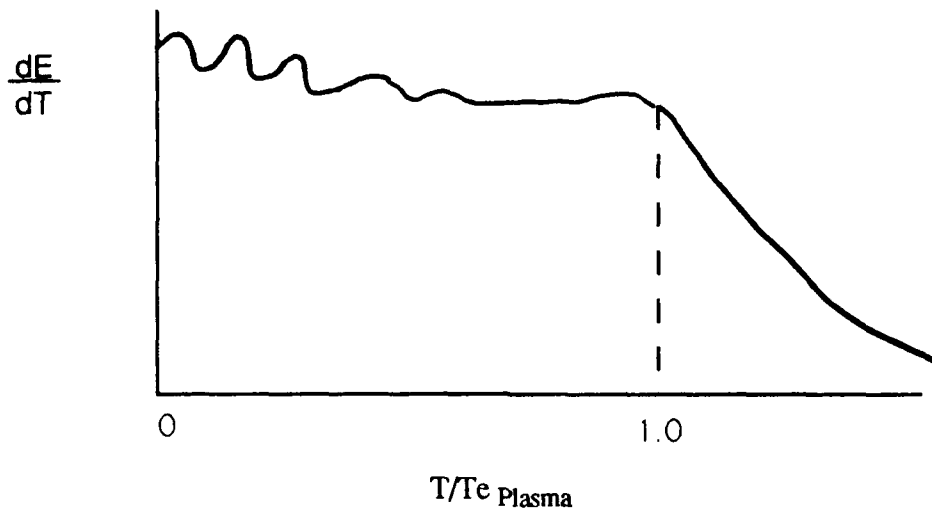
Figure 4. Schematic of radiation spectrum from a fusion plasma.

Ignition. Fuels that ignite tend to have less recirculating power requirements than those that don't. Therefore, ignitability has a high-weighted score. Table 9 shows the scoring for the four fuels.

Ignition occurs when the fusion charged particle power in the fuel exceeds all losses. These losses are made up of conduction and convection of ions and electrons, and the photon radiation discussed above. Even with depressed electron temperatures, radiation losses with p-^{11}B, p-^{6}Li, and ^{3}He-^{3}He are so great that ignition cannot occur even with perfect confinement. D-^{3}He is the only fuel that has a chance of igniting and therefore is the only fuel that gets a nonzero score.

Low Radiation Loss. The higher the operating temperature, the greater the photon radiation loss. The four fuels of interest all operate at temperatures high enough that Bremsstrahlung radiation is a major, if not the total, loss mechanism. If magnetic fields are present, cyclotron radiation is also severe. Table 10 shows Bremsstrahlung radiation loss fractions for electron temperatures at half the ion temperature. In general, this would require low density plasmas because at high density, thermal equilibrium occurs at a rate much faster than power production. Yet high density is needed because the reactivity of these fuels is so poor. Table 10 is therefore quite optimistic. For D-^{3}He, at least 20% of the charged particle power leaves by radiation. If it can be held to this low level, ignition may be possible. While the radiation loss fraction for p-^{11}B is under 100%, any reasonable transport scaling law shows that this fuel cannot be ignited. Similarly, even with perfect energy confinement (excluding radiation), the other two fuels are in the subignition region. While all of the fuels score badly here, D-^{3}He is still the best.

TABLE 7

EXOTHERMIC REACTIONS
(Weight = 10)

	D-^{3}He	p-^{11}B	p-^{6}Li	^{3}He-^{3}He
Charged Particle Energy, MeV	18.4	8.7	4.0	12.9
Score (1-10)	10	5	2	7
Score x Weight	100	50	20	70

TABLE 8

LOW NEUTRONS AND GAMMA
(Weight = 8)

	D-^{3}He	p-^{11}B	p-^{6}Li	^{3}He-^{3}He
Neutrons from D-D	yes	no	no	no
T_{burn}, keV	55	150	90	1000
Penetrating X- and γ-rays (% of total power)	10%	50%	40%	100%
Score (1-10)	6	7	8	6
Score x Weight	48	56	64	48

TABLE 9

IGNITION
(Weight = 9)

	D-^{3}He	p-^{11}B	p-^{6}Li	^{3}He-^{3}He
Radiation with Te/Ti = 0.5	20%	60%	100%	100%
Confinement Requirements	High	Very High	Very High	Very High
Score (1-10)	7	0	0	0
Score x Weight	63	0	0	0

TABLE 10

LOW RADIATION LOSS
(Weight = 6)

	D-^{3}He	p-^{11}B	p-^{6}Li	^{3}He-^{3}He
Radiation with $T_e/T_i = 0.5$	20%	60%	100%	100%
Score (1-10)	6	0	0	0
Score x Weight	36	0	0	0

Reacting Isotope Availability. Hydrogen, boron, and lithium are readily available on earth in the required quantities. Helium-3 is available only in small quantities which are insufficient for anything but small experiments. There is a large quantity adsorbed in the lunar surface and there is interest in exploiting it [9]. Once space stations and lunar colonies are in place, then helium-3 may be as utilizable as any on earth. Until that time, however, preference is for terrestrial sources and therefore fusion requiring ^{3}He scores low. This is summarized in Table 11.

TABLE 11

FUSION FUEL AVAILABILITY
(Weight = 5)

	D-^{3}He	p-^{11}B	p-^{6}Li	^{3}He-^{3}He
Earth	Low	High	High	Low
Moon	High	-	-	High
Score (1-10)	1	8	8	1
Score x Weight	5	40	40	5

Reactivity: The parameter $<\sigma V>$ is a measure of the reactivity of the fusion fuel. This, times the energy release per reaction, gives the power density of the reaction. Figure 3 shows power densities for several fuels. It is worth noting the strong temperature dependence and particularly the difference between the fuels at lower temperatures. Ideally, one wants high

reactivity at low temperature because then the power produced for a given fuel pressure confined is greatest.

Table 12 shows the analysis for cross sections for the four fuels. The fourth entry, $<\sigma V>/T^2$ was discussed earlier. It is the reactivity for a given fuel pressure. For each fuel, it peaks at a certain optimum temperature, shown in the table. The higher the temperature, the more difficult to achieve it. Reaching the required temperature for ^{3}He-^{3}He would be very difficult indeed.

The second entry in Table 12 shows the cross section at that temperature. The third entry shows for convenience these cross sections normalized to the ^{3}He-^{3}He value. Surprisingly, all but the p-^{6}Li are about the same. But this is not what matters. If one were to score this item based on cross section alone, ^{3}He-^{3}He would win.

TABLE 12

REACTIVITY
(Weight = 10)

	D-^{3}He	p-^{11}B	p-^{6}Li	^{3}He-^{3}He
T for peak $<\sigma V>/T^2$, keV	55	150	90	1000
Peak $<\sigma V>$, 10^{-23} m^3/s	9.5	10	1	12
Ratio of $<\sigma V>$	0.79	.83	.1	1.0
Peak $<\sigma V>/T^2$, 10^{-27} m^3/s keV^2	580	39	5	1.5
Ratio	1.0	.067	.009	.003
Score (1-10)	5	0.3	0	0
Score x Weight	50	3	0	0

What does matter is the reactivity per unit pressure because all of the effort in fusion is going to contain that pressure. The fourth entry is the magnitude of the maximum reactivity per unit pressure. The fifth entry shows these normalized to D-^{3}He for convenience. The scores correspond to these values.

Good Storage and Handling. While not considered urgent enough to be heavily weighted, some consideration must be given to prosaic issues like storage and handling. Table 13 gives an evaluation of this issue. Compounds of hydrogen and boron exist that are solid at room temperature (e.g., decaborane $B_{10}H_{14}$). This is also true with hydrogen and lithium (LiH). Deuterium and helium-3 both require cryogenic storage; and $D^{-3}He$ requires storage at two temperatures. Lithium is chemically the most active of the fuels.

The scores reflect these storage and handling characteristics with $p^{-11}B$ scoring highest and $D^{-3}He$ lowest.

No Radioactive Secondary Reactions. Table 14 shows that some radioactive products are produced by these so-called "clean" fuels. $D^{-3}He$ produces tritium from the side D-D reactions. Since tritium density is very low, it generally will tend to migrate out of the fuel before reacting. Therefore, some sort of low-volume tritium handling is required with this fuel. The proton-based fuels produce trace amounts of other radioactive isotopes. The scoring puts $D^{-3}He$ at the bottom because of the tritium.

TABLE 13

GOOD STORAGE AND HANDLING
(Weight = 3)

	$D^{-3}He$	$p^{-11}B$	$p^{-6}Li$	$^3He^{-3}He$
Room Temperature Solid	No	Yes	Yes	No
Single Temperature Liquid	No	-	-	Yes
Score (1-10)	1	10	6	3
Score x Weight	3	30	18	9

TABLE 14

NO RADIOACTIVE SECONDARY REACTIONS
(Weight = 6)

	$D\text{-}^3He$	$p\text{-}^{11}B$	$p\text{-}^6Li$	$^3He\text{-}^3He$
Tritium	Yes	-	-	-
^{14}C, etc	-	Yes	^8Be, ^9Be	-
Score (1-10)	2	8	8	10
Score x Weight	12	48	48	60

Low Ignition/Burn Temperature. With lower ignition temperature, less heating power is needed. The lower the burn temperature, the less radiation loss of charged particle power. Table 15 shows an evaluation of this issue. D- ^3He is the only fuel that is likely to ignite, even with depressed electron temperatures limiting radiation loss. It also has the lowest burn temperature of the four fuels. It is the only fuel that rates a nonzero score here.

Evaluation Summary. Table 16 gives a summary of the alternate fuel evaluation based on all of the criteria. D-^3He receives the highest total score, which is 50% higher than the next contender p-^{11}B. The other two fuels are not worth any further consideration.

TABLE 15

LOW IGNITION/BURN TEMPERATURE
(Weight = 10)

	$D\text{-}^3He$	$p\text{-}^{11}B$	$p\text{-}^6Li$	$^3He\text{-}^3He$
Ignition Temperature, keV	55	-	-	-
Burn Temperature, keV	70	150	90	1000
1/product of above	>0	0	0	0
Score (1-10)	5	0	0	0
Score x Weight	50	0	0	0

TABLE 16

FUSION FUEL ASSESSMENT SUMMARY

TOTAL SCORE x WEIGHT

	D-^{3}He	p-^{11}B	p-^{6}Li	^{3}He-^{3}He
Exothermic Reactions	100	50	20	70
Low Neutrons or Gamma Rays	48	56	64	48
Ignition	63	0	0	0
Low Radiation Loss	36	6	0	0
Reacting Isotope Availability	5	40	40	5
Large Cross Section	50	3	0	0
Good Storage and Handling	3	30	18	9
No radioactive Secondary Reactions	12	48	48	60
Low Ignition/Burn Temperatures	50	0	0	0
Total Sum	367	233	190	192

In view of this ranking, and considering that D-T was eliminated because of present concerns over tritium handling and accidental releases, the reactor evaluation portion of this study concentrated on confinement concepts appropriate to D-^{3}He fuel.

SUMMARY

The only two viable fusion fuels are D-T and D-^{3}He. This conclusion is drawn from an elaborate evaluation based on numerous criteria. While one would like to consider p-^{11}B because of its truly aneutronic characteristics, it simply does not have the power density to meet the demanding requirements for compactness in fusion rockets. If tritium and neutron issues can be resolved, the D-T is by far the best choice because of its high power density and availability. Otherwise, the only choice is D-^{3}He, and it will be necessary to mine it from the moon if large quantities are required.

EVALUATION OF FUSION CONFINEMENT CONCEPTS

In this section we explore the many different means that are being attempted to create fusion power and sort out those that appear most suited to space propulsion.

INTRODUCTION

Fusion research has focused on ground-based reactors, primarily electricity producers. Weight and bulk have been a consideration only with respect to their impact on costs and reliability. For space propulsion, costs are less of an issue; but reliability requirements are even tighter. Low mass and compact size override everything, because otherwise fusion propulsion cannot compete with other sources like fission. Desirable features of a fusion rocket are listed in Table 17 and are discussed below.

Low mass and volume generally require high fusion power density. Limitations on power density stem from the confining forces required such as magnetic fields, and the ability of nearby materials to take the heat flux.

When the mass of peripherals such as power supplies are included, often an optimum power density exists beyond which total mass increases because of increased recirculating power. Fusion reactors are sized for a given useful power output. When recirculating power to run the reactor is required, it must be added to the useful output, increasing reactor and peripheral size and cost.

The hardest part of using fusion for thrust is getting the fusion power to the propellant without harming the fusion reaction. Fusion is more difficult in this regard than fission because the fission fuel is usually solid and the fission reaction is therefore unaffected by contact with a flowing propellant. Fusion fuel, being gaseous, is greatly affected by contact with large amounts of cold gas needed to produce high thrust. In this respect, it is like the gaseous core fission concept.

TABLE 17

FUSION ROCKET DESIRABLE FEATURES

Low total mass and volume including peripherals

Low recirculating power to run reactor

Ease of getting fusion power to propellant

Quick starting with minimum startup energy

High thrust and specific impulse

Wide thrust variation

Low radioactivity and afterheat

The problem is worse with steady or long burn fusion reactions because of the time overlap between the fusion burn and the propellant heating. Unless a material wall protects the fusion reaction, the propellant (which expands upon heating) will try to enter the fusion reaction, putting it out. Because the total fusion energy produced must be many times the instantaneous thermal energy in the reaction, the energy produced must flow to the propellant while the reaction proceeds.

Propellant addition in inertial confinement fusion is easier because the fusion burn is over in nanoseconds and the fusion energy is dumped into the propellant in such a short time that it hardly expands.

Fusion is thermonuclear and therefore the fuel must be heated to get it going. This takes energy and power and so there is a finite startup time that is required. Generally, small, high-power density reactors with low losses will have the shortest startup time.

Thrust and specific impulse tend to oppose each other. As discussed later, the required fusion power is proportional to FI_s, where F is the rocket thrust and I_s is the specific impulse. High thrust with high specific impulse therefore requires high power. These requirements are fundamental and apply to both fission and fusion.

Thrust variation with fusion is likely to be easier with pulsed systems where the fusion burn is always the same, only the rep rate is changed. With steady state or long burn fusion, only a modest power variation is likely since fusion reactors will inherently run best at full power.

Fusion should have lower radioactivity than fission and most certainly will have low afterheat. Afterheat is generally high enough with fission to require reactor cooling during off periods. This should be unlikely with fusion. Even with D-T, as discussed in the previous section, the tritium presents a rather low level radiation hazard compared to fission products. Clever design can greatly reduce the irradiated materials problem.

There are other fusion reactor characteristics that have been listed in the past, but are actually inherent in those shown in Table 17. For example, the desire for ignition and high beta (ratio of fusion fuel pressure to confining pressure) reflects the wish for low recirculating power and low mass. Also, a requirement for much of the fusion output in charged particles reflects the wish for high thrust.

BASIC FEATURES OF A FUSION ROCKET

A generic fusion rocket is shown schematically in Figure 5. A reaction chamber is required to contain the fusion reaction. In space, this can be less massive than on earth because their is no atmospheric pressure overload. Some method is required to limit thermal losses from the fusion reaction. Magnet coils are shown here, but they could also be inertial confinement drivers. Thermal losses are limited in ICF by creating fusion burns that are much more rapid than any heat loss rate. Fusion fuel must be supplied either by injecting pellets, compact tori, or equivalent. Also, some means should exist to recover unburned fuel or fusion fuel consumption may be excessive.

Some power must be recycled to heat the fusion fuel during startup or to maintain temperature if subignition occurs. Finally, propellant must be added, heated, and then exhausted out a rocket nozzle. Propellant addition is required because the specific impulse from the fusion products alone is way too high and the thrust far too low to be useful for Air Force missions.

38
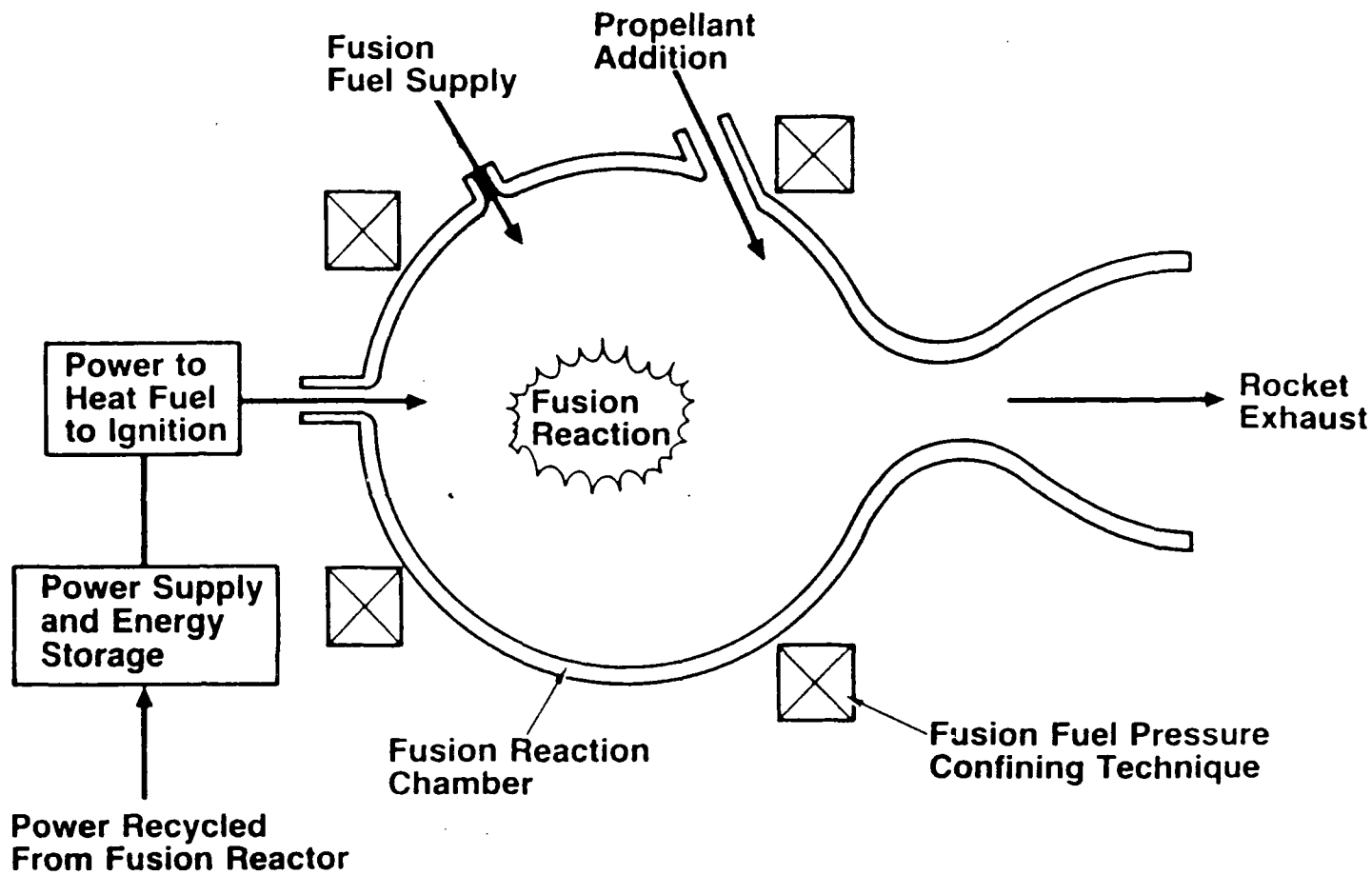
Figure 5. Principle features of a generic fusion propulsion system.

PROSPECTIVE FUSION CONFINEMENT SYSTEMS

There are a large number of fusion confinement systems than can be considered as candidates for propulsion. Because of the issue of propellant addition, they are divided here into low initial density systems, in which it will probably be difficult to add propellant, and high density, where propellant addition should be easier. Table 18 shows the candidates divided in this way.

TABLE 18

PROSPECTIVE FUSION CONFINEMENT SYSTEMS

■ Low initial density ($<10^{18}$cm^{-3})

- ● Magnetic
  - Tokamak
  - RFP
  - FRC (includes moving ring)
  - LINUS
  - TCT
  - Stellarator
  - Mirror
  - Plasmak

- ● Electrostatic

- ● Transpiration-cooled Wall Confined

- ● MIGMA/non-Maxwellian

■ High initial density ($>10^{18}$ cm^{3})

- ● Inertial
  - Impact
  - Explosive compression
  - ICF (laser or particle)
    - o X-D-N shield
    - o Multistage
    - o Magnetically insulated (MICF)
  - ORION

- ● Quasi S.S.
  - μ_o - catalyzed (could be low n)
  - Z - pinch
  - Beam

Low Density Systems.

Among low density machines are the magnetically-confined, electrostatic, wall-confined, and non-Maxwellian systems. In these, density tends to be limited by the stresses in the confining system. For example, in magnetically-confined, magnetic fields are limited to below about 15 Tesla[*].

The tokamak (Figure 6) has dominated fusion research for two decades. The reasons are because it has achieved the best plasma confinement, the highest plasma temperatures, and the highest $n\tau$ [**] values. Its success seems to stem from the strong embedded field parallel to the plasma current. This field, called the toroidal field, provides resistance to a variety of plasma instabilities, the most notable being the sausage and kink instabilities. The first pinches the plasma off while the second forces it to bulge out of its circular shape. Both essentially destroy plasma confinement.

While the strong toroidal field has helped plasma confinement, the large and heavy magnets needed to create that field have rendered the tokamak questionable even for ground-based applications. Mass-power densities tend to be below 200 kW(th)/tonne of nuclear island, which consists of the reactor, shielding, magnets, and coupled heating systems. Peripherals such as power supplies and energy storage lower this value even further. It is therefore not a viable candidate for fusion propulsion.

---

[*] The pressure due to a 15 T field is 90 MPa (13,000 psi). This pressure induces stresses on the magnet structure much like a gas pressure in a tank. It varies with the square of the field. Small magnets with special materials may go to 25 T.

[**] $n\tau$ is the Lawson Criterion denoting the energy breakeven conditions.
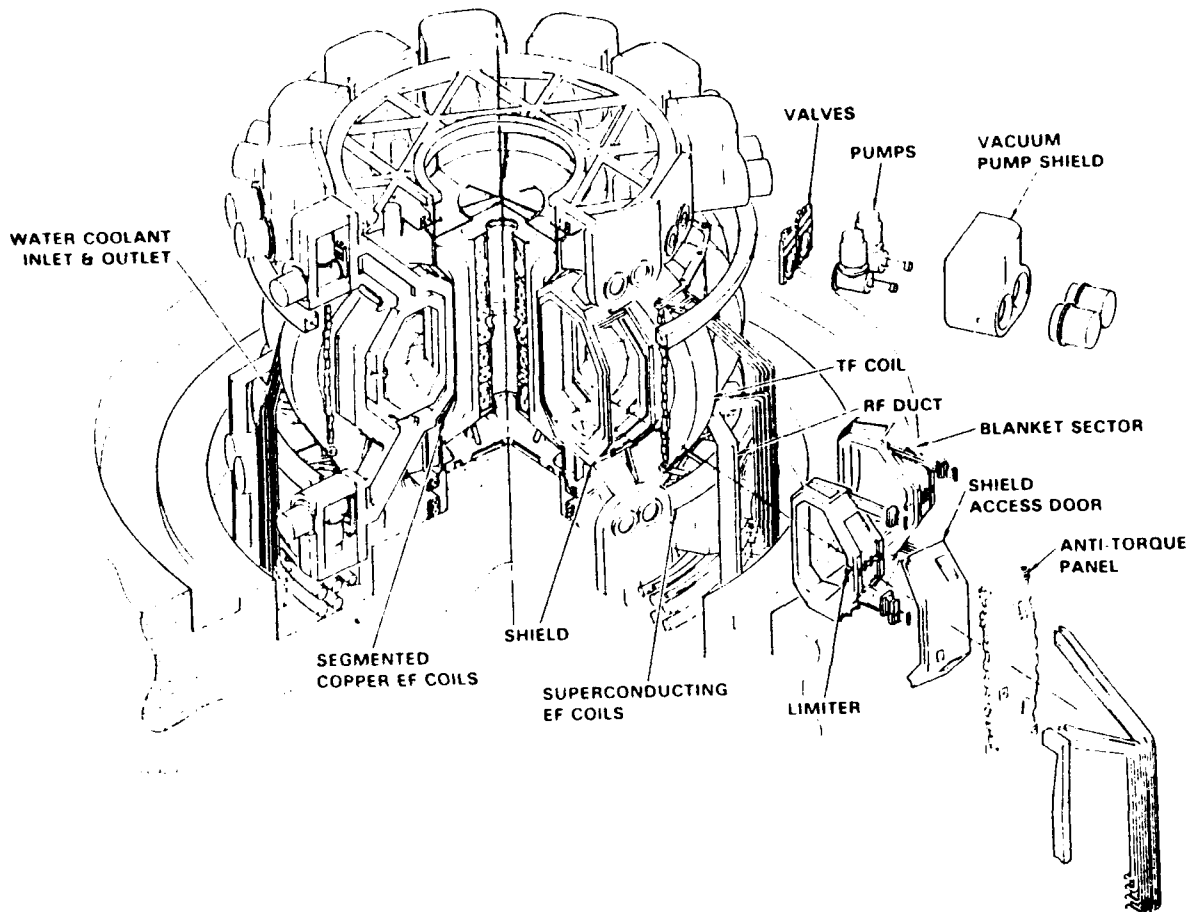
Figure 6. The Starfire Tokamak (Ref. 10).

The reversed-field pinch RFP (Figure 7) is similar to a tokamak except that much of the toroidal field is generated by the plasma current itself, which in this case spirals through the plasma everywhere except exactly on the plasma axis. A curious feature is that the toroidal field actually reverses near the outer edge of the plasma. This, along with a close-fitting conducting shell, provides the required plasma stability.
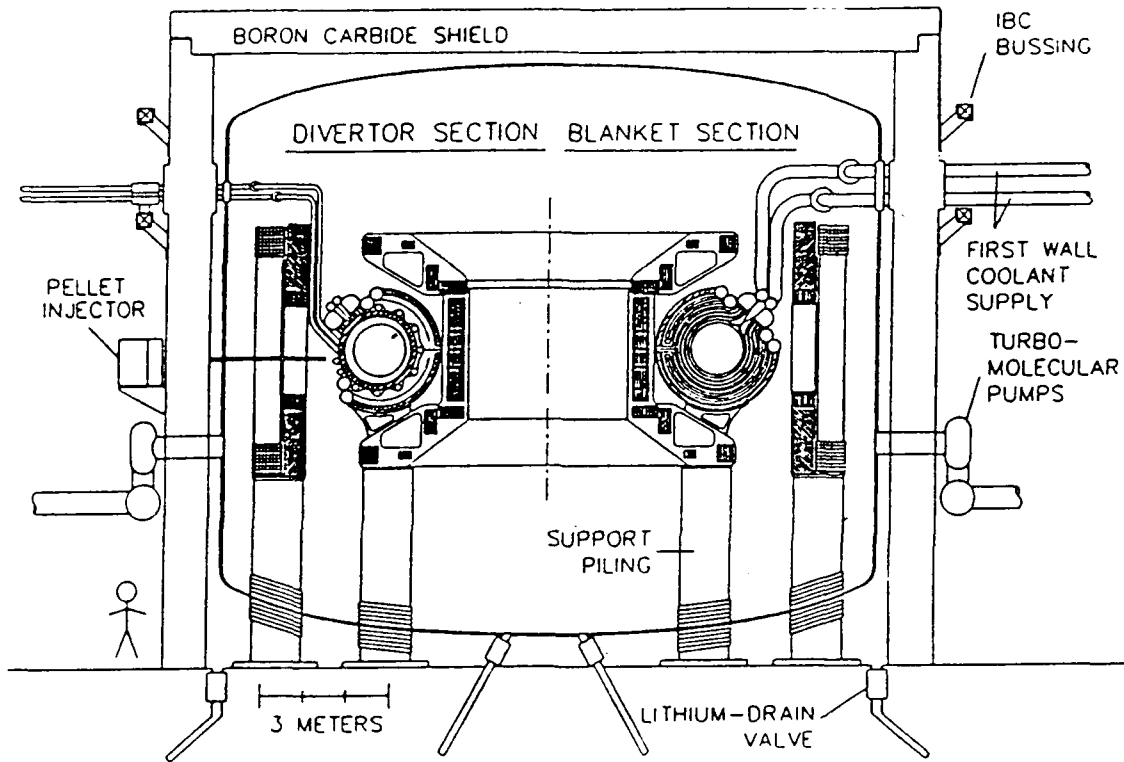
Figure 7 The Titan Reversed-Field Pinch Reactor (Ref. 11).

Like the tokamak, an external toroidal field is needed in the RFP; but now it is more of a seed field which is multiplied 5-fold in the plasma by the plasma current. The power density is therefore not limited by magnetic fields as in tokamaks, but rather by wall heating constraints. Mass power densities of 1500 kW(th)/tonne may be possible.

The closed toroidal configuration of the RFP still presents problems in applying it to fusion propulsion. One could conceivably take the charged particle power though a divertor and mix in a propellant. However, as will be shown in the next chapter, propellant to charged particle mass ratios are several million to one. Therefore, only a small fraction of the propellant moving back to the plasma would quench the reaction. This is a common problem with virtually all of the low density systems: the plasmas are quite ephemeral and it takes very little to destroy them.

The field-reversed configuration (FRC) is similar to the RFP except field reversal takes place axially rather than radially. There are both open and closed field lines, and the plasma is capable of translating (Figure 8). An advantage of the FRC is that propellant addition may be easier than the RFP because of the open field lines. Propellant could be injected axially at one end and expelled out the other end. The same problem of quenching the plasma still exists, however. Another problem is that the FRC has not demonstrated very good confinement in the experiments to date, even compared to the RFP.
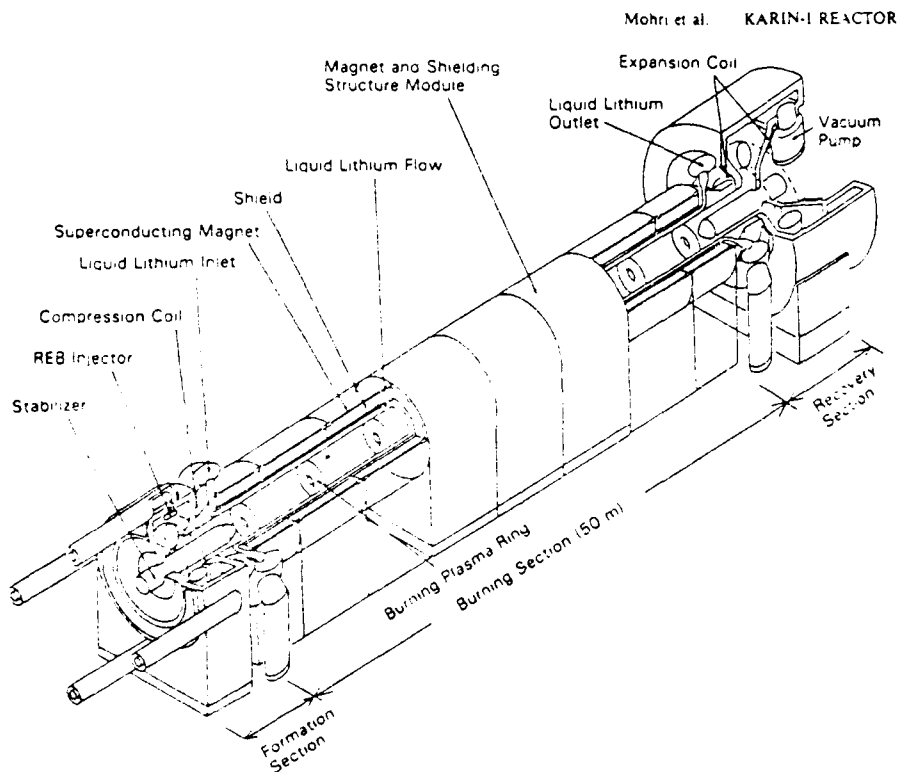
Figure 8. A field-reversed moving ring reactor (Ref. 12).

Liner Fusion (LINUS) starts with a low initial density plasma, either in the form of a long column or field-reversed, inside a rotating liquid lithium liner (Figure 9). The liner is imploded, compressing the plasma to high density. In a field-reversed configuration, this system could be relatively compact. One of the major issues with LINUS is the demanding simultaneity of compression required along the entire plasma. Another is the intense heating of the inner liner wall. If one could accept lithium vapor as the propellant, LINUS could potentially be made into a rocket. However, the specific impulse from lithium is lower than hydrogen because of the high atomic mass. However, lithium may be attractive as a propellant for some missions because it can be stored as a powder at normal temperatures or as a liquid at about 200° C. Unlike hydrogen, cryogenic or hydride storage is unnecessary..
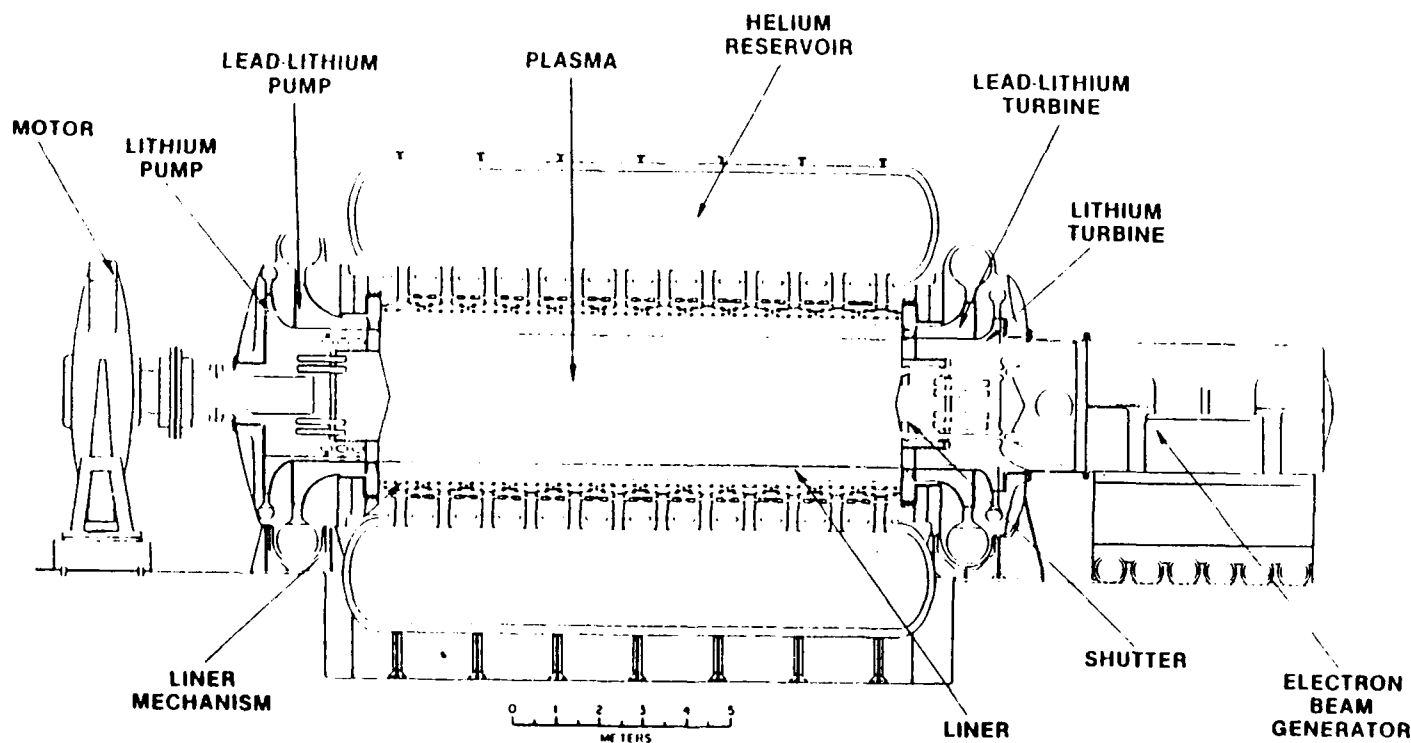
Figure 9. A liner fusion (LINUS) reactor (Ref. 13).

45

The Translating Compact Torus TCT employs two field-reversed configurations in the form of spheromaks accelerated to very high velocity, over 1000 km/s. These values have already been achieved experimentally. Then the kinetic energy is converted to plasma thermal energy by either driving them into converging conducting channels or colliding two into each other. This concept is discussed in detail in the next section and Appendix C.

The Stellarator (Figure 10) was an earlier attempt at toroidal confinement and is similar to a tokamak except for the absence of an internal plasma current. Like the tokamak, it tends to be low power density and quite large and heavy.
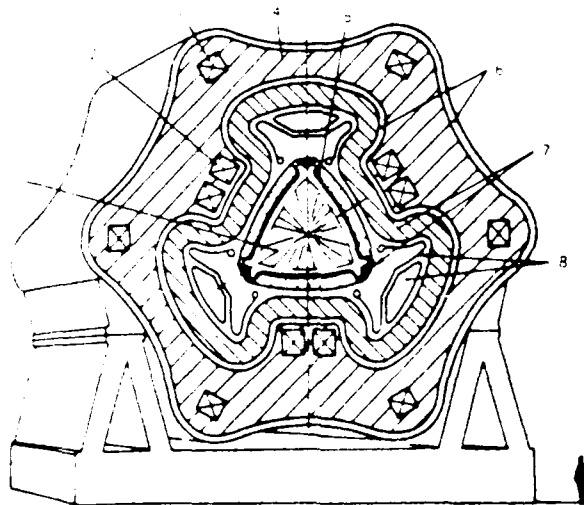
Figure 10. The stellarator (Ref. 14).

The Mirror (Figure 11) has an ideal axial configuration for propulsion. However, it has low power density and requires large magnets and a very complex RF and neutral beam heating system. Therefore, while appealing at first glance, it is really no more attractive than the tokamak. In addition, experiments have shown disappointing confinement.
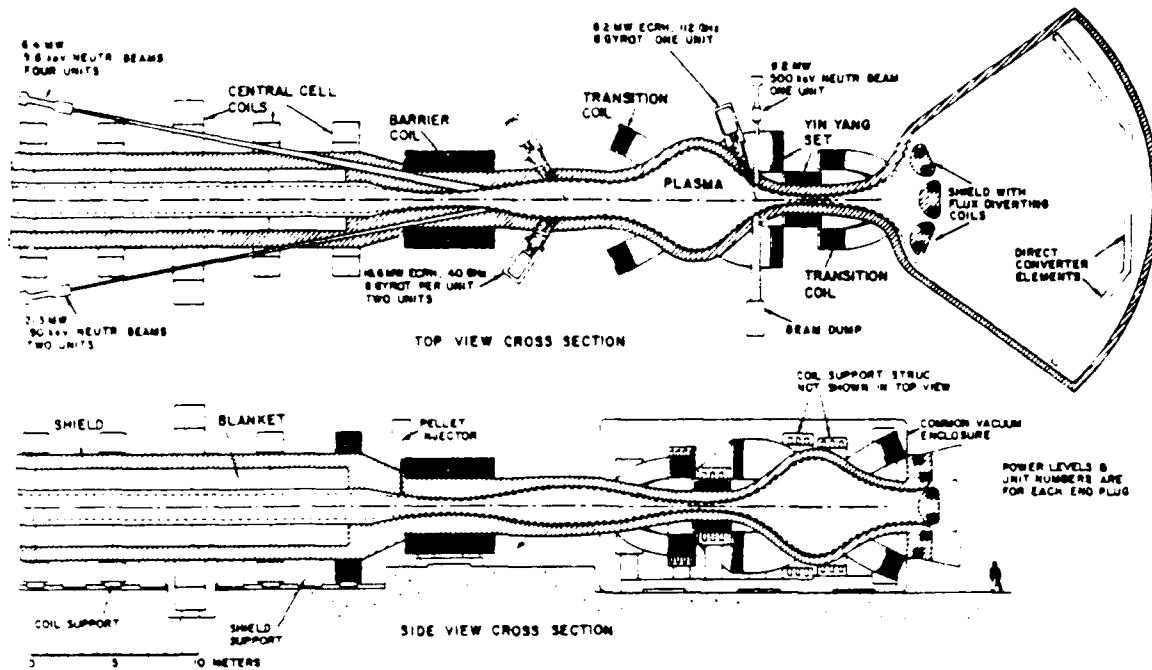
Figure 11. One end of the WITAMIR-I tandem mirror reactor (Ref. 15).

The Plasmak (Figure 12) is a spheromak concept stabilized by a relativistic electron ring which in turn is stabilized by a neutral gas. The concept, while potentially interesting, is strictly in the conceptual stage and is greatly in need of detailed analysis.

Electrostatic confinement was first tried in the 1960's but later abandoned when it was learned that the neutrons produced where not due to fusion but due to photodissociation (i.e., fissioning of deuterium by energetic photons). The appeal of electrostatic confinement has always been the spherical symmetry not achievable with magnetic systems.

Wall-confined plasmas (Figure 13) were considered experimentally but generally showed poor confinement, as would be expected. Some magnetic fields are needed to reduce thermal losses, and this introduces the same problems of axial end loss as in mirrors.
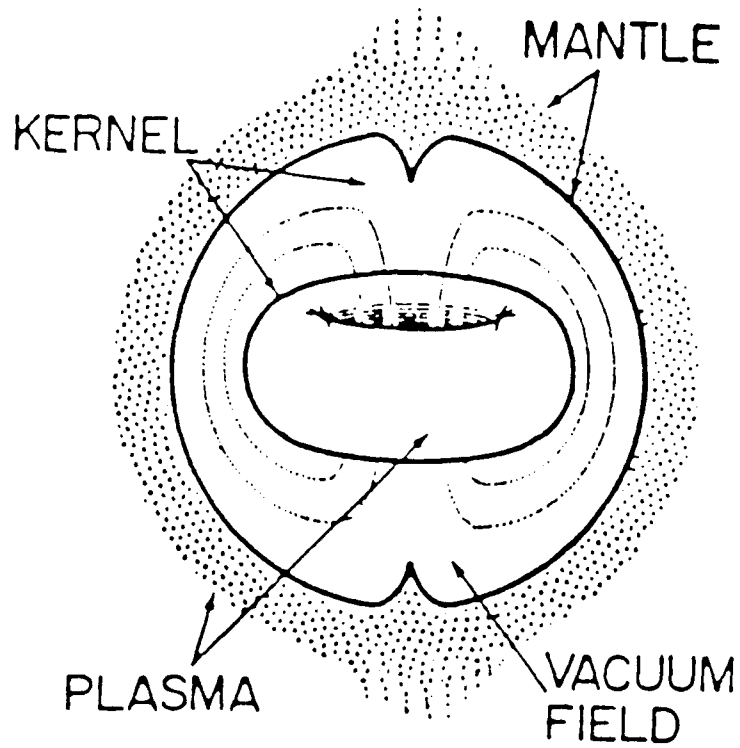
Figure 12. The Plasmak configuration (Ref. 16).
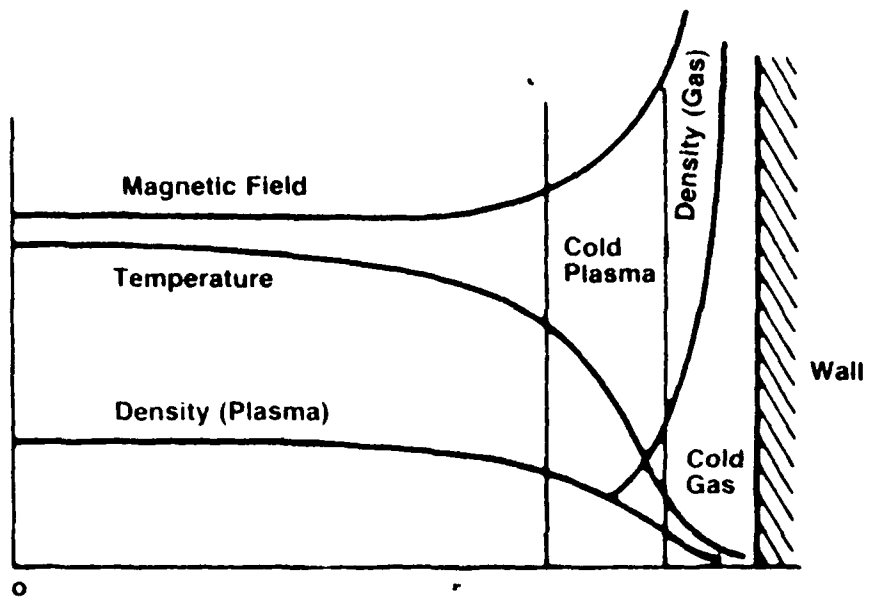
Figure 13. Wall-confined plasma internal profiles (Ref. 17).

Self-colliding monoenergetic beams such as MIGMA (Figure 14) are still being considered experimentally. These beams tend to require very high recirculating power and are therefore likely to remain only laboratory experiments.

There are a number of high initial density configurations that may show promise, particularly with respect to compatibility with propellant addition. They are discussed below:
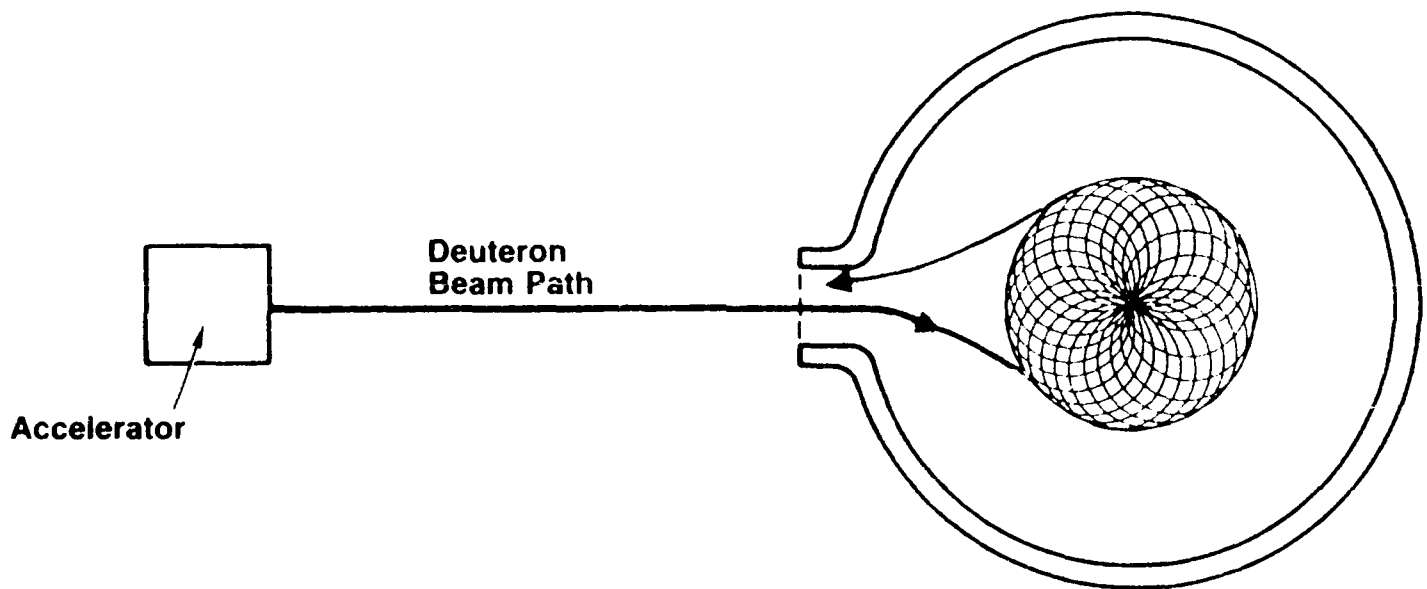
Figure 14. MIGMA monoenergetic colliding beam concept (Ref. 18).

High Density Systems.

The high-density confinement systems are divided into inertial, where the fusion reaction occurs faster than the expansion rate of the fusing fuel, and quasi-steady-state, where means must be available to confine the fuel for a significant period of time.

Fusion by high-velocity impact would require colliding frozen fusion fuel pellets at velocities of 100 km/s and up. Considering that current railguns have difficulty achieving 4-10 km/s with relatively strong projectiles like polycarbonate, it will be difficult to accelerate a slushy substance like hydrogen ice to 10-20 times that velocity. Perhaps a similar but better approach is to collide spheromaks at much higher velocities (like the TCT discussed earlier and in the next section).

Explosive compression also offers some interesting possibilities. Once a cold plasma is established, it could be compressed adiabatically to high temperature using crushable conducting sheils driven by explosives. As long as the shell does not go into low order buckling and maintains spherical shape, this can be an efficient method of compression. As discussed in Appendix C, however, most of the energy during compression goes into magnetic energy with a lesser fraction going to the thermal energy desired.

With explosive compression, the fusion energy released could be deposited into the explosion products and the vaporized conducting shell. It is important that the atomic weight of this mix be low, however, in order to maximize the specific impulse of the rocket. If the shell is lithium and the explosion products are hydrogen-rich, acceptable values of I_s may be achievable.

Inertial confinement fusion (ICF) appears to offer the greatest promise of being able to heat the propellant without quenching the fusion reaction. This is because the fusion burn is over in a matter of nanoseconds, too fast for a hot propellant to expand and interfere. Figure 15 shows an ICF concept called the propellant surround rocket. Here a ball of frozen hydrogen is placed around the target. Radial openings admit the laser driver energy. Fast closures (not shown) close off everything except the nozzle after the laser pulse. Virtually all of the fusion energy is deposited in the hydrogen, which turns to a hot, high pressure gas, fills the chamber, and expands out the nozzle. With D-T, a significant fraction of the neutron energy is also absorbed in the hydrogen rather than wasted, as is likely with other concepts.

High Thermal Diffusivity Chamber

Solid H_2, etc., Sized to Totally Vaporize and Reach 1-2 eV Avg Temp Min $\Delta R \sim 30$ cm for Neutrons

5 m

1 m

0.3 m

M = 4

Rocket Nozzle

Laser Light

Any Driver That Works

Any ICF Target/Fuel That Works
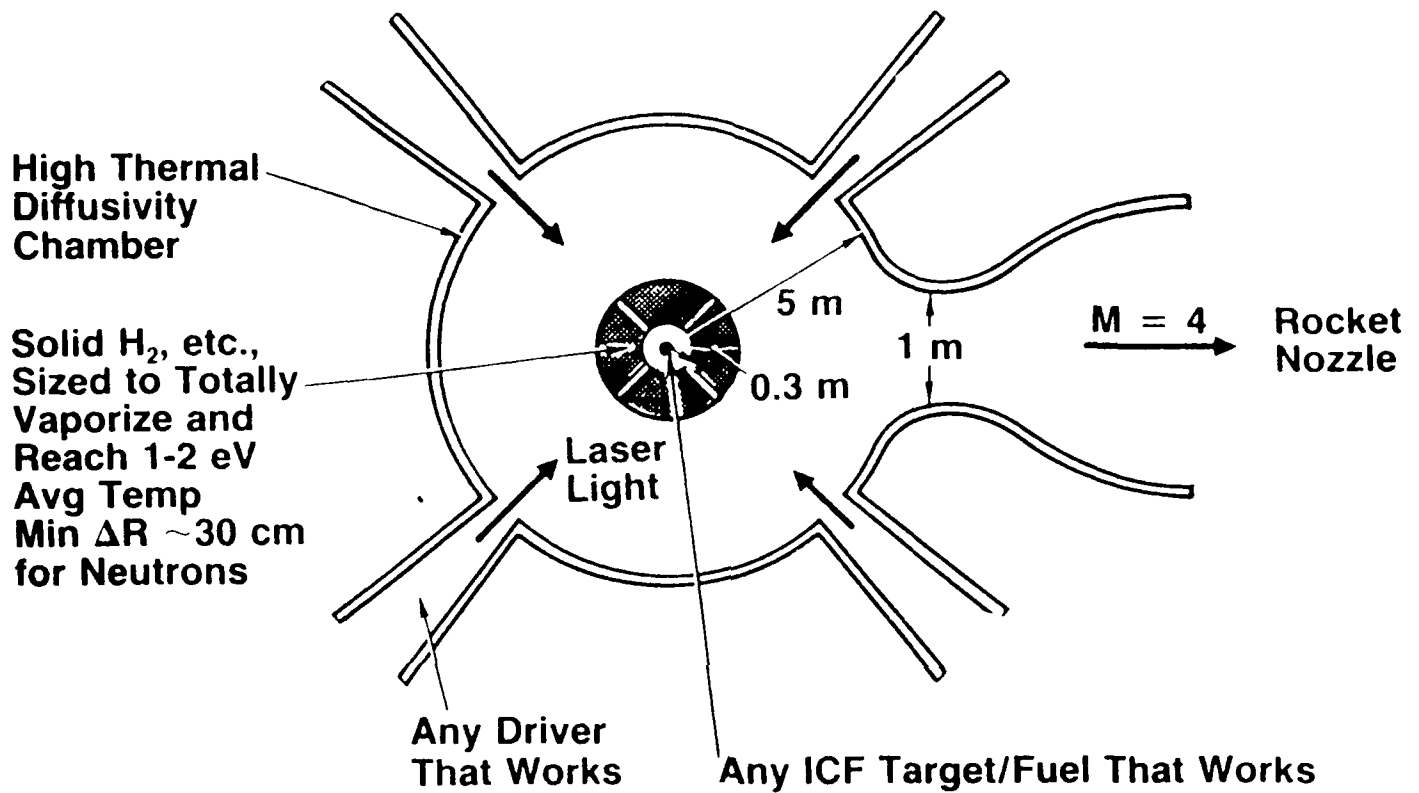
Figure 15. The propellant surround ICF rocket concept.

Calculated results of a typical propellant surround concept are shown in Figures 16 and 17 With this system, it appears that I_s values of up to 2500 s are possible. Major disadvantages are the complexity of having to fabricate frozen hydrogen propellant surrounds, and the pulsed nature of the thrusting.
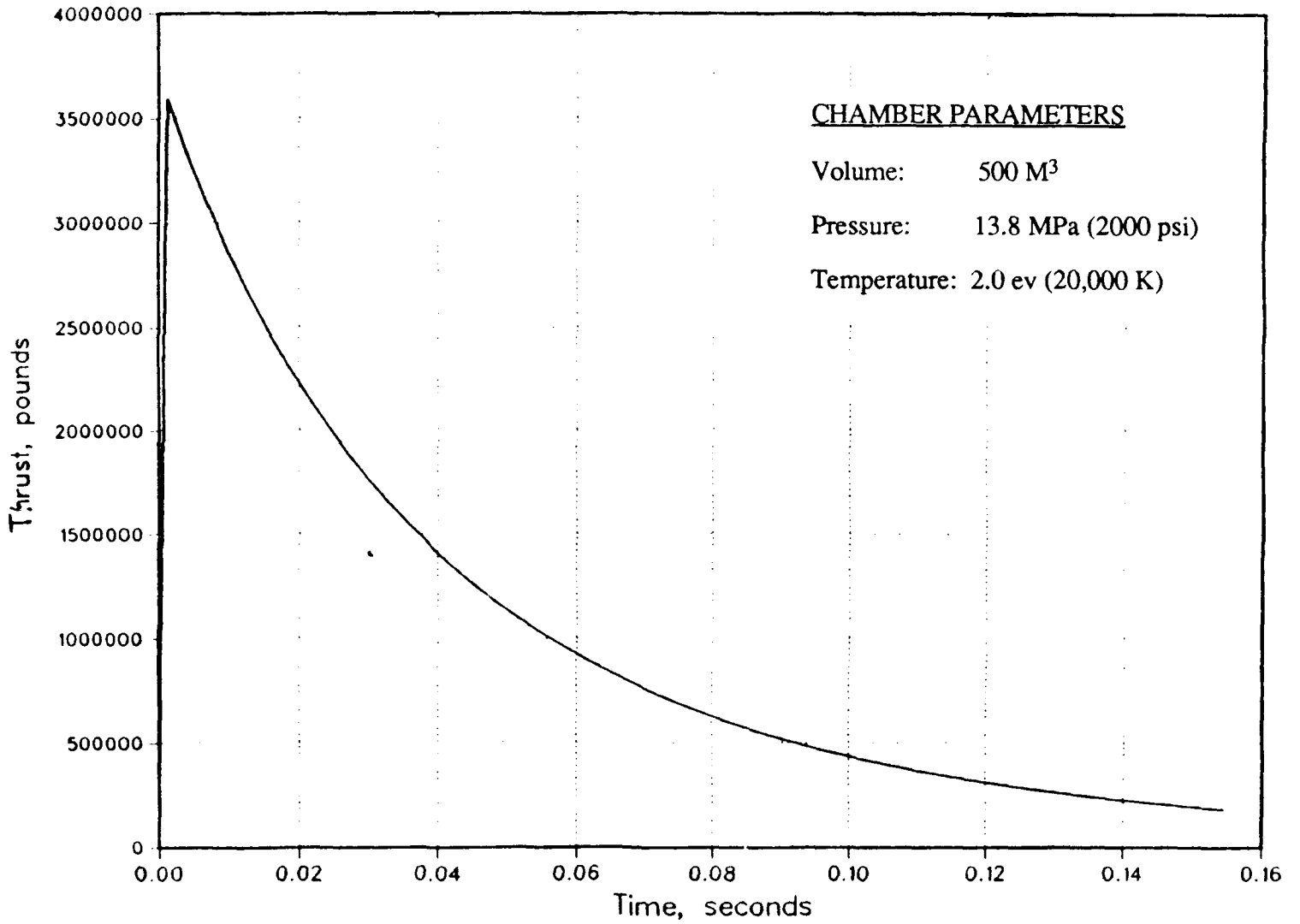
Figure 16.   Thrust vs. time for a propellant surround rocket.
Throat diameter is 1.0 m.
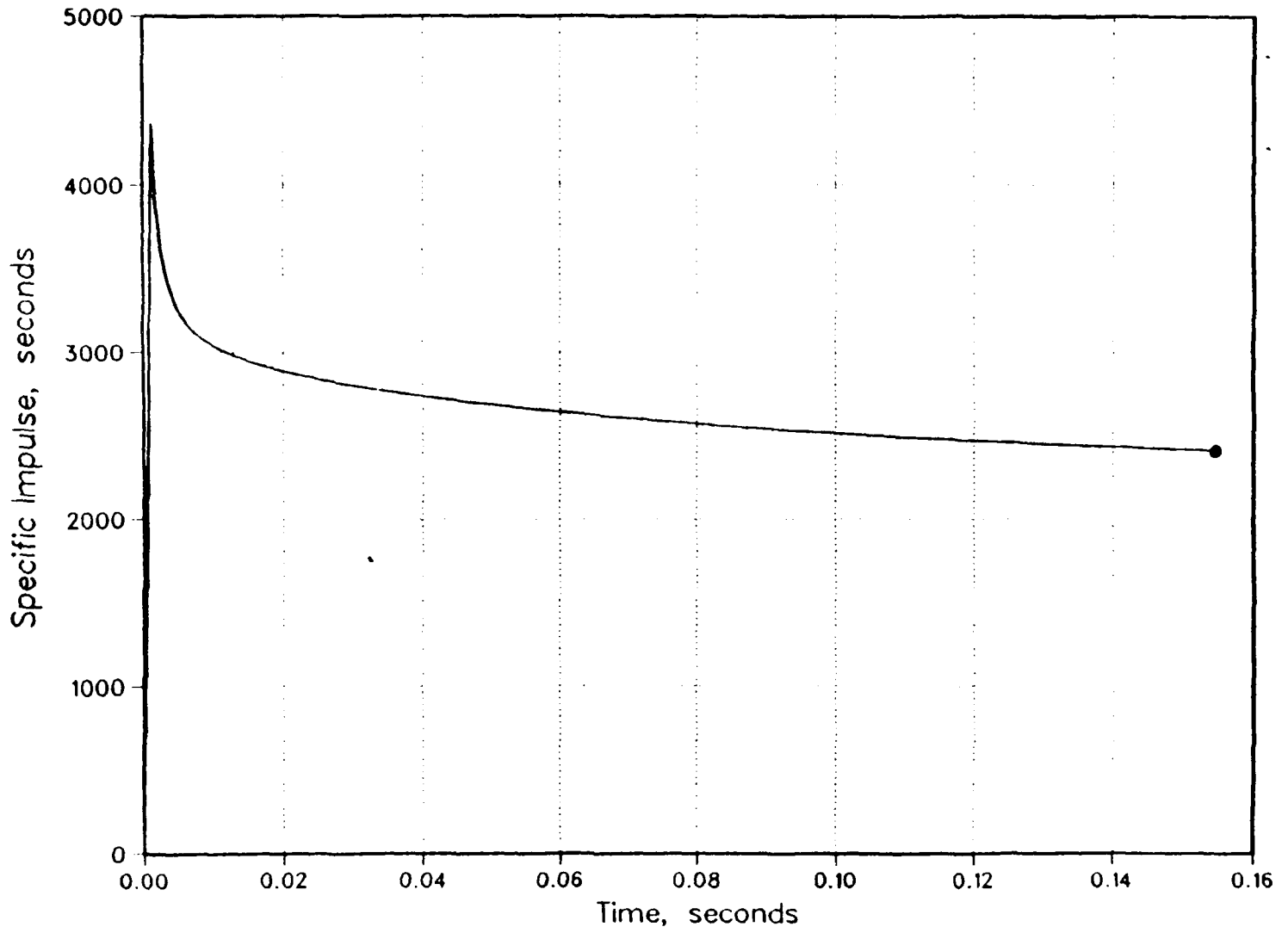
Figure 17. <u>Specific impulse vs. time for the ICF propellant
surround rocket.</u>

54

Another ICF concept is the VISTA[19,] shown in Figure 18. Here the target is exploded external to the spacecraft. The expanding plasma compresses the fields of a superconducting magnet and mass is preferentially directed rearward, providing thrust. The curious conical shape of the spacecraft places the payload in the shadow of the neutron shield (D-T is the fuel) thereby protecting it from direct neutrons (some scattered neutrons will hit the payload, however).

The VISTA spacecraft would be intended for planetary missions. Specific impulse is 17,000 s and total ΔV is 80-120 km/s. Little if any propellant can be added because the resulting gas must be hot enough to ionize so it can deflect magnetic fields.

The ultimate inertial confined concept is ORION[20] where actual fusion bombs are ejected out the back and exploded. Some of the energy released impinges on a pusher plate which, with a series of shock absorbers, drives the spaceship. Figure 19 shows a schematic of Orion. This concept was investigated over 30 years ago and has been well characterized. Specific impulses in the 4000 s range appear possible. The major disadvantage is that a lot of radioactive debris is vented into space. Also, the EMP output from a large (1.0 kt and up) nuclear detonation can damage electronics both on board the space station and a considerable distance away.

There are a few other concepts that are high density but are not inertial in nature.

If electron orbits could be made closer to the nucleus, then incoming nuclei would see a much lower repulsive force until very close. More nuclei could penetrate the coulomb repulsion barrier and fuse. A possible way of doing is by muon-catalysis[21].

Here muons, which are negatively charged, replace the electrons. Being far more massive than electrons, their orbits are closer. However, muon lifetimes are only microseconds, enough for less than 200 fusions to take place. They require GeV energies to be produced in accelerators. The net result is that all of the fusion energy produced and then some goes back to the accelerator to make more muons and no net energy is available. The muon is the only subatomic particle with sufficient mass and lifetime to be considered for "low-temperature" fusion.

The Z-pinch is a high density pinch device that employs a converging stream of plasma with a strong axial electrical current. Adiabatic compression occurs along the direction of flow much like the compressor of a ramjet. Like muon-catalyzed, it is unlikely that this method can produce any net power because recirculating powers are very high.
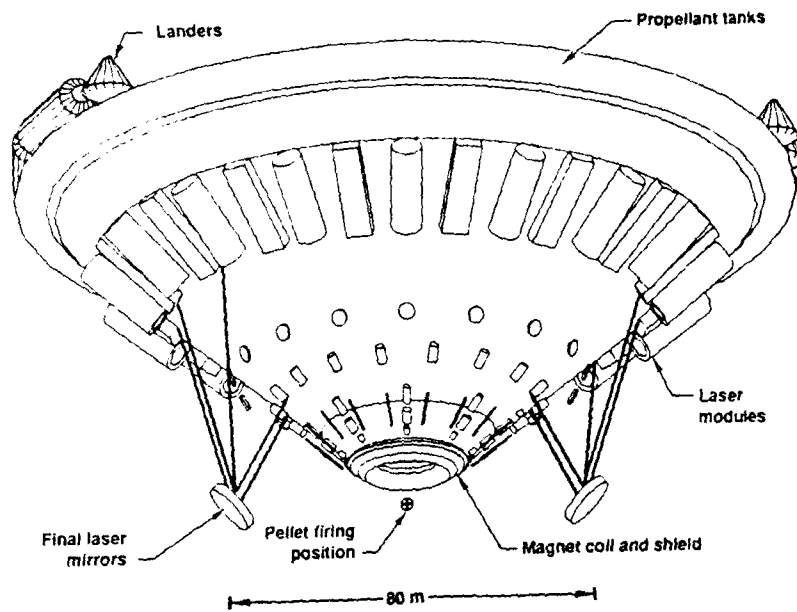
Figure 18. The VISTA ICF spacecraft (Ref. 22).
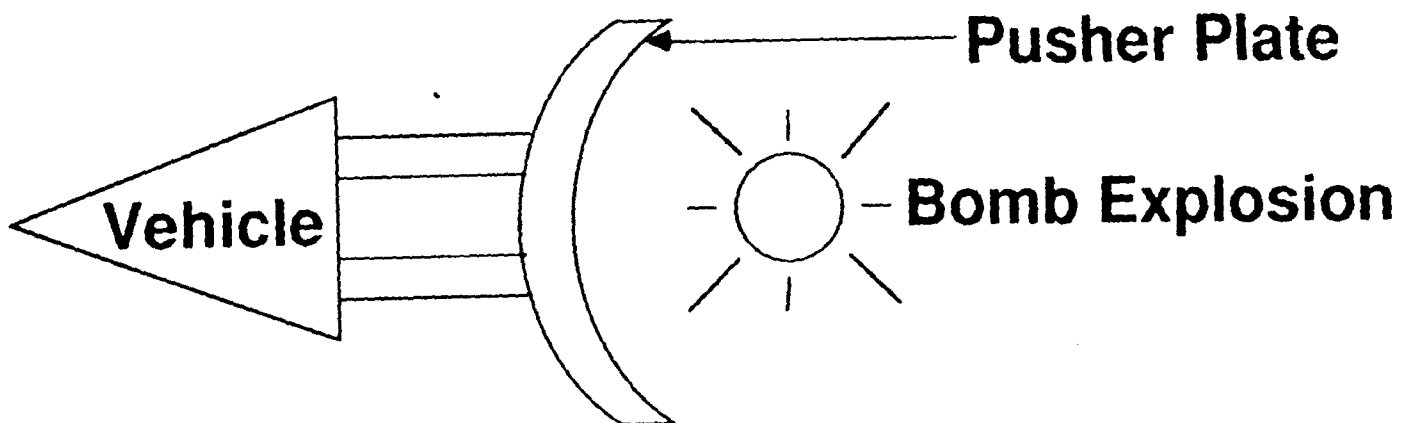
Figure 19. The Orion propulsion concept.

High recirculating powers also plague colliding beam systems. This in fact was one of the first attempts at fusion. However, because fusion cross sections are so small, the beams tend to be scattered to the wall before enough fusions take place.

REACTOR SELECTED FOR FURTHER STUDY

Two reactor concepts held enough potential for Air Force missions to be worth further study: the ICF propellant surround and the translating compact torus (TCT). However, the TCT was ultimately selected for the following reasons:

The ICF concept has the best propellant/plasma coupling. Specific impulse is very high. It is adaptable to all target/fuel/driver combinations that have discrete and small beam lines. In particular, it is amenable to D-T operation because much of the neutron power is usable and the propellant shields the chamber wall. Finally, it makes use of the mainline DOE ICF program. The overriding disadvantage is the pulsed thrusting, with large accelerating forces separated by dwell intervals. While some sort of shock absorber would smooth these forces out, it was deemed such a disadvantage that the edge was given to the TCT.

The TCT has the advantage of high power density and compact envelope. The technology uses the mainline DOE magnetic confinement program. While pulsed, operation should be much smoother than the ICF approach. The power supply and driver requirements for the TCT appear easier to deal with than for ICF. Propellant addition remains a major problem, however, and it is hoped that a solution can be found by clever innovation.

The two modes of TCT operation are adiabatic compression and collision. The results from Appendix C suggest that the later holds more promise. It is therefore the subject of a detailed analysis in the next section.

57

COLLIDING TCT D - ^{3}He SCOPING STUDY

In this section, we explore the TCT as a possible fusion reactor for propulsion. Considerable background information about this concept can be found in Appendix C.

BACKGROUND

Compact tori (ct) are a class of toroidal plasma configurations with internal toroidal currents and no external magnetic fields. The internal currents are distributed in such a way as to provide both toroidal and poloidal confining magnetic fields. Configurations with the poloidal field dominating are called "field-reversed" configurations (FRC's). Those with roughly equal toroidal and poloidal fields are called "spheromaks". Spheromaks may have better confinement than FRC's and are therefore considered here. Because there are no external fields, they are free to translate, a feature that is exploited in the translating compact torus (TCT) concept.

It is shown in Appendix C that the colliding TCT has the advantage over the compression TCT in that the velocity to which it must be accelerated is lower. Also, preheating to minimize compression ratio is unnecessary. The main disadvantages are the uncertainty of successful merging and the greater poloidal circuitry required.

The TCT rocket analysis in this section combines the TCT physics of Appendix C with the rocket analysis given in the next section. Reactors are sized for particular missions. Estimates are made of component and propellant masses, and optimum specific impulses are established for particular missions.

DESCRIPTION OF THE SCOPING CODE

A fast-running FORTRAN code, TCT FOR, was written to perform the parameter runs. This code, about 500 lines long, uses the input shown in Table 19. A full listing of the code is given in Appendix F. Some of the more obscure entries are discussed below.

Specific impulse is treated as a parameter. With this and thrust specified, fusion power is established (an iteration loop allows inclusion of recirculating power).

Fusion repetition rate is also treated as a parameter. The higher the rate, the smaller the components. However, the time available to burn the fusion fuel to the specified burnup is also reduced. This is a minor problem with D-T fuel, but, as will be seen, a major one with D-^{3}He.

There are both resistive and coupling losses in the magnets needed to form the compact tori. Resistive losses are due to ohmic dissipation in the conductor while coupling losses are due to the fact that not all of the magnet energy gets into the plasma. The input EFFMAG accounts for both.

The electrical energy required to run the reactor is assumed to be supplied by a turbine driven by propellant gases bled off the rocket nozzle. This turbine in turn drives a compulsator, (compensated pulsed alternator - like an alternator, but provides pulsed voltage spikes instead of continuous output). Transpiration cooling and thermal barrier coatings are assumed to provide the required thermal tolerance. The efficiency EFFEL is then the turbine adiabatic efficiency (>70%) and not a thermodynamic cycle efficiency (<45%) because the exhaust is not discarded but used as thrust.

TABLE 19

TCT FOR INPUT LIST

NO.	NAME	DESCRIPTION
1	THRUST	ROCKET THRUST, NEWTONS
2	ISP	SPECIFIC IMPULSE, SECONDS
3	RATE	FUSION REP RATE, HZ
4	BURNUP	FUSION BURNUP FRACTION (0 TO 1)
5	EFFMAG	ELEC TO MAGNETIC CONVERSION EFFICIENCY
6	EFFEL	THERMAL TO ELECTRICAL CONVERSION EFF ASSUMES TURBINE IN ROCKET THROAT WITH EXHAUST GOING TO THRUST.
7	KFUEL	FUSION FUEL OPTIONS: 1=D-T, 2=D-3HE
8	BPOL	POLOIDAL FIELD AFTER MERGING, TESLA
9	BETA	POLOIDAL BETA AFTER MERGING
10	KPROFL	PLASMA PROFILE: 1=FLAT, 2=PARABOLIC
11	ASPECT	PLASMA ASPECT RATIO, R/A
12	DELTAV	DESIRED DELTA V, M/SEC
13	PAYLOD	PAYLOAD MASS, KG
14	KPRINT	PRINT OPTION: 1 FOR PRETTY OUTPUT, 2 FOR PLOT TABLES.

Two fuel options are included in the code, D-T and D-^{3}He. For D-T, it is assumed that 9 MeV out of 14.1 MeV are absorbed by the propellant and therefore effectively utilized. Burn temperatures are assumed to be 12 keV for D-T and 55 keV for D-^{3}He. All of the parameter runs discussed later used D-^{3}He.

The poloidal field after merging, BPOL, combined with the poloidal beta, BETA, the required fusion power (determined internally), the repetition rate, and the plasma profile factor, KPROFL, establish the plasma size and density, and the plasma current. Magnitudes of poloidal field and beta are limited and therefore it is best to specify them explicitly.

The compact torus will tend toward a low aspect ratio. It is generally specified in the code at around 1.2.

The last two relevant inputs in the table are space mission related. DELTAV is the mission velocity increment, a cumulative value if appropriate. The payload mass was fixed in all cases at 36000 kg.

The code first establishes the total required fusion power using a rough estimate of recirculating power. This is iterated upon with actual calculated values. Plasma dimensions and density are established next. Power density, burn time to the specified burnup, and power and energy flux through the plasma last surface are then determined. This is followed by calculations of plasma current, Ohmic heating, and total magnetic and thermal energies. This in turn provides the basis for calculating recirculating power.

An estimate is made of the required total energy confinement time, including radiation, needed to maintain a steady burn at the specified temperature. If the actual value is less, the burn would extinguish. If greater, a thermal excursion would occur, greatly reducing the time needed to consume the fuel. Since it is uncertain (in fact unlikely) that the plasma will remain intact for the time needed to consume the D-^{3}He fuel at steady temperature, any boost in reactivity will help.

The above confinement time estimate is compared with two scaling laws normally used for tokamaks: neoclassical and Goldston. Goldston scaling[23] is the most representative and is given by

$$\tau = 0.052 \frac{I_p R^{1.75}}{\sqrt{P_f} a^{0.37}}$$

where I_p is the plasma current in MA, R is the major radius in meters, P_f is the fusion charged particle power in MW and a is the plasma radius in meters. Note that Goldston scaling is fairly accurate for tokamaks. Experimental evidence is showing, however, that confinement in CTs is worse[24]. The problem is that no experiments have been conducted so far to permit the establishment of a scaling law that can be extrapolated to fusion temperatures. One would expect, however, greater improvement in confinement is more dependent on plasma current while in tokamaks confinement also depends on applied external fields. The scale-up of CT confinement to the reactor level might therefore approach tokamaks.

The code then calculates the pre-merging plasma conditions. In general, pre-merging plasma dimensions are double and plasma current is half the post-merging values. Pre-merging poloidal field is therefore 1/4 the post-merging value. The pre-merging beta is taken at an arbitrary plasma temperature of 1.0 keV. A full time-dependent analysis would be necessary to establish actual temperatures.

The code then calculates the translational velocity needed to provide the kinetic energy which, once thermalized after merging, will give the desired plasma burn temperature. While one could in principle provide only enough energy to reach ignition temperature, in fact confinement is so poor that any ignition will be at close to burn temperature. The velocity required is

$$v = \left[\frac{3kT}{m} \right]^{1/2}$$

where k is Boltzmann's constant, T is the desired temperature after thermalization, and m is the ion mass.

In order to keep the plasma intact during acceleration, the force is kept to 1/20 times the body force holding it together. That force is conservatively taken to be the pre-merging magnetic energy divided by the plasma diameter.

The code also calculates the coaxial current and field required for acceleration. The inductance per unit length is

$$I = \frac{\mu_o}{2\pi} \ln \frac{R+a}{R-a}$$

and so for an accelerating force F.

$$I_{coax} = \left[\frac{2F}{I}\right]^{1/2}$$

and the maximum magnetic field, which occurs at the central conductor, is

$$B_{max} = \frac{\mu_o I_{coax}}{2\pi (R-a)}$$

where μ_o is the magnetic permeability constant (1.26×10^{-6} H/m).

Reactor system weight estimates are made once these calculations are completed. These are based on specific weights culled from a variety of sources and are given in Table 20. Note that the 9.2 kJ/kg for capacitor banks is well above the current value of 0.2. This optimistic prediction assumes advanced development with emphasis on low weight and bulk rather than low cost, high reliability and environmental hardness. A contingency of 100% is used to account for the many components not included in this scoping study.

TABLE 20
SPECIFIC WEIGHTS FOR REACTOR COMPONENTS

Item	Assumed	Source	Current
Capacitors	9.2 kJ/kg	DNA[25]	0.2
Compulsators	10 kJ/kg	GA[26]	10
Magnets	50 kJ/kg	GA[26]	50

Chamber material density - 2 gm/cc
Contingency - 100% of total weight

Finally, the code calculates rocket performance using calculated weights and specified input. To account for propellant tank structure, the specific impulse (an input) is discounted 5%. Calculated are the initial spacecraft mass, the rocket burn time, the minimum acceleration, the propellant mass, and the fusion fuel mass. The ratio of the last two masses is then calculated. This is important because, if it is very large, it would be easy for a small quantity of propellant to quench the fusion reaction. More extensive and detailed calculations of system performance and mass breakdown by component are found in a later section.

DETAILED RESULTS FROM A TYPICAL CODE RUN

In this section, we discuss a single point design from a code run. The purpose is to provide a better understanding of the parametric runs discussed in the following section. Table 21 summarizes some of the parameters and assumptions used in the code runs.

The input variables are shown in Table 22. This example is for a low-earth orbit (LEO) to geosynchronous earth orbit (GEO) transfer vehicle. The ΔV of 9000 m/s is for a round trip.

Iterated output for this sample run is shown in Tables 23 through 25. Some of the entries are discussed below.

The fusion power level for this example is in the range of that expected for terrestrial applications. As discussed in the next section, however, this power can reach extraordinary values at higher thrusts and specific impulses.

The compressed plasma is very small, R = 8.2 cm, and plasma current, 20.45 MA, very high. This is the result of having the input poloidal field after merging being 60 Tesla.

TABLE 21

ASSUMPTIONS AND FIXED PARAMETERS USED IN THE CODE

Flat plasma profiles

T_{burn} = 12 keV for D-T, 55 keV for D-^{3}He

E_{fusion} = 12.5 MeV for D-T, 18.35 MeV for D-^{3}He

Pre-merging Size = 0.5 post-merging Size

F_{accel} = 0.1 Fbody

Capacitors provide accelerator energy

Magnets provide magnetic energy

Compulsator provides total energy and is driven

by a turbine adjacent to the rocket nozzle

Propellant chamber sized for 4000 psi gas (σ_{hoop} = 50 ksi)

Propellant tank mass accounted for by decreasing Is by 5%

TABLE 22

INPUT VARIABLES FOR SAMPLE D-^{3}He

COLLIDING TORUS FUSION THRUSTER

1	Thrust, N	100,000
2	Specific Impulse, s	1500.
3	Repetition Rate, Hz	4.00
4	Fuel Burnup Fraction	0.500
5	Electrical to Magnetic Efficiency	0.600
6	Thermal to Electrical Efficiency	0.600
7	Fuel Option 1=D-T, 2=D-^{3}He	2
8	Poloidal Field After Merging, Tesla	60.0
9	Poloidal Beta After Merging	0.800
10	Plasma Profile Factor	1
11	Plasma Aspect Ratio, R/A	1.200
12	Desired Delta V, m/s	9000.
13	Payload Mass, kg	36000.

This does not have to be initially supplied, however. As seen in the bottom entries in Table 24 only 15 Tesla needs to be supplied, which may be feasible. Considerable ohmic heating will initially result from these high currents, a benefit that has not been included. It is through ohmic heating that magnetic energy can be converted to thermal. The extent of the ohmic heating once the burn temperature is reached is small, however, as seen by the long L/R resistive decay time of 14.15 seconds.

TABLE 23

ITERATED OUTPUT FOR SAMPLE CODE RUN

Thrust Power, MW	735.
Total Fusion Power, MW	913.
Major Radius, m	0.082
Plasma Radius, m	0.068
Plasma Current, MA	20.45
Fusion Burn Time, s	0.1219
Burn Time/Max Burn	0.487
Plasma L/R Time During Burn, s	14.153
Energy Flux to Wall/Propellant, MJ/m^2	1037.0
Magnetic Energy to Plasma, MJ	11.0
Thermal Energy to Plasma, MJ	4.1
Total Recirc Thermal Energy, MJ	44.2
Total Fusion Energy, MJ	228.3
Recirc Thermal Power Fraction	0.195
Electrical Recirculating Power, MW(e)	107.

TABLE 24

OUTPUT, CONTINUED

Ave. Ion Density, m^{-3}	1.30E+23
Assumed Burn Temp, eV	55000.
Reqd Total Energy Conf Time for SS, s	0.00438
No. Confinement Times in Burn	27.8
Ratio of Goldston Confinement Time to Reqd	0.27
Ratio of Propellant to Fusion Fuel Mass	1.31E+06
Pre-Merging Major Radius, m	0.164
Pre-Merging Plasma Current, MA	10.22
Pre-Merging Ion Density, m^{-3}	8.13E+21
Pre-Merging Poloidal Field, Tesla	15.0
Pre-Merging Beta at 1.0 keV	0.029

65

TABLE 25

OUTPUT, CONCLUDED

CT Injection Velocity, km/s	2515.3
Acceleration Length, meters	2.237
Acceleration Time, μs	1.78
Acceleration Current, Amp	1.96E+06
Max Accelerator Field, Tesla	28.7
Reaction Chamber Diameter, m	2.5
Estimated Total Mass, kg	15,700
Capacitor Banks, kg	892
Compulsator, kg	2650
Magnet Coils, kg	367
Reaction Chamber, kg	3960
Miscellaneous Mass, kg	7870
Min Acceleration, g	0.104
Initial Mass, kg	98,600
Rocket Burn Time, min	109.
Reactor Mass Power Density, kg/kW(th)	0.017
Mass Utilization Factor, kW(th)/tonne	58,000

The D-^{3}He fusion burn time of 0.12 seconds is very long (D-T burns are 1/10 as long) and there is the question of whether the plasma can stay together that long. Also, with a rep rate of 4 Hz (0.25 sec between pulses), the burn time is approaching 50% of the maximum available time. It will be shown later that this fusion burn limit places an upper limit on repetition rate. Clearly, high repetition rate is otherwise desirable because it reduces the size and weight of all the reactor components.

A surprising result is that recirculating powers are quite reasonable, about 20%. This value seemed to be independent of the type of fusion fuel (fusion fuel mainly affected burn time).

The average ion density of $1\cdot3 \times 10^{23}$ m^{-3} is 1000 times greater than in a tokamak. That is why power density is so high. In order to at least maintain steady state, an energy confinement time of 4.38 ms is needed. This is determined simply by dividing the thermal plasma energy by the fusion power deposited in the plasma. This time, divided by an optimistic Goldston energy confinement time established for tokamaks, gives 0.27 which, being less than 1.0, means that this reactor must have confinement 1/0.27 times better than tokamaks. This is unlikely. While tokamaks have problems of their own, they so far provide the best energy confinement.

66

There are 27.8 energy confinement times during the course of the burn. This also means that the total fusion energy produced is 27.8 times the instantaneous plasma thermal energy. Therefore, 27.8-1 = 26.8 times the plasma thermal energy must go to the propellant while the burn proceeds. And the propellant cannot do anything, like expand, to quench the burn during this time. This is a major challenge, particularly because the propellant mass is 1,310,000 times greater than the fusion fuel in the plasma Material walls can provide the separation, but at a great cost in specific impulse because of the reduced propellant temperature.

The CT injection velocity of 2500 km/s is not much above what has already been achieved with good efficiency. Because of the high plasma current, the CT is quite robust and therefore can withstand a very high acceleration force. The length of the accelerator of 2.2 m (two of them facing each other) is trivial. The acceleration time of 1.78 ms indicates that only capacitors can be used as the energy supply. Of course, these are minimum values and both acceleration length and times can be increased to ease hardware requirements.

The reaction chamber is sized to hold the entire propellant at 27.6 MPa (4000 psi). It is assumed to be some superstrong woven carbon composite.

The total reactor system mass is 15.7 tonnes, which includes a factor of two for contingency. The mass is dominated by the compulsator long-term (millisecond) energy storage and the reaction chamber. The capacitors contribute little, but the DNA estimate of 9.2 kJ/kg for future capacitors could be very optimistic. Nevertheless, a factor of 2-3 increase in capacitor mass will have only a minor effect. The mass power density is 0.017 kg/kW(th), a very low value and comparable to fission rockets. The fusion community tends to use the inverse, called the mass utilization factor. Here it is 58,000 kW(th)/tonne, over 60 times better than a high power density RFP D-T reactor. Actual achievement of this mass will be quite challenging.

PARAMETRIC ANALYSIS RESULTS

The first set of parameter runs were made with a 4 Hz fusion rep rate and I_s was swept from 500 (the range for chemical rockets) to 4000 s (an upper limit for most Air Force missions). The LEO to GEO round trip mission was selected (see Table 22). As seen in a later section, each mission has an optimum specific impulse where total vehicle mass is minimized. Figure 20 shows total spacecraft mass as a function of I_s. A broad optimum in specific impulse occurs at 2000-2500 s. Note that the reactor mass remains a small fraction of the total until Is exceeds about 2500 s. This is an artifact of the estimates of specific masses, particularly the capacitors. The

67

masses of the capacitors, magnets and compulsator are called out in the figure. If the capacitors turn out to be heavier, the optimum specific impulse will drop due to the higher reactor system mass. As seen in a earlier section, radiation losses make it difficult to achieve I_s values over 2000 s. Because of this and with the broad optimum, we choose I_s = 1500 s for the rep rate parameter runs discussed later on.

The total fusion power is shown in Figure 21. It gets quite high at high I_s. At the chosen optimum of 1500 s, the power is about 1000 MW(th), about the same as a small terrestrial powerplant.
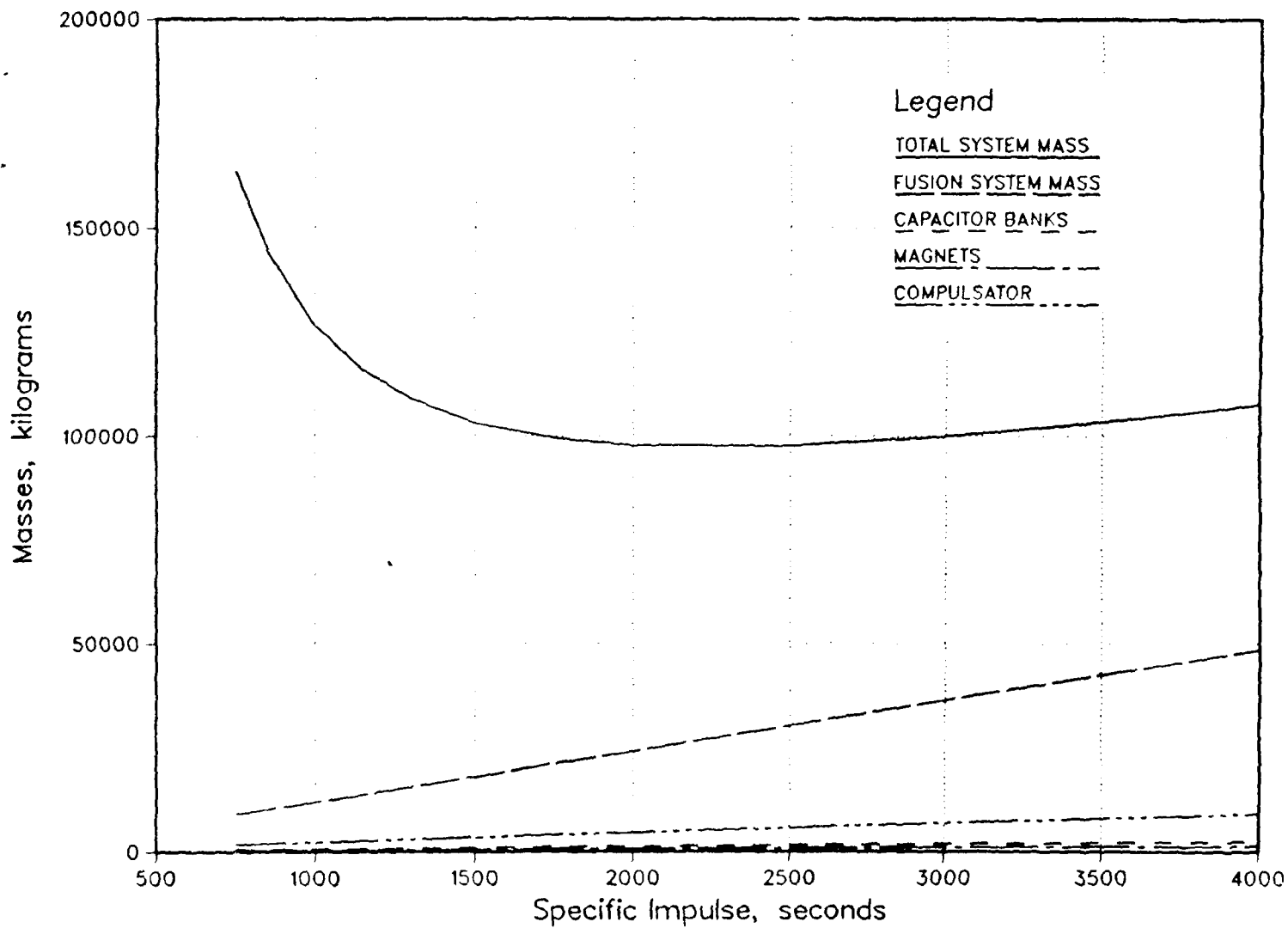
Figure 20. Total spacecraft mass for a LEO-GEO round trip.
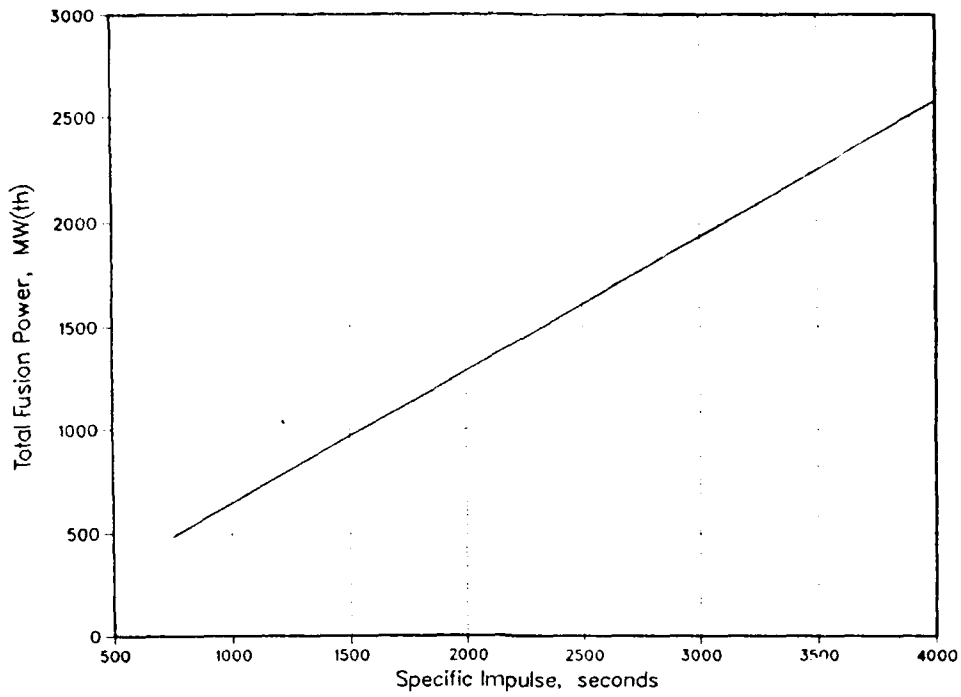
Figure 21. Total reactor fusion power for LEO-GEO m...on.

One of the biggest issues for the TCT reactor is energy confinement, particularly with D-^{3}He fuel. Figure 22 shows the required energy confinement time for steady state burn, which is a minimum condition, divided into projected confinement time based on Goldston tokamak scaling.
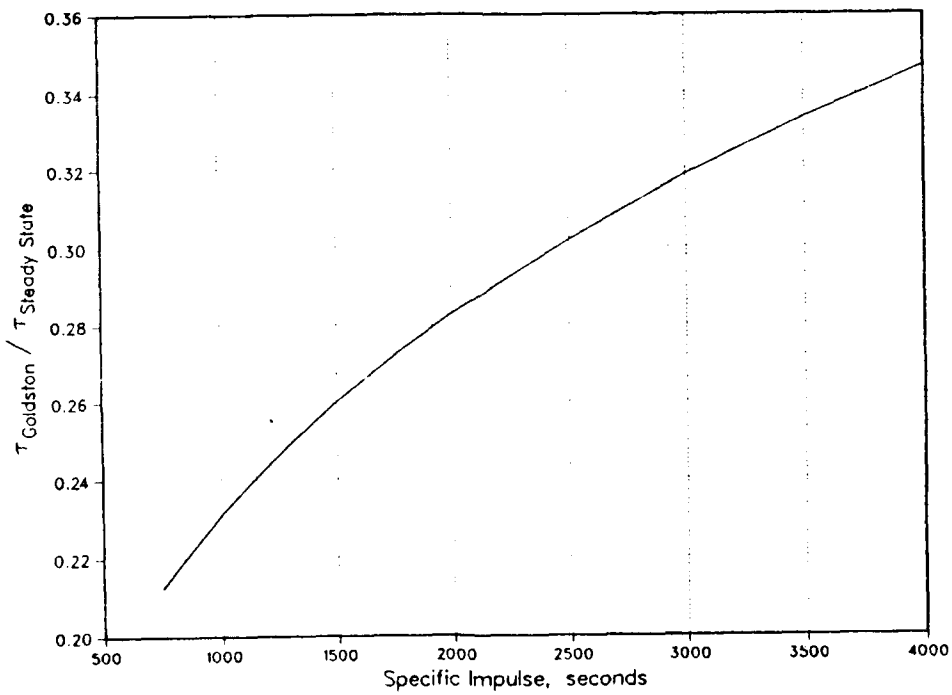
Figure 22. Required confinement time relative to Goldston scaling.

70

A confinement time less than this could not sustain the burn. The fact that it is in the range of 0.25 to 0.33 means that confinement must be 3 to 4 times better than tokamaks, which is rather difficult for compact tori. This remains a major concern in using D-^{3}He in compact tori. When D-T is used, the ratio is just about 1.0, indicating that compact tori will work if their confinement is as good as tokamaks. Again, because CT confinement is expected to be less, this is a matter of concern.

The major radius of the plasma is shown in Figure 23 for a fixed repetition rate of 4 Hz. Note that the radii are very small and possess very large power densities and plasma currents. Because the aspect ratio is so low, 1.2, the plasma minor radii are not much smaller.
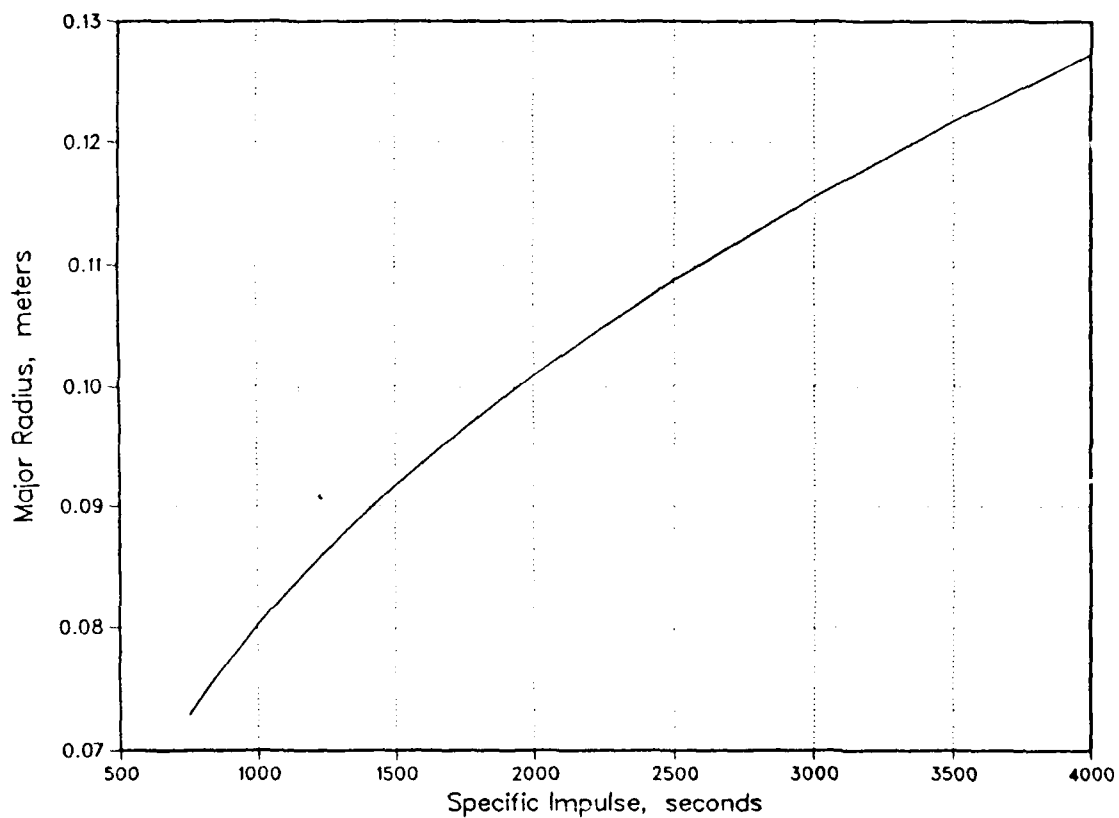
Figure 23. Plasma major radius for 4 Hz rep rate.

71

A major feasibility issue is propellant addition. In order to tailor specific impulse to the mission, much more mass must be expended than is available in the fusion products. Figure 24 shows the magnitudes of propellant addition required. For a given thrust, propellant mass goes inversely with specific impulse and reaches magnitudes millions of times greater than the fusion fuel. Even if a trivial fraction of propellant got in to the plasma, it would displace most of the fusion fuel, quenching the burn.
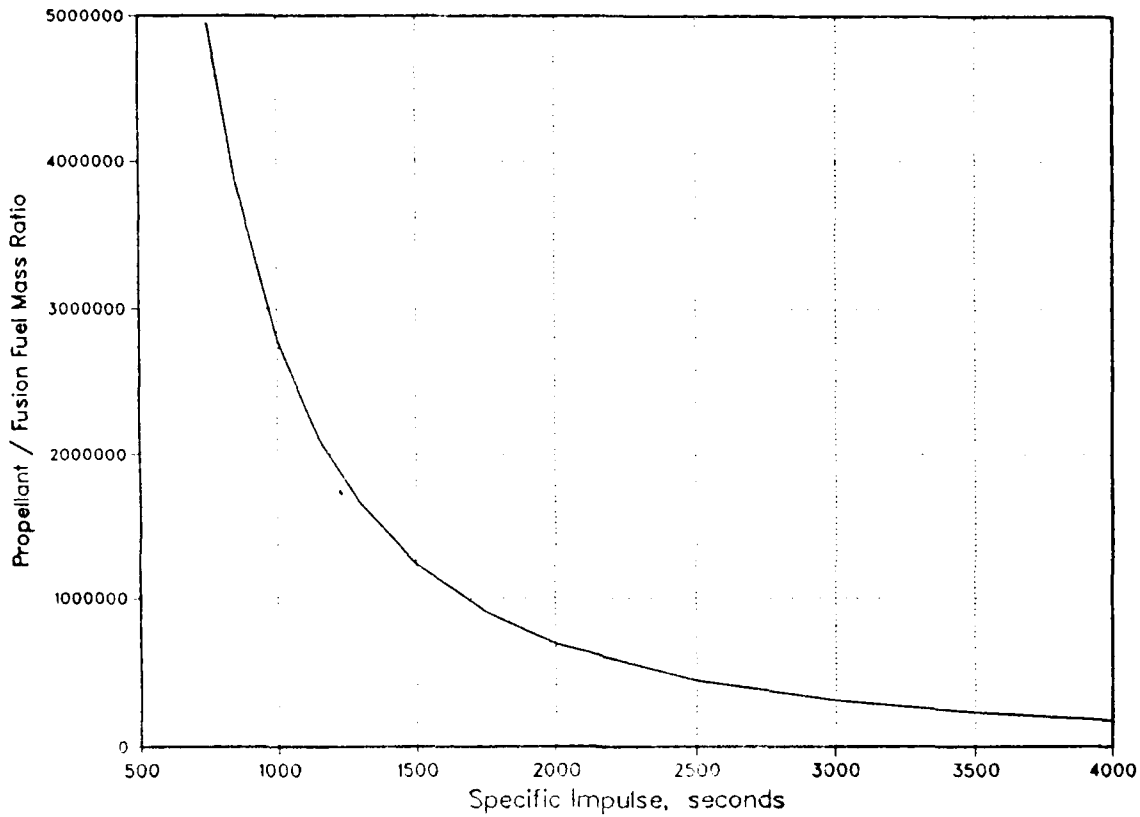
Figure 24. Propellant addition required to achieve specified I_s.

The above scoping was done at a fixed 4 Hz repetition rate. Below we fix the specific impulse at 1500 s and vary the repetition rate from 0.25 to 10 Hz.

Approximate total spacecraft and fusion system masses are shown in Figure 25. It is to be noted that low repetition rates produce very high masses. This is due mainly to the increased weight of the fusion system. The remaining increase is due to the larger propellant mass needed to accomplish the mission. Incentives exist to increase repetition rate to 3-4 Hz, beyond which there is a diminishing return because by then the fusion system mass has become unimportant.
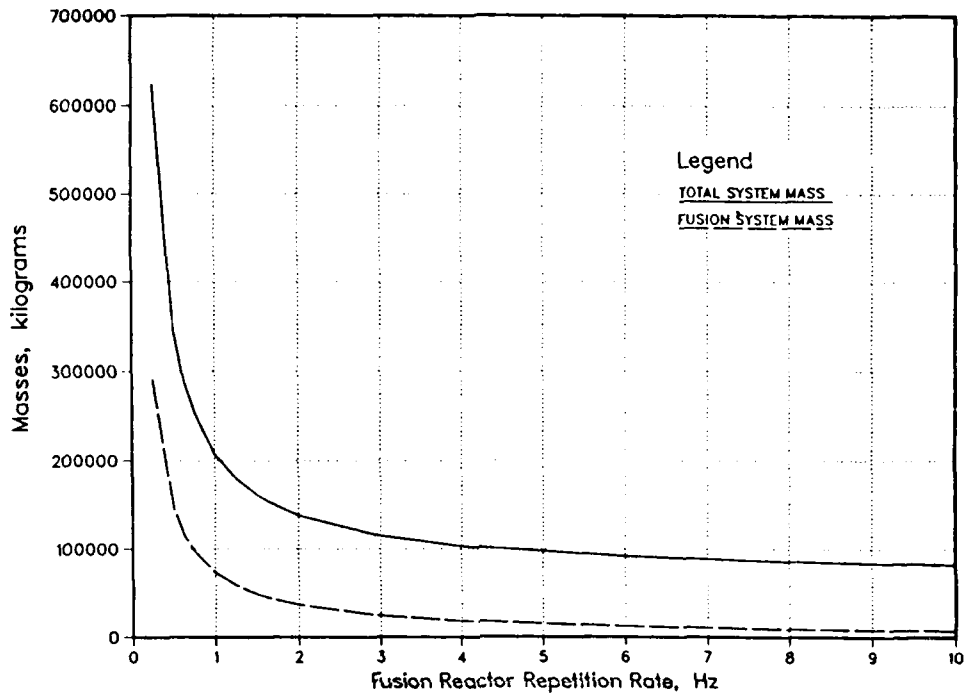
Figure 25. Total and fusion system masses for $I_s = 1500$ s,
$\Delta V = 9$ km/s, 100 kN thrust, and 36,000 kg payload.

73

With decreasing repetition rate, the fusion energy per pulse must increase to maintain the same average fusion power. Plasma size therefore increases, and this is shown in Figures 26 and 27. At 0.25 Hz, major radius is a substantial 47 cm and plasma current is 58 MA. Note that $I \approx R$ in all cases. The plasma radii are reduced by half due to merging while plasma current doubles. This is from the requirement of conversion of magnetic energy and assumes geometrically similar plasmas before and after merging. If this is so, then the plasma inductance, which is proportional to radius, must drop by half after merging.
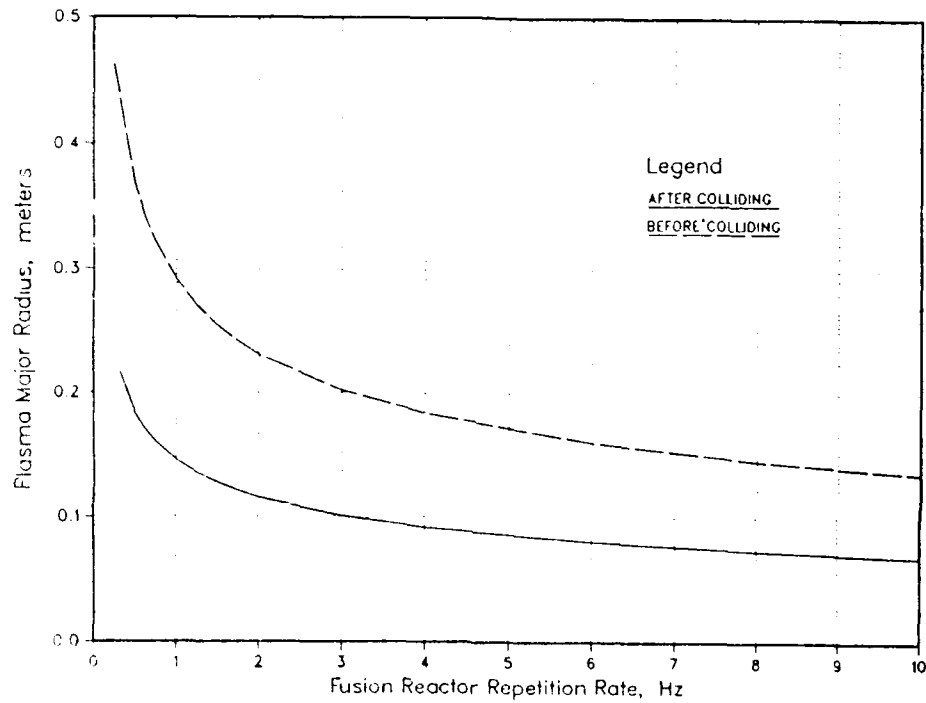
Figure 26. **Plasma radii before and after merging.**
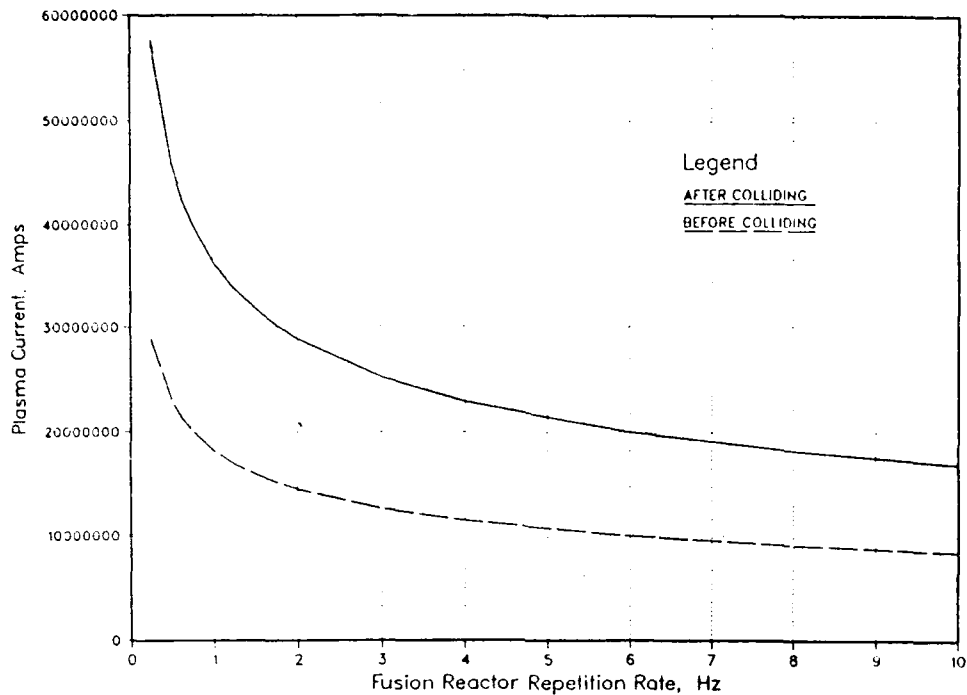
Figure 27. Plasma currents before and after merging.

While low repetition rate increases mass, it also increases the likelihood of success. Confinement is greater in larger plasmas. However, the required energy confinement time for steady state burn doesn't change. This is because, as the rate decreases, both the plasma thermal energy and the fusion power increase at the same rate. It is the ratio of the two that gives the steady state energy confinement time. Figure 28 shows the ratio of Goldston tokamak confinement time to the required steady state value. The greater the ratio the better. At about 1/3 Hz, for example, CT confinement could be half that of Goldston and still burn. The ratio falls below 1.0 at about 0.75 Hz, which bodes ill for higher repetition rates.

75
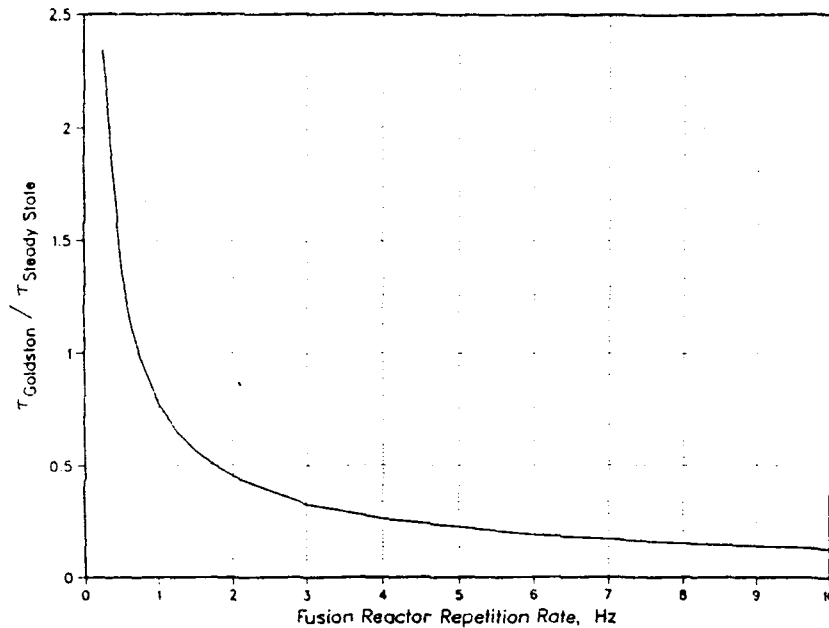
Figure 28. <u>Ratio of Goldston tokamak energy confinement time</u>
<u>to CT confinement time needed for fusion burn at</u>
<u>steady temperature.</u>

There is another upper limit to repetition rate and that is the amount of time available to burn the fusion fuel. As the rate increases, this time decreases. And, although fusion power density increases as well, it is not fast enough. Figure 29 illustrates this point. Above a repetition rate of about 6 Hz, there is not enough time available to burn the fuel to the specified burnup fraction (50% in this case). When allowance is made for the time needed to refresh the chamber after each pulse, the maximum rate will probably drop to 4-5 Hz.
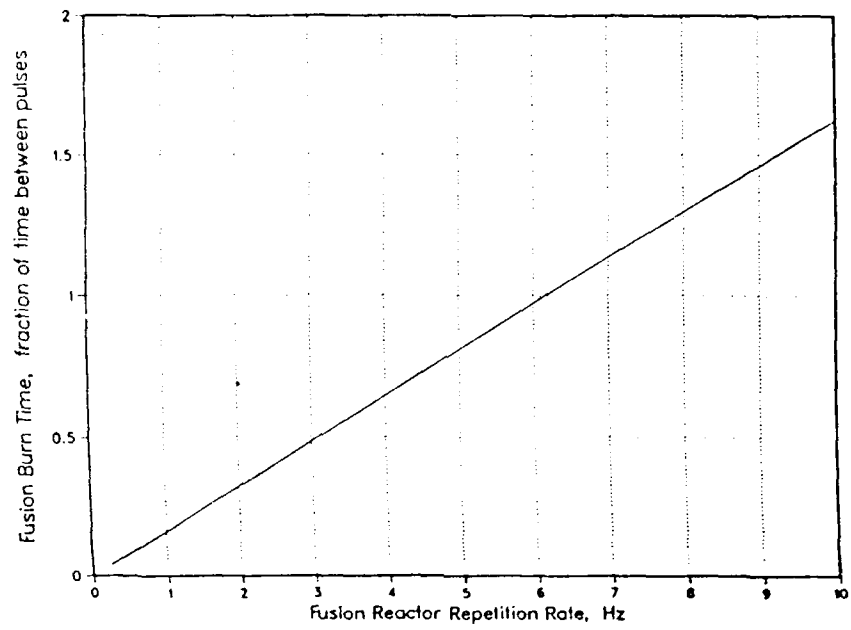
Figure 29. <u>Ratio of fusion burn time to allowable time.</u>

PHYSICAL CONFIGURATIONS

Figures 30 and 31 show two possible configurations for TCT rockets. Both have coaxial accelerators that are angled slightly away from colinear. This allows a small perpendicular velocity component to remain after collision for translation into the propellant addition region. As long as the translational velocity exceeds 15 km/s, the terminal expansion velocity of hydrogen propellant at 2 eV, quenching of the plasma should not occur. The propellant backflows to fill the accelerator chambers, eliminating the need for fast valves. While this reduces pressure, it merely increases the total thrusting time and has no effect on impulse. After each pulse, the entire chamber is automatically pumped by the space environment.

The compulsator provides the energy for both the capacitors for acceleration and the magnets for startup. It is driven off the rocket exhaust gases. This will require very high temperature materials, transpiration cooling, and thermal barrier coatings. It is by far the most efficient way to extract power because the heat "rejected" also produces the thrust. An alternate scheme is to provide a side stream of propellant for a power turbine and dump the exhaust back into the nozzle.

The circular track configuration shown in Figure 31 allows the plasma to travel around a continuous loop until the burn goes out. After collision, the plasma moves into a spiral chute that directs it into a circular track which it can orbit as long as necessary. The intense heat flux blows off propellant wicked through a transpiration cooled wall. The propellant immediately vents to space at terminal velocity without passing through a nozzle. This external configuration has the advantage similar to Orion discussed earlier in that high pressure chambers are not needed and higher specific impulses may be possible.

78
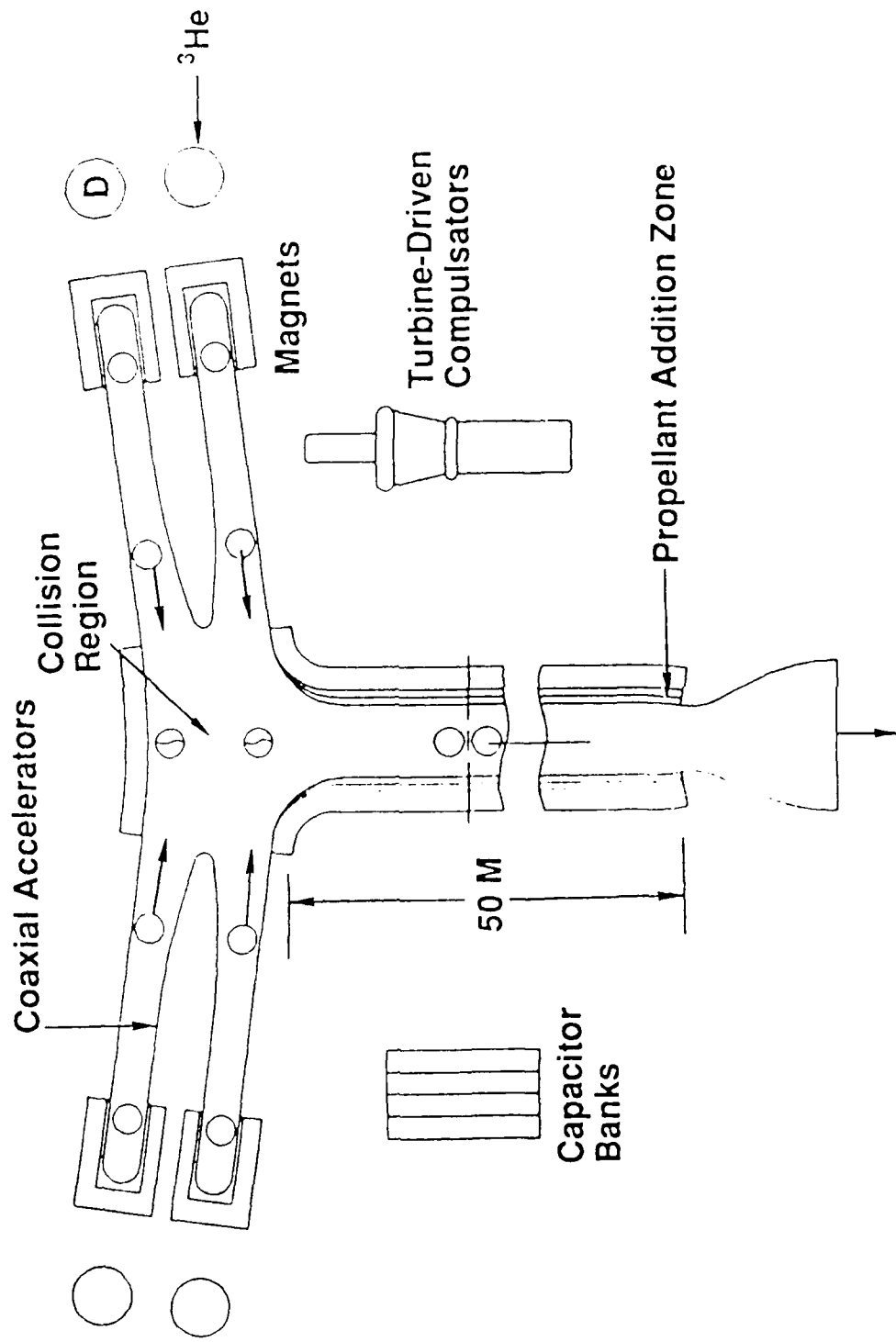
Figure 30. TCT rocket configuration with internal propellant addition.

Figure 31. TCT with external propellant addition.

U_e , Thrust

Plasmold
Initiator/Accelerator
(Both Sides)

Plasmold
Collision
Region

Spiral Feed Chute
to Circular Track

U_e , Thrust

Plasmold Spins Around
Circular Track

Propellant
Addition
Wick
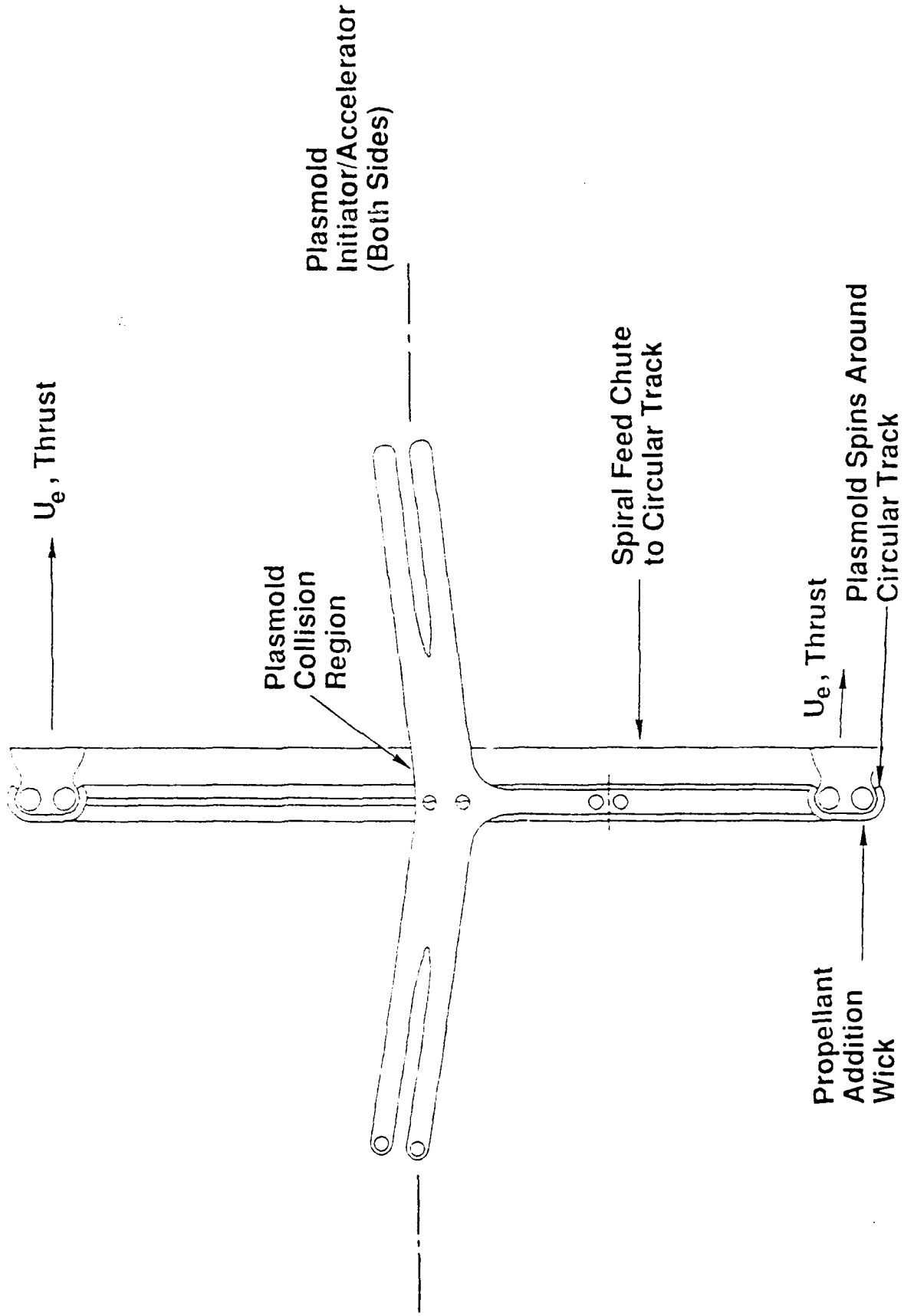
SUMMARY

The colliding translating compact torus may be capable of compact size, light weight, and high power density, thereby making it an interesting candidate for space propulsion. Thrust rate can be varied by varying the repetition rate, giving it the same advantage as ICF without the complex drivers.

The hardware requirements are not extraordinary. A compulsator is required for energy storage with pulsed output. Capacitor banks are needed to provide the acceleration energy. Copper magnets are needed for initial CT startup. And some sort of propellant chamber and rocket nozzle are also needed.

Key issues are the very high plasma current densities, which may be difficult to initiate, the questionable energy confinement (particularly with D-^{3}He fuel), the plasma integrity during the fusion burn (again, this is more serious with D-^{3}He), and the means of getting the fusion energy to the propellant without having the propellant gas quench the plasma.

SYSTEMS ANALYSES

The topic of systems and mission analysis formed the main thrust of the study where the fusion fuel cycle and fusion reactor concepts are applied and integrated into a usable vehicle system. This task is therefore accomplished by defining and analyzing the various subsystems and components as well as the requirements and their integration into a complete system. In the process the system design and trade studies are identified, the criteria and algorithms are formulated and the system optimization studies are conducted.

SYSTEM DEFINITION AND REQUIREMENTS

The vehicle system is composed of a set of major subsystems and components whose description, purpose (role) and requirements are as follows:

Propulsion Subsystem

The propulsion subsystem is the source of all energy, power and force (thrust) required for the operation and motion of the vehicle, the delivery of the payload and the return of the cargo vehicle for subsequent reuse.

In the case of fusion propulsion the system is composed of the following parts and components:

(a) Fusion Reactor: This is the basic plasma generation/formation source which is used to heat the propellants required for thrust and power generation. The present study has selected the translating compact toroid (TCT) with colliding beams as the reactor of choice; the fuel cycle of choice is D-^{3}He. Descriptions of these items are given in the previous section.

(b) Thruster Unit: This unit is composed of the propellant injection and mixing chamber and the expansion deLaval nozzle. An integral part of this unit is the attendant power drive equipment, such as turbines, energy storage such as advanced batteries, compulsators, or flywheels, and electric generation which, in turn, power the capacitors, the magnets and the propellant pumps. The turbines are driven by hot (warm) gas which is extracted from a heat exchanger powered by the regeneratively cooled thrust chamber jacket. The whole system power and energy balance is somewhat similar to the classical liquid rocket

82

bootstrap method with the turbine exhaust gas either manifolded into the rocket expansion nozzle or exhausted separately. Typical system power, energy and mass flow balances are given in the TCT/D-^{3}He scoping section.

(c)   Propellant Feed: This subsystem contains all the flow channels, pumping equipment and control valves which provide for the delivery of propellants from the propellant tanks to the reactor heating chamber. With the exception of the specific area where propellants are injected into the chamber, the system is similar, if not identical, to any liquid propellant (hydrogen, in this case) rocket feed system.

(d)   Propellant Tankage and Pressurization: These subsystems consist of the propellant tanks used to store the propellants and the pressurization used to expel them or simply supply a constant pressure feed at the propellant pump inlet. The problems of long term cryogenic storage, settling, sloshing, multiple start, etc. are still present but they are well developed and somewhat easy to handle.

(e)   Miscellaneous: Under such a title one can include the various shielding requirements, be they thermal, meteroid protection or neutron, as in the case of a fusion reactor system using D-^{3}He as fuel, thrust structure, plus a variety of components that may be required for refueling, accessing or performing system maintenance.

(f)   Payload: This is the final remaining item that when added to the delivery vehicle, finalizes the complete vehicle configuration. Other than the effects of size, the problems imposed by the payload itself are in no way considered serious or very difficult to handle.

It is the task of the system designer to properly integrate these subsystems into an operational vehicle. Pressurization systems, for example, may be packaged around the propellant tanks or they may be stored inside, as was done in the case of the SATURN-APOLLO S-IVB vehicle.

SYSTEM DESIGN AND TRADES

Whereas the system definition and requirements may result in a conceptual definition of the overall vehicle, it is the actual design and trade studies that put the finishing touches and identify each subsystem and component. The mission studies determine the propellant mass for example, but it is the actual system design and packaging that will lay out the propellant tank configurations and their interconnecting with the other subsystems, e.g., propulsion and pressurization.

83

In the system design and trade studies conducted here, certain geometric configurations needed to be assumed in order to arrive at specific masses and mass distributions. The propellant tanks, for example, were considered to be cylindrical with elliptical top caps and conical bottoms. As it turns out, in this study the fusion propulsion system is such that this type of configuration may not be the most desirable or optimum. However, this geometry serves as a start in order to initiate the comparative studies between the various propulsion system alternatives, i.e., nuclear fission and cryogenic liquid bipropellant. These comparative studies produce a relative ranking between the candidates, and the clear winner or the top two contenders are examined in detail for further comparison if necessary.

The trade studies assessed the total vehicle size and mass for a given mission and payload. The velocity requirements, along with the propulsion system delivered specific impulse, establish the required propellant mass which, in turn, allows the computation of the propellant tank volume and mass and also the masses of the various auxiliary subsystems such as pressurization, meteroid and thermal shield protection. When each candidate system is put through these trade study loops, the result is a final vehicle of specified envelope and mass. Optimum system is by definition the one of minimum mass.

DESIGN ALGORITHMS AND OPTIMIZATION

The details of the system design algorithms and computational routines are discussed in Appendix G. It will suffice here to state that the chemical and nuclear propulsion systems use the already developed and/or existing rocket engines.

(a) Chemical: Bipropellant liquid O_2/H_2 PL-10 used in the CENTAUR program and the J-2 engine from the SATURN APOLLO program.

(b) Nuclear: The Los Alamos National Laboratory (LANL) ALPHA nuclear thermal solid core engine which was designed for the orbit transfer vehicles (OTV) that would have operated from the Space Shuttle.

Both of these systems have fixed performance, envelope and mass and as such they represent constant quantities in the optimization process. The fusion propulsion system, however, is new and all design parameters are part of the system optimization. In particular, it is noted that the mass of the system depends on the required power to be generated; e.g., high power require

84

large capacitor banks, large magnets and larger attendant flow channels. A brief discussion of these issues is given in the section that follows:

RELEVANT PROPULSION ISSUES

This section, reviews the relevant issues of rocket propulsion in space including specific impulse and power requirements, and mission optimization. The differences between chemical and other forms of propulsion, such as fusion and fission, are also discussed. It is included here because of the expected diversity of readership from the fusion and the aerospace communities.

Thrust and Power

To create thrust, mass must leave the system with an exhaust velocity u_e and a mass flow $\dot{m}$. The thrust F is[27]

$$F = \dot{m}u_e \tag{1}$$

The power in the exhaust stream is

$$P = \frac{1}{2}\dot{m}u_e^2 = \frac{1}{2}Fu_e \tag{2}$$

This power is leaving the rocket system and must be supplied by some means. In chemical rockets, it is the fuel flow rate times its heating value. In fission and fusion, it is the nuclear reaction rate times the nuclear energy released per reaction.

The ratio of thrust to power, from (1) and (2), is

$$\frac{F}{P} = \frac{2}{u_e} \tag{3}$$

Therefore, while Eq. (1) shows that a high exhaust velocity will reduce propellant mass flow (which is desirable), it also reduces the thrust for a given power (which is not). As is discussed later, tradeoffs are clearly required.

Specific Impulse

Rather than deal with exhaust velocity, it is common to use the term specific impulse, which is the impulse imparted per unit mass of propellant. It is given by

$$I_s = \frac{F}{\dot{m}g} \tag{4}$$

where the g (9.8 m/s^2) is used to give it the more convenient unit of seconds The specific impulse depends on the type of gas, the reservoir temperature, and the rocket nozzle expansion. With an infinite expansion, it is given by[27]

$$\text{Max } I_s = \frac{1}{g}\left[\frac{2\gamma}{\gamma - 1}\frac{R}{M}T_o\right]^{1/2} \tag{5}$$

where γ is the specific heat ratio, R is the universal gas constant (8315 J/kg-mole-K), M is the gas molecular weight (e.g., 4 kg-moles for helium), and T_o is the temperature of the gas (Kelvin) in the reservoir upstream of the rocket nozzle throat. For real rocket nozzles that expand out to Mach numbers of about 4.0, specific impulse is about 90% of the infinite expansion value.

Figure 32 shows maximum specific impulses for hydrogen, helium, and lithium based on ideal gas theory. Obviously, the lower the molecular weight of the element the better. Note that dissociation, recombination, and ionization are not included in th figure, and these mechanisms have a profound effect on I_s. To achieve specific impulses greater than about 1500 s, temperatures must be above 4000 K even for atomic hydrogen. In reality, there will be a mix of atomic, molecular, and ionized hydrogen and therefore the actual I_s curve will lie somewhat below that for atomic hydrogen. Therefore, to get $I_s > 1500$ s, temperatures over 5000 K are required. Because no known engineering materials can withstand such temperatures, the propellant must receive its energy without having that energy pass across material walls, such as a heat exchanger. In chemical rockets there are no walls because the energy source is in the propellant itself. However, temperatures are not high enough in chemical rockets for this to be a serious issue. For fusion and fission, the energy source is the nuclear fuel. This energy must be transferred to the propellant without crossing material walls or impairing the nuclear reaction. The latter is of greater concern in fusion because the fusion reaction tends to be very tenuous and little effort is required to quench it.
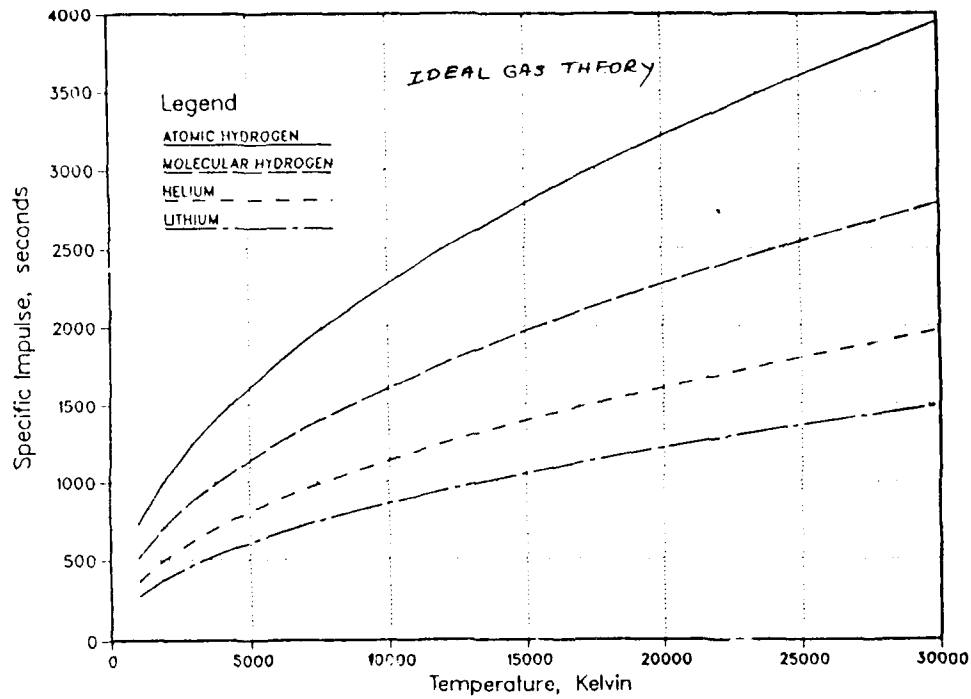
Figure 32. Maximum specific impulses for hydrogen, helium, and lithium. Assumes infinite expansion and ignores dissociation, recombination, and ionization.

At the high end of the temperature scale, 30,000 K (about 3 eV), radiation from Bremsstrahlung becomes so great that power is lost so fast that it is unlikely that such propellant temperatures can be maintained. While less of a problem in low density ion propulsion, here gas densities are so high that this loss can be overwhelming.

Bremsstrahlung radiation power for hydrogen is given by[28*].

$$P_B = 1.625 \times 10^{-38} \, n_e^2 \sqrt{T_e}, \quad W/m^3 \qquad (6)$$

where n_e is the free electron density and T_e is the electron temperature in eV. For example, at 2 eV (about 20,000 K) and 13.8 MPa (2000 psi), hydrogen is about 50% ionized and $n_e = 2 \times 10^{25}$ m^{-3}. The Bremsstrahlung radiation is then 10^7 MW/m^3. Even if 99.99% of this were reabsorbed, the net loss would still be 1000 MW/m^3. If reabsorption is total, the gas is a black body and then the surface radiation is on the order of σT^4, where s = 5.73×10^{-14} MW/m^{2}K^4 is the

---

* Ref 28, p241, equa. (7-69)

Stefan-Boltzmann constant. At 2 eV, this power flux is 9200 MW/m². These values are greater or comparable to the fusion power. Therefore, propellant temperatures are likely to be well under 2 eV. The upper bound in I_s is therefore likely to be about 3000 s for hydrogen and about 1500 s for helium and lithium.

The appeal of helium and lithium as propellants is that they do not dissociate (which absorbs energy). Studies in low density arc jets have in fact showed that helium delivers higher energy efficiency than hydrogen for specific impulses under 2000 s. Helium also has a very high first ionization potential, 24.5 eV vs. 13.6 eV for hydrogen.

Many fusion confinement concepts require a close-fitting conducting shell around the plasma. One could envision using a solid lithium shell for this purpose. The fusion energy would vaporize the shell, and it would become the propellant. With a low ionization potential, 5.4 eV, one could envision using magnetic fields to deflect the hot lithium ions from material walls. However, to deliver high I_s, temperatures of 3 eV or more are needed, which would be hard to achieve because of the intense Bremsstrahlung radiation loss.

It is clear from the above u. 't any high thrust rocket will have difficulty achieving specific impulses over about 3000 s. The constraints lie in the propellant and not the low density fusion power source. If only the fusion "ash" is used for thrust, I_s values over 250,000 s are possible, but only at very low density and hence low thrust. There is, therefore, no reason to categorically state that fusion can deliver higher specific impulse than fission or any other power source when operated at high thrust. As discussed below, the maximum specific impulse is not necessarily the best because, as I_s increases, so do the onboard power requirements.

Mass/Power Ratios

Unlike chemical rockets, considerab ` hardware is needed to supply the power in fission or fusion. Therefore, not only must one consider specific impulse, but the mass per unit power $\alpha \equiv M_r/P$ and, of course, the total power. M_r is the mass of the nuclear reactor and all the other components, such as power supplies, needed to run it. In fusion reactors, α can range from a heavy 10 kg/kW for a tokamak[10] to a low of $2 \cdot 10^{-2}$ kg/kW for the translating compact torus concept discussed in the preceding section.

It can be shown that the ratio of thrust to reactor mass, a measure of acceleration, is given by

$$\frac{F}{M_e} = \frac{2}{\alpha g I_s} \qquad (7)$$

Increases in specific impulse clearly harm thrust-to-mass ratio. With this conflict, there is obviously an optimum specific impulse that depends on mission profile and α. This is discussed in detail in a previous section. There are many missions which have optimum specific impulses below 2500 s, and therefore the Bremsstrahlung radiation limit on propellant temperature is no great issue.

The power that must be supplied by the reactor for this thrust is, from Eqs. (2) and (4)

$$P = \frac{g}{2} F I_s \qquad (8)$$

This is plotted in Figure 33 for several thrust levels. At high thrust and I_s levels, (e.g. 1000 kN and 1000 s) the thermal power required from the reactor far exceeds that of any single reactor ever built. While this power level is easily achieved in chemical rockets, it is very expensive to provide in nuclear reactors. Further, the total reactor system mass tends to be proportional to power level.

Typical Space Shuttle performance is also shown in Figure 33 for comparison. The Shuttle main engines produce 5×10^6 N (1.125×10^6 lb) thrust with an average $I_s \approx 400$ s. The Solid Rocket Boosters produce a total of 2.36×10^7 N (5.2×10^6 lb) thrust with $I_s \approx 200$ s. The thrust-average specific impulse is then only about 235 s. After SRB separation at high altitude, the main engines continue to burn, and their performance is also shown in the figure. Because this is closer to space operation, this value is a more appropriate comparison. Clearly, even if fusion propulsion achieves I_s values of 800-1000 s, it will be a significant advantage over the existing shuttle[29].

89
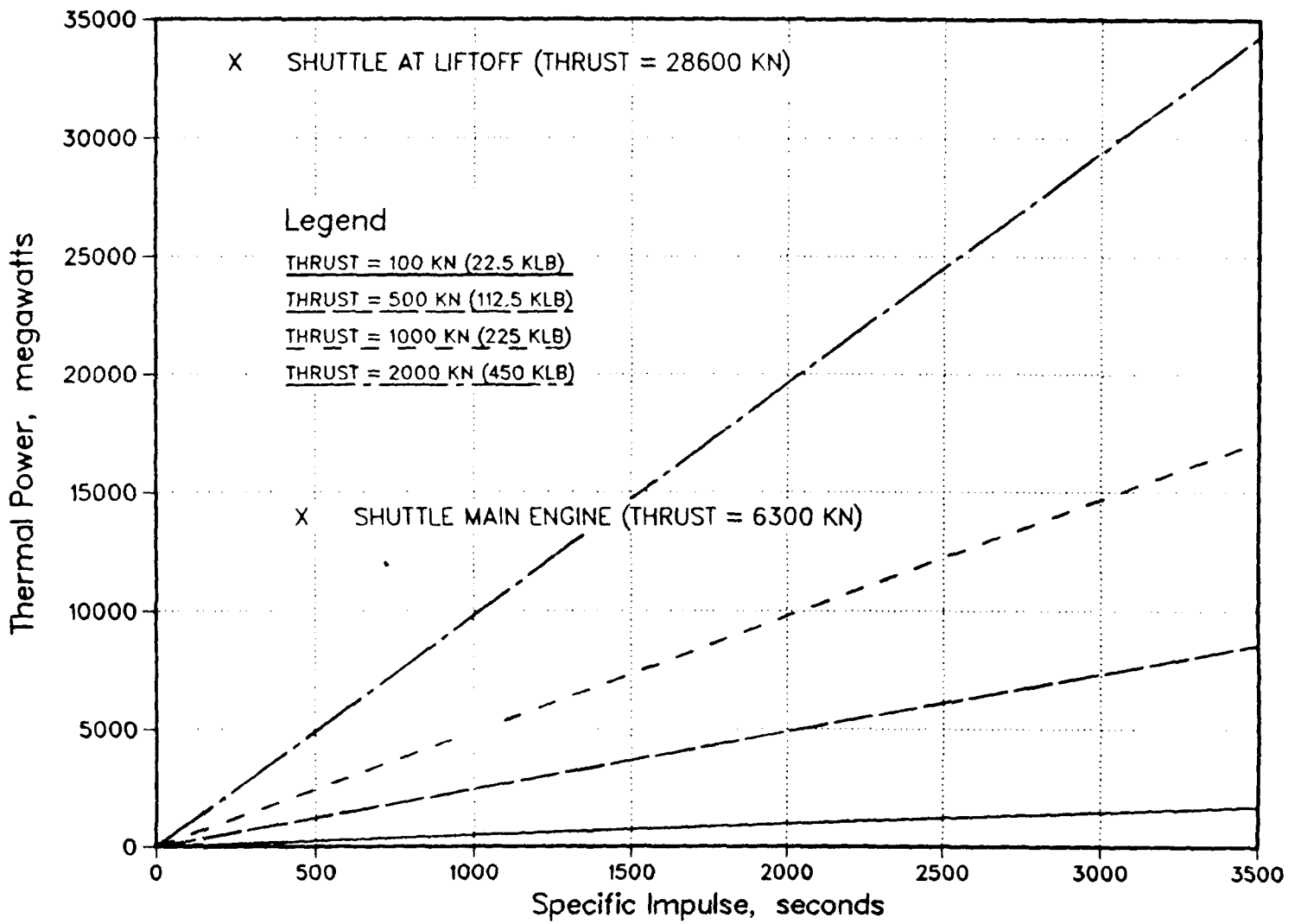
Figure 33. Power levels required as a function of thrust and specific impulse. Typical Space Shuttle values are shown for comparison.

90

SPACE MISSIONS

To complete this section on relevant propulsion issues, we state the basic expressions for space missions. The fundamental mission parameters are the velocity increment Δv, the initial mass M_i, and the final mass M_f. Clearly, $M_i - M_f$ is the propellant expended to achieve Δv. M_i is made up of the payload, reactor system, structure, and propellant. It can be shown that

$$\frac{M_i}{M_f} = e^{\Delta v / g I_s} \tag{9}$$

and the rocket burn time is

$$\tau = \frac{M_f g I_s}{F} \left(\frac{M_i}{M_f} - 1 \right) \tag{10}$$

Lastly, the acceleration is given by

$$a = \frac{F}{M} = \frac{F}{M_i - \dfrac{Ft}{g I_s}} \tag{11}$$

where Eq. (4) has been used and M here is the instantaneous mass.

SUMMARY

With fusion or fission powered rockets, the maximum specific impulse is not necessarily the best. As I_s increases, so does the reactor power that must be supplied. Because this increases system weight, tradeoffs were made to establish the optimum I_s for a given mission.

The temperatures required to achieve a given I_s depends upon the propellant molecular mass, the lower being the better. Even with the lightest, atomic hydrogen, to achieve $I_s \geq 1500$ s requires temperatures over 4000 K and therefore the reactor power must be transmitted to the propellant without crossing material walls. Temperatures above about 20,000 K are unlikely in any case with high density propellants because of the severe radiation power loss. The realistic upper bound for I_s is therefore about 3500 s.

Even if I_s values of 800 - 1000 s were all that could be achieved with fusion, it would still be 2-3 times better than the Space Shuttle. And if D-^{3}He fuel can be made to work, radioactivity levels would be far less than fission.

The present optimization trade studies set the thrust level a priori and allow the specific impulse to vary. A schematic representation of the optimization process is shown in Figure 34. As the delivered specific impulse increases, the propellants and all the propellant dependent masses (e.g., tanks, pressurization, etc.) decrease, but the propulsion unit (power plant) mass increases. The trends of these two counter-varying groups of masses are such that at some intermediate point an optimum (minimum total mass) point is found.
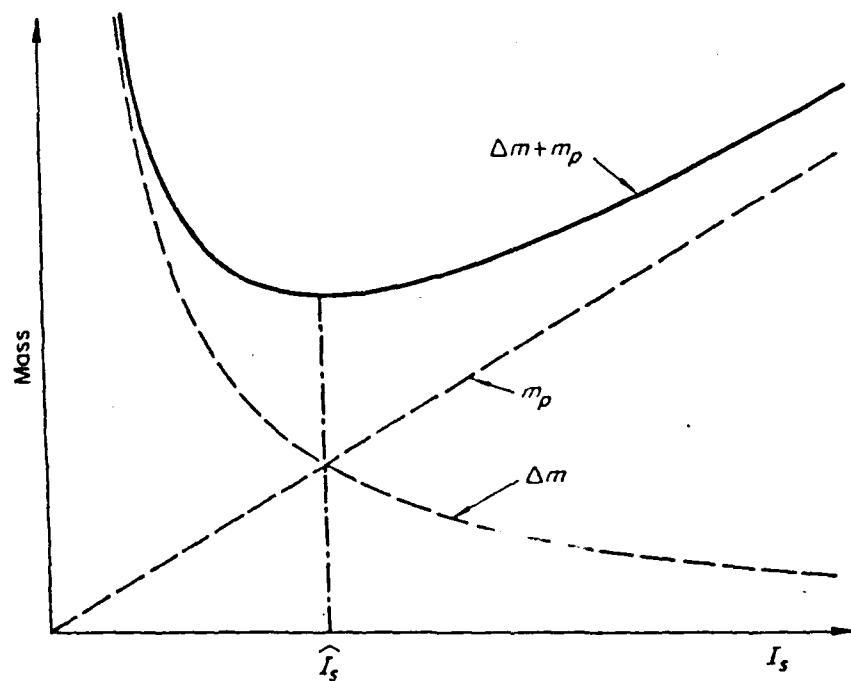
Figure 34. Dependence of propellant mass Δm

In the next section the specific numerical values of these optimization studies are presented for the subject missions selected.

92

MISSION ANALYSES AND PERFORMANCE

This section represents the culmination of the efforts of all previous sections. In the previous sections the following topics were discussed, analyzed and evaluated:

1. Air Force Missions reviewed
2. Fusion fuel cycles assessed
3. Fusion reactor concepts evaluate
4. Systems analyses and optimization studies defined

Here we attempt to answer the question "Are there any Air Force Missions where fusion propulsion could play a constructive role in a manner competitive with or superior to other alternate propulsion systems?"

MISSION SELECTION AND RATIONALE

Because of time schedule and budgetary constraints, only a limited number of applications were considered. Reference is made to the special section where the Air Force Mission scenario is constructed (Figure 2), and also the list of systems contained in AF PF II is given. One mission that appears to have attractive features is the Reusable Orbit Transfer Vehicle (ROTV), AF PF II PS-28. To quote its definition in the AF PF II, this system is

- **A totally reusable vehicle for transporting payloads between low earth orbit and higher (up to several times geosynchronous) orbits, enabling routine space operations, satellite retrieval, and dormant sparing.**

- **The objective of this program is to provide affordable access to space through routine transportation between various orbits, and on-orbit repair and reconstitution of Space Systems, which will ultimately provide a truly operational space capability in support of ground, air, and space-based forces.**

Additionally,

1. The ROTV system is in the plans of all agencies concerned with space operations and transportation.

2. It offers a great potential for high performance systems to prove their value and advantages because of the extended operations and long life requirements.

93

3. It has special requirements for moving large payloads and high delta velocity missions.

4. This system offers a great growth potential, especially as space operations expand to Mars and other planetary missions.

The first item to be selected was the velocity requirements for the mission to be examined. Since an ROTV could be called upon to perform a variety of missions of orbit change, a collage of such missions was examined and the velocity requirements for each mission computed. These missions involve both transfers from low earth orbit (LEO) to higher earth orbits (HEO), such as geosynchronous (GEO), orbit plane changes and LEO to lunar orbits and return. A summary of the velocity increments of the subject missions is shown in Tables 26 and 27. All these velocity values include a gradual orbit plane change of 28.5 degrees.

The velocity increments of 4,500 m/s and 9,000 m/s were selected for one-way and return missions, respectively. These mean values of delta velocity are within the "ball park" of all the values shown in the cited tables and can serve as the basis for the comparative evaluation between the alternate propulsion systems. The conclusions reached from these studies will not be altered significantly by the minor perturbations in the exact velocity requirement values for each specific mission.

The advantages of a high energy and performance ROTV become more evident as both the delta velocity and the mass of payload become large. The payload mass for this part of the study is set at 36,000 kg, which is significantly large so as to serve as an indicator of whether fusion propulsion offers any promise for Air Force Space Missions. In the addendum, some larger and more specific payloads are evaluated.

With this information at hand, the algorithms and the optimization computations discussed in Appendix G and the preceding section are put to use. The results are discussed below.

Table 26. ORBIT PLANE ROTATION VELOCITY REQUIREMENTS

Δ Φ	(DEG)	28	42	62	90
	Altitude				
	100 n.mi.	3,780	5,600	8,047	11,047
ΔV	300 km	3,747	5,550	7,977	10,952
m/s	1100 km	3,541	5,245	7,538	10,349

Table 27. LEO TO GEO AND HEO VELOCITY REQUIREMENTS

LEO ORBIT DATA

Altitude:	185.2 km (100 n.mi.)
Velocity:	7,744 m/s
Inclination:	28.5 deg.

HIGH EQUATORIAL ORBIT

RADIUS (km)	ALTITUDE (km)	Δ V (m/s)	r/r_{geo}
42,163	35,793	4,296.3	1
84,325	77,955	4,323.3	2
126,488	120,058	4,265.1	3

NOTE: 1) LEO to lunar circular orbit and return

ΔV ≈ 8,400 m/s to 10,400 m/s

2) Descent to lunar surface and return

ΔV ≈ 3,600 m/s to 4,000 m/s

VEHICLE AND PROPULSION SYSTEM TRADES

Here the fusion-powered vehicles to accomplish the selected missions are sized, i.e., parametric cases are computed and the points where the total vehicle mass attains a minimum are determined.

A cursory evaluation of the thrust level effects established that high thrust and high specific impulse fusion rocket engines are very massive. This in turn results in a low specific impulse for a minimum total vehicle mass. Therefore, attention was turned to lower values of thrust which are more compatible with the selected ROTV vehicle and mission. This general trend can be seen in Figures 35 where the thrust levels of 100 kN and 1,000 kN are evaluated. The lower thrust level of 100 kN (22.5 klb) optimizes at a specific impulse of 2300s whereas the 1,000 kN thrust level optimizes at $I_s = 1,000$s. The effect of the low specific impulse is to substantially increase the propellant and all the propellant-dependent masses (tanks, pressurization, etc.) with the net result making the fusion-propelled vehicle very massive. This can be seen seen in Figures 36 and 37 where the chemical cryogenic vehicles utilizing RL-10 and J-2 engines and the nuclear vehicle powered by the Los Alamos National Laboratory (LANL) developed ALPHA nuclear rocket engine, are compared.

COMPARISONS OF CHEMICAL, NUCLEAR, AND FUSION PROPULSION

As shown in Figure 36 and 37 the two chemical systems are comparable between themselves but both are substantially more massive than the nuclear. The 100 kN thrust fusion-powered vehicle is the least massive and hence it would be the system of choice for this mission. The advantage is further accentuated when the mission delta velocity requirements are increased to 9,000 m/s, which represents the case of delivering the 36,000 kg payload from LEO to GEO and return it (or one of equal mass) to LEO again. This example is shown in Figure 37.

It is noted that because the thrust level is set the corresponding burning times vary between the systems. No consideration is given here as to whether a J-2 engine can be made to operate for this length of time. In this respect, the figures simply refer to "some" propulsion system of comparable mass, thrust and performance levels as the RL-10, J-2 and the ALPHA, respectively.

Taking another approach to the mission and fixing the burning time, the thrust is allowed to vary accordingly and the optimizations and performance are evaluated in an identical manner. Figure 38 shows the pertinent vehicle mass and performance data for a chemical ROTV utilizing 6 RL-10's, 4 ALPHA's and a 208 kN thrust fusion engine for a burning time of 3,675 s. Again, it
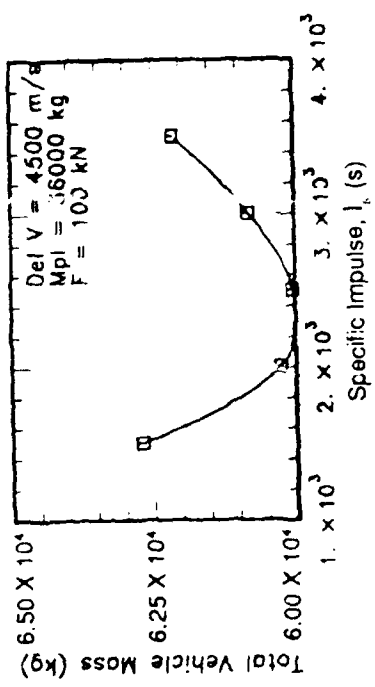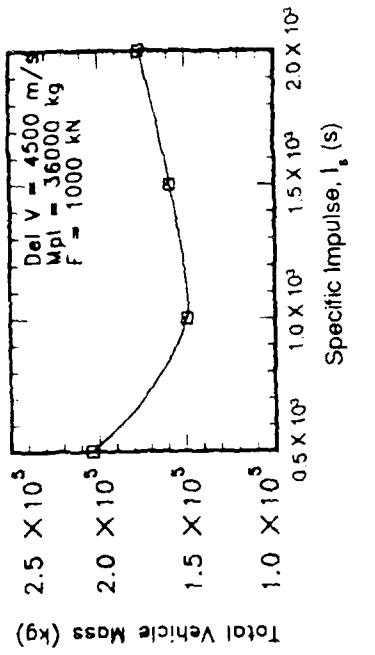
Engine Specific Mass 0.01 kg/kW
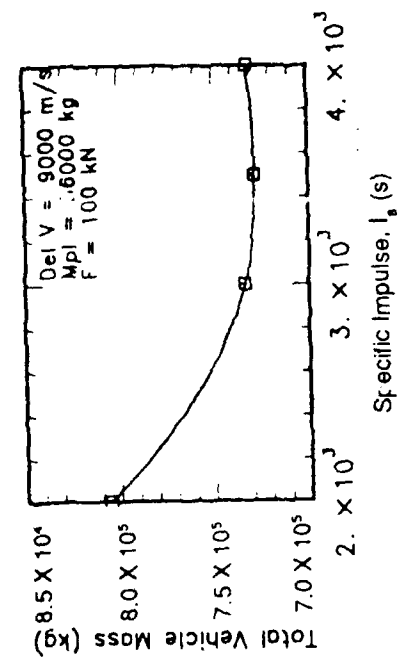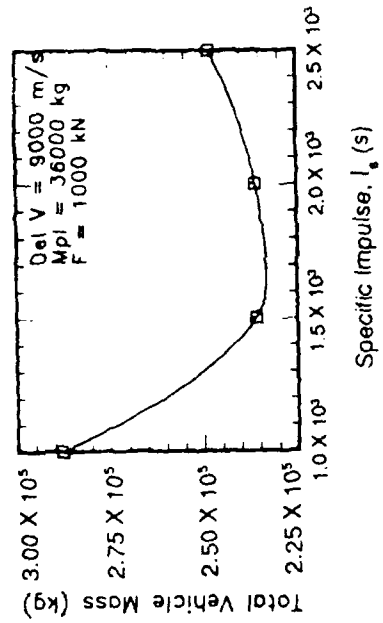
Figure 35. <u>Fusion Vehicle Mass Optimization</u>

Figure 36   **SPACE TRANSFER VEHICLE DESIGN DATA**

LEO to GEO Mission Data :   Payload Mass   36,000 kg
Velocity Increment   4,500 m/s

		CRYOGENIC (O2/H2)		NUCLEAR FISSION	FUSION	
		RL - 10	J - 2	LANL ALPHA 2	NEW	NEW
ROCKET ENGINE						
Thrust	(kN)	66.7	902	71.7	100	1,000
Specific Impulse	(s)	450	429	860	2,300	1,000
MASS BREAKDOWN						
PROPELLANTS	(kg)	68,712	77,695	30,877	10,849	54,858
Fuel (LH2)		10,571	11,953	-	-	
Oxidizer (LOX)		58,141	65,742	-	-	
PROPELLANT TANKS						
Total Volume	(m3)	200	226	495	174	879
Mass	(kg)	1,681	1,901	3,324	1,168	5,905
PRESSURIZATION						
(He system)	(kg)	283	320	560	197	995
ENGINE	(kg)	132	1,579	2,567	11,282	49,050
MISCELLANEOUS	(kg)	703	730	1,390	488	2,470
TOTAL VEHICLE MASS	(kg)	107,512	118,291	74,719	59,984	149,279

Figure 37 . **SPACE TRANSFER VEHICLE DESIGN DATA**

LEO to GEO With Return   Payload Mass   36,000 kg
Mission Data :   Velocity Increment   9,000 m/s

		CRYOGENIC (O2/H2)		NUCLEAR FISSION	FUSION	
		6 RL - 10's	J - 2	LANL ALPHA 2	NEW	NEW
ROCKET ENGINE						
Thrust	(kN)	400.3	902	71.7	100	1,000
Specific Impulse	(s)	450	429	860	3,500	1,650
MASS BREAKDOWN						
PROPELLANTS	(kg)	333,291	396,423	109,120	16,792	99,869
Fuel (LH2)		51,275	60,988			
Oxidizer (LOX)		282,015	335,435	-	-	-
PROPELLANT TANKS						
Total Volume	(m3)	970	1,154	1,748	269	1,600
Mass	(kg)	8,156	9,701	11,746	1,808	10,751
PRESSURIZATION						
(He system)	(kg)	1,374	1,635	1,979	305	1,811
ENGINE	(kg)	792	1,579	2,567	17,168	80,933
MISCELLANEOUS	(kg)	3,411	4,058	4,913	756	4,497
TOTAL VEHICLE MASS	(kg)	383,024	449,394	166,326	72,828	233,861

Figure 38. **SPACE TRANSFER VEHICLE DESIGN DATA**

LEO - GEO - LEO Mission ; Mpl = 36,000 kg ; Del V = 9 km/s ; Burn Time = 3675 s (Constant)

		CRYOGENIC , 6 RL-10's	NUCLEAR , 4 ALPHA 2's	FUSION , Me=12 (Is)
ROCKET ENGINE				
Thrust	(kN)	400	278	208
Specific Impulse	(s)	450	860	2500
<u>MASS BREAKDOWN</u>				
PROPELLANTS	(kg)	333,291	134,548	34,685
Fuel	(LH2)	51,275		
Oxidizer	(LOX)	282,015	-	-
PROPELLANT TANK(S)				
Total Volume	(m³)	970	1,937	499
Mass	(kg)	8,156	10,849	2,797
PRESSURIZATION				
He System	(kg)	1,374	1,828	471
ENGINE(S)	(kg)	792	10,270	30,000
MISCELLANEOUS	(kg)	3,411	4,538	1,170
TOTAL VEHICLE MASS		383,024	198,033	105,123

is seen that the fusion-propelled vehicle has distinct mass and size advantages over its chemical and nuclear fission competition.

In all these cases, the 9,000 m/s delta velocity implies that the vehicle transfers the full 36,000 kg payload from LEO to GEO and back to LEO. This is the true reusability of the subject vehicle.

The mass variation of an ROTV as it is used to transfer various payloads on the return trip is shown in Figure 39 for the nuclear fission-powered vehicle and in Figure 40 for both the nuclear fission and fusion vehicles. Again, it is shown that as the requirements increase so does the relative superiority of the high-performing fusion-propelled vehicle.

Finally, Figures 41 and 42 show the mass breakdown data for two reusable fusion-propelled ROTVs, one using I_s = 1500 s, the other 2,000 s. As discussed earlier, the 1500-s specific impulse power plant is more feasible , therefore it was selected for final vehicle design layout and configuration evaluation which is shown in Figure 43.

FUSION VEHICLE DESCRIPTION

The vehicle shown in Figure 43 is assembled in three distinct sections: The payload (shown in "Phantom" lines), an interstage structure and the propulsion unit.

NOTE: The dimensions given below are estimates and are intended to provide a scale reference for the reader.

- The payload is snown as a 10 m diameter by 20 m long cylinder. This configuration will accept payloads of the established values, e.g., 36,000 kg, which will interface with the 10-m diameter load ring in the interstage structures.

- The interstage structure is of conventional frame and longeron construction, but with an external meteroid and radiation shield. Command and control electronic packages are located within this section. The illustration shows a 4-m long section.

Figure 39. **NUCLEAR REUSABLE ORBITAL TRANSFER VEHICLES**

UTILIZING THE LANL ALPHA 2 ENGINE :   PAYLOAD MASS = 36,000 kg

MISSION TYPE		LEO - GEO ONLY	LEO-GEO-LEO; EMPTY RETURN	LEO-GEO-LEO; W/ SAT
Thrust	(kN)	72	72	72
Specific Impulse	(s)	860	860	860
Burn Time	(s)	3,552	3,846	11,880
MASS BREAKDOWN				
PROPELLANT (Liquid H2)	(kg)	33,598	36,379	112,363
PROPELLANT TANK				
Total Volume	(m^3)	484	524	1,618
Mass	(kg)	2,709	2,933	9,060
PRESSURIZATION				
He System	(kg)	456	494	1,527
ENGINE	(kg)	2,567	2,567	2,567
MISCELLANEOUS	(kg)	1,133	1,227	3,789
TOTAL VEHICLE MASS		76,464	82,778	165,307

Figure 40. TOTAL VEHICLE MASS vs. RETURNED PAYLOAD FROM GEO
Assumes Each Vehicle Has Delivered a 36,000 kg Payload to GEO
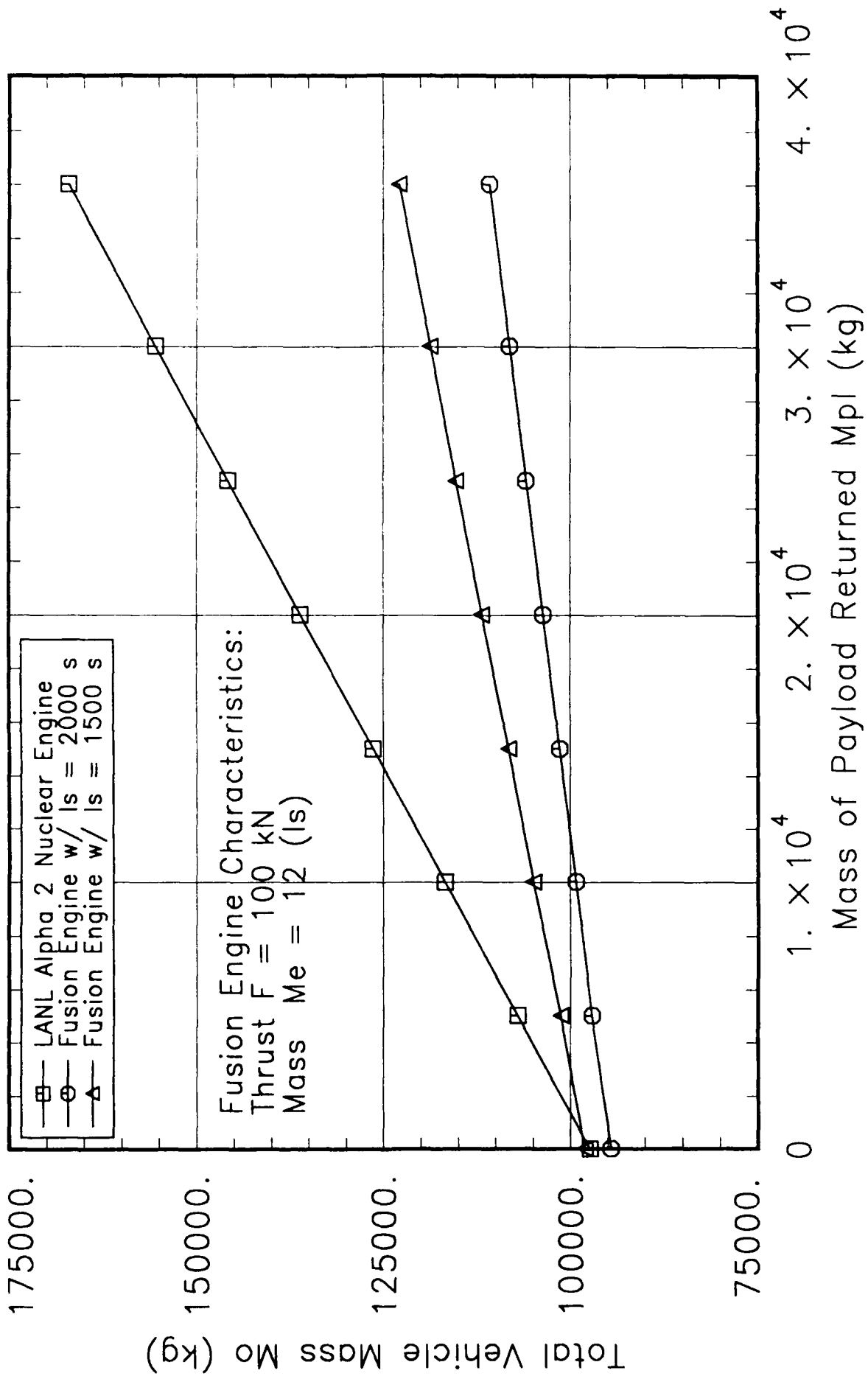
Figure 41

MDAC-GA FUSION SPACE TRANSFER VEHICLE SIZING DATA

Mission: Transfer 36,000 kg to Geosynchronous Orbit (GEO)
Return Vehicle Empty and with Original Payload

Engine: GA Fusion Engine

Is = 1500 s, Thrust = 100 kN, Mass = 12 (Is)

Mass Breakdown		LEO-GEO Empty Return	LEO-GEO Return Payload
Propellant	kg	27,910	57,597
Propellant Tanks			
Total volume	m³	402	829
Mass	kg	2,251	4,644
Pressurization	kg	379	783
Engine	kg	18,000	18,000
Miscellaneous	kg	941	1,942
Total Vehicle Mass	kg	98,070	118,967

Figure 42

MDAC-GA FUSION SPACE TRANSFER VEHICLE SIZING DATA

Mission: Transfer 36,000 kg to Geosynchronous Orbit (GEO)
Return Vehicle Empty and with Original Payload

Is = 2000 s, Thrust = 100 kN, Mass = 12 (Is)

Engine: GA Fusion Engine

Mass Breakdown		LEO-GEO Empty Return	LEO-GEO Return Payload
Propellant	kg	21,074	42,379
Propellant Tanks			
Total volume	m³	303	610
Mass	kg	1,699	3,417
Pressurization	kg	286	576
Engine	kg	24,000	24,000
Miscellaneous	kg	710	1,430
Total Vehicle Mass	kg	94,549	107,801

THIS PAGE LEFT INTENTIONALLY BLANK

Figure 41 FUSION-PROPELLED
REUSABLE ORBIT TRANSFER VEHICLE

PAYLOAD
(20 M LONG x 10 M DIAMETER SHOWN)

COMMAND AND CONTROL ELECTRONICS

FORMING AND ACCELERATING MAGNETS

ACCELERATOR FAIRING

COUNTER ROTATING
TURBINE/
COMPULSATOR/
FUEL PUMP
MODULES

(14) LH$_2$ TANKS

PROTECTIVE SHIELD

(2) GHe
PRESSURANT TANKS

(2) RESTART
TANKS

INTERSTAGE AND THRUST CONE

CAPACITOR BANKS

D AND ^{3}He STORAGE

NEUTRON SHIELDING

PLASMA/PROPELLANT MIXING TUBE
(50 M LONG)

MULTILAYER INSULATION
ON ALL CRYOGENIC TANKS

NOMINAL 829 M^3 FUEL STORAGE
PLUS ULLAGE
FOR ALL TANKS COMBINED

PLASMA TUBE STRUCTURE
AND NEUTRON SHIELDING

FUEL PLENUM

POROUS CERAMIC LINER

NOZZLE

nej 12/88

107

- The propulsion unit contains all the components associated with the fusion propulsion system. This section is constructed from ISOGRID * skins and external meteoroid and radiation shielding of 9 m diameter and 58 m length. Liquid hydrogen fuel is contained within 16 cylindrical tanks with spherical end caps, of 2.5 m diameter and 13.75 m overall length. This volume will accommodate the 57,597 kg of propellant mass given in Figure 41, plus the nominal ullage volume and tank wall thicknesses. Each tank is individually insulated with Multilayer Insulation (MLI) to reduce boil-off. The tanks are manifolded and have fill, vent, pressure relief and supply valves. Two additional tanks of 2.5 m diameter and 10.5 m overall length are provided for the storage of the high pressure gaseous helium pressurant. In addition, two auxiliary tanks of 2.5 m diameter each are provided for restart capabilities. The start tanks are equipped with wick and screen assemblies to assure restartability under microgravity environment conditions.

- The accelerator/propulsion tube configuration of the engine draws D and ^3He from spherical storage tanks of one-meter diameter. These fuels are injected under pressure into the plasma generator regions from where magnetic fields and electric currents accelerate them down the accelerator "Arms" to the point of collision. Following the successful collision and subsequent compression, the resulting high temperature (T = 55 keV) plasma is driven down the close-fitting propulsion tube of 50 m length. This tube is lined with a porous ceramic liner. Hydrogen is supplied via manfolding to a plenum behind the liner and diffuses through the liner into the propulsion tube where it is heated and then expands through the exhaust nozzle.

- The nozzle is cooled regeneratively by passing LH_2 through the nozzle wall. Portions of the resulting hot gas are fed into a pair of counter-rotating turbines with compulsators and pumps to provide the power and fluid flow control. Power is conditioned and stored in the high efficiency capacitor banks for subsequent use in the accelerators. A neutron shield surrounds the propulsion tube, the "Arms" and the collision zone of the accelerators.

The estimated propulsion parameters for this system are shown in Table 28 and the variation of specific impulse for H_2 as a function of temperature, accounting for dissociation, is shown in Figure 44.

---

* A tank wall design which employs a milled skin and rib pocket geometric configuration for high strength.

108

Table 28

FUSION PROPULSION SYSTEM PARAMETERS

Thrust (kN)	100
Specific Impulse (s)	1500
Propellant	H_2
Chamber* Temperature (K)	5000
Chamber* Pressure (MPa)	27.6 (4,000 PSI)
Propellant Flow Rate (kg/s)	6.8
Nozzle Expansion Area Ratio	75:1
Total Power (MW(th))	1000

---

* Nozzle Stagnation
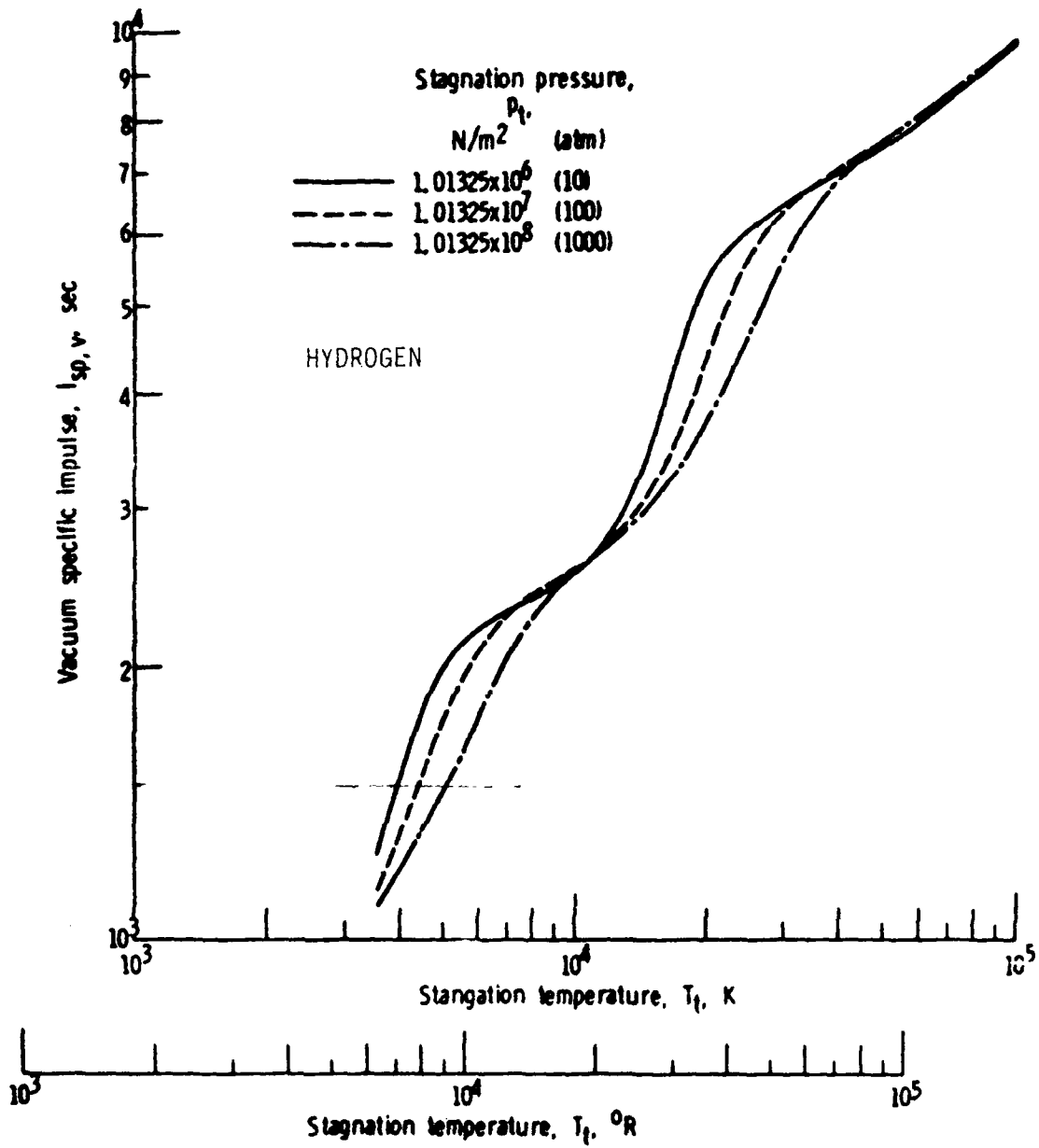
Figure 44.   Vacuum specific impulse for choked nozzle flow with shifting chemical
              equilibrium in Debye-Huckel approximation. Ratio of nozzle-exit pressure
              to stagnation pressure of 10^{-4} (Ref. 30)

110

REMAINING ISSUES

A modest study such as this could not possibly resolve all the issues of fusion propulsion. In fact, many fundamental issues in the fusion process itself remain which must be resolved before the development of fusion propulsion can be pursued with the expectation of some degree of success. Some of these issues that remain yet unresolved and related to fusion propulsion are as follows.

CONFINEMENT

This is perhaps the most important of the fundamental problems in the fusion program for very little can be accomplished without a successful confinement scheme of the very high temperature plasma. The major focus of the fusion program has been to limit the heat loss from fusion fuels in order to achieve ignition and net energy output. The characteristic minimum confinement time needed to maintain a fixed burn temperature is the fuel thermal energy divided by the fusion heating power (charged particle power). Longer confinements would help because they would cause a thermal excursion to higher, more reactive, temperatures.

ICF DRIVERS

Inertial confinement fusion (ICF) may have the greatest probability of success in being able to effectively use propellant. The major concern is the bulk and weight of the drivers. Higher power density lasers will be required than currently exist. Also, while direct drive ICF may be more efficient than indirect drive, the requirement for uniform illumination would be awkward to implement in a spacecraft. Indirect drive, with beams coming from one, or at most two, directions would be preferred although there may be a penalty of decreased efficiency.

MATERIALS

Fusion materials must withstand high temperatures, high heat fluxes, and, in the case of D-T fuel, high neutron fluxes. In space, material reliability is paramount because little replacement material can be carried on board.

In order to achieve high specific impulse, high rocket nozzle temperatures are needed, up to 20,000 K. It is unlikely that bulk materials can be developed for this temperature. However, thin

film thermal barrier coatings should be pursued. Magnetic insulation (e.g., magnetic nozzles) is also a useful technique and should be pursued.

PROPELLANT ADDITION

This is an issue of great concern. Propellant must be added in such a way that very high temperatures (up to 2eV ≈ 20,000 K) can be achieved without having the resulting gas prematurely quench the fusion burn. With ICF, the fusion burn is over in 10 nsec, and during that time a vaporized propellant can move no more than about 5 cm (e.g. hydrogen ions heated to 50 keV). It is therefore easy to keep the propellant out of the fuel during that time. The problem is harder with confinement schemes having slower fusion burns. If the fusioning plasma is fixed in the reactor, it will be difficult to keep propellant from quenching the burn. Because the mass of propellant can be millions of times greater than the fuel, only a tiny fraction can completely push out the fuel. If the plasma is moving at a velocity greater than 10's of km/s, then it may be possible to sweep past a film of liquid hydrogen, vaporizing it with its intense fusion power density, and then getting out of the way of the expanding gas. This is the scheme discussed earlier with the translating compact torus.

The problem would be less severe if the total fusion energy released during the burn could be stored in the plasma until the end. Then that ball of hot gas could be fired into a waiting ball of propellant. This is not the case, however, because about 30 times more fusion energy is released than the stored plasma thermal energy, and this energy must go to the propellant while the burn is continuing. If a material wall separates the plasma from the propellant, then there is no quenching problem. However, that would bring temperatures down to the level of fission, reducing the peak achievable I_s to about 800 s. One could of course convert the fusion energy to electricity and use arc heating to heat a propellant. This can produce I_s values of up to 2000 s. If direct conversion of fusion charged particle energy can be done efficiently, this may be one of the few viable ways to utilize magnetic fusion energy for thrust. A schematic of this scheme is shown in Figure 45. it would be especially appealing with D-^{3}He fuel because most of the output is in charged particles.
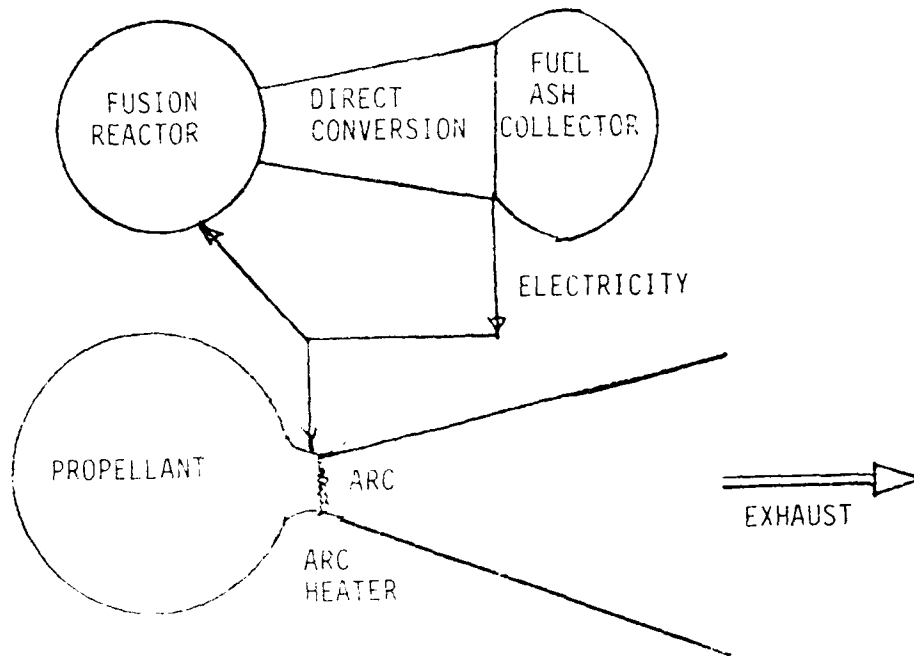
Figure 45. Schematic of a D-^{3}He Direct-Converted Arc Jet.

PLASMA PRESSURE

Fusion power density increases with the square of the plasma pressure in the optimum burn temperature regime. Obviously, one therefore wishes to maximize fuel pressure which is usually some fraction of the pressure needed to contain the fuel. In magnetic confinement, that fraction is the "beta" defined by

$$\beta = \frac{n_i T_i + n_e T_e}{B^2/2\mu_o}$$

where the magnetic field B depends on who is doing the defining. Physicists tend to use B in the middle of the plasma while engineers tend to use B at the magnet coil. They can differ by factors of as much as five.

113

There is never a reason to operate at less than maximum beta. If power density is too high, magnetic field strength can be reduced with an accompanying cost and weight reduction. The desirability of a confinement concept depends much on its achievable beta. If betas could be raised to the 30% range without paying too high a price, then power densities would be high enough, and masses low enough, to make even tokamaks attractive for space applications.

D - T VS. OTHER FUELS

Eventually one may wish to address the tritium and neutron issues with D - T fuel and compare these features with its 50-fold higher power density (minimum) when compared to other fuels. Tritium is relatively benign and its soft beta activity is easily shielded. Information is needed on the effect of a single dose due to a known accident, and also the short and long-term effect of a large release of tritium into the atmosphere.

If the neutron energy from D - T can be absorbed by the propellant, as appears likely with ICF, then neutron effects on first wall materials would be no worse than the neutrons from D -^{3}He or D - D.

D -^{3}He is appealing because most of its output is in charged particles and because it is the only "aneutronic" fuel that has any hope of ignition. Requirements for n τ are 10 to 20 times greater than for D - T, and this will manifest itself in more massive and expensive hardware required for heating. There may be benefits from "enhancements" such as non-Maxwellian temperature distributions and spin-polarization. More work must be done here. However, these techniques introduce complexity and constraints. Therefore, tradeoffs will be required.

POLOIDAL FIELD

The ratio of plasma current to plasma radius, I_p/a, is a measure of the poloidal field in the plasma. Very high values tend to be needed for D -^{3}He reactors with high power density. Whether or not startup mechanisms can be engineered to achieve such fields is yet to be resolved.

114

RECOMMENDED DEVELOPMENT PLAN

Some of the specific tasks called out in the statement of work (SOW) require that:

(a)   A preliminary system and mission analysis be carried out to illustrate the potential payoffs of the most promising fusion propulsion concept(s) in relation to chemical and nuclear fusion propulsion concepts.

(b)   People, groups of people, or organizations be identified that can best analyze and propose solutions to the remaining and problems

(c)   A development plan for the favored fusion propulsion concept(s) be recommended which identifies research, exploratory and advanced development efforts and includes pertinent information on the supporting technologies planned and reasonable financial and technological constraints.

The system and mission analysis potential payoffs, comparisons with other propulsion concepts, and a brief discussion of the several fusion technology problems that will require resolution are presented in the two immediately preceding sections.

In this section a recommended development plan is presented. It is shown schematically in Figure 46 and lists the various pertinent technologies and some financial information. The recommended time span covers up to the year 2025 as per the information given in the addendum to this report. The various parts of this development plan are as follows:
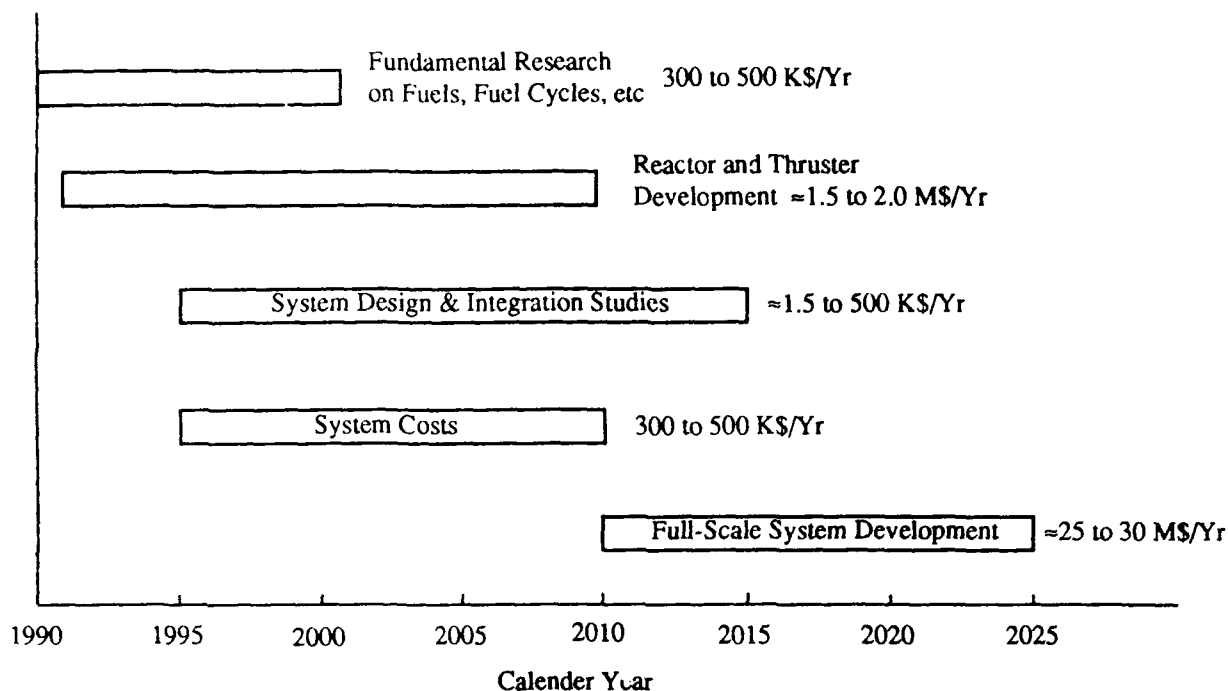
Figure 46. Fusion propulsion development program.

FUELS AND FUEL CYCLES

Fusion cross sections for Maxwellian thermal distributions for all fuels of interest are well developed. In some cases, such as p-^{11}B, accuracies may be as low as ±25%. Yet this is still sufficient for the levels of detail required in the near future.

Interesting work can be done, however, on non-thermal fusion and on spin polarization enhancement, especially for D-^{3}He. These may provide higher power density for a given plasma pressure.

Muon-catalyzed fusion is another interesting possibility. Muons generated from GeV accelerators if injected into a high pressure fuel, e.g. D-T, gas at T~500 ° C displaces the electrons in their orbit and, having smaller orbital radii, greatly decrease the range of coulomb repulsion seen by the D and T nuclei. Fusion can therefore take place at low temperature.

Currently, it appears that muon lifetimes are not long enough to produce net energy output. However, there may be synergistic effects that would enhance muon fusion. Could muons be

116

used with very high pressure D-T gas? Can muons enhance other fusion fuels? Can clever ways be found to produce muons at lower energies? Currently they are produced by atomic collisions which is a brute force approach.

Traditionally, this type of work is performed by small university-type research groups. However, as the knowledge matures and practical applications and specific designs are considered, it may be advisable to involve industrial-type research groups who are more application-oriented.

REACTOR AND THRUSTER DEVELOPMENT

Exploratory fusion reactor development work should first be undertaken to verify that the colliding beams in the selected TCT will indeed work as envisioned. In case the results are negative then other reactor concepts will need to be examined; e.g. the propellant-surround ICF concept.

In any event, reactor development could and should be leveraged off the mainline fusion program with special emphasis in tailoring the development of reactor concepts suitable for space propulsion. Since this task would begin around 1995, it is not unreasonable to expect that a wider experimental data base may be available which may allow a reactor concept selection and development to be made easier.

Thruster development should be directed on the primary issue of propellant addition. If the selected TCT reactor becomes feasible, as a fusion reactor concept, then the problem of injecting the propellant down the long flow channel via the discussed porous wall should be verified experimentally. The basic question that must be answered is "How can a very hot, high pressure gas propellant co-exist with an on-going fusion reaction without destructive interference"?

In a way, this problem is similar to that of developing and designing the injectors of liquid bipropellant rocket engines of the recent past.

Other problems that will need to be tracked and resolved are materials in the high temperature zones. In the cases discussed here where the delivered specific impulse is in the 1500 s to 2000 s range the nozzle stagnation temperatures for hydrogen propellant are in the vicinity of

117

5000 K. This is beyond the current state-of-the-art but it does not appear to be the most formidable of the problems.

Traditionally, industrial-type research and development groups are best suited to pursue these development efforts, where prototype hardware should be the goal, with inputs from more basic research-oriented university-type groups or individuals.

SYSTEM STUDIES

The fusion reactor, the thruster unit and the entire propulsion system which includes propellant tanks, pressurization, pumps, feed systems, manifolds, protective shields, etc., must be integrated into a functional system. This requires detailed layouts of the components, subsystems and their interfaces. Flow and power balanced details must be calculated and proper auxiliary components, such as control valves and start tanks need to be incorporated into the system.

Operational problems, e.g. propellant loading and transfer, plus the requirements for system mass center control, thrust vector control and vehicle attitude control are part of the complete system integration package before a full scale development program is committed. Key experiments at the component and subsystem level need to be conducted early in the system development program.

System design, integration and hardware development are costly activities and they are contingent upon successful outcomes in the fusion programs, particularly the experimental results.

It is therefore important that along with all the aforementioned technical development studies, the systems costs for all facets through life-cycle-cost operations be assessed and scoped. Especially, since fusion propulsion is to be competitive with the chemical, nuclear fusion or other alternative propulsion concepts.

The system design, integration and cost activities are best done by the organizations that develop and build the hardware with specialized inputs and consultations from special economic study and analysis groups.

118

FULL SYSTEM DEVELOPMENT

This task has been slated to begin on or about the year 2010, i.e. approximately 20 years following the beginning of this overall program. It is anticipated that by then all pertinent issues concerning the fusion fuels and the fusion reactor concepts will have been fully resolved. Furthermore, all of the basic work in the development of the thruster hardware, the propellant injection and associated materials and hardware will have matured and developed. In addition, the combined national and perhaps international activities in space will have resulted in permanent fuel depots and an expanded space travel program where fusion propulsion will prove to be far more beneficial than this study has indicated.

With all this given then, a full program development can commence with prototype flight vehicles becoming available sometime before 2020 to be followed by fully operational vehicles by the year 2025.

This task, of course, to be completed by a major aerospace systems contractor, with pertinent inputs and consultations from various speciality smaller R&D groups.

NOTE: The financial figures shown in Figure 46 are rough estimates in 1988 dollars.

119

CONCLUSIONS

The purpose of this study was to evaluate fusion power for space propulsion. Implicit in this goal was to advise the Air Force on the level of participation that should be pursued both in the near and far term. Primary tasks were to evaluate fusion fuels and fuel cycles and explore known fusion confinement concepts. Emphasis was on propulsion, especially in investigating whether there are any missions where fusion propulsion can play a constructive role as compared to other viable propulsion systems.

The study reviewed numerous fuel cycles and fusion reactor concepts. Based on the requirement constraints, one of which is the need to eliminate or minimize neutron radiation, and the evaluation criteria, we selected D-^{3}He and the translating compact torus (TCT) as the fuel and reactor of choice respectively.

The study was able to show that a reusable orbit transfer vehicle (ROTV) operating in the near earth region, ferrying large payloads from LEO to GEO or X-GEO and return would be an excellent application of fusion propulsion.

Furthermore, the systems integration studies showed that the desired level of specific impulse is in the 1500 s to 2000 s range. This results in nozzle stagnation temperature in the 5000 K range. This makes the material and heat containment problems in the rocket nozzle solvable and also allows the injection of high propellant mass flow rates, thus achieving high thrust. In addition, it substantially alleviates the bremstrahlung and photon radiation problems which are known to be major energy losses in the fusion processes.

Additional work, of course, needs to be done. For example, more work could be done to fully assess the trade-off between D-^{3}He and D-T fuels, especially if neutron radiation can be used rather than being a menace. D-T will be easier to confine and ignite. In fact, because of the high photon radiation loss, there is concern that D-^{3}He may not ignite in many confinement concepts. The implications of subignition are high recirculating powers. The inherently low power density of D-^{3}He means that power reactors will be larger as will input powers. Because D-^{3}He produces some neutrons, shielding is still required and, considering the larger reactor, shield volume could be as large as would be required for an equal power D-T reactor.

Three confinement concepts that are worth further study are (1) the colliding translating compact torus (TCT), (2) the propellant-surround ICF, and (3) a direct-converted fusion electric arc jet.

This study evaluated the TCT in detail. In this concept, compact tori, such as spheromaks, are accelerated toward each other at high velocity and merged, their kinetic energy thereby being converted to thermal. The biggest issues are those of confinement and stability during the fusion burn, particularly with D-^{3}He. There are conflicting experimental results which indicate very good or very poor confinement, but the preponderence of the evidence shows that the selected configuration is closer to the former.

An appealing TCT concept is translating the reacting torus after collision along a linear or circular track that has been wetted with liquid propellant. The propellant blowoff velocity is lower than the translational velocity of the reacting torus, so interference with the burn does not occur.

The ICF propellant-surround, as mentioned above, appears to avoid the propellant addition problem that plagues all the others. In this concept, an ICF target is surrounded by a sphere of frozen hydrogen which absorbs most of the fusion energy. There are questions of driver size and mass, installation and alignment, and surround fabrication. One of the biggest advantages here is the possible use of D-T fuel with the neutrons and their energy being largely absorbed by the propellant.

The fusion arc jet idea came along toward the end of the study and little analysis has been done. The basic idea is to use a compact fusion reactor, direct-convert the charged particle energy into electricity and then heat a remote flowing propellant by an electric arc. Not only are very high specific impulses possible, but the propellant addition problem is solved. This concept is superior to fission electric because no thermal power conversion is needed, and conversion efficiencies are 50-70% vs. 10% for fission thermionic or thermoelectric systems. It also encourages the use of aneutronic fusion fuels, which produce mainly charged particle exhaust.

A useful analogy to fusion propulsion is that of powered flight which, if one starts with da Vinci, took some 400 years to develop. The key to success was the parallel development of the compact and lightweight internal combustion engine. Later, powered flight had another boost with the development of the still more compact gas turbine. If all that were available were the Corliss

steam engine, powered flight would never have occurred. And if all that remains available in fusion is the low-beta tokamak, fusion propulsion will never occur. But there appear to be a number of promising fusion concepts that hold the potential of high power densities needed for space applications. What is needed at this stage are medium-sized experiments to sort them out and locate a winner.

Fusion space propulsion will be harder to achieve than fission. The payoff, however, would be greater. Our ultimate recommendation to the Air Force is therefore to continue to pursue fusion propulsion. Emphasis should be placed on influencing the mainline program to devote some effort to confinement concepts that would be suitable to space propulsion.

REFERENCES

1. Horn, F. L., Powell, J. L. and Lazareth, D. W. "Particle Bed Reactor Propulsion Vehicle Performance and Characteristics as an Orbital Transfer Rocket", Space Nuclear Power Systems, 1986, Chapter 36, pp. 375-381, M. S. El-Genk and M. D. Hoover, Editors, Orbit Book Company, Malabar, FL 1987.

2. J. J. Pass, Jr., "Fusion, and Advanced Fuel, Reaction Bibliography - Particle Reactions from H1 to B11", Air Force Astronautics Laboratory Report AFAL TR-87-073, August 1987.

3. Handbook of Chemistry and Physics, 50th ed., Chemical Rubber Company.

4. E. P. Cronkite and J. S. Robertson, "Somatic and Teratogenic Effects of Tritium", in Tritium, A. A. Moghissi and M. W. Carter, editors, Messenger Graphics (Phoenix and Las Vegas), 1973, pp. 198.

5. W. Seelengtag, "Two Cases of Tritium Fatality", ibid., pp. 267.

6. L. Quintana, General Atomics Health Physics Department, personal communication, 1988.

7. "Standards for Protection Against Radiation", US Nuclear Regulatory Commission, Code of Federal Regulations, Title 10, Chapter 1, Part 20, Revised January, 1986.

8. "Manual of Protective Action Guidelines and Protective Actions for Nuclear Incidents", Environmental Protection Agency AD/A119 287, September, 1975.

9. J. F. Santarius, "Lunar and ^{3}He, Fusion Propulsion, and Space Development", University of Wisconsin UWFDM-764, August, 1988.

10. "Starfire - A Commercial Tokamak Fusion Power Plant Study", Argonne National Laboratory Report ANL/FPP-80-1, September, 1980.

11. "The Titan Reversed-Field Pinch Fusion Reactor Study", Scoping Phase Report UCLA-PPg-1100, January, 1987.

12. A. Mohri, Y. Fujii-E, K. Ikuta, et al, "Conceptual Design of A Moving-Ring Reactor: Karin-I", Fusion Technology, Vol 9, May, 1986, pp. 422.

13. A. E. Robson, "A Conceptual Design for An Imploding-Liner Fusion Reactor (Linus)", Naval Research Laboratory NRL Memorandum Report 3861, September, 1978.

14. R. L. Miller, "Recent Progress in Stellarator Reactor Conceptual Design", Fusion Technology, Vol 8, No. 1, July, 1985, pp. 1581.

15. J. Santarius, K. Audenaerde, J. Beyer, et al, "WITAMIR-I, A Tandem Mirror Reactor with Non-Zero Nu", University of Wisconsin UWFDM-380, September, 1980.

16. "The PLASMAK™ Solution: The Answer for Space Power and Propulsion", Prometheus II Limited, Box 222, College Park, MD 20740, 1988.

17. D. K. Bhadra, General Atomics, personal communication, 1988.

18. B. C. Maglich, S. Menasian, R. A. Miller, et al, Phys. Rev. Letters, 54, 1985, pp. 796.

19. C. D. Orth, G. Klein, N. Hoffman, et al, "Interplanetary Propulsion Using Inertial Fusion", LLNL Report UCRL-95275 SUM, Rev. 1, October, 1986.

20. J. C. Nance, "Nuclear Pulsed Propulsion", General Atomic Company Report GA-5572, October 1964.

21. S. E. Jones, "Engineering Issues in Muon-Catalyzed Fusion", Fusion Technology, Vol 8, No. 1, July 1985, pp 1511.

22. Orth. C., et al, "Transport Vehicle for Manned Mars Missions Powered by Inertial Confinement Fusion" Paper No. AIAA-87-1904, presented at the AIAA/SAE/ASME/ASEE 23rd Joint Propulsion Conference, June 29-July 2, 1987, San Diego, California.

23. R. J. Goldston, "Energy Confinement Scaling in Tokamaks: Some Implications of Recent Experiments with Ohmic and Strong Auxiliary Heating", Plasma Physics and Controlled Fusion, Vol 26, No. 1A, January, 1984, pp. 87.

24. J. C. Fernandez, C. W. Barnes, T. R. Jarboe, et al, "Energy Confinement Studies in Spheromaks with Mesh Flux Conservers" Nuclear Fusion Vol 28, No. 9, 1988, pp. 1555.

25. J. Farber, Defense Nuclear Agency, Quoted in "Military Space", June 24, 1985, pp 6-7.

26. M. Dew, General Atomics Magnet Group, personal communication, 1988.

27. P. G. Hill and C. R. Peterson, Mechanics and Thermodynamics of Propulsion, Addison-Wesley, (Reading, MA), 1965.

28.   J. Reece Roth, Introduction Fusion Energy, Ibis Publishing Charlottesville, VA), 1986.

29.   "Space Shuttle System Summary", Rockwell International Space Systems Group Document SSV80-1, May, 1980.

30.   Patch, R. W., "Thermodynamic Properties and Theoretical Rocket Performance of Hydrogen to 100,000K and 1.01325×10^8 N/M^2" NASA SP-3069, NASA Lewis Research Center, 1971.

APPENDIX A

AN EVALUATION OF FUSION FUELS FOR SPACE PROPULSION

APPENDIX A

AN EVALUATION OF FUSION FUELS FOR SPACE PROPULSION

Summary

We briefly examine D-T and D-^{3}He for use as fuel for space propulsion. It is concluded that, even when the D-T neutron heating is thrown away and the neutron flux is shielded to a level comparable to the unshielded flux from D-^{3}He, D-T is a hard fuel to beat. This remains so even if the fuel mix in the D-^{3}He case is arranged so as to minimize neutron production.

Introduction

The current emphasis on "aneutronic" fusion fuels seems to be overlooking the fact that these fuels are generally quite difficult to utilize. In this memo, we attempt to make an honest evaluation of the "aneutronic" D-^{3}He fuel compared to D-T fuel. The truly aneutronic fuel, p-^{11}B, is also briefly examined.

Background

The qualitative features of fusion power are briefly reviewed below before commencing the detailed analysis. In thermonuclear fusion a certain density of fusion fuel is heated to ignition temperature, where the reaction is self-sustaining, and burned at a still higher temperature. The product of density and temperature is pressure or energy density, and one must be able to supply the energy needed to heat the fuel to ignition and also must contain the fuel pressure during the burn.

How much energy must be supplied depends on the confinement method used, the size of the device, and the fusion fuel. How much pressure must be contained depends on these and also on the power density desired. The energy can be supplied by ohmic heating, compression,

collision, radiofrequency, or particle beams. Also, D-T fusion fuel and, possibly, antimatter can be used to heat other fuels. The fuel pressure can be contained by magnetic fields, by inertia, or mechanically by rigid walls or gas blankets.

The magnitude of the energy that must be supplied to reach ignition is the sum of fuel internal energy at ignition plus the integrated energy losses from the fuel during the heating period. The latter can greatly exceed the former. These losses are made up of conductive and convective ion and electron losses plus photon radiation from hot electrons. The radiation losses are (1) Bremsstrahlung due to electron-ion interactions, (2) cyclotron due to electrons orbiting around magnetic field lines, and (3) line radiation due to impurities that are not fully ionized.

It is common to lump all of these losses into a characteristic "confinement time" defined as the fuel internal energy at steady state divided by the total power loss from the fuel. The product of fuel density and this confinement time is what is commonly called the "Lawson Criterion" and refers to the minimum confinement time and density product needed for ignition. It becomes mainly irrelevant after ignition is achieved. Then the issue is how much power can be produced during the burn and therefore how much fuel pressure can be contained. The quality of confinement is then important and this is usually indicated by the ratio of fuel pressure to confining pressure, commonly referred to as the "beta". This is discussed later.

With this qualitative background, we turn now to some of the quantitative expressions for fusion and examine the characterisics of different fusion fuels.

Fusion Reaction Rate

The fusion reaction rate per unit volume is given by

$$R = \begin{cases} n_1 n_2 \langle \sigma V \rangle \leq n^2 \langle \sigma V \rangle / 4 \\ n^2 \langle \sigma V \rangle / 2 \end{cases} \tag{1}$$

where n is the total fuel density (ions/m³) and $\langle \sigma V \rangle$ is the fusion reaction probability or cross section. The upper branch is for unlike fuels 1 and 2 (e.g., deuterium and tritium), while the lower branch is for single species fuels (e.g., D-D). The $\leq$ sign is included because reactivity falls off if $n_1 \neq n_2$, as is discussed later.

The fusion cross section $\langle \sigma V \rangle$ is a function of the mean fuel temperature and the temperature distribution. It is typically given for a Maxwellian distribution, although there are cases where other distributions are more suitable. It is a strong function of temperature and does not become at all significant until temperatures of over 2000 eV are reached (1.0 eV $=$ 11,600 K). It is because such high temperatures are required that most of the effort in controlling fusion has been to overcome the heat losses due to the astonishing temperature gradients (order 10^8 K/meter) either by limiting the time for such losses (inertial confinement) or effectively reducing the thermal conductivity of the fuel (magnetic confinement).

Reactivity At Constant Pressure

While $\langle \sigma V \rangle$ is an important measure of fusion fuel performance, a *more significant* quantity is reaction rate for a given fuel pressure, since all of the reactor engineering effort goes into containing that pressure. It is actually more convenient to use the square of the pressure since that eliminates density, i.e.,

$$\frac{R_{fusion}}{p^2} \sim \frac{n^2 \langle \sigma V \rangle}{(nT)^2} = \frac{\langle \sigma V \rangle}{T^2} \tag{2}$$

noting that pressure is nT. Fusion fuel products are either energetic neutrons or charged particles. The latter are of greater usefulness in fusion propulsion. Table 1 shows the product energy breakdown for four fuels of interest. Note that the D-D reaction branches into two product sets having about equal probability of reaction. Note also that the so-called "aneutronic" D-^{3}He fuel also produces neutrons from the D-D reaction. While the production rate is small, it is significant enough to warrant considerable study, as discussed below.

The most useful figure of merit for space propulsion is $\langle \sigma V \rangle Q^+/T^2$ because it gives a measure of charged particle power available per unit fuel pressure. This is shown for three fuels in Fig. 1.

The curves in Fig. 1 are plotted with linear coordinates to show proper perspective of the differences in power levels and temperatures for the three fuels. This tends to be obscured in log-log plots. It is seen from the figure that maxima in $\langle \sigma V \rangle Q^+/T^2$ exist *for each of the*

TABLE 1
FUSION FUEL REACTION PRODUCT ENERGIES

FUEL	Q^+, CHARGED PARTICLE ENERGY, MeV	Q_n, NEUTRON ENERGY, MeV
D-T	3.52	14.1
D-D (n)	0.817	2.45
D-D (T)	4.03	0.
D-^{3}He	18.35	2.45
p-^{11}B	8.664	0.
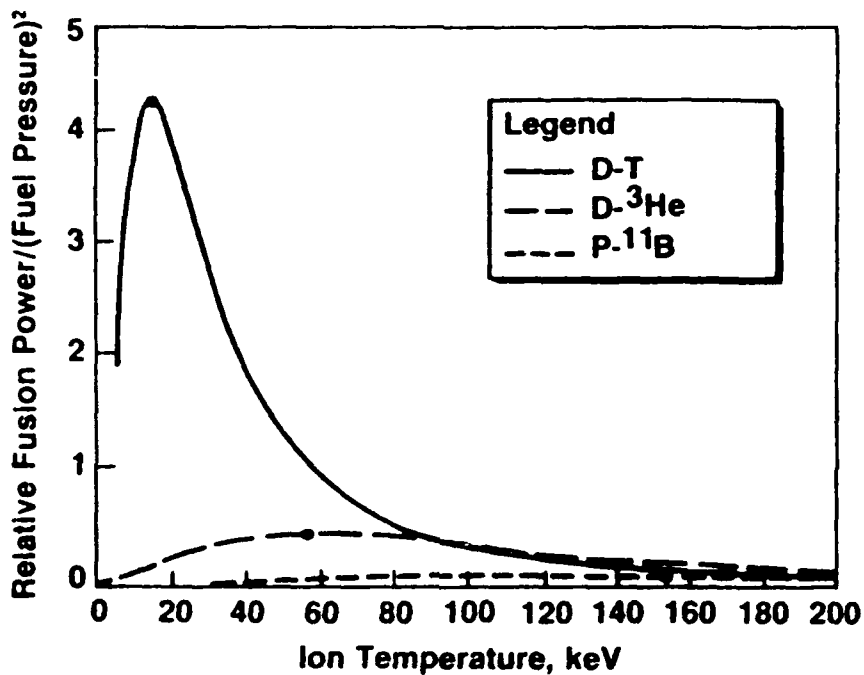
Figure 1. Fusion fuel charged particle power for a given fuel pressure

fuels. For D-T, it is centered around 13 keV, around 55 keV for D-^{3}He, and around 140 keV for p-^{11}B.

An unescapable point shown in Fig. 1 is that D-^{3}He has 1/10 the charged particle power density as D-T for the same fuel pressure. The fuel p-^{11}B has 1/100 the charged particle power density of D-T. When D-T neutrons are included, the gap is 50 to 1 for the first two fuels.

The nominal ignition temperatures vary considerably depending on the kind of confinement and the impurity level. D-T ignites at about 6 keV, well below the optimum, while D-^{3}He ignites at 60 keV, just about at the optimum. The third fuel, p-^{11}B may ignite only if the electron temperature is well under the ion temperature. However, because reactivity is so low, high fuel densities are needed for reasonable power density. At such densities, heat conduction between ions and electrons is greater than the fusion power produced, and therefore electrons will be about at the same temperature as the ions. Table 2 summarizes ignition requirements and optimum burn temperatures for the fuels shown in Fig. 1.

D-D fuel is not shown in Fig. 1 because it is not of interest for propulsion: Not only does it produce considerable neutrons as D-T does, but its reactivity is much lower than D-T. There is a variant of D-D, called "catalyzed-D", that has reactivities approaching D-^{3}He. Here the ^{3}He and tritium products of the D-D reaction, which migrate out of the fuel before reacting, are separated out and reinjected into the fuel and reacted. They do not react prior to leaving the reactor because, being a reaction product themselves, their density is very low. Their reaction rate is therefore much lower than the transport rate out of all known methods of confinement. Because catalyzed-D requires a relatively elaborate separation and reinjection scheme and, considering that reactivites are still less that D-^{3}He, it does not appear that attractive for fusion space power.

TABLE 2
CHARACTERISTIC FUSION FUEL TEMPERATURES
(keV)

FUEL	IGNITION	BURN
D-T	6	15
D-^{3}HE	60	75
P-^{11}B	–	140

Effect of Fuel Choice on Reactor Design

Let us now consider the effect of these differences in power density on reactor parameters. First note that the total charged particle fusion power is given by

$$P^+ = RQ^+V \quad , \tag{3}$$

$$P^+ \sim \frac{\langle \sigma V \rangle}{T^2} p^2 Q^+ V \quad , \tag{4}$$

where Eq. (2) has been employed and V is the fuel volume. Regardless of confinement method, there is always a figure of merit that ratios the fuel pressure to the confining pressure. Taking magnetic confinement as an example, this ratio is called the "beta", defined by

$$\beta = \frac{p}{p_m} \sim \frac{p}{B^2} \quad , \tag{5}$$

where p is the plasma pressure and p_m is the magnetic confining pressure. Using this in Eq. (4) gives,

$$P^+ \sim \frac{\langle \sigma V \rangle}{T^2} Q^+ \beta^2 B^4 V \quad . \tag{6}$$

It is clear that, for example, if $\langle \sigma V \rangle Q^+ / T^2$ is reduced by a factor of 10, as it is when one goes from D-T to D-^{3}He (see Fig. 1), then the combination $\beta^2 B^4 V$ must be increased by the same factor. And since the limits on β and B are independent of fusion fuel, they would be at peak values in any case. This assumes that other limits, such as wall heat

flux, have not been reached first, which seems appropriate for this futuristic study. Therefore, the fuel volume V must be a factor of 10 larger for D-^{3}He compared to D-T.

Needless to say, this factor of 10 increase has a profound effect on other reactor components. Not only are plasma chambers, reactor blankets, magnets and other nuclear island components increased accordingly, but power supplies and energy storage requirements increase as well. This is discussed later.

Neutron Production With D-^{3}He Fuel

The only reason to use D-^{3}He fuel is to minimize neutron production. As seen in Table 1, some 2.45 MeV neutrons are produced from the D-D reaction. To minimize this, we need to minimize the fraction of deuterium in the fuel. How this affects performance is discussed below.

If f_d is the deuterium fuel density fraction, then the fusion power level is proportional to $f_d(1 - f_d)$. The neutron production rate due to the D-D(n) reaction chain is proportional to f_d^2. Therefore, for a fixed fusion power, the neutron production rate is proportional to $f_d/(1-f_d)$. These are plotted in Fig. 2 for deuterium fuel fractions from 0 to 0.5. Relative values are used, and therefore are independent of temperature. Clearly, in reducing the number of neutrons, a price is paid in lower fusion power. Most likely, one would not go below a 50% power reduction and therefore the minimum deuterium fraction would be limited to about 0.15. For a given fuel density, the neutron production rate would be only 9% of the maximum rate, which occurs with 50% deuterium. However, to maintain a given power level, fuel volume must be increased by a factor of two. The factor of ten increase in fuel volume over an equal-power D-T reactor now becomes a factor of 20. With this 15% deuterium fraction, the neutron production rate at fixed fusion power is about 18% of the maximum value. How this compares with D-T is discussed below.
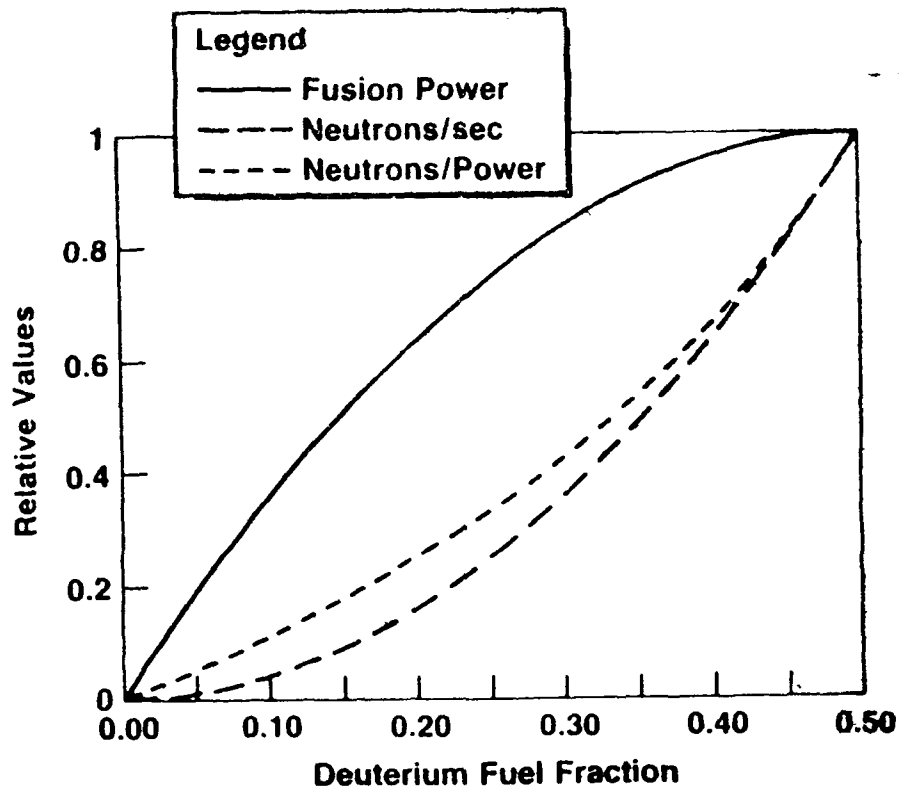
Figure 2. Effect of Deuterium fuel fraction for D-³He fusion fuel

Comparison of D-³He and D-T Neutron Production

In this section we compare the neutron production from two equal-power reactors: One with D-T and the other with D-³He running with 15% deuterium to minimize neutron production. The purpose of this comparison is to examine, with respect to neutron production, the relative overall penalties of using the two fuels. We use the example

of magnetic confinement, although it is likely that the same general conclusions will apply to all forms of confinement. Based on arguments presented earlier, we assume that

$$\beta_{DT} = \beta_{DH} \quad , \quad B_{DT} = B_{DH} \quad ,$$

and therefore, $P_{DT} = n_{DT}T_{DT} = P_{DH}$. $\quad (7)$

In Eq. (7), DH refers to D-^{3}He fuel. Using the burn temperatures shown in Table 2, for equal fuel pressure p,

$$n_{DT} = 5n_{DH} \quad . \quad (8)$$

The neutron production rate for each fuel is

$$\dot{N}_{nDT} = \frac{n_{DT}^2}{4} \langle \sigma V \rangle_{DT} V_{DT} \quad ,$$

$$\dot{N}_{nDH} = \frac{(.15n_{DH})^2}{2} \langle \sigma V \rangle_{DH} V_{DH} \quad . \quad (9)$$

It is not total neutron production rate but neutron flux I (n/sec-cm^2) that must be estimated:

$$I = \frac{\dot{N}}{A} \sim \frac{\dot{N}}{V^{2/3}} \quad . \quad (10)$$

It was shown above that $V_{DH} = 20V_{DT}$, which includes the factor of two power loss due to running helium-rich. Using this and Eq. (9) gives

$$\frac{I_{DT}}{I_{DH}} = 200 \ \frac{\langle \sigma V \rangle_{DT}}{\langle \sigma V \rangle_{DH}} \quad . \tag{11}$$

We would expect to operate the two fuels at their respective peaks in $\langle \sigma V \rangle / T^2$ shown in Fig. 1. The optimum D-T temperature is 15 keV and here $\langle \sigma V \rangle = 2.72 \cdot 10^{-22}$ m^3/sec. The optimum D-^{3}He temperature is 75 keV and here $\langle \sigma V \rangle = 1.295 \cdot 10^{-22}$ m^3/sec. Using these cross sections, the ratio of neutron fluxes is

$$\frac{I_{DT}}{I_{DH}} = 430 \quad . \tag{12}$$

Solid shielding reduces the neutron flux exponentially roughly according to

$$\frac{I}{I_o} = e^{-x/\lambda} \tag{13}$$

where I_o is the neutron flux incident on the shield and λ is a characteristic e-fold length that is dependent on the shield material, void fraction, and neutron spectrum. For earth-bound fusion reactors, the shield material might be high-density stainless steel, which has $\lambda \simeq 10$ cm for neutron spectra above about 1.0 MeV. For space use, we wish to radiate the heat at high temperature and therefore would probably opt for low-density ceramics such as SiC and carbon. Although the total mass of shield would be about the same, it would be thicker because $\lambda \simeq 20$ cm with these low-Z materials.

The question at hand is, how much extra shielding is needed for the D-T neutron flux compared to D-^{3}He? The required shield thickness is, from Eqs. (12) and (13),

$$x = \lambda \ln 430 = 6.1\lambda \quad ,$$

which, for our low density shield, gives $x = 122$ cm. This is the additional shielding that a D-T fuel reactor requires to give an escaping neutron flux equal to a D-^{3}He reactor running with 15% deuterium. While this may seem like a lot, it must be remembered that this shield envelops a much smaller first wall area because the D-T reactor is so much more compact. At issue is the total mass of the D-T reactor with 1/20th the plasma volume but with 1.2 m of shield vs. the D-^{3}He reactor with no shield but with 20 times the plasma volume and comparably larger nuclear island, power supplies, and energy storage.

Because the D-^{3}He reactor produces some neutrons, it also requires shielding. How much depends on allowable leakage fluxes. The 75 keV D-^{3}He plasma also produces penetrating X-rays that may also require shielding. It is fair to ask, then, how much shielding thickness in the larger D-^{3}He reactor would be required to equal the mass of the D-T reactor shield? The shield volume is

$$V_s = x A_{wall} \quad ,$$

where A_{wall} is the first wall area and is proportional to $V_{plasma}^{2/3}$ so can therefore show that, for equal shield volumes,

$$\frac{x_{DT}}{x_{DH}} = \left(\frac{V_{DH}}{V_{DT}}\right)^{2/3} = 20^{2/3} = 7.37 \quad .$$

Therefore, if $x_{DH} = x_{DT}/7.37 = 122/7.37 = 16.6$ cm, the shield volumes are equal and D-^{3}He shows no advantage with respect to shielding. As mentioned above, shielding of this thickness range may be needed in any case.

Heat Rejection

Eighty percent of the DT fusion power is in neutrons. If only the charged particle energy is used, the neutron power must be disposed of by radiating into space. While this may seem wasteful, it must be remembered that, even considering charged particle energy only, D-T is ten times more energetic than D-^{3}He (20 times if an effort is made to reduce neutrons from D-^{3}He). The area required for the T^4 radiated energy, assuming $\varepsilon = 0.9$, is shown in Fig. 3. In this futuristic study, it is safe to assume that high temperature ceramic radiators will be viable. Silicon carbide can safely withstand temperatures to 1700 K while graphite can go to perhaps 3000 K. In the last case, it is seen from the figure that only about 25 m^2 per 100 MW(th) are needed to get rid of the heat. It is likely therefore that the back surface of the shield itself can be used as radiator; no additional radiator will be required. Heat pipes embedded in the shield can be used to transfer the internal heating to the radiator surface.

Power Supplies and Energy Storage

It is easy to forget that the mundane equipment on the periphery can overshadow the reactor itself. Because fusion is thermonuclear, heat must be supplied to get it going. How much depends on the required internal energy at ignition and the losses that result during the heating. In this section, we form a crude ratio of heating energies for the reactors discussed above.

The ignition temperatures for D-T and D-^{3}He are given in Table 2 and are 6 and 60 keV, respectively. The fuel density for equal pressure at burn is given by Eq. (8) which shows the D-T density to be 5 times the D-^{3}He density. The D-^{3}He fuel volume for equal power with 15% D was shown above to be 20 times the D-T volume. The minimum internal energy required to heat the fuel to ignition is $3nkT_{ign}/2$. With this information, it can be shown the the ratio of ignition energies is
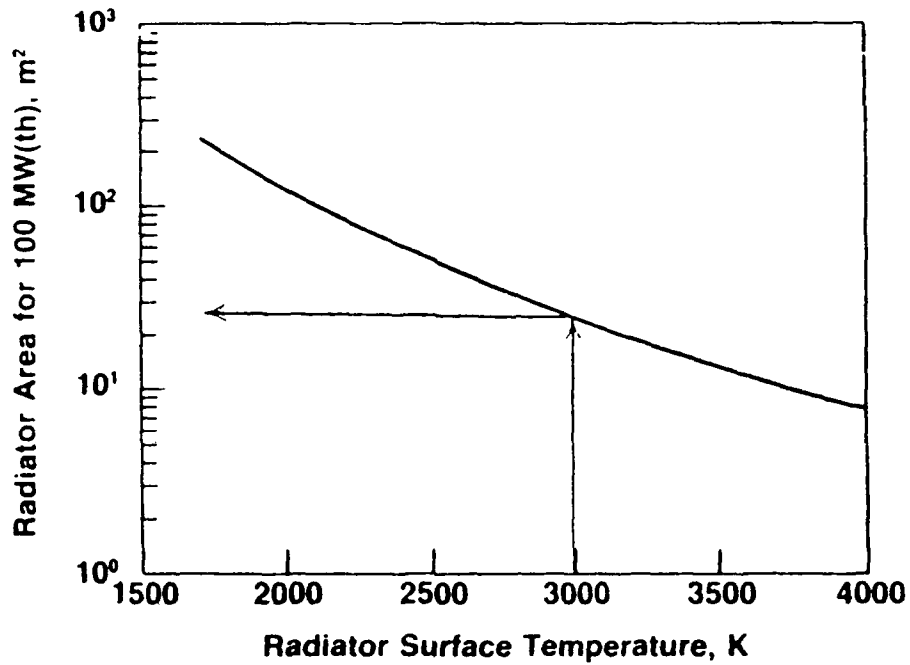
Figure 3. D-T NEUTRON POWER REJECTION

$$\frac{E_{DH}}{E_{DT}} = \frac{n_{DH} \cdot 60 \text{ keV}}{5n_{DH} \cdot 6 \text{ keV}} = 2 \quad .$$

Twice the energy must go into heating D-^{3}He as D-T for equal power, equal pressure reactors. Therefore, twice the energy must be stored presumably resulting in twice the energy storage hardware mass.

A-14

This simple analysis ignores power losses during the ignition ramp, which can dominate the process. These losses are a complicated issue and beyond the scope of this work. However, some words are in order because the losses are so significant. If the plasma confinement increases with dimension, then the D-^{3}He reactor will be better confined and losses may be less than D-T. However, if losses increase with temperature gradient, then the reverse will be true and the factor of 2 above will increase. The actual loss mechanism is specific to the reactor concept.

Conclusions

The incentive for using D-^{3}He fusion fuel is to reduce neutron production. There is no other reason. This analysis has shown that the price paid in reduced reactivity is excessive, especially considering that a reasonable shield around the D-T reactor will also reduce escaping neutron flux to acceptable levels.

The truly aneutronic p-^{11}B fuel has reactivities so far below D-T as to place it out of the running. To make things worse, temperatures required are over 100 keV, which are very difficult to achieve. Finally, this fuel does not ignite and therefore large power inputs are continuously required to keep it going.

These conclusions are dependent mainly on fuel reactivities and not on reactor embodiments. Therefore, it is unlikely that progress in fusion confinement research will alter them.

APPENDIX A

REFERENCES

1.   J. Rand McNally, Jr., "Physics of Fusion Fuel Cycles", Nuclear Technology/Fusion, Vol 2, Jan. 1982, p. 9.

2.   J. Rand McNally, Jr., K. E. Rothe, and R. D. Sharp, "Fusion Reactivity Graphs and Tables for Charged Particle Reactions", Oak Ridge National Laboratory ORNL/TMN-691, Aug. 1979.

APPENDIX B

THE EFFECT OF BREMSSTRAHLUNG RADIATION ON THE UTILIZATION OF FUSION FUEL CHARGED PARTICLE POWER FOR PROPULSION

APPENDIX B

THE EFFECT OF BREMSSTRAHLUNG RADIATION ON THE
UTILIZATION OF FUSION FUEL CHARGED PARTICLE POWER
FOR PROPULSION

Summary

The photon radiation from the interaction of electrons with ions
in a fusion plasma, called Bremsstrahlung radiation, is a basic loss
mechanism that is independent of the method of confinement. We examine
the ratio of Bremsstrahlung radiation to fusion charged particle power
produced for D-T and D-^{3}He fuels and conclude that this radiation loss
is minor for a D-T plasma but is more than half for a D-^{3}He plasma when
one attempts to minimize neutrons by running helium-rich. This makes
the latter fuel hard to utilize for space propulsion.

Introduction

Alternate fusion fuels such as D-^{3}He produce reaction products
that are mainly charged particles. These particles thermalize with the
main plasma and maintain the plasma at burn temperature. Utilization
of this energy directly for space propulsion requires that the energy
remain in the plasma as particle kinetic energy. Then it can be
readily transferred by dilution to a propellant. On the other hand, if
this energy is lost to the surrounding hardware, then the same material
temperature limits that restrict other methods of propulsion will apply
here as well.

A fundamental loss mechanism that cannot be avoided is
Bremsstrahlung radiation which results from the motion of electrons in
the vicinity of ions. This radiation is dependent upon the plasma
makeup alone and not on the particular confinement concept. Being of
UV through soft X-ray wavelengths, it propagates through a plasma
without being reabsorbed, and is absorbed by solid walls without being
reflected. If it is a large fraction of the charged particle power
produced, then that power cannot be effectively utilized for propulsion

except in the conventional manner that involves heat transfer from material walls. While this is acceptable for electric power generation, it poses problems for direct conversion of plasma energy to propulsive momentum by means of propellant injection.

In this memo, we examine the ratio of Bremsstrahlung power to fusion charged particle power produced for the two fuels of interest for propulsion: D-T and D-^{3}He. We examine the latter under differing conditions of electron to ion temperature ratios and D/^{3}He fuel mix proportions.

Analysis

The Bremsstrahlung power density in watts/m^3 is given by (Ref. 1)

$$P_b = Sn_e^2 Z_{eff} T_e^{1/2} \quad , \tag{1}$$

where $S = 1.625 \cdot 10^{-38}$ is the Bremsstrahlung constant, n_e is the electron density in m^{-3}, T_e the electron temperature in eV, and Z_{eff} is the effective atomic number of the plasma and is given by

$$Z_{eff} = \frac{1}{n_e} \sum_j n_{ij} Z_j^2 \quad ,$$

where $\hspace{10cm}$ (2)

$$n_e = \sum_j n_{ij} Z_j \quad .$$

In Eq. (2), Z_j is the atomic number of ion species j. In this memo, species 1 is D or T for D-T and D for D-^{3}He. Species 2 is ^{3}He. Clearly, $Z_1 = 1$ and $Z_2 = 2$.

The fusion charged particle power density fuel species 1 and 2 is given by

$$P_f = n_1 n_2 \langle \sigma V \rangle Q^+ \quad , \tag{3}$$

where $\langle \sigma V \rangle$ is the fusion reaction cross section in m^3/sec and Q^+ is the charged particle energy per reaction. All this was discussed in Ref. 2. For a 50-50 D-T mix, $n_1 n_2 = n_i^2/4$ where n_i is the total ion density. For a D-^{3}He mix, we would expect to run it helium-rich to minimize neutron production. The most extreme proportion is about 15% deuterium (85% helium), and then $n_1 n_2 = 0.128 n_i^2$. With this mix, fusion power density is cut in half, and neutron production at fixed fusion power is cut by a factor of 5 (Ref. 2). This D-He mix also gives $n_e = 1.85 n_i$ and $Z_{eff} = 1.92$. For any mix of D-T, $n_e = n_i$ and $Z_{eff} = 1.0$.

Note that the introduction of impurities will raise both n_e and Z_{eff}, and can greatly increase the radiation loss. For a given fuel pressure limit, these impurities also displace fuel, lowering fusion power. Bremsstrahlung radiation, like fusion power, depends on n^2. Therefore, the ratio of the two is independent of density. However, the radiation goes like $\sqrt{T}$ while fusion power, in the optimum temperature region, goes like T^2. The ratio of the two then goes like $T^{-3/2}$. This is strictly true only when $T_e = T_i$. In the results below, we also look at the case when the $T_e < T_i$, which would reduce the radiation loss.

Results with $T_e = T_i$

Fig. 1 shows the ratio of Bremsstrahlung power loss to fusion charged particle power for D-T and D-^{3}He fuels. Here the electron temperature is equal to the ion temperature and the D-^{3}He fuel mix is 15% D, 85% ^{3}He, which minimizes neutron production. Results are also shown later for other fuel mixes and ratios of T_e/T_i. The theoretical ignition point is when this ratio is 1.0 (solid line). It is around 4.0 keV for D-T and 55 keV for D-^{3}He. Actual ignition points are higher because of impurities, other forms of photon radiation, and plasma conductive and convective losses.
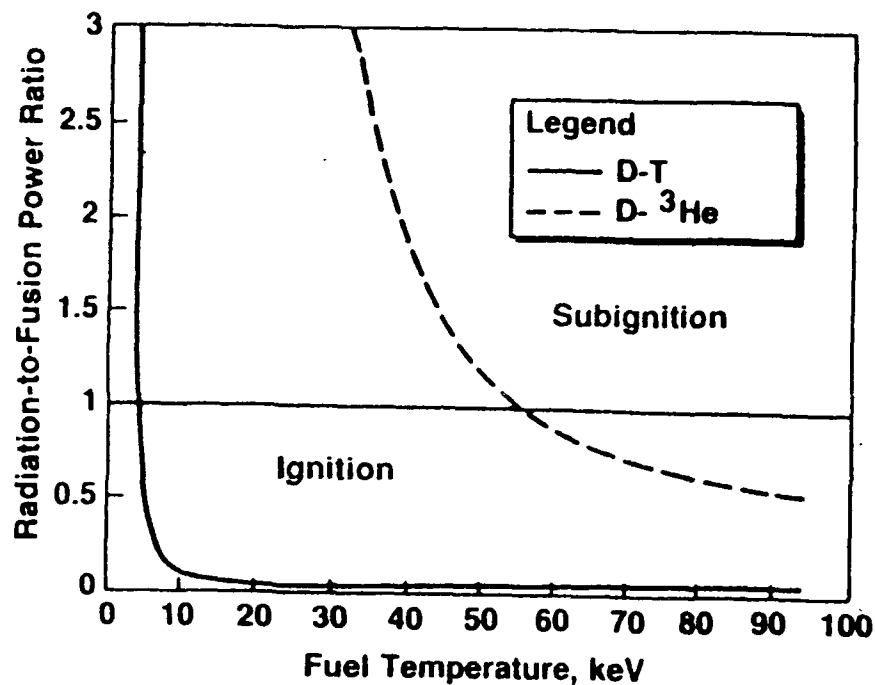
Figure 1. COMPARISON OF BREMSSTRAHLUNG RADIATION POWER-TO-FUSION CHARGED PARTICLE POWER

Auxiliary heating of the plasma is required until this power ratio falls below 1.0. It may be possible to heat D-T ohmically up to the 4.0 keV ignition point. However, because plasma resistivity goes like $T_e^{-3/2}$, it is very unlikely that enough $I^2 R$ heating can be supplied to bring a D-^{3}He plasma up to the 55 keV ignition point.

Optimum burn temperatures are 13 keV for D-T and 75 keV for D-^{3}He. These temperatures are where the fusion reactivity for a given pressure is maximum (see Ref. 2). For D-T, the Bremsstrahlung radiation loss has dropped to about 6% of the charged particle power at 13 keV. However, for D-^{3}He at 75 keV, the radiation is 67% of the fusion power. To be self-sustaining, other losses cannot exceed 33% of the fusion

power. This is highly unlikely: In real confinement devices, conductive and convective losses are considerable. If magnetic fields are present, cyclotron radiation also occurs. Finally, line radiation may occur near the plasma boundary resulting from impurities that are not fully stripped. These other losses may well add up to drive a D-^{3}He plasma to subignition even at temperatures over 80 keV. D-T Bremsstrahlung losses, on the other hand are so low that it would take substantial other losses to drive D-T to below ignition.

If one wishes to transfer the fusion power to a propellant during the fusion burn, it must be done via the conductive and convective heat transport across the plasma boundary. If all that is left of D-^{3}He fusion power after losses from radiation is 33% of the total, the viability of that fuel is cast into serious doubt. On the other hand, up to 94% of the charged particle power is retained in a D-T plasma after Bremsstrahlung loss. Up to this much can therefore be transferred to a propellant.

Effect of Lowering Electron Temperature

It was mentioned earlier that Bremsstrahlung radiation loss goes with electron temperature while fusion power goes with ion temperature. At very high temperatures, these tend to decouple from each other and electron temperature will drop off somewhat. Fig. 2 shows the effect of this on radiation to power ratio for T_e/T_i from 0.1 to 0.9 (1.0 is shown in Fig. 1).

While depressing electron temperature has an effect, it goes with $\sqrt{T}$ and is therefore not as great as one would like. At reasonably high power densities, it is unlikely that T_e would fall below about 0.7 T_i (see Refs. 3-7). Still fully half of the fusion power would be lost to Bremsstrahlung.
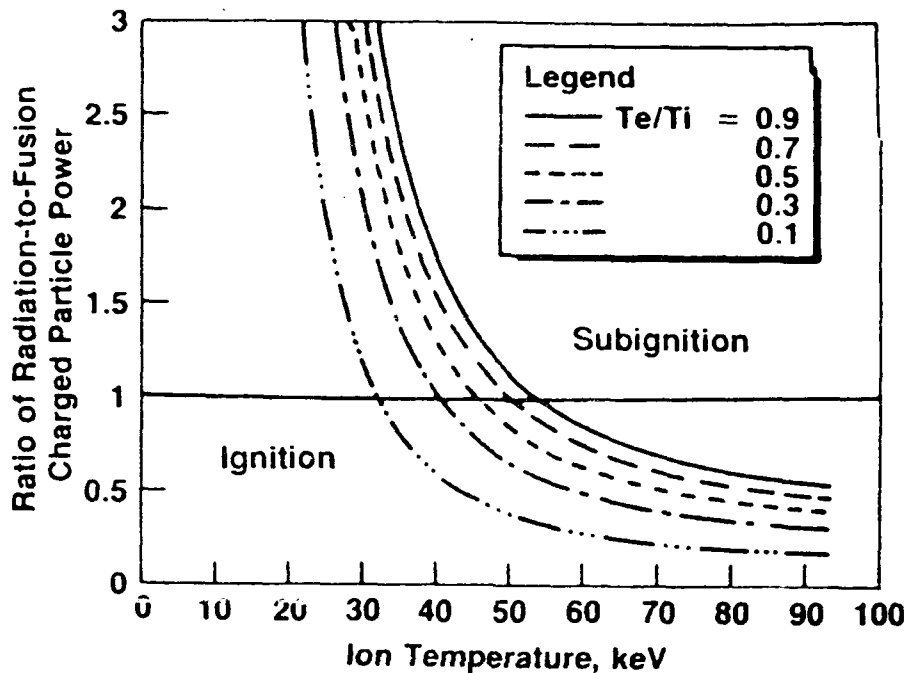
Figure 2. D-³He BREMSSTRAHLUNG RADIATION -TO-FUSION CHARGED PARTICLE POWER RATIO AS A FUNCTION OF ELECTRON TEMPERATURE

Effect of Different D-³He Fuel Mixes

The results above are for the extreme case os 15% D and 85% ³He, chosen to reduce neutron production to an absolute minimum. If one relaxes this condition and runs the fuel with more deuterium, then the ratio of Bremsstrahlung to charged-particle power is reduced, but at the cost of increased neutrons. This is shown in Fig. II-3 for four deuterium fractions and $T_e/T_i = 0.7$, which is the lowest probable ratio likely. Clearly, by going to 25% deuterium, the radiation fraction at $T_i = 75$ keV drops from about 55% to about 30%. With a 50-50 mix, the
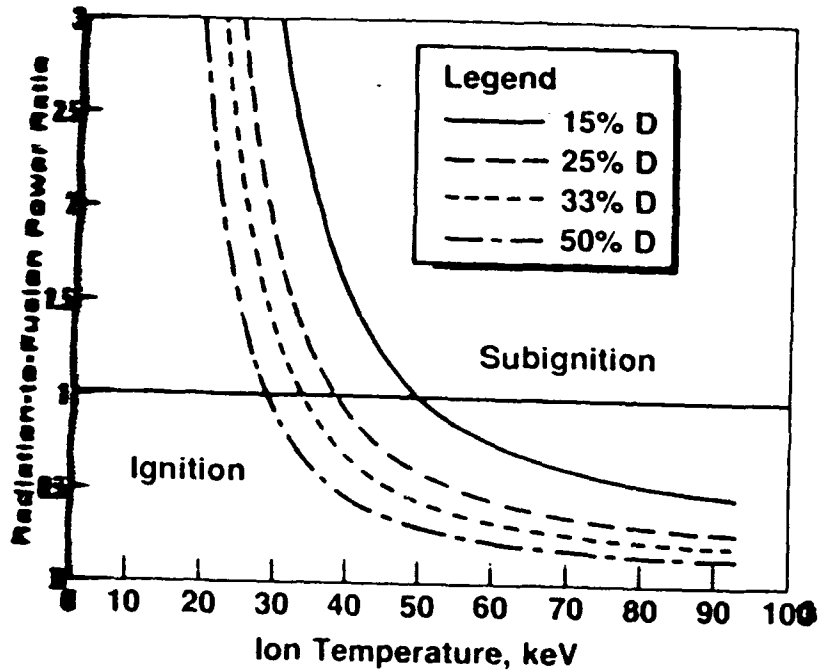
Figure 3. D-^{3}He BREMSSTRAHLUNG RADIATION -TO-FUSION CHARGED PARTICLE POWER RATIO FOR 4 DEUTERIUM CONCENTRATIONS (Te/Ti = 0.7)

radiation fraction is under 20%. These numbers approach acceptability but, again, at the cost of increased neutron production.

Discussion

There may be a way of utilizing Bremsstrahlung radiation for thrusting. Clement Wong of GA has suggested using metal particles. This could be generalized to perhaps smoke or carbon soot entrained in the propellant gas. Being opaque, they would absorb the radiation until they vaporized. The resulting propellant temperature could be as

high as the vaporization temperature of carbon, about 4000 K, resulting in fairly high I_{sp}.

The radiation to fusion power ratio may be altered by changing the energy distribution of the plasma. Dilip Bhadra has commented that all of the above applies only to a Maxwellian plasma distribution. Results could be very different if the plasma energy distribution were closer to monoenergetic.

Also, spin polarization may achieve the same result in suppressing neutron production (Ref. 4) as running the fuel helium-rich. However, this could yield an enhancement in power rather than a decrease.

These ideas, while innovative, also serve to restrict the options available. Considering the inherent difficulty in getting fusion to work at all, it is not clear if that is the proper direction to move toward.

Conclusions

Bremsstrahlung radiation may be a dominant loss mechanism for D-³He fuel and therefore it could be very difficult to utilize this fuel for propulsion purposes. When combined with other losses, it may not be possible to ignite D-³He at all. The most severe case is when attempts are made to limit neutron production by running the fuel helium-rich.

On the other hand, Bremsstrahlung loss is negligible for D-T fuel, making it much easier to use for propulsion and more likely that it will remain ignited.

Recommendation

D-T fuel should not be overlooked even though it produces neutrons. In order for D-^{3}He to be at all viable, it must be run near a 50-50 fuel mix and therefore will also produce significant neutrons. We should explore the ramifications of using D-T including shielding, tritium supply, and mitigation of material damage due to neutrons.

We should also explore the possibility of using entrained particles to absorb radiation losses from D-^{3}He plasmas.

Finally, we should explore the ramifications of using a non-Maxwellian plasma temperature distribution and/or spin polarization.

References

1. J.R. Roth, Introduction to Fusion Energy, Ibis Publishing, Charlottesville, VA, 1986.

2. R.F. Bourque, "An Evaluation of Fusion Fuels for Space Propulsion", Fusion Propulsion Technical Memorandum No. 2, March 21, 1988.

3. J.F. Santarius, "Very High Efficiency Fusion Reactor Concept", Nuclear Fusion, 27 No. 1 (1987), p. 167.

4. G.W. Shuy, A.E. Dabiri, and H. Gurol, "Conceptual Design of a Deuterium-^{3}He Fueled Tandem Mirror Reactor Satellite/Breeder System", Fusion Technology, v. 9, May 1986, p. 459.

5. J. Galambos and G.H. Miley, "Effects of Enhanced Ion/Electron Equilibria", 5th ANS Topical Meeting on the Technology of Controlled Fusion Energy, Knoxville, TN, April 26-28, 1983.

6. J.F. Clarke, "Hot-Ion Mode Ignition in a Tokamak reactor", Nuclear
   Fusion 20, No. 5 (1980), p. 563.

7. J. R. McNally, "Physics of Fusion Fuel Cycles", Nuclear
   Technology/Fusion, v. 2, Jan 1982, p. 9.

APPENDIX C

**AN EVALUATION OF TRANSLATING COMPACT TORI
FOR FUSION SPACE PROPULSION**

APPENDIX C
AN EVALUATION OF TRANSLATING COMPACT TORI
FOR FUSION SPACE PROPULSION

SUMMARY

We explore two modes of translating compact tori such as spheromaks as possible fusion reactors for space propulsion. The first mode uses adiabatic compression by injecting the torus into a converging conducting channel. The second uses the collision and merging of two tori travelling in opposite directions. It is found the the latter may hold more promise from a technology point of view but the former has shown greater likelyhood of working.

INTRODUCTION

Compact tori are a class of toroidal plasma confinement where poloidal and toroidal magnetic fields are comparable and where both fields are generated internally by a plasma current that has considerable pitch off-axis. Examples of compact tori are the spheromak and the field-reversed configuration (FRC). The former, which we will devote most of the time here, is shown in Fig. 1.

Because compact tori have no external magnetic fields, they are free to move about. It is this feature that makes them attractive to us because it opens up two mechanisms for heating to ignition: (1) adiabatic compression by firing them into a converging channel, and (2) firing two of them at each other in such a way that the merge into one and convert their kinetic energy to thermal. These two concepts are shown schematically in Fig. 2. The actual plasma cross section is shown. However, the analysis below will used a simplified circular cross section. The conducting shells provide image currents that stabilize the plasma. When the plasma is moving with respect to the conducting shell, the penetration of flux into the shell, which is a waste of flux and energy, is negligible and the shell acts as if it
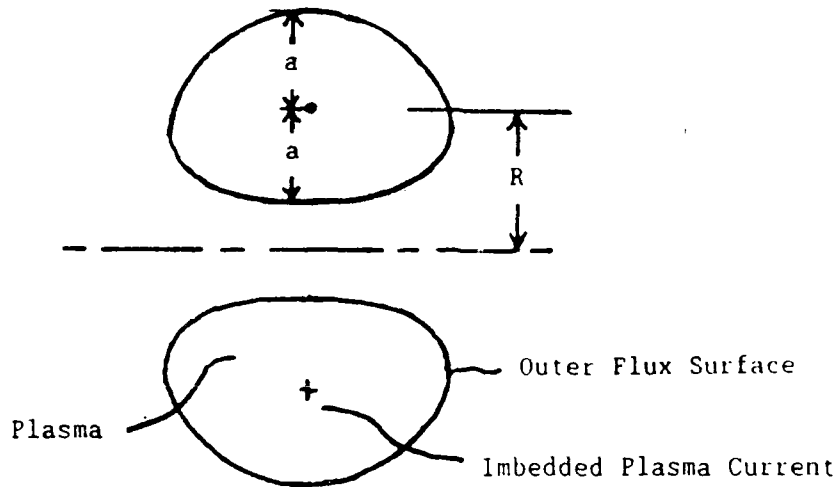
Fig.   1.   The spheromak configuration.

were superconducting. Therefore, virtually any conducting material can be used.

Acceleration of spheromaks to high velocities has been achived experimentally. In the RACE experiment at LLNL, velocities over 1,500,000 m/sec have been achieved with acceleration forces comparable to the magnetic forces holding the plasma together[1]. Energy efficiencies have been as high as 30%, defined as the resulting plasma kinetic energy divided by the accelerator electrical energy.

Spheromaks have also been successfully driven toward each other and merged. In the TRISOPS VIII experiment, adiabatic compression has been combined with merging to produce ion temperatures up to 6 keV and

---

* Numbers refer to references at the end of this memo.
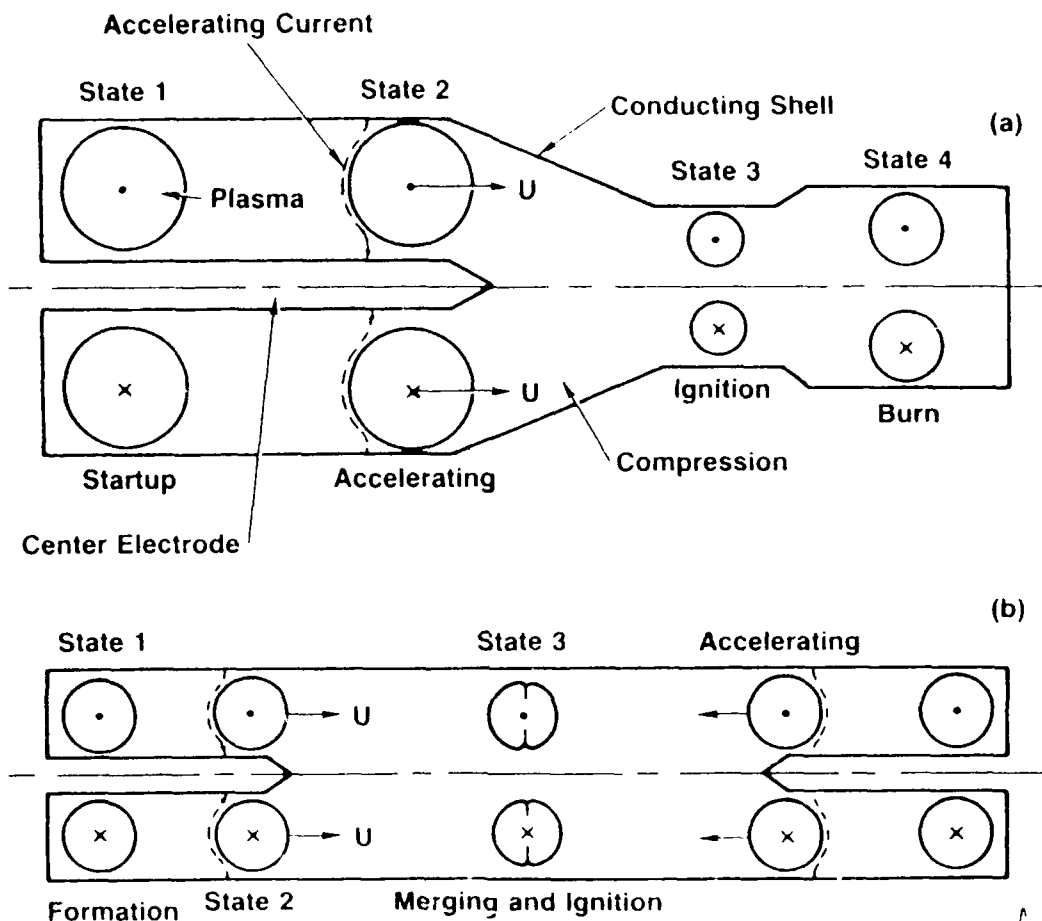
Fig.   2. Schematic of two methods for heating compact tori:
            (a): Adiabatic compression.   (b): Merging.

significant neutron production with deuterium[2]. It is because of the
success of these experiments that these two approaches warrant
considerable study for fusion propulsion.

In the next section, we examine the dynamics of adiabatic
compression. After that, we look at the prospect of merging spheromaks
by firing them at each other.

ANALYSIS OF ADIABATIC COMPRESSION

General

In the translating adiabatic compression system, a spheromak is initially formed, then accelerated to high velocity, then compressed in a converging conducting channel, and finally moved to a fusion burn chamber. This is shown schematically in Fig. 2a.

The spheromak is formed in state 1, either by electrodes or inductively, and ohmically heated to modest temperature, perhaps 100 eV. It is accelerated using a coaxial railgun to high velocity (state 2). The sheet current that does the accelerating stays around the edge of the plasma because not enough time is available to allow it to soak through to the interior. At state 2, the plasma is still at about 100 eV but the velocity corresponds to a directed energy which, after compression, gives an plasma ion temperature of 6 keV, the nominal ignition temperature for D-T (See Ref. 2 for a discussion of why this is the preferred fuel). The plasma is slowed and compressed to state 3 by driving it into a converging channel. Image currents in the channel keep the plasma off the wall.

The spheromak is restained from its natural tendency to tilt during acceleration by the central electrode and during compression by the convergence of the channel. The latter is understood by visualizing a portion of the spheromak moving ahead of the rest. This portion would be compressed more than the rest and therefore slowed down, allowing the rest of the spheromak to catch up.

After ignition, because of the resulting thermal runaway, the plasma can be allowed to expand a little and moved to a burn chamber where fusion burning takes place at state 4 until either fuel depletion occurs or the plasma dissipates. During this burn some mechanism for

propellant injection must be employed to provide sufficient momentum for thrust.

Key issues are the degree of compression required, the magnitude of the directed velocity, the ratio of plasma to magnetic pressure (the β), and the breakdown between magnetic and thermal energy.

Scaling Laws

In the analysis that follows, subscript 'm' refers to magnetic, 't' to thermal, and 'd' to directed. We assume that the spheromak retains geometric similarity, i.e., $R/a = A = $ constant.

Adiabatic compression for a plasma follows the same laws as that for a monatomic gas where $\gamma = C_p/C_v = 5/3$:

$$\frac{n_3}{n_2} = \left(\frac{a_2}{a_3}\right)^3 \quad , \tag{1}$$

$$\frac{T_3}{T_2} = \left(\frac{V_2}{V_3}\right)^{\gamma-1} = \left(\frac{a_2}{a_3}\right)^{3(\gamma-1)} = \left(\frac{a_2}{a_3}\right)^2 \quad . \tag{2}$$

We can assume that compression is rapid enough so that the magnetic flux Φ contained within the plasma has no time to dissipate and is therefore conserved:

$$\Phi \sim BaR \sim \frac{I}{a}aR \sim IR \sim Ia = \text{constant} \quad ,$$

$$\text{and therefore} \quad \frac{I_3}{I_2} = \frac{a_2}{a_3} \quad . \tag{3}$$

In the above, B is the poloidal field produced by the imbedded plasma current I. Note that plasma current increases during compression.

We need to establish the effect of compression on plasma β where

$$\beta = \frac{P_{plasma}}{P_{magnetic}} \sim \frac{nT}{B^2} \sim \frac{nT}{(I/a)^2} = \frac{nTa^2}{I^2} \quad .$$

from Eqs. (1-3), we obtain

$$\frac{\beta_3}{\beta_2} = \frac{n_3 \, T_3 \, I_2^2 \, a_3^2}{n_2 \, T_2 \, I_3^2 \, a_2^2} = \frac{a_2}{a_3} \quad . \tag{4}$$

We also need to determine how adiabatic compression affects the partitioning of energy between magnetic energy and thermal. Obviously, we want as much as possible to go to thermal to provide plasma heating to ignition.

The magnetic energy in the plasma is

$$E_m = \frac{1}{2} \, LI^2 \quad .$$

where L is the plasma inductance. For R/a = constant, $L \sim R \sim a$, and therefore

$$\frac{E_{m3}}{E_{m2}} = \frac{L_3}{L_2} \left(\frac{I_3}{I_2}\right)^2 = \frac{a_2}{a_3} \quad . \tag{5}$$

The plasma thermal energy is

$$E_t = \frac{3}{2} nTV \quad,$$

where V is the plasma volume. During compression, E_t scales like

$$\frac{E_{t3}}{E_{t2}} = \frac{n_3 \, a_3^3 \, T_3}{n_2 \, a_2^3 \, T_2} = \left(\frac{a_2}{a_3}\right)^2 \quad. \tag{6}$$

One can readily see that the ratio of thermal to magnetic energy goes like $1/a_3$, and therefore an increasing fraction of the energy of compression goes into thermal rather than magnetic energy. While the direction is favorable, we must establish the magnitudes of this energy partitioning. This is done below.

Energy Partitioning

Between states 2 and 3, no additional energy is introduced to the plasma and therefore

$$E_{t2} + E_{d2} + E_{m2} = E_{t3} + E_{d3} + E_{m3} \quad.$$

In most cases, $E_{t2} \ll E_{d2}$ and $E_{d3} \ll E_{t3}$ so that

$$E_{t3} = E_{d2} + E_{m2} - E_{m3} \quad. \tag{7}$$

We wish to write the magnetic energies E_m in terms of the thermal energies E_t for reasons that will soon be apparent. It is necessary then to determine E_t/E_m.

For parabolic plasma current profiles, the inductance is given by[3]

$$L = \mu_o R \left[\ln\frac{8R}{a} - 1.542 \right] \quad , \tag{8}$$

so that, for an aspect ratio of $R/a = 1.5$,

$$L = 0.943\mu_o R = 1.42\mu_o a \quad ,$$

and therefore the magnetic energy in the plasma is given by

$$E_m = 0.71\mu_o a I^2 \quad .$$

We wish to write the thermal energy in terms of β where

$$\beta = \frac{nT}{B_p^2/2\mu_o} \quad , \tag{9}$$

and B_p is given by

$$B_p = \frac{\mu_o I}{2\pi a} \quad . \tag{10}$$

The result is

$$E_t = \frac{3}{2}nTV = \frac{3}{2} \frac{\beta \, \mu_o^2 I^2}{8\pi^2 \mu_o a^2}V$$

$$= \frac{3\beta \, \mu_o I^2 V}{16\pi^2 a^2} \quad .$$

The ratio of thermal to magnetic energy is then

$$\frac{E_t}{E_m} = \frac{0.264\beta V}{\pi^2 a^3} \quad .$$

The plasma volume for a torus with circular cross section is

$$V = \pi a^2 \, 2\pi R \simeq 3\pi^2 a^3 \quad \text{for} \quad \frac{R}{a} = 1.5 \quad .$$

Substituting this in the preceding equation gives the desired ratio:

$$\frac{E_t}{E_m} \simeq \frac{4}{5} \beta \quad . \tag{11}$$

A very important point here is that, because MHD stability restricts β to no more than about 0.20, only a small fraction of the total directed energy goes into thermal energy to heat the plasma. The magnitude of the directed energy required is, from Eqs. (6-11),

$$\frac{E_{d2}}{E_{t3}} = 1 + \frac{5}{4\beta_3}\left(1 - \frac{a_3}{a_2}\right) \quad . \tag{12}$$

Compression of a D-T Plasma

With Eq. (12), we can determine the directed energy required to compress a given plasma to a specified temperature. For example, consider a D-T plasma, which is by far the easiest to ignite. With nominal transport and radiation losses, a typical ignition temperature is 6 keV. We assume that the initial plasma can be heated Ohmically to 1.0 keV. The compression ratio required is, from Eq. (2),

$$\frac{a_2}{a_3} = \left(\frac{6.0}{1.0}\right)^{1/2} = 2.45 \quad .$$

If we place a maximum limit on β of 0.2 due to MHD limits, then the ratio of directed to final thermal energy is, from, Eq. (12),

$$\frac{E_{d2}}{E_{t3}} = 4.7 \quad .$$

This is the fundamental problem with adiabatic compression: not much energy goes into heating. To raise the plasma from 1.0 to 6.0 keV, a directed kinetic energy per particle of 4.7(6.0) = 28.2 keV must be supplied. This does not automatically eliminate the concept, but does make achieving an attractive energy balance that much more difficult. If one wishes to get 20 times the energy out as put in, or 28.2(20) = 564 keV, then the fuel burnup fraction must be 564 keV/3.52 MeV = 16%. This is a high burnup fraction and requires that the fusion burn be sustained for some time. However, it is not completely unreasonable and means may be found to achieve the degree of confinement needed.

The velocity corresponding to 28.2 keV directed energy is, for D-T,

$$U = \left(\frac{3kT}{m}\right)^{1/2} = \left(\frac{3(1.38 \cdot 10^{-23})(28.2 \cdot 10^3)(11,600)}{2.5(1.67 \cdot 10^{-27})}\right)^{1/2}$$

$$= 1.75 \cdot 10^6 \text{ m/sec} = 1750 \text{ km/sec} \quad .$$

This velocity has already been achieved in the RACE experiment at LLNL[1]. It is a modest velocity, representing only 0.006 times the speed of light.

Note that the electrons move at the same velocity. Since their mass is 1/4600 the average mass of a D-T ion, the added energy during acceleration is only $26.2 \cdot 10^3 /4600 = 6$ eV. Therefore, they essentially remain at their initial energy of 1.0 keV. While some thermalization takes place during the compression and burn, they will tend to stay cool, reducing both radiation and electron transport losses. Their pressure contribution is also reduced, allowing one to more fully utilize the allowable β by increasing the fuel ion density. On the negative side, any heating of the electrons by the ions will tend to pull the ion temperature down and decrease the compression efficiency.

For other fuels, such as D-^{3}He, the requirements are much higher. For ignition, about 50 keV thermal energy is required. It can be shown that about 320 keV of directed kinetic energy will be needed. Considering the low reactivity of D-^{3}He, it is difficult to sustain a fusion burn long enough to multiply this energy investment enough to achieve a usable net energy balance.

Plasma Sizing for Compression of D-T

Using the example above, we briefly size out a D-T plasma to see if the numbers appear realistic. The reactor is based on 100 MW of charged particle power, a repetition rate of 1.0 Hz, and a fusion burn time of 0.5 seconds. The power density is determined from the neutron wall loading at the plasma surface and is here taken to be 100 MW_n/m^2. While no material wall can take such a high heat flux, remember that the burning plasma does translate back and forth in the burn chamber distributing the heat over perhaps five times the area. This reduces the neutron wall loading down to about 20 MW_n/m^2, which has been deemed acceptable in current reactor conceptual designs[4]. Even though the neutron heat is discarded, it still is the limiting heat flux.

The other parameters required have already been established: β = 0.2, compression ratio a_2/a_3 = 2.45, and 16% burnup. We also assume that the fusion burn takes place at average ion and electron temperatures of 10 and 5 keV, respectively.

The above specifications give 100 MJ per 200 MW burn. Since each fusion produces 3.52 MeV charged particle power ($5.63 \cdot 10^{-13}$ J), the total number of α-particles produced is

$$N_\alpha = \frac{100 \cdot 10^6}{5.63 \cdot 10^{-13}} = 1.78 \cdot 10^{20} \quad .$$

There is one D and one T ion consumed for each α-particle. With 16% burnup, the total fuel ions is

$$N_{D-T} = \frac{2(1.78 \cdot 10^{20})}{0.16} = 2.22 \cdot 10^{21} \text{ ions D-T} \quad .$$

The average ion density is established by the neutron wall loading at the plasma surface. For R/a = 1.5, the surface has area $A_{plas} = 6\pi^2 a^2$. For D-T, the neutrons produce 80% of the power and the α-particles 20%. The required plasma surface area is therefore

$$A_{plas} = \frac{.80}{.20} \frac{P_{chg}}{q_n} = 4 \frac{200}{100} = 8 \text{ m}^2 \quad .$$

The plasma radius is therefore $a_3 = 0.37$ m and the major radius is $R_3 = 0.55$ m. The total diameter is $D_3 = 2(R + a) = 1.8$ m. These parameters prior to compression are

$$a_2 = 2.45(.37) = 0.91 \text{ m}$$
$$R_2 = 2.45(.55) = 1.34 \text{ m}$$
$$D_2 = 2.45(1.8) = 4.40 \text{ m} \quad .$$

This shows another problem with adiabatic compression: initial plasmas tend to be rather large.

It is also necessary to determine if the imbedded plasma current and its associated poloidal field falls in the realm of reasonablity. This requires determining the plasma density. The compressed plasma volume is, for R/a = 1.5,

$$V_{plas} = 3\pi^2 a^3 = 1.5 \text{ m}^3 \quad .$$

and therefore the average ion or electron density is $2.22 \cdot 10^{21}/1.5 = 1.49 \cdot 10^{21}$ m^{-3}. The plasma pressure is, assuming $n_e = n_i$,

$$P_{plas} = (\langle n_i T_i \rangle + \langle n_e T_e \rangle)e$$

$$= (1.49 \cdot 10^{21}(10,000 + 5,000)(1.602 \cdot 10^{-19})$$

$$= 3.57 \cdot 10^6 \text{ N/m}^2 = 520 \text{ psi} \quad .$$

Because $\beta = 0.2$, the magnetic confining pressure must be 5 times this or $1.78 \cdot 10^7$ N/m^2 (2600 psi). This magnetic pressure is given by

$$P_{mag} = \frac{B^2}{2\mu_o} \quad , \text{ where }$$

$$B = \frac{\mu_o I}{2\pi a} \quad .$$

This pressure corresponds to a field of 6.7 T and a plasma current of $I_3 = 12.4$ MA. This current is high but reasonable for reactors of this size. Prior to compression, the current is only $12.4/2.45 = 5.1$ MA, which should be relatively easy to produce.

Discussion

It appears feasible to produce adiabatic compression by accelerating a compact torus to high velocity and then decelerating and compressing it by driving it into a converging channel. However, less than 20% of this directed kinetic energy goes into plasma thermal energy. With D-T fuel, by far the most reactive, a 100 MW (α-power only) reactor with a neutron wall loading of 100 MW/m^2 at the plasma surface is about 2 m in diameter after compression and has a plasma current of about 12 MA. This could be reduced by increasing the repetition rate. However, a substantial burn time is required to produce net energy. The pre-compressed plasma is actually quite large: about 4.4 m in diameter, and has a plasma current of 5 MA. While not an unreasonable current, a considerable investment in energy storage and power supplies will be needed to create it.

Because of these shortcomings, we now explore another potential method of converting directed kinetic energy into plasma thermal energy: colliding compact tori.

ANALYSIS OF COLLIDING COMPACT TORI

General

Colliding compact tori differ from collision of plasma blobs in that the imbedded plasma currents should induce merging rather than having the two plasmas merely pass through each other. Upon merging, the two plasmas each with plasma current I and density n should form a single plasma with current 2I and density 2n. Even if the plasma temperature is negligible prior to merging, the temperature afterwards should correspond to the directed kinetic energy to which the plasmas had been accelerated. As mentioned in the last section, the electron temperature increase will be negligible and most of the heating during

collision will be in the ions. The merging stages are shown in Fig. 2b.

Analysis

After acceleration but prior to merging, each of the compact tori have directed kinetic energy E_d and internal magnetic energy E_m given by

$$E_d = \frac{1}{2} LI^2 \quad ,$$

$$E_m = \frac{1}{2} MU^2 \quad ,$$

where L is the plasma inductance and is given by Eq. (8), I is the plasma current, U the directed velocity, and M is the total plasma mass which, for a toroidal plasma, is given by

$$M = 2\langle n_i \rangle \pi^2 Ra^2 m \quad , \tag{13}$$

where m is the ion mass.

We postulate that two compact tori will merge into one whenever the magnetic energy E_{m3}, which holds the plasmas together, equals or exceeds the directed kinetic energy E_{d2}, which attempts to blow them apart. This assumption is based on the results of the RACE experiment at LLNL[1] where it was found that spheromaks could be accelerated intact with forces comparable to the body force E_m/R holding the plasma together. Obviously, further justification of this assumption will be necessary.

For $E_{d2} = E_{m3}$,

$$MU_2^2 = LI_3^2, \quad \text{and} \quad M = \frac{LI_3^2}{U_2^2} \quad .$$

We wish to determine the plasma β where this condition occurs. If it is above any MHD limit (typically $\beta = 0.2$), then merging should be successful. We can eliminate M with Eq. (13) above and U by noting that

$$U^2 = \frac{3kT_i}{m} \quad , \tag{14}$$

where T_i is the ion temperature after merging. Implicit in this equation is that all of the directed kinetic energy goes to ion thermal energy. This is a big improvement over adiabatic compression where it was shown that most of the directed energy went into magnetic energy. Using Eqs. (13-14), with $A = R/a$, we obtain

$$\langle n_i \rangle = \frac{mLI^2}{2\pi^2 Aa^3 m \ 3kT_i} \quad . \tag{15}$$

This can be written in a β-like form

$$\frac{\langle n \rangle kT}{(I/a)^2} = \frac{\mu_0[\ln(8R/a) - 1.5]}{6\pi^2} \quad . \tag{16}$$

Combining Eqs. (9), (10), and (16) gives,

$$\beta = \frac{4}{3} [\ln(8R/a) - 1.5] \quad .$$

For a spheromak, $R/a \simeq 1.5$ and therefore

$$\beta \simeq \frac{4}{3} \quad .$$

That is, provided $\beta \leq 4/3$, merging will occur. Since MHD stability limits β to well below this limit, merging should occur presuming, of course, that our original assumption is correct.

Even if it is off by a factor of several, merging is still likely. MHD β limits are about 0.2, or 0.15 times the merging limit. If the MHD limit is adhered to,

$$\frac{E_d}{E_m} \leq 0.15 \quad .$$

Note that the directed energy is a modest fraction of the magnetic energy. Also, to heat D-T to 6 keV, the directed energy must be 6 keV, rather than 28.2 keV for adiabatic compression. This greatly reduces the accelerator hardware and energy storage requirements. However, the initial plasma has a higher plasma current and therefore the initial magnetic energy is higher. Again there is no free lunch. With any magnetic confinement scheme, most of the energy in the system is magnetic. The main advantage of the merging system is that the magnetic energy is supplied initially by mundane inductive drive rather than later by the more exotic coaxial acceleration. Also, preheating of the plasma to limit compression ratio is not needed.

One item that remains unclear is the energy balance before and after merging. Because the two plasma currents also merge so that $I_3 = 2I_2$, the $LI^2/2$ magnetic energy increases by a factor of four. Half of this can be accounted for by the merging. The other half either must be supplied by the directed kinetic energy or it doesn't exist and the plasma makes an automatic adjustment in inductance so that $L_3 = L_2/2$.

This would require that $R_3 = R_2/2$. The physical mechanism for either is not obvious. However, project constraints prevent us from pursuing this further and so this factor of two uncertainty cannot be resolved at this time.

Plasma Sizing for Merging of D-T

If we take the same parameters as for adiabatic compression (and ignore the factor of two uncertainty above), then the main issue is whether or not the desired velocity can be achieved. Upon merging, this directed kinetic energy must convert to 6 keV thermal energy in the ions. The required velocity is

$$U = \left[\frac{3kT}{m} \right]^{1/2} = \left[\frac{3(1.38 \cdot 10^{-23})(6000)(11,600)}{2.5(1.67 \cdot 10^{-27})} \right]^{1/2}$$

$$= 8.3 \cdot 10^5 \text{ m/sec} \quad .$$

From the previous case, the total fuel ions is $N = 2.22 \cdot 10^{21}$ which, for D-T, has a mass of $M = 9.3 \cdot 10^{-6}$ kg. The directed kinetic energy is then

$$E_{d2} = \frac{1}{2} MU^2 = 3 \cdot 10^6 \text{ J} \quad .$$

The magnetic energy is $L_3 I_3^2/2$. From Eq. (8) with $R_3 = 0.55$ m and $a_3 = 0.37$ m, $L_3 = 6.8 \cdot 10^{-7}$ h. With a 12.4 MA plasma current, we obtain

$$E_{m3} = 5.2 \cdot 10^7 \text{ J} \quad .$$

The ratio of the two is then

$$\frac{E_{d2}}{E_{m3}} = 0.062 \quad ,$$

which is 41% of the limit shown above of 0.15. This is helpful because, even with the factor of two uncertainty discussed above, merging should still occur.

DISCUSSION AND SUMMARY

After considering all elements of the problem, it is clear that both adiabatic compression and merging are viable means of heating a D-T plasma to ignition. In both cases, much more energy must be supplied to the magnetic system than to the thermal system. In adiabatic compression, this is done by accelerating the compact torus to higher velocities and converting much of that kinetic energy to magnetic. In merging, this is done by inductively driving the initial plasmas to higher currents.

The main advantage of merging is that lower velocities are required. The main disadvantage is that there is less evidence that it will work. The RACE experiment clearly demonstrated adiabatic compression. The TRISOPS VIII experiment combined compression with merging and so the results are not as clear-cut.

Because so much energy must be supplied, a considerable amount of fusion energy must be produced to make the investment worthwhile. It was shown that about a 0.5 second burn could produce a total charged particle energy output 20 times greater than the energy input. This is a very long sustainment time for current spheromaks, which typically last a few milliseconds. High plasma temperatures may help confinement, but that is not certain.

Another issue than is common to all fusion plasma devices designed to produce thrust is how the charged particle fusion power can be converted into momentum. This must be done in such a way as to not quench the plasma. Ideally, it should be independent of material surfaces or specific impulse will suffer because of the lower temperature. For most missions, it is expected that exhaust velocities will be optimized so as to limit the power required for thrust. Therefore, mass flows could be so high as to swamp the tenuous fusion plasma. Under these circumstances, a physical material wall separating the plasma from the propellant may be necessary.

REFERENCES

1. J.H. Hammer, C.W. Hartman, and J.L. Eddleman, "Recent Results of the RACE CT Accelerator Experiment", in Proc. 8th Symposium on the Physics and Technology of Compact Toroids, Univ. of MD, College Park, MD (June 1987).

2. D.R. Wells, P.E. Ziajka, and J.L. Tunstall, "Hydrodynamic Confinement of Thermonuclear Plasmas TRISOPS VIII (Plasma Liner Confinement), Fusion Technology, v. 9, Jan 1986, p. 83.

3. M.J. Schaffer, General Atomics, private communication, Feb 1988.

4. "The Titan Reversed-Field Pinch Fusion Reactor Study", UCLA-PPG-1135, March 1988.

APPENDIX D

PULSED NUCLEAR PROPULSION

"Pulsed Nuclear Propulsion"

D.K. Bhadra

ABSTRACT

The prospect for using pulsed-nuclear systems for propulsion appear very attractive. We review the ORION and SIRIUS projects. An external system, using driven low-yield thermonuclear reactions burning aneutronic fuel may be an attractive propulsion concept for Air Force missions.

PULSED NUCLEAR PROPULSION
D.K. Bhadra

1. Introduction

Pulsed Nuclear Propulsion, Project ORION in particular, was considered as a viable candidate for space travel during the late fifties and early sixties. This was about the time when the Russian Sputnik went up and before the U.S. was committed to a big space program with chemical propulsion. The ORION project started in 1957 and ended in 1965. The project was funded initially by ARPA of DOD and later by the Air Force and also by NASA in a minor role. A review of the project is available in [Ref. 1].

2. ORION Concept

A schematic of the basic features of the ORION vehicle is shown in Fig. 1. The propulsion system is very simple in concept. A nuclear explosion was to be produced underneath the vehicle, some of the expanding debris of which would be intercepted by the base of the vehicle, thereby transferring momentum to it from the explosion products. The expansion velocity of an atomic explosion may be of the order of 10^8 cm/sec, and if this could be directed and intercepted efficiently, a very high exhaust velocity could be reached (a specific impulse of 10^5 sec if an exhaust velocity $\sim 10^8$ cm/sec could be achieved). However, to increase the vehicle thrust, it is better to reduce the expansion velocity of the explosion by loading the unit with a cheap propellant like polyethylene. The interaction time of the expanding plasma debris and the vehicle would be around a millisec or less. Such a very short interaction period and high momentum transfer would result in excessive shock loading of the vehicle and so a special "pusher plate" was designed to be mounted on the vehicle via shock absorbers. It was found that a very thin coating of silicon grease on an aluminum pusher plate would drastically reduce the ablation of such a pusher plate. To prevent the plate from being destroyed by mechanical shock waves, correct shaping of the

pusher plate thickness was required. The shock absorber system consisted of two different sets of pneumatic devices. The other main system components are the magazine holder and pulse unit feed system; the charge injection system, achieved by means of compressed nitrogen which propelled the charge through a hole in the center of the pusher plate; a low-thrust attitude control system and, of course, the nuclear charges themselves.
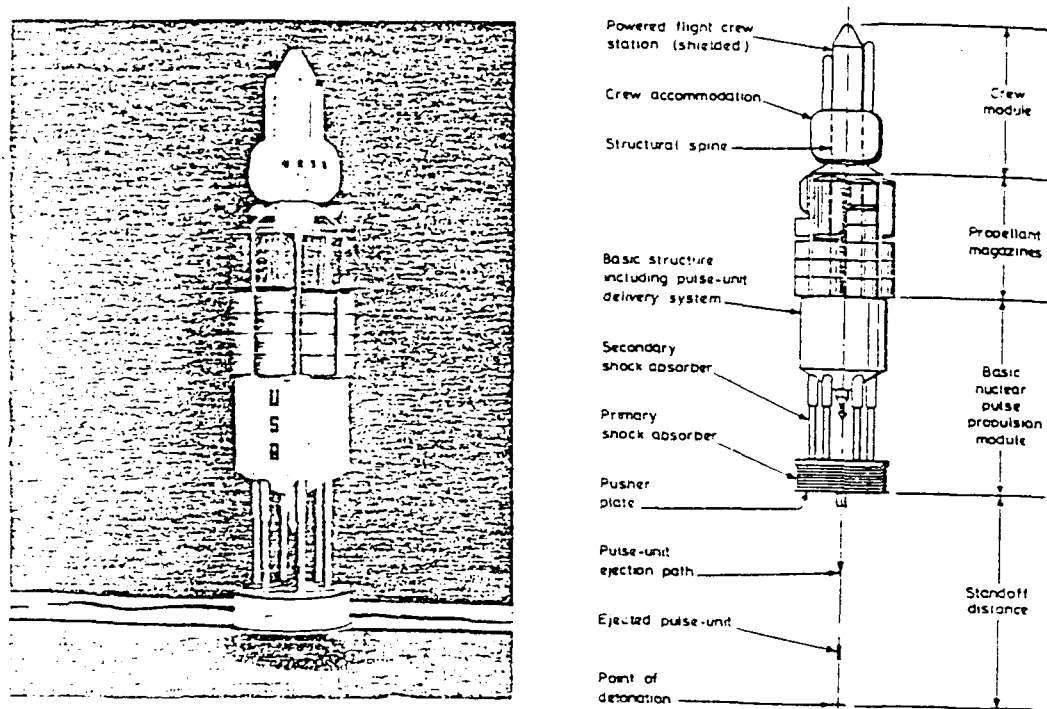
FIG. 1. Schematic of an ORION rocket.

The nuclear charges were mostly based on conventional atomic weapons technology. The use of thermonuclear fusion charges was mentioned in the GA report GA-4891 (1964). The use of a hydride composition to reduce the quantity of fissile material employed in the construction of an atomic weapon for propulsion purposes was originally suggested by Everett and Ulam [Ref. 2].

3. Vehicle Parameters and Specific Impulse

During the early years, the United States Air Force design requirements guided the development of the project vehicle. The vehicle was to be propelled by small explosions of about 0.01 kiloton to 0.1 kiloton yield, released from the vehicle at 1 to 10 sec intervals, and detonated between 30 to 300 meters behind the pusher assembly. For an earth launch, the size of the nuclear yield can be reduced by one or two orders of magnitude in the lower atmosphere and hence reduce the contamination problem. At higher altitudes, the yield of the pulse unit would approach about 1 kiloton if a high level of acceleration is to be maintained.

The characteristics of the USAF vehicles were as follows:

TABLE 1

Launch Mass	$\approx 3.3 \times 10^9$ kg
Payload Mass	$\approx 9 \times 10^5$ kg
Exhaust Velocity	$\simeq 40$ km/sec
Acceleration	≥ 10 m/sec^2
Explosion Repetition Rate	~ 1 to 0.1 per sec
Launch	$= 3.3 \times 10^6$ kg

The vehicle was designed to become a full-blown space battleship with guidance systems and directional nuclear weapons for bringing down missiles. It has been said that such a vehicle could present its pusher plate to anything that came near it, with the expected capacity of being able to resist a megaton explosion as close as 500 feet away.

The pulse units, mentioned earlier, consisted of systems in which propellant mass was incorporated along with a shaped nuclear charge. Such shaping of nuclear charges also helped increasing the fraction of debris intercepted by the pusher plate almost to 0.5. To obtain the estimates for specific impulse limits for such a system, one considers the mean propellant velocity, pulse unit fraction, mass loss via ablation, collimation factors to account for charge shaping, the formation of stagnant layers at the surface of the pusher plate, and varying explosive yields. It was found that there is an optimum explosive pulse energy to give the maximum specific impulse with a given vehicle size (keeping the

separation distance between the vehicle and the explosive charge at a minimum as dictated by pressure limitations). The effective specific impulse is given by:

$$I_{sp}^{eff} = \alpha_c \, \alpha_m \, I_{sp}^{base}$$

where α_c = fraction of pulse unit mass which intercepts the pusher, and

$$\alpha_m = \text{ablation mass factor.}$$

Figure 2 shows the effective specific impulse as a function of the size of the push-plate for various explosive yields. It appears that the maximum specific impulse for such a system is ~4000 to 5000 sec and increasing the base specific impulse (i.e., increasing the mean propellant velocity) does not lead to large increases in the effective specific impulse. However, increasing the vehicle size does lead to higher specific impulses, as long as the pulse energy is maintained at the optimum value for that size.

Another complication in such a design concept was the fact that excessive propellant pressure against the pusher plate will cause spallation if the resulting internal tensile stresses exceed the strength of the pusher plate material.

4. How About an Internal System?

Such configurations, studied in the sixties (e.g., HELIOS system, [Ref. 3]), generally consist of a pressure vessel with a conventional rocket nozzle; the explosion takes place inside of the vessel into which is fed liquid hydrogen, or water, radially through the wall, acting as a coolant. Shock waves, as a result of explosion, propagate through the hydrogen until it is reflected from the wall. This reflection process goes on back and forth in the vessel, increasing the internal energy of the hydrogen. After a few milliseconds, hot gas is expanded through the nozzle while the pressure vessel is refilled with the propellant.

EFFECTIVE SPECIFIC IMPULSE (ORION)
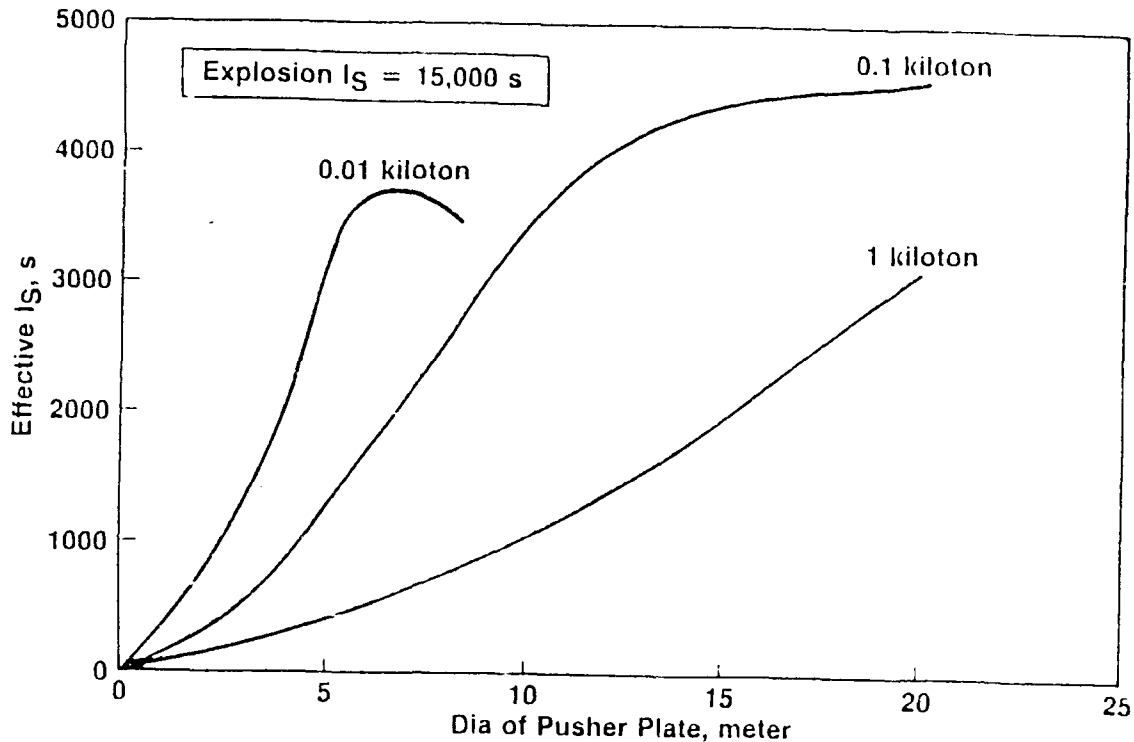
FIG. 2. Effective specific impulse (ORION).

At the beginning, the internal pulsed propulsion concept appeared attractive as the efficiency with which the explosion energy could be converted into impulse is very high. The energy of the explosion was almost totally absorbed by the propellant, and the nozzle directed the propellant into the well-collimated exhaust. However, the internal system possesses several disadvantages compared to the external system and was the main reason why it was given up fairly early in the game.

There are two main limitations to the performance of an internal system:

(a) Heating of the vehicle due to radiation — neutrons produced from the explosion (both fission and fusion) will deposit energy directly to the structure through collision and by inducing γ-reactions in the material. The vehicle then requires cooling and this is the dominant performance limiting factor in the internal design.

The use of advanced fuels may mitigate this state of affairs to a considerable extent.

(b) Higher mass of such a vehicle — when one tries to optimize such an internal system from the point of view of minimizing the total vehicle mass required to deliver a given payload by a combination of minimizing the propellant load through an increase in specific impulse and the minimizing of the propulsion system mass, one comes to the conclusion that the minimum mass of the external system will always be less than that of an internal system, for the same payload and mission.

5. Radiation Consideration

Here we discuss some relevant points regarding the radiation environment which results from the explosions (fission or fusion). There are several areas of concern:

(a) Neutron heating of the pusher plate.

(b) Neutron heating and radiation damage in the rest of the vehicle.

(c) Dose rate for the payloads.

(d) Gamma-ray effects resulting from neutron capture.

Shielding considerations for the ORION   hicle were based on the allowable propulsion radiation dose of 50 rem per mission (this dosage rate is higher than the presently accepted one). Three major ways of shielding a payload were considered:

(a) The pulse unit — critical parts were configured so as to subtend relatively small solid angle from the explosion location.

(b) An expendable attenuating material can be placed between the explosion and the pusher plate (for each explosion!), implying a reduction of the system specific impulse directly as this mass is increased.

(c) Direct shielding of the payload area to reduce the dosage.

It appears, for some of the work carried out for the ORION vehicle design during the later stages of the program, that, even for D-T, the shielding of the payload may not involve a horrendous amount of added mass in order to reduce the dose levels to acceptable values.

6. Low-Yield Thermonuclear Reaction Concept

A less potent version of the ORION concept is the possibility of initiating low-yield thermonuclear reactions by the use of an intense laser pulse to heat to ignition a very small pellet of fusionable material (presumable, 0.01 to 0.1 kiloton equivalent of TNT). Under the title of PROJECT SIRIUS, (unofficial name — SIRIUS is the principal star in the constellation *Canis Major* which follows close to ORION in the sky), this project looked in detail at internal and external designs. The external design relied on ablation of the pusher plate (as in the ORION design). Their studies indicate a maximum specific impulse for an internal system of about ∼2500 sec, whereas that for an external system may achieve ∼7000 sec.

The neutron and γ-ray radiation in the forward part of the vehicle was minimized by an elongated design. The payload area is very far forward and benefits from both the effect of distance and the effective shielding due to the entire vehicle. The waste heat is to be dumped via large fin-shaped plates of a radiator system. The laser was supposed to have two components, *viz.*, a permanent first-stage carried on-board the vehicle and a disposable final stage deployed with the explosive charge. Such a final stage can be conveniently deployed with the explosive since the laser reactants will probably not be reusable and the final focusing mirror will be destroyed in the explosion. Some of the vehicle masses and performance parameters are shown in Table 2.

TABLE 2

Energy per Explosion	$\sim 7.5 \times 10^{10}$ J
Explosion Rate	1 sec^{-1}
Exhaust Velocity	$\sim 4 \times 10^{4}$ M/sec
Specific Impulse	~ 4500 sec
Thrust	$\sim 2 \times 10^{5}$ N
Various Masses:	
Laser	~ 500 kg
Momentum Conditioner	~ 1800 kg
Pusher Plate	~ 1800 kg
Propellant	~ 4000 kg
Structure	2000 kg
Total Vehicle Mass	~ 20 tons
Payload	~ 9.5 tons

7. Epilogue

The performance potential for propulsion using nuclear-pulsed systems is attractive. Such a system offers the possibility of effective utilization of fusion energy with the potential for minimal adverse side effects.

Such propulsion systems would contain pulse units, located either internally or externally to the system, imparting an impulse to the spacecraft. Such pulse units are sequentially discharged and initiated until the necessary spacecraft velocity is reached. Means of shock absorption and shielding against fast neutrons (when using D-T fuel) are needed for meaningful operation of the vehicle. An internal system, where the explosion is surrounded by a high-density propellant, generally yields a specific impulse which is considerably less than that of a similar external system, but would utilize a larger fraction of the explosion yield.

An external system, using driven low-yield thermonuclear reactions, may be an attractive design for Air Force missions. In order to be able to use exotic fuels (like D-^{3}He or p-^{11}B), it may be necessary to achieve some form of multistage optimally-shaped implosion in the fusion charge in order to get very high pellet gain. A study for the feasibility of such a system for fusion power propulsion will be presented in a separate memorandum.

References

[1] J.C. Nance, General Atomic report GA-5572 (1964).

[2] C.J. Everett and S.M. Ulam, Los Alamos National Laboratory report #LAMS-1955 (1955).

[3] J.W. Hadley, T.F. Stubbs, M.A. Jensen and L.A. Simmons, University of Calif. report #UCRL-14238 (1965).

APPENDIX E

"CAN ANTIPROTONS BE USED FOR PROPULSION BY FUSION POWER?

APPENDIX E

Fusion Propulsion Technical Memorandum

No. 5, April 5, 1988

"CAN ANTIPROTONS BE USED FOR PROPULSION BY FUSION POWER?"

D. K. Bhadra
General Atomics
(619) 455-3118

Abstract

Antiproton-driven inertially confined fusion concept does not appear feasible for propulsion purposes at present. However, synergistic schemes using the intermediary of fission processes may be viable for producing implosion in a micro-target resulting in fusion of the appropriate fuel.

"CAN ANTIPROTONS BE USED FOR PROPULSION BY FUSION POWER?"

D. K. Bhadra

INTRODUCTION

It is well known that the developments in experimental nuclear physics have often resulted in some applications in other fields of science. It has been suggested (Ref. 1) that antimatter could be used as an ultimate fuel for propulsion. In this context, thrust generated from antiproton annihilation has been considered as a possible propulsion mechanism. With the advent of accelerators and devices capable of producing and storing some antiprotons, such propulsion mechanisms may be considered to have moved from the realms of "fantasy" to regimes of future possibility. The availability of magnetic storage ring devices like LEAR (Low Energy Antiproton Ring) at CERN (see Ref. 2), with its high beam quality (comparable to that for protons from electrostatic tandem generators) and the possibility of accumulating a sufficient number of antiprotons in the ring, lead us to consider the possibility to obtain an enormous energy release (in a small volume) via antiprotons. Such a mechanism could then be used to trigger possible microexplosions in a micro-target, similar to present-day Inertially Confined Fusion (ICF) schemes.

Thermonuclear Plasma by Antiprotons?

Scientists involved in ICF experiments are primarily interested in generating implosion in a target via ablation using high-power laser or light-ion beams as drivers. Let us briefly explore whether antiprotons could be used for such a driver. Before one proceeds, it is worth noting that the present-day wisdom in ICF confinement phys. dictates a driver energy ~1 MJ to 10 MJ to be delivered within the inertial confinement time $\leq$ 10 to 100 nsec.

The antiprotons can travel quite a distance in the target and a significant amount of energy is released near the point where the antiproton is stopped. Figure 1 shows an example of specific energy loss along the path of an antiproton (the "straggling phenomenon" for antiprotons). The straggling parameter (dE/dr) has been computed assuming that the antiproton has an initial energy of about 300 MeV.
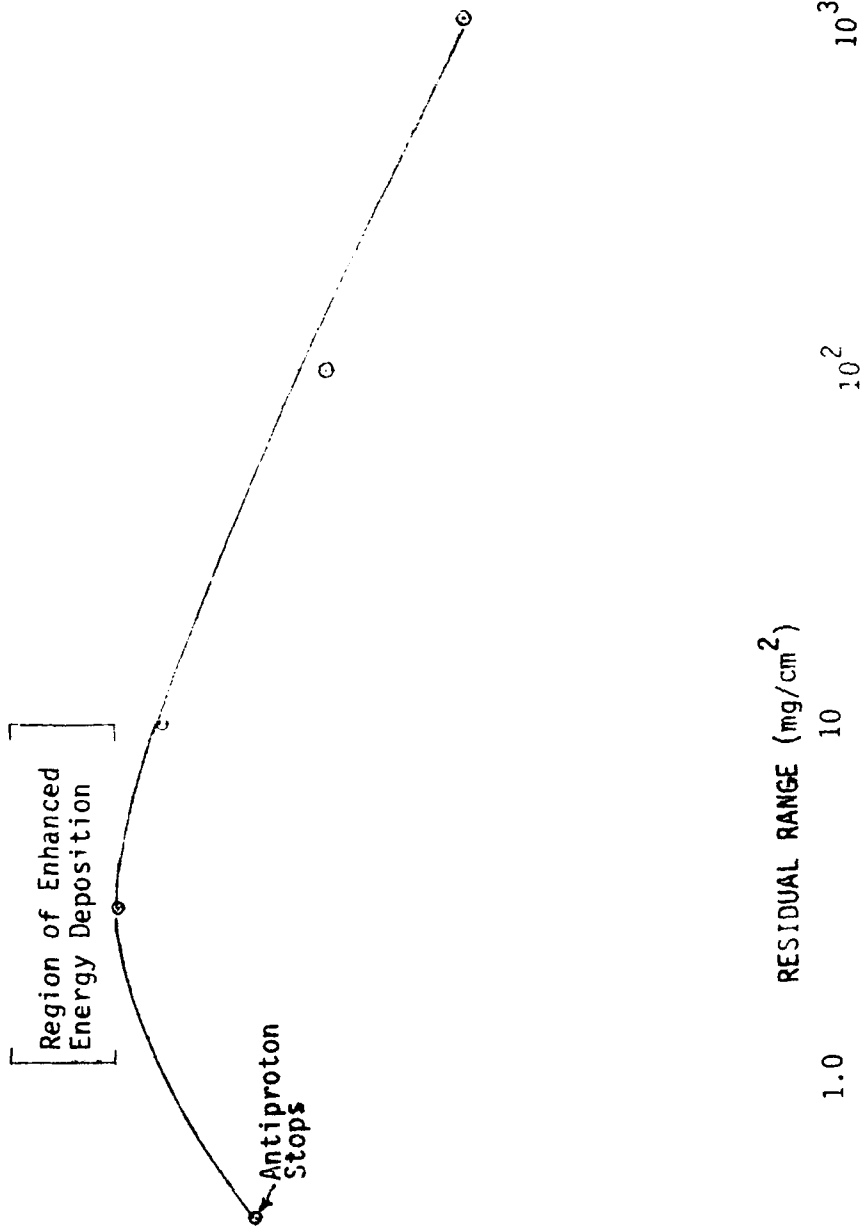
Figure 1. Specific Energy Loss Along the Antiproton Trajectory

E-2

In order to shorten the actual penetration distance of such anti- pro-
tons, it may be necessary to surround the ICF-target with a thin mantel of
tungsten or uranium. A good quality beam of antiprotons (e.g., the type
generated in LEAR) may be focussed to a size of the order of 1 sq. mm.
Considering a beam of antiprotons with momentum corresponding to an energy
of 300 MeV, the stopping range in uranium could be about 0.2 to 0.4 gm.
This is obtained from knowing the density of uranium and the straggling
distance of the antiproton (from Fig. 1), and considering a beam
cross-section of 1 square mm. One then could possibly fabricate an
ICF-target with a diameter of about a mm or so and a very thin mantle of
uranium to tailor the antiproton energy deposition in the target (see
Fig. 2).

Unless we have a very large number of antiprotons available, it is
difficult to see how one can generate large transfer of momentum onto the
target resulting in its compression. As calculated later, one needs a very
large number of antiprotons for that purpose and there are significant num-
ber of technological problems in that context. However, if one decides to
use an uranium mantle, then it may be possible to use an appropriate
fissile isotope of that element with the intention that any induced fission
processes would enhance the probability of target implosion via ablation of
fission debris (see Figure 1). This is somewhat similar to the case of
laser-driven implosion where the "light pressure" itself is much smaller
than the pressure that could be generated through ablation. The large mass
of fisson products could play a significant role in generating enough
momentum-flux to drive an implosion in the ICF-target. To understand such
a possible mechanism better, one requires to study the details of the
fission events caused by the antiproton dump (each fission even carried
somewhere around 150 MeV of kinetic energy) in the fissile mantle of the
target. More significantly, one needs to explore possible ablation caused
by such debris (preferably in a time scale $< 10^{-7}$), the resulting implosion
of the target material, assuming that the thermal front follows behind the
hydrodynamic shock front as the implosion proceeds with target preheat
being negligible. Such synergistic antiproton-triggered fission-driven
ablation may be a viable ICF scheme for power production for propulsion.
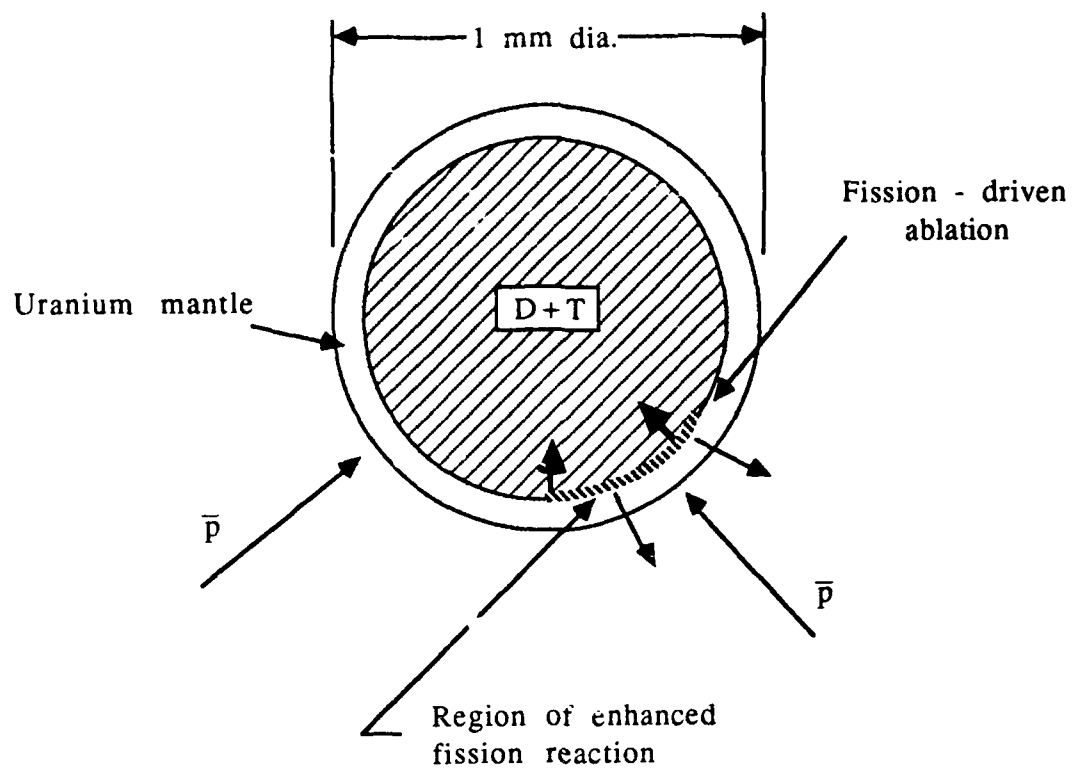
Figure 2 Fission - Induced Ablation

Some Issues of Significance

One of the major issues related to the available antiproton dump is the question of how many antiprotons can be stored and carried on board a space vehicle.

A number of experimenters have recently proposed to decelerate the antiprotons down to almost zero velocity and put them into a Penning trap (see Ref. 2). The Penning trap uses only static electric and magnetic fields and can trap charged ions. In a cryogenically cooled ultra-high vacuum Penning trap, the longivity of antimatter may be quite high. Figure 3 shows the schematic of a Penning trap consisting of a small trapping region containing an axial magnetic field and bounded by a ring electrode and a pair of cap electrodes. The charging of the various electrodes is shown in Figure 3, suitable for trapping a negatively charged anti- proton. Such a combination of electric and magnetic fields has been shown to help confine charged particles.

One of the primary limitations in such a device arises from the concept of space-charge build up. Approximate estimates, obtained in present-day scientific literature, indicate that the number density may vary from 10^{11}/cc (for a 2 cm radius trap) to about 10^{14}/cc (for a large 50 cm radius trap). In addition, another limitation arises from the fact that the angular rotation of the particles in the crossed electric and magnetic fields should remain less than the gyrofrequency of the particles, as a condition for particles remaining trapped. If one assumes that the self-consistent electric field E is related to a space-charge buildup with density n of antiprotons, then one has $E = 4 \pi ner$; and the above-mentioned condition can be shown to be given by ω^2_p/Ω^2_c, where ω_p is the plasma frequency for the antiprotons and Ω_c is their gyrofrequency. For a magnetic field B = 10 Tesla, this condition corresponds to an upper limit for density of antiprotons ~5 x 10^{11}/cc. The total annihilation energy delivered by such a density of particles ~35 J/cc, assuming optimum conditions. (Half of the energy is lost through other channels). In order to obtain an
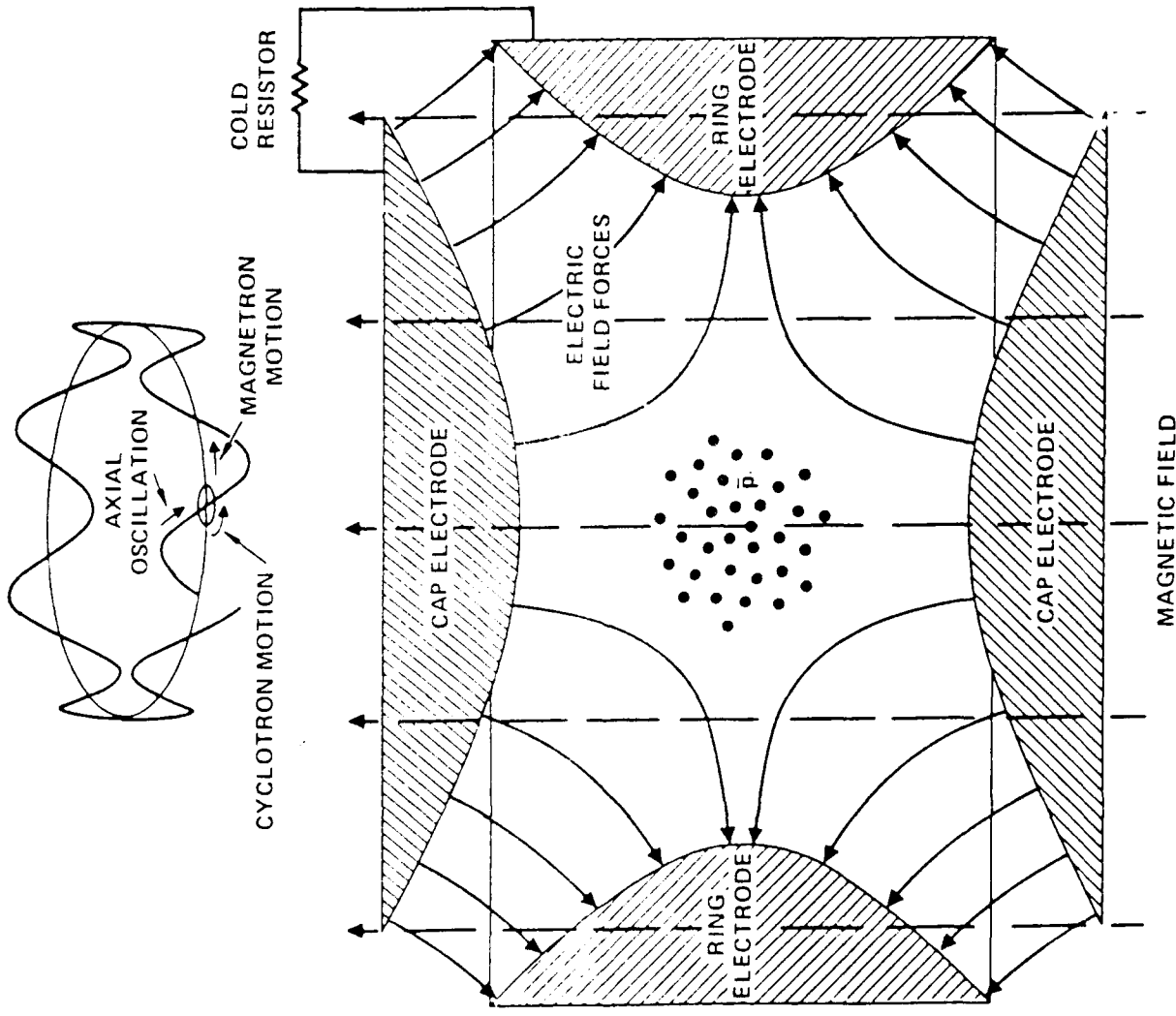
Figure 3

TRAPPING OF
ANTIPROTON IONS
USING
PENNING TRAP

G. Gabrielse, U. Washington (1985)

energy delivery in the range of a 1 MJ to 10 MJ, one would require a trap of volume 20000 c.c. to 200000 c.c.! Additionally, one would assume a dump of all the antiprotons (in the trap) on the target within a very short time interval.

At present, one faces a number of severe limitations in this context. No knowledge exists regarding the feasibility of building such large Penning traps. Even if a trap that large could be built, it is not clear how one would dump all the antiprotons on a micro-target (~1 mm or so diameter) in a time-span of the order of inertial confinement time. Additionally, the production of the necessary high intensity magnetic (~10 Tesla or more) requires peripheral equipment not very different from what would be needed for a conventional magnetically confined plasma device.

Even if all the antiprotons that we need to drive an ICF-target directly could be produced here on earth today, we do not have the necessary form of storage, transportation and delivery capabilities for antiprotons onto a micro-target. This all has to be done on board a space vehicle. Surprise-free and reasonable extrapolations of present-day technology seem to point towards a negative conclusion. However, if we focus our attention away from the conventional direct drive concept onto some novel synergistic approach (like the one discussed earlier), then it is possible that antiprotons could become a viable mechanism to drive an ICF-target, at least in principle, especially if we allow ourselves a reasonable measure of extrapolation of the technology available at present.

DISCUSSION

A brief exploration of the antiproton-driven micro-explosion concept unveils that fact that direct ICF-drive does not appear feasible at present. Synergistic drives, like the one mentioned earlier, may become feasible but further study needs to be done. Limitations of the presently

available Penning-type traps seem to be very significant, since, even if we assume that, here on earth, we can produce all the antiprotons we need for the ultimate purpose of power generation for propulsion, we do not know how to store, transport and appropriately deliver them, particularly onto a micro-target.

Another improvement, in this context, may arise from using anti- hydrogen (an antiproton surrounded by an orbiting positron as possible fuel. For such antihydrogen, the storage restrictions in a trap would not be nearly as severe as in the case of the antiprotons in a Penning-type trap. Thus, a hydrogen-antihydrogen mixture could be used to generate power for propulsion.

References

1. R. L. Forward, Air Force Rock t Propulsion Laboratory Report No. AFRPL TR-85-034 (1985).

2. U. Gastaldi and R. Klapisch, et., "Physics at LEAR with Low-Energy Cooled Antiprotons," Plenum Press (N.Y.) 1984.

NATURE OF p⁺-p⁻ INTERACTION

The interaction of antiproton with proton leads to the following major processes:

$$\pi^+ + \pi^- + 2\pi^\circ \quad (35\%)$$

$$2\pi^+ + 2\pi^- + 2\pi^\circ \quad (21\%)$$

$$p^+ + p^- \rightarrow \quad 2\pi^+ + 2\pi^- + \pi^\circ \quad (18\%)$$

$$\pi^+ + \pi^- + \pi^\circ \quad (3\%)$$

$$K^+ + K^- + K^\circ \quad (2\%)$$

. . . . .

. . . . .

There is prompt γ-radiation produced by the annihilation process and also large amount of delayed radiation from the decay of π°. The charged pions decay to μ-mesons (the latter having a lifetime $\geq 10^{-6}$ sec.) and neutrinos within $^-10^{-8}$ sec. Roughly, half of the $p^+ + p^-$ annihilation energy goes to the charged particles, the remainder going primarily to the neutrinos. The energy per unit mass released from the above annihilation reaction is roughly $^-4.5 \times 10^{13}$ J/gm which is about two orders of magnitude higher than the corresponding energy released from a typical nuclear fusion reaction. For collision energies above 100 eV, the direct annihilation cross-section is the significant one, the radiative capture cross-section being negligible for $p^+ - p^-$ interactions at all energies of interest.

The antiproton will also interact with nuclei heavier than the proton. The antiproton will annihilate with a neutron (as well as a proton) inside a heavy nucleus. Such antiproton annihilation will produce different numbers of the various types of charged and uncharged pions and kaons as compared to $p^+ - p^-$ process.

APPENDIX F

TCT. FOR CODE LISTING

```
C+++++++++++++++++++++++++++++++++++++++++++++++++++++++++++++++++++
C  TCT.FOR
C+++++++++++++++++++++++++++++++++++++++++++++++++++++++++++++++++++
C
C  A SCOPING CODE FOR TRANSLATING COMPACT TORUS FUSION ROCKET.
C       COLLIDING TORI VERSION.
C
C  AUTHOR: R.F. BOURQUE, GENERAL ATOMICS
C  BEGUN ON JUNE 27, 1988.
C  LAST EDITED ON 10/5/88.
C
C  EXTERNAL:  FCNSIG.FOR
C    TO USE, TYPE:  FOR TCT.FOR,FCNSIG.FOR
C               THEN:  LIN TCT,FCNSIG
C
C  MKS, EV UNITS
C
       IMPLICIT REAL (I-J, L-N)
       CHARACTER*12 DATA,DDATE,TITLE(5)
       DIMENSION V(20)
C
       PI = 355./113.
       MU = 4.*PI*1.E-7
       E = 1.602E-19
C
       KOUT = 21
C
       WRITE(*,153)
   153 FORMAT(5X,'DAT FILE:')
       READ(5,154) DATA
   154 FORMAT(A)
C
       OPEN(UNIT=21, FILE=DATA, STATUS='NEW')
       CALL DATE(DDATE)
C
C------------------------------------------------------------------
C  INPUT LIST:
C------------------------------------------------------------------
C
C   NO.     NAME         DESCRIPTION
C
C   1       THRUST       ROCKET THRUST, NEWTONS
C   2       ISP          SPECIFIC IMPULSE, SECONDS
C   3       RATE         FUSION REP RATE, HZ
C   4       BURNUP       FUSION BURNUP FRACTION (0 TO 1)
C   5       EFFMAG       ELEC TO MAGNETIC CONVERSION EFFICIENCY
C   6       EFFEL        THERMAL TO ELECTRICAL CONVERSION EFF
C                        ASSUMES TURBINE IN ROCKET THROAT WITH
C                        EXHAUST GOING TO THRUST.
C   7       KFUEL        FUSION FUEL OPTIONS: 1=D-T, 2=D-3HE
C   8       BPOL         POLOIDAL FIELD AFTER MERGING, TESLA
C   9       BETA         POLOIDAL BETA AFTER MERGING
```

```
C    10      KPROFL        PLASMA PROFILE: 1=FLAT, 2=PARABLOIC
C    11      ASPECT        PLASMA ASPECT RATIO, R/A
C    12      DELTAV        DESIRED DELTA V, M/SEC
C    13      PAYLOD        PAYLOAD MASS, KG
C    14      KPRINT        PRINT OPTION: 1 FOR PRETTY OUTPUT,
C                          2 FOR PLOT TABLES.
C
C-------------------------------------------------------------
C  DEFAULT INPUT:
C-------------------------------------------------------------
C
       V(1) = 100000.
       V(2) = 1500.
       V(3) = 4.
       V(4) = .5
       V(5) = .6
       V(6) = .6
       V(7) = 2
       V(8) = 60.
       V(9) = 0.80
       V(10) = 1
       V(11) = 1.2
       V(12) = 9000.
       V(13) = 36000.
       V(14) = 1.
C
C-------------------------------------------------------------
C  CHANGE DEFAULTS:
C-------------------------------------------------------------
C
  111 CONTINUE
       READ(5,27) (TITLE(K), K=1,5)
   27 FORMAT(5A)
  112 WRITE(*,2)
    2 FORMAT(10X,'OK')
       READ(5,*) KV,VAR
       IF(KV .EQ. 0) GO TO 88
       IF(KV .EQ. 99) GO TO 99
       V(KV) = VAR
       GO TO 112
C
   88 CONTINUE
C
C-------------------------------------------------------------
C  ASSIGN VARIABLE INPUT NAMES:
C-------------------------------------------------------------
C
       THRUST = V(1)
       ISP = V(2)
       RATE = V(3)
       BURNUP = V(4)
       EFFMAG = V(5)
       EFFEL = V(6)
       KFUEL = V(7)
       BPOL = V(8)
       BETA = V(9)
```

```
           KPROFL = V(10)
           ASPECT = V(11)
           DELTAV = V(12)
           PAYLOD = V(13)
           KPRINT = V(14)
      C

           EFFACC = 0.5
           FTBURN = 1.0
      C
      C------------------------------------------------------------
      C  PRINT INPUT LIST:
      C------------------------------------------------------------
      C

           IF(KPRINT .EQ. 1)
          & WRITE(KOUT,29) DDATE, (TITLE(K),K=1,5)
      C
        29 FORMAT(1H1,/,
          & 5X,'R.F. Bourque  13-156  X2140',
          & 28X,A,//,10X,5A)
      C

           IF(KPRINT .EQ. 1)
          & WRITE(KOUT,28) (V(K), K=1,13)
      C
        28 FORMAT(/,T35,'INPUT LIST',//,
          & 10X,'1    Thrust, Newtons',T57,G9.3,/,
          & 10X,'2    Specific Impulse, seconds',T57,F6.0,/,
          & 10X,'3    Repetition Rate,  Hz',T57,F6.2,/,
          & 10X,'4    Fuel Burnup Fraction',T57,F6.3,/,
          & 10X,'5    Electrical to Magnetic Efficiency',T57,F6.3,/,
          & 10X,'6    Thermal to Electrical Efficiency',T57,F6.3,/,
          & 10X,'7    Fuel Option 1=D-T, 2=D-3He',T57,F3.0,/,
          & 10X,'8    Poloidal Field After Merging, Tesla',T57,F5.1,/,
          & 10X,'9    Poloidal Beta After Merging',T57,F6.3,/,
          & 10X,'10   Plasma Profile Factor',T57,F3.0,/,
          & 10X,'11   Plasma Aspect Ratio, R/A',T57,F6.3,/,
          & 10X,'12   Desired Delta V, m/sec',T57,F6.0,/,
          & 10X,'13   Payload Mass, kg',T57,F7.0,/)
      C
      C------------------------------------------------------------
      C  FUSION FUEL OPTIONS:
      C------------------------------------------------------------
      C
           IF(KFUEL .EQ. 1) THEN
           TBURN = FTBURN*12000.
           SIGV = SDT(TBURN)
           ECHG = 3.517E6
      C 9 MEV NEUTRON HEATING OUT OF 14.1 ASSUMED ABSORBED BY PROPELLANT:
           EN = 9.E6
           MASS = 2.5
           ELSE
           TBURN = FTBURN*55000.
           SIGV = SDHE3(TBURN)
           ECHG = 18.351E6
           EN = 0.
           MASS = 2.5
           END IF
```

```
C
C------------------------------------------------------------
C  POWER REQUIREMENTS:
C------------------------------------------------------------
C
      PTHRST = (9.8/2.)*THRUST*ISP
C  INITIAL ESTIMATE OF TOTAL FUSION POWER:
      ETOT = 0.5*PTHRST/RATE
   78 PRECIR = ETOT*RATE
      PTHTOT = PTHRST+PRECIR
C
C  FUSION ENERGY AND MAX BURN TIME:
C
      EFUSN = PTHTOT/RATE
      MAXBRN = 1./RATE
C
C
C------------------------------------------------------------
C  NO. FUSIONS, FUEL TOTAL NO. AND DENSITY:
C------------------------------------------------------------
C
      NFUSN = EFUSN/((ECHG+EN)*E)
      NIONT = 2.*NFUSN/BURNUP
C  TE ASSUMED << TI:
      NION = (BETA/E)*(BPOL**2/(2.*MU*TBURN))
C
C  DENSITY PROFILE FACTOR:
C
      FPROFL = 1.
      IF(KPROFL .EQ. 2) FPROFL = 0.67
      NIAVE = NION*FPROFL
C
      VPLAS = NIONT/NIAVE
      A = (VPLAS/(2.*PI*ASPECT))**(1./3.)
      R = A*ASPECT
C
C------------------------------------------------------------
C  POWER DENSITY, BURN TIME, POWER AND ENERGY FLUX:
C------------------------------------------------------------
C
      PFUSN = 0.25*(NIAVE*SIGV)*NIAVE*((ECHG+EN)*E)*VPLAS
      BURN = EFUSN/PFUSN
      FBURN = BURN/MAXBRN
      ASURF = 4.*PI**2*R*A
      EFLUX = EFUSN/ASURF
      PFLUX = PFUSN/ASURF
C
C------------------------------------------------------------
C  PLASMA CURRENT AND OHMIC HEATING:
C------------------------------------------------------------
C
      IP = 2.*PI*A*BPOL/MU
      AXC = PI*A**2
      J = IP/AXC
C
C  OHMIC HEATING:
```

```
C
      FANOM = 3.
      LOGLAM = 17.
      Z = 1.5
      ETA = 5.34E-5*Z*LOGLAM/TBURN**1.5
      RESIST = 2.*ETA*R/A**2
      POHMIC = ETA*J**2*VPLAS
      TAUOHM = 2.*1.5*NIONT*TBURN*E/POHMIC
C
C  EXTERNAL ENERGY SUPPLY:
C
      LI = 0.5
      IF(KPROF .EQ. 2) LI = 11./12.
      INDUCT = MU*R*(ALOG(8.*ASPECT)-2.+LI/2.)
C  L/R TIME:
      LOVRR = INDUCT/RESIST
C
      EMAG = 0.5*INDUCT*IP**2
      ETHERM = 1.5*NIAVE*TBURN*E*VPLAS
      ETOLD = ETOT
      ETOT = (EMAG/EFFMAG+ETHERM/EFFACC)/EFFEL
C
C  ACTUAL RECIRCULATING POWER FRACTION:
C
      PELREC = PRECIR*EFFEL*1.E-6
      FRACTH = PRECIR/PTHTOT
      FCONV = ABS((ETOT-ETOLD)/ETOLD)
      IF(FCONV .LE. .01) GO TO 77
      GO TO 78
   77 CONTINUE
C
C------------------------------------------------------------------
C  REQUIRED ENERGY CONFINEMENT TIME FOR STEADY STATE AT TBURN:
C------------------------------------------------------------------
C
      PCHG = PFUSN*ECHG/(ECHG+EN)
      TAUE = 2.*1.5*NIONT*TBURN*E/PCHG
C  NO. OF CONFINEMENT TIMES DURING BURN:
      NCONF = BURN/TAUE
C
C  REQUIRED N-TAU (10**14 SEC/CM**3):
C
      NTAU = NIAVE*TAUE/1.E20
C
C  GOLDSTON SCALING (P. POLITZER 7/7/88):
C
      TAUGLD = .052*R**1.75*IP*1.E-6/
     & (SQRT(PTHTOT*1.E-6)*A**.37)
C
      RTAUG = TAUGLD/TAUE
C
C  NEOCLASSICAL ENERGY CONFINEMENT TIME DUE TO ION
C       THERMAL CONDUCTIVITY (P. POLITZER 9/88):
C
      IPMA = IP*1.E-6
      TAUN = 0.11*IPMA**2/((NIAVE/1.E20)*2.)*
```

F-5

```
     &  SQRT(TBURN/1000.*ASPECT/MASS)
C
      RTAUN = TAUN/TAUE
C
C-------------------------------------------------- ----------
C  PRE-MERGING CONDITIONS:
C----------------------------------------------------------
C
C  BASED ON CONSERVATION OF MAGNETIC ENERGY:
C
      RPRE = 2.*R
      IPPRE = IP/2.
      VPLPRE = 8.*VPLAS
      NIPRE = (NIAVE/2.)/8.
      BPOLP = BPOL/4.
C  PRE-MERGING BETA AT 1.0 KEV:
      BETPRE = 2.*NIPRE*1000.*E/(BPOLP**2/(2.*MU))
C
C
C-----------------------------------------------------------
C  ACCELERATION:
C-----------------------------------------------------------
C
C  ACCELERATES TO BURN TEMP (CONSERVATIVE):
      VEL = SQRT(3.*1.38E-23*TBURN*11600./(MASS*1.67E-27))
      VKMSEC = VEL/1000.
C
C  WANT ACCELERATION FORCE = 0.1*BODY FORCE:
      FBODY = (EMAG/2.)/(2.*(R+A))
      FACCEL = 0.05*FBODY
      MTOT = (NIONT/2.)*MASS*1.67E-27
      ACCEL = FACCEL/MTOT
      TACCEL = VEL/ACCEL
      SACCEL = 0.5*ACCEL*TACCEL**2
      TACCMS = TACCEL*1.E6
C
C  COAXIAL ACCELERATOR CURRENT AND FIELD:
C
      LPRIME = MU/(2.*PI)*ALOG((R+A)/(R-A))
      IACCEL = SQRT(2.*FACCEL/LPRIME)
      RIN = R-A
      BMAX = MU*IACCEL/(2.*PI*RIN)
C
C-----------------------------------------------------------
C  WEIGHT ESTIMATES (KG):
C-----------------------------------------------------------
C
C  ACCELERATOR CAPACITORS:
C  FROM: J. FARBER, DNA: 9.2 KJ/KG BY 1990:
      ECAP = (ETHERM/1000.)/EFFACC
      WCAP = ECAP/9.2
C
C  COMPULSATOR ENERGY STORAGE:
C  FROM: SAE PAPER 859131 (H.J. SCHMIDT, ET.AL.) 10 KJ/KG:
      ECOMP = (ETOT/1000.)*EFFEL
      WCOMP = ECOMP/10.
```

```
C
C  COILS:
C  FROM: MIKE DEW, GA, 50 KJ/KG IN CRYOGENIC COILS:
       ECOIL = (EMAG/1000.)/EFFMAG
       WCOIL = ECOIL/50.
C
C  PROPELLANT CHAMBER (2 EV HYDROGEN AT 4 KSI):
       NHTOT = EFUSN/(2.0*E)
       VCHAM = NHTOT/8.61E25
       DCHAM = (6*VCHAM/PI)**.333
C  CHAMBER STRESSED TO 50 KSI:
       TCHAM = 4000.*DCHAM/(2.*50000.)
       WCHAM = 2000.*PI*TCHAM*DCHAM**2
C  DOUBLE FOR MISC WEIGHT (TRANSFORMERS, POWER SUPPLIES, ETC):
C
C  TOTAL WEIGHT:
       WTOT = (WCAP+WCOMP+WCOIL+WCHAM)*2.0
       WMISC = WTOT/2.
C  MASS POWER DENSITY IN KG/KILOWATT:
       MSPWR = WTOT/(PTHTOT/1000.)
C  MASS UTILIZATION FACTOR IN KW(TH)/TONNE:
       MASSUF = (PTHTOT/1000.)/(WTOT/1000.)
C
C-------------------------------------------------------
C  ROCKET PERFORMANCE:
C-------------------------------------------------------
C
C  PROPELLANT TANK MASS = 0.05*PROPELLANT MASS:
       IEFF = 0.95*ISP
C
C  END OF BURN MASS:
       MFIN = WTOT+PAYLOD
C  INITIAL MASS:
       MINIT = MFIN*EXP(DELTAV/(9.8*IEFF))
C  ROCKET BURN TIME IN MINUTES:
       TRBURN = (9.8*IEFF/THRUST)*(MINIT-MFIN)/60.
C
C  MIN ROCKET ACCELERATION, GEES:
C
       GEES = THRUST/(9.8*MINIT)
C
C  RATIO OF PROPELLANT TO FUSION FUEL MASS:
C
       MPROP = THRUST*MAXBRN/(9.8*ISP)
       MFUEL = NIONT*MASS*1.67E-27
       RATIO = MPROP/MFUEL
C
C-------------------------------------------------------
C  OUTPUT:
C-------------------------------------------------------
C
C
       PTSMW = PTHRST*1.E-6
       PTHMW = PTHTOT*1.E-6
       IPMA = IP*1.E-6
       TAUMS = TAUE*1000.
```

```
      IPPMA = IPPRE*1.E-6
      EFLXMJ = EFLUX*1.E-6
      PFLXMJ = PFLUX*1.E-6
      EMAGMJ = EMAG*1.E-6
      ETHMJ = ETHERM*1.E-6
      ETOTMJ = ETOT*1.E-6
      EFUSMJ = EFUSN*1.E-6
C
      IF(KPRINT .EQ. 1)
     & WRITE(KOUT,30) PTSMW,PTHMW,R,A,IPMA,BURN,FBURN,LOVRR,EFLXMJ,
     & EMAGMJ,ETHMJ,ETOTMJ,EFUSMJ,FRACTH,PELREC,NIAVE,TBURN,
     & TAUE,NCONF,RTAUG,RATIO,RPRE,IPPMA,NIPRE,BPOLP,
     & BETPRE,VKMSEC,SACCEL,TACCMS,IACCEL,BMAX,DCHAM,
     & WTOT,WCAP,WCOMP,WCOIL,WCHAM,WMISC,GEES,
     & MINIT,TRBURN,MSPWR,MASSUF
C
   30 FORMAT(T32'ITERATED OUTPUT',//,
     & 10X,'Thrust Power, MW',T57,F7.0,/,
     & 10X,'Total Fusion Power, MW',T57,F7.0,/,
     & 10X,'Major Radius, meters',T57,F6.3,/,
     & 10X,'Plasma Radius, meters',T57,F6.3,/,
     & 10X,'Plasma Current, MA',T57,F6.2,/,
     & 10X,'Fusion Burn Time, seconds',T57,F7.4,/,
     & 10X,'Burn Time/Max Burn',T57,G9.3,/,
     & 10X,'Plasma L/R Time During Burn, sec',T57,F7.3,/,
     & 10X,'Energy Flux to Wall/Propellant, MJ/m**2',T57,F7.1,/,
     & 10X,'Magnetic Energy to Plasma, MJ',T57,F6.1,/,
     & 10X,'Thermal Energy to Plasma, MJ',T57,F6.1,/,
     & 10X,'Total Recirc Thermal Energy, MJ',T57,F6.1,/,
     & 10X,'Total Fusion Energy, MJ',T57,F6.1,/,
     & 10X,'Recirc Thermal Power Fraction',T57,F6.3,/,
     & 10X,'Electrical Recirculating Power, MW(e)',T57,F7.0,/,
     & 10X,'Ave. Ion Density, m**-3',T57,G9.3,/,
     & 10X,'Assumed Burn Temp, eV',T57,F6.0,/,
     & 10X,'Reqd Total Energy Conf Time for SS, sec',T57,F8.5,/,
     & 10X,'No. Confinement Times in Burn',T57,F4.1,/,
     & 10X,'Ratio of Goldston Confinement Time to Reqd',
     & T57,F5.2,/,
     & 10X,'Ratio of Propellant to Fusion Fuel Mass',T57,G9.3,/,
     & 10X,'Pre-Merging Major Radius, m',T57,F4.3,/,
     & 10X,'Pre-Merging Plasma Current, MA',T57,F6.2,/,
     & 10X,'Pre-Merging Ion Density, m**-3',T57,G9.3,/,
     & 10X,'Pre-Merging Poloidal Field, Tesla',T57,F5.1,/,
     & 10X,'Pre-Merging Beta at 1.0 keV',T57,F4.3,/,
     & 10X,'CT Injection Velocity, km/sec',T57,F6.1,/,
     & 10X,'Acceleration Length, meters',T57,F7.3,/,
     & 10X,'Acceleration Time, microsec',T57,F6.2,/,
     & 10X,'Acceleration Current, Amp',T57,G9.3,/,
     & 10X,'Max Accelerator Field, Tesla',T57,F6.1,/,
     & 10X,'Reaction Chamber Diameter, m',T57,F4.1,/,
     & 10X,'Estimated Total Mass, kg',T57,G9.3,/,
     & 15X,'Capacitor Banks, kg',T57,G9.3,/,
     & 15X,'Compulsator, kg',T57,G9.3,/,
     & 15X,'Magnet Coils, kg',T57,G9.3,/,
     & 15X,'Reaction Chamber, kg',T57,G9.3,/,
     & 15X,'Miscellaneous Mass, kg',T57,G9.3,/,
```

```
      & 10X,'Min Acceleration, gees',T57,F5.3,/,
      & 10X,'Initial Mass, kg',T57,G9.3,/,
      & 10X,'Rocket Burn Time, minutes',T57,G9.3,/,
      & 10X,'Reactor Mass Power Density, kg/kW(th)',T57,G9.3,/,
      & 10X,'Mass Utilization Factor, kW(th)/tonne',T57,G9.3)
C
C  TABULATED OUTPUT FOR PLOT FILES:
C
      IF(KPRINT .EQ. 2) WRITE(KOUT,38)
      & ISP,RATIO,MINIT,WTOT,WCAP,IP,IPPRE,
      & RTAUG,R,RPRE,
      & FBURN,GEES
   38 FORMAT(16(1X,E10.4))
C
      GO TO 111
C
   99 CONTINUE
      CLOSE(UNIT=21, DISPOSE='SAVE')
      STOP
      END
C
```

APPENDIX G

VEHICLE DESIGN OPTIMIZATION

APPENDIX G

VEHICLE DESIGN OPTIMIZATION

This section describes the algorithms and procedure used in optimizing the space vehicle design. The problem begins with the subject mission which is normally expressed as the need to deliver a given payload to a given destination, e.g., transfer a 36_ tonnes (36,000 kg) payload mass from low earth orbit (LEO) to geosynchronons orbit (GEO). The mission as stated automaticlaly defines a delta velocity (ΔV) requirement that must be imported to the payload and, of course, the vehicle delivering this payload, an integral pat of which is the propulsion system. The problem in optimum vehicle design is then reduced to the design and construction of a vehicle with minimum total mass which is capable of delivering the specified payload to the designated target point. Sine the propulsion system and the required propellants are an integral part of the total vehicle, then a set of iterative procedures are required to arrive at the final and complete vehicle design.

In this section the procedure and algorithms used in the design and optimizatin are presented. They are for a single stage vehicle but the procedure is similar for multiple-stage vehicles. Besides, the purpose of fusion propulsion is to have a propulsion system whose energy capacity and engine performance are such that single stage vehicles can accomplish missions with high delta velocity (ΔV) requirements; i.e., missions which require multi-stage, chemically propelled vehicles.

Vehicle Sizing Algorithms

The basic problem is the delivery of a specified payload mass (M_{PL}) to a given target which defines the delta velocity required. The basic rocket equations which describe the single-stage vehicle/payload/rocket propulsion system integration are:

$$\Delta V = I_s \, g_0 \, \ln R \tag{1}$$

and

$$\frac{M_{PL}}{M_o} = 1 - \frac{1}{\lambda}\left(1 - \frac{1}{R}\right) \tag{2}$$

Since the mission defines the velocity requirements and a specific rocket propellant and engine design define the specific impulse, the vehicle mass ratio ($R = \frac{M_i}{M_f}$) is determined. The sizing procedure is: Given ΔV and I_s compute

$$R = \exp\left[\frac{\Delta V}{I_s g_o}\right] \qquad (13)$$

Then construct a plot of $\frac{M_{PL}}{M_o}$ vs λ from equation (2) and proceed as follows:

Assume a value of λ which also defines M_{PL}/M_o and for a given M_{PL}, the initial vehicle mass M_o is completely determined based on the assumed value of the propellant mass fraction of λ. The iteration loop is

$$\lambda = \frac{M_P}{M_o - M_{PL}} = \frac{M_P/M_{PL}}{\left(\frac{M_o}{M_{PL}} - 1\right)}$$

$$\text{or} \qquad M_P = M_{PL}\left[\lambda\left(\frac{M_o}{M_{PL}} - 1\right)\right]$$

The propellant-dependent and other structural masses are,

    1. Propellant Tank(s)
$$M_{PT} = F(W_P) = f(V_{PT}) \qquad (4)$$

    2. Pressurization System
$$M_{PRESS} = f(V_{PT}, P, T) \qquad (5)$$

    4. Tank Insulation and Shielding
$$M_{sh} = f(V_{PT}, T) \qquad (6)$$

    5. Miscellaneous

        (a) Thrust Structure
$$M_{TH \cdot St} = f(F, V_{PT}) \qquad (7)$$

        (b) Lines, valves, pumps, etc.
$$M_{misc} = f(M_P, V_{PT}) \qquad (8)$$

    where $M_P = F/I_S \qquad (9)$

6. Engine

$$M_{eng} = f(F, I_S) \qquad (10)$$

Thus, the complete vehicle mass can be determined by adding all the computed masses

$$M_{PROP\ STAGE} = M_0 - M_{PL}$$
$$= M_P + M_{PT} + M_{Press} + M_{SH}$$
$$+ M_{TH \cdot St} + M_{misc} + M_{eng} \qquad (11)$$

now compute

$$\lambda_{comp} = \frac{M_P}{M_{PROP.\ STAGE}} \qquad (12)$$

and compare with the assumed value.

If $\left| \lambda_{comp} - \lambda_{assumed} \right| \geq \delta$

then assume a new value of λ

e.g. $\lambda = \frac{1}{2} \left(\lambda_{comp} + \lambda_{assumed} \right)$

and repeat the procedure until

$\left| \lambda_{comp} - \lambda_{assumed} \right| \leq \delta$

The results are schematically shown in Figure 1.

Having converged to the proper vehicle mass, the various other parameters of interest are:

Propellant flow rate: $\quad \dot{M}_P = \frac{F}{I_S}$

Burning Time: $\quad t_b = \frac{M_P}{\dot{M}_P}$

Acceleration: $\quad a = \frac{F}{M_0 - \dot{M}_P \Delta t}$

The computation of various structural components, e.g., the engine pumps, the shield and insulation, etc., depend on numerous empirical relations which have been developed over the years of activity in aerospace design practice. The algorithms used here have been based on past vehicle system design studies at MDAC, most notably the SATURN-APOLLO S-IVB stage and the nuclear stage vehicles utilizing the NERVA rocket engine.

Vehicle Sizing Algorithms
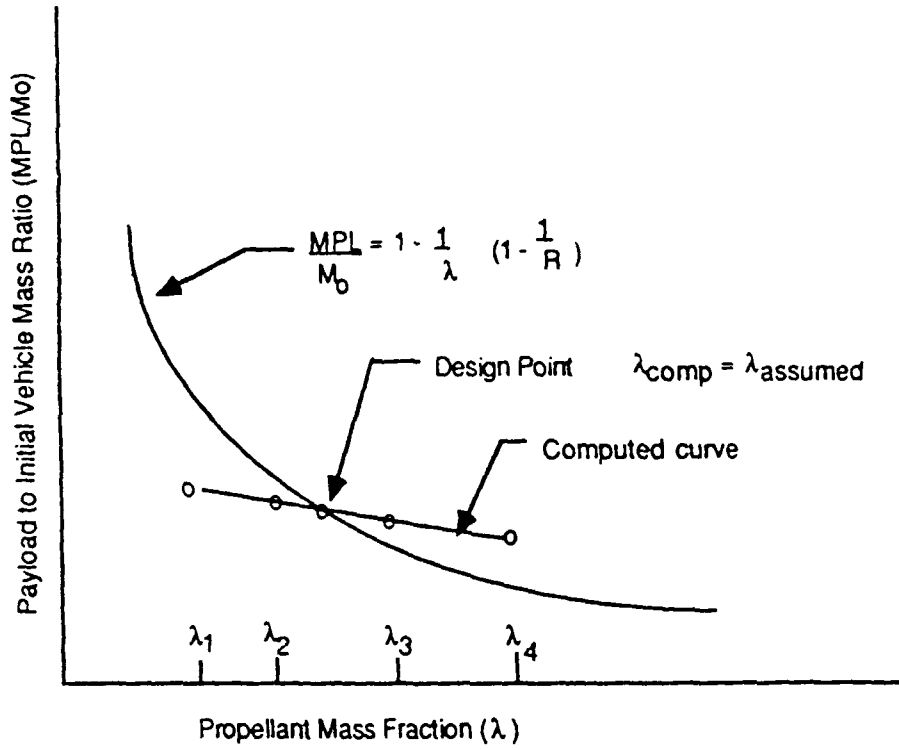
Figure 1. Vehicle Sizing Computational Procedure

REFERENCES

1. (U) Aerospace Forum Report, May 1986 (Secret)

2. (U) DoD Space Transportation Mission Requirements Definition

    VOLUME I: Discussion, (Unclassified)
    Aerospace Report No. TOR-0086 (6460-01)-1

    VOLUME II: Database, (Secret Report)
    Aerospace Report No. TOR-0086A (2460-01)-1

    Air Force Systems Command/Space Division
    12 Dec. 1986

APPENDIX H

BIBLIOGRAPHY ON FUSION FUEL CYCLES

BIBLIOGRAPHY ON FUSION FUEL CYCLES

Ajzenberg-Selove, F., *Nucl. Phys. A*, **320**, 1 (1979).

Bahcall, N.A., and W.A. Fowler, *Astrophys. J.*, **157**, 645 (1969); see also *Astrophys. J.*, **161**, 119 (1970).

Baker, C.C., *et al.*, "Technology Implications of Advanced Fusion Fuel Cycles," IEEE 79CH1410-0, *Proc. 1979 Intl. Conf. Plasma Sci.*, 50 (1979).

Bethe, H.A., *Phys. Today*, **21**, 36 (1968).

Conn, R.W., *et al.*, "Alternate Fusion Fuel Cycle Research," *Proceedings of the 8th International Conference on Plasma Physics and Controlled Nuclear Fusion Research*, IAEA–CN–38/V–5, Brussels, July 1980.

Coppi, B., F. Pegoraro, and J.J. Ramos, "Instability of Fusing Plasma and Spin-Depolarizing Processes," *Phys. Rev. Lett.*, **51**, 892–895 (1983).

Chu, T., and G.H. Miley, "Energy Balances for D–D Systems," *Proc. Symp. Technology of Controlled Thermonuclear Fusion Experiments and the Engineering Aspects of Fusion Reactors, University of Texas, Austin, Texas, November 1972*, AEC Symp. Ser. 31, CONF.-7211, National Technical Information Service, Springfield, Virginia, 1974.

Crocker, V.S., S. Blow, and C.J.H. Watson, "Nuclear Cross-Section Requirements for Fusion Reactors," Paper CN–26/99 in CLM–P 240, Culham Laboratory, Abingdon, England, 1970.

Davison, J., *et al.*, "Low Energy Cross Sections for ^{11}B$(p,3\alpha)$," LAP–165, California Institute of Technology, 1978.

Dawson, J.M., "Enhanced Reactivity of Fusion Reactors," *Proceedings of the Alternate Fuels Fusion Reaction Workshop, December 7-8, 1981, La Jolla, California*, SAI–023–82–008LJ APS–83, SAI Energy Systems Group, August 1982.

Dawson, J.M., H.P. Furth, and F.H. Tenney, "Production of Thermonuclear Power by Non-Maxwellian Ions," *Phys. Rev. Letters*, **26**, 1156 (1971).

Devaney, J.J., and M.L. Stein, "Plasma Energy Deposition from Nuclear Elastic Scattering," *Nucl Sci. Eng.*, **46**, 323 (1971); p, d, t, ^{3}He, ^{4}He on d.

Furth, H.P., and D.L. Jassby, "Power Amplification Conditions for Fusion Reactor Plasmas Heated by Reacting Ion Beams," MATT–1040, Princeton Plasma Physics Laboratory, Princeton, New Jersey, 1974.

Fusion, E. Teller (ed.), Academic Press, New York, 1981 v. 1, (Parts A and B).

Gamow, G., and E. Teller, "The rate of Selective Thermonuclear Reactions," *Phys. Rev.*, **53**, 608–609 (1938).

Gordon, J.D., et al., "Evaluation of Proton-Based Fuels for Fusion Power Plants," RP 1063-1, Final Report on EPRI Project, 1981.

Gordon, J.D., et al., "p–^{11}B Multiple Evaluation," presented at *Third IAEA Technical Committee Meeting and Workshop on Fusion Reactor Design and Technology*, Tokyo, Japan, October 5–16, 1981.

Hauss, B.I., and T.K. Samec, "Fusion Reactivity Enhancement by Non-Maxwellian Ion Tail Formation," *BAPS*, **27**, 1144 (1982).

Hauss, B.I., and T.K. Samec, "The Impact of Synchrotron Radiation on the Burning of Advanced Fuels," *BAPS*, **24**, 1042 (1979).

Heckrotte, W., and J.R. Hiskes, "Some Factors in the Choice of D–D, D–T, or D–^{3}He Mirror Fusion Power Systems," *Nucl. Fusion*, **11**, 471 (1971).

Hofmann, H.M., and D. Fick, "Fusion of Polarized Deuterons," *Phys. Rev. Lett.*, **52**, 2038–2040 (1984).

Hosea, J., et al., *Proc. 8th Int. Conf. Plasma Physics and Controlled Nuclear Fusion Research*, Brussels, Belgium, July 1–10, 1980, International Atomic Energy Agency, to be published.

Howerton, R.J., "Maxwell–Averaged Reaction Rates $(\overline{\sigma v})$ for Selected Reactions Between Ions with Atomic Mass $\leq$ 11," UCRL–50400, v. 21, (Part A), Lawrence Livermore National Laboratory, 1979. Report contains data for 24 reactions.

Kulsrud, R.M., et al., "Fusion Reactor Plasmas with Polarized Nuclei," *Phys. Rev. Lett.*, **49**, 1248–1251 (1982).

Lawson, J.D., *Proc. Phys. Soc. London B*, **70**, 6 (1957).

Levush, B., and S. Cuperman, "On the Potentiality of the Proton-Boron Fuel for Inertially Confined Fusion," *Nuclear Fusion*, **11**, 1519 (November 1982).

Mark, J.C., "Report on Conference on the Super," LA–575, Los Alamos National Laboratory, June 1946, sanitized version, May 1971; see also "A Short Account of Los Alamos Theoretical Work on Thermonuclear Weapons, 1946–1950," LA–5647–MS, Los Alamos National Laboratory, 1974.

Maxon, M.S., and E.G. Corman, *Phys. Rev.*, **163**, 156 (1967).

McNally, J.R., Jr., "Nuclear Fusion Resonance Reactions of Possible CTR Interest," ORNL/TM–3233, Revised, Oak Ridge National Laboratory, 1971.

McNally, J.R., Jr., *Proc. Conf. Nuclear Cross Sections and Technology*, NBS Special Publication 425, v. 2, U.S. National Bureau of Standards, 1975, p. 683; see also *Proc. 6th IEEE Symp. Engineering Problems of Fusion Research*, Institute of Electronics and Electrical Engineers, 1976, p. 1012.

McNally, J.R., Jr., and K.E. Rothe, *Int. Conf. Plasma Science Abstracts*, 79CH1410–0 NPS, Institute of Electronics and Electrical Engineers (1979), p. 52.

McNally, J.R., Jr., K.E. Rothe, and R.D. Sharp, "Fusion Reactivity Graphs and Tables for Charged Particle Reactions," ORNL/TM–6914, Oak Ridge National Laboratory, 1979. Updated tables containing $\langle \sigma v \rangle$ data for 37 reactions are available from the first author.

Miley, G., *et al.*, "Cat–D and D–^{3}He Fusion Reactor Systems," *Proc. 2nd Int. ANS Topical Mtg. on the Tech. of Cont. Nuclear Fusion*, 1, 119–133 (1976).

Miley, G.H., "Advanced Fuels and the Development of Fusion Power," FSL–54, University of Illinois, 1981; see also "Potential and Status of Alternate-Fuel Fusion," COO–2218–175, University of Illinois, 1980.

Miley, G.H., "Charged-Particle Cross Section Data for Fusion Plasma Applications," *Proc. Brookhaven National Laboratory Workshop*, September 22–26, 1980.

Miley, G.H., "Comments About p–^{11}B Ignition," in *Proc. Rev. Mtg. AF Fusion*, C. Choi (ed.), ER–536–SR, EPRI, Palo Alto, California, 1977.

Miley, G.H., Fusion Energy Conversion, *The American Nuclear Soc.*, La Grange Park, Illinois, 1976.

Miley, G.H., "Potential Role of Advanced Fuels in Inertial Confinement Fusion," *Proc. Fifth Workshop on Laser Interaction with Matter*, University of Rochester, November 1979.

Miley, G.H., and H. Towner, "Cross-Sections and Reactivities for Two-Component Fusion Calculations," *Proc. APS Conf. Nuclear Cross Sections and Technology, Washington, D.C., March 1975*, CONF.–750303, National Bureau of Standards, Washington, DC, 1975.

Miley, G.H., H. Towner, and N. Ivich, "Fusion Cross Sections and Reactivities," COO–2218–17, Nuclear Engineering Program, University of Illinois, Urbana, Illinois, 1974.

Miley, G.H., et al., "Catalyzed-DD and D-^{3}He Fusion Reactor Systems," *Second Topical Meeting on Technology of Controlled Nuclear Fusion*, v. 1, Richland, American Nuclear Society, 1976, pp. 119-133.

Mills, R.G., "Catalyzed Deuterium Fusion Reactors," PPL-TM-259, Princeton Plasma Physics Laboratory, 1971.

Perkins, S.T., and D.E. Cullen, "Elastic Nuclear Plus Interference Cross Sections for Light-Charged Particles," *Nucl. Sci. Eng.*, 77, 20 (1981); p, d, t, ^{3}He, ^{4}He with each other.

Persiani, P.J., W.C. Lipinski, and A.J. Hatch, "Some Comments on the Power Balance Parameters Q and ϵ as Measures of Performance for Fusion Power Reactors," *Nucl. Fusion*, to be published.

Persiani, P.J., W.C. Lipinski, and A.J. Hatch, "Survey of Thermonuclear-Reactor Parameters," *Proc. Symp. Technology of Controlled Thermonuclear Fusion Experiments and the Engineering Aspects of Fusion Reactors, University of Texas, Austin, Texas, November 1972*, AEC Symp. Ser. 31, CONF.-7211, National Technical Information Service, Springfield, Virginia, 1974.

Proc. EPRI Advanced Fuel Reactor Review Mtg., EPRI ER-536-SR, C. Choi, (ed.), Electric Power Research Inst., 1977.

Proc Second United Nations Int. Conf. Peaceful Uses of Atomic Energy, Geneva, Switzerland, September 1-13, 1958, v. 31-33, United Nations, 1958.

Rand McNally, J., Jr., "Advanced Fuels for Nuclear Fusion Reactors," *Proc. APS Conf. Nuclear Cross Sections and Technology, Washington, D.C., March 1975*, CONF.-750303, National Bureau of Standards, Washington, DC, 1975.

Rand McNally, J., Jr., "Autocatalytic Burning of ^{6}LiD Nuclear Fuel Via the $\rho+^9$Be Resonance Reaction," *Nucl. Fusion*, 11, 554 (1971).

Rand McNally, J., Jr., "Fusion Chain Reactions-II," *Nucl. Fusion*, 11, 189 (1971).

Rand McNally, J., Jr., "Fusion Chain Reactions-III, The Production of MeV Plasmas," *Nucl. Fusion*, 11, 191 (1971).

Rand McNally, J., Jr., "Modified Lawson Criterion for D-Li^6 Fuelled Fusion Reactors," *Nucl. Fusion*, 13, 289 (1973).

Rand McNally, J., Jr., "Nuclear Fusion," *Encyclopedia of Chemistry*, 3rd ed., C.A. Hampel and G.G. Hawley (eds.), Van Nostrand-Reinhold Company, Princeton, New Jersey, 1973, p. 481.

Rand McNally, J., Jr., "Nuclear Fusion Chain Reaction Applications in Physics and Astrophysics," IAEA/SM-170/49, International Atomic Energy Agency, Vienna, Austria, 1973.

Rand McNally, J., Jr., "Prospects for Alternate Fusion Fuel Cycles at Ultra-High Temperatures," ORNL–TM–3783, Oak Ridge National Laboratory, Oak Ridge, Tennessee, 1972.

Rand McNally, J., Jr., "Speculations on the Configurational Properties of a Fusioning Plasma," *Nucl. Fusion*, 12, 265 (1972).

Rand McNally, J., and K.E. Rothe, "Advanced Fusion Fuels — A Review," *Second Int'l. Conf. Emerging Nucl. Eng. Sys.*, Lausanne, Switzerland, April 23–25, 1980.

Reinmann, J.J., and W.D. Rayle, "Deuterium-Helium–3 Fusion Power Balance Calculations," NASA TM X–2280, NASA Lewis Research Center, Cleveland, Ohio, 1971.

Rose, D.J., "On the Feasibility of Power by Nuclear Fusion," ORNL/TM–2204, Oak Ridge National Laboratory, 1978; see also *Nucl. Fusion*, 9, 183 (1969).

Ruby, L., and T.P. Lung, "Effect of ^{6}Li$+^6$Li Reactions in a Fusion Reactor Operating on ^{6}Li$(p, \alpha)^3$He," *Nucl. Sci. Eng.*, 69, 107 (1979).

Schultz, J.H., L. Bromberg, and D.R. Cohn, *Nucl. Fusion*, 20, 703 (1980).

Shuy, G.W., "Advanced Fusion Fuel Cycles and Fusion Reaction Kinetics," UWFDM–335, University of Wisconsin, Madison, Wisconsin, 1979.

Shuy, G.W., and R.W. Conn, "Physics Phenomena in the Analysis of Advanced Fusion Fuel Cycles," PPG–522, University of California, Los Angeles, 1980; see also "Charged Particle Cross Section Requirements for Advanced Fusion Fuel Cycles," *Proc. Int. Conf. Nuclear Cross Sections for Technology*, NBS Special Publications 594, U.S. National Bureau of Standards, 1980, p. 254.

Spitzer, L.J., Jr., *Physics of Fully Ionized Gases*, Wiley-Interscience Publishers, New York, 1962.

Takahashi, H., "Some Thoughts on Muon-Catalyzed Fusion Reactor," *Muon-Catalyzed Fusion*, 1, 375 (1987).

Tamor, S., "Studies of Emission and Transport of Synchrotron Radiation in Tokamaks," LAPS–71, SAI–023–81–110LJ, Science Applications, Inc., 1981.

Trubnikov, B.A., *J. Exp. Theor. Phys.*, 16, 1 (1972).

Weaver, T., G. Zimmerman, and L. Wood, "Exotic CTR Fuels: Non-Thermal Effects and Laser Fusion Applications," UCRL–74938, Lawrence Livermore National Laboratory, October 1973.

Weaver, T., G. Zimmerman, and L. Wood, "Prospects for Exotic Thermonuclear Fuel Usage in CTR Systems," UCRL–74191, UCRL–74352, Lawrence Livermore National Laboratory, 1972; see also "Exotic CTR Fuels: Non-Thermal Effects and Laser Fusion Applications," UCRL-74938, Lawrence Livermore National Laboratory, 1973.

APPENDIX I

BIBLIOGRAPHY ON FUSION CONFINEMENT

BIBLIOGRAPHY ON FUSION CONFINEMENT

Alfven, H., "Magnetohydrodynamics and the Thermonuclear Problem," *Proc. 2nd U.N. Conf. Peaceful Uses of Atomic Energy*, 31, 3 (1958).

Alikhanov, S.G., *et al.*, "Studies of Model Thermonuclear Systems with Liners," *Proc. 6th Int. Conf. Plasma Physics and Controlled Nuclear Fusion*, Berchtesgaden, Federal Republic of Germany, October 6–13, 1976, CONF–761012, IAEA-CN–35/E19–2, v. III, International Atomic Energy Agency, 1977, p. 517.

"Alternate Concepts in Controlled Fusion," F.F. Chen (ed.), EPRI–429–SR, Electric Power Research Institute, May 1977.

Anderson, O.A., *et al.*, "Neutron Production in Linear Deuterium Pinches," *Phys. Rev.*, 110, 1375 (1958).

Angelo, J.A., and D. Buder, *Space Nuclear Power*, (Orbit Book Company, Malabar, Florida, 1985), p. 101.

Armstrong, W.T., *et al.*, "Compact Torus Experiments and Theory," *Proc. 8th Conf. Plasma Physics and Controlled Fusion Research*, Brussels, July 1–10, 1980, IAEA–CN–38/R–3, International Atomic Energy Agency, 1980.

Artiugina, I.M., *et al.*, "Thermonuclear Power Station Based on a Reactor with a Partially Evaporating Liner," *Seriia: Termoiadernyi Sintez*, 1, 3, 62 (1979).

Artsimovich, L.A., *Nucl. Fusion*, 2, 215 (1972).

Badger, B., *et al.*, *HIBALL-II — An Improved Conceptual Heavy Ion Fusion Reactor Study*, UWFDM–625, University of Wisconsin, Madison, Wisconsin, 1984.

Baker, C.C., *et al.*, "The Impact of Alternate Fusion Fuels on Fusion Reactor Technology," ANL/FPP/TM–128, Argonne National Laboratory, November 1979.

Baker, C.C., *et al.*, "STARFIRE — Commercial Tokamak Fusion Power Plant Study," ANL/FPP–80–1, Argonne National Laboratory, 1980; see also, M.A. Abdou, *et al.*, "STARFIRE — A Conceptual Design of a Commercial Tokamak Power Plant," *Proc. 8th Int. Conf. Plasma Physics and Controlled Nuclear Fusion Research*, Brussels, July 1–10, 1980, IAEA–CN–38/E–1, International Atomic Energy Agency, 1980; see also, C.C. Baker, *et al.*, "STARFIRE — A Commercial Tokamak Power Plant Design," *Nucl. Eng. Des.*, to be published.

Baldwin, D.E., B.G. Logan, and T.K. Fowler, "An Improved Tandem Mirror Fusion Reactor," UCID-18156, Lawrence Livermore National Laboratory, 1979.

Bangerter, R.O. "Heavy-Ion Inertial Fusion: Initial Survey of Target Gain Versus Ion-Beam Parameters," *Phys. Lett.*, **88A**, 5 (1982).

Barnes, C.W., *et al.*, "Confinement Time and Energy Balance in the CTX Spheromak," *Proc. 6th U.S. Compact Toroid Symp.*, Princeton, New Jersey, 1984, p. 80.

Bathke, C., H. Towner, and G.H. Miley, "Fusion Power by Non-Maxwellian Ions in $D-T$, $D-D$, $D-He^3$ and $p-B^{11}$ Systems," *Trans. Am. Nucl. Soc.*, **17**, 41 (1973).

Benford, J., *et al.*, "Electron Beam Heating of Linear Fusion Devices," *Proc. 1st Int. Topl. Conf. Electron Beam Research and Technology*, Albuquerque, New Mexico, November 3-6, 1975, CONF-751108, 1976.

Bertolini, E., *Proc. 3rd Topl. Mtg. Technology of Controlled Nuclear Fusion*, Santa Fe, New Mexico, May 9-11, 1978, CONF-780508, American Nuclear Society, 1978, p. 38.

Blink, J.A., *et al.*, *The High-Yield Lithium-Injection Fusion-Energy (HYLIFE) Reactor*, UCRL-53559, Lawrence Livermore National Laboratory, Livermore, California, 1985.

Book, D.L., *et al.*, "Stabilized Imploding Liner Fusion Systems," *Proc. 6th Int. Conf. Plasma Physics and Controlled Nuclear Fusion Research*, Berchtesgaden, Federal Republic of Germany, October 6-13, 1976, CONF-761012, IAEA-CN-35/E19-1, v. III, International Atomic Energy Agency, 1977, p. 507.

Bourque, R.F., "OHTE as a Fusion Reactor," *Proc. 4th Topl. Mtg. Technology of Controlled Nuclear Fusion*, King of Prussia, Pennsylvania, October 14-16, 1980, to be published.

Bourque, R.F., "OHTE Reactor Concepts", GA Report GA-A-16458, General Atomic Co., September 1981; also paper 67-25 presented at the *9th Symposium on Engineering Problems of Fusion Research*, Chicago, Illinois, October 26-29, 1981.

Bourque, R.F., K.R. Schultz, and Project Staff, *Final Report: Innovative Approaches to Inertial Confinement Fusion Reactors*, GA Report GA-A18574, GA Technologies Inc., San Diego, California, 1986.

Busemann, A., "Plasma Physics and Magnetohydrodynamics in Space Exploration," NASA SP-25, 1, National Aeronautics and Space Administration, 1962.

Bussac, M.N., *et al.*, "Low-Aspect-Ratio Limit of the Toroidal Reactor: The Spheromak," *Proc. 7th Int. Conf. Plasma Physics and Controlled Nuclear Fusion Research*, IAEA-CN-37/X-1, v. III, International Atomic Energy Agency, 1978, p. 249.

Bustraan, M., *et al.*, "A Reactor Study on the Belt-Shaped Screw Pinch," Jutphaas Report ECN-77, Netherlands Energy Research Foundation, October 1979.

Carlson, G.A., *et al.*, "Conceptual Design of the Field-Reversed Mirror Reactor," UCRL-52467, Lawrence Livermore National Laboratory, May 1978.

Chen, F.F., "Alternative Concepts in Magnetic Fusion," *Phys. Today*, 32, 36 (May 1979).

Cohn, D.R., *et al.*, "High Field Compact Tokamak Reactor (HFCTR)," RR-78-2, Massachusetts Institute of Technology Plasma Fusion Center, March 1978.

Condit, W.C., *et al.*, "Preliminary Design Calculations for a Field-Reversed Mirror Reactor," UCRL-52170, Lawrence Livermore National Laboratory, 1976.

Conn, R.W., *et al.*, "Aspects of Octopoles as Advanced Cycle Fusion Reactors," in *Fusion Reactor Design Problems*, IAEA, Vienna, 1978.

Cooper, R., "A Shock-Heated, Wall-Confined Fusion Reactor Conceptual Design," PIFR-1154-1, Physics International, June 1979.

Dove, W.F., "Advanced Fusion Concepts Program," *Proc. 3rd Topl. Mtg. Technology of Controlled Nuclear Fusion*, Santa Fe, New Mexico, May 9-11, 1978, CONF-780508, 1, 51 (1978).

Fleischman, H.H., and T. Kammash, "System Analysis of the Ion-Ring Compressor Approach to Fusion," *Nucl. Fusion*, 15, 1143 (1975).

Fowler, T.K., and B.G. Logan, "The Tandem Mirror Reactor," *Comments on Plasma Physics*, 2, 167 (1977).

Fraley, G.S., *et al.*, "Thermonuclear Burn Characteristics of Compressed DT Microspheres," *Phys. Fluids*, 17, 474 (1974).

Frank, T.G., and C.E. Rossi, "Technology Requirements for Commercial Applications of Inertail Confinement Fusion," *Nucl. Tech./Fusion*, 1, 359 (1981).

Fuller, G.H., *et al.*, "Developing Maintainability for Tokamak Fusion Power Systems," COO-418426, McDonnel Douglas Astronautics Company, November 1978.

Furth, H.P., "The Compact Torus," *J. Vac. Sci. Technol.*, 18, 1073 (1982).

Furth, H., "The Compact Torus Concept and the Spheromak," *Proc. US/Japan Joint Symp. Compact Toruses and Energetic Particle Injection*, Princeton, New Jersey, December 12-14, 1979, 1980, p. 3.

Furth, H.P., *Nucl. Fusion*, 15, 487 (1975).

Furth, H.P., "U.S. Tokamak Research," PPPL-1598, Princeton Plasma Physics Laboratory, October 1979.

"Fusion Reactor Remote Maintenance Study," ER-1046, Electric Power Research Institute, April 1979.

Galambos, J.D., et al., "Operating Parameters for a Moving Plasmoid Heater (MPH) Reactor Concept," *Trans. Am. Nucl. Soc.*, **32**, 28 (1979).

Gautier, P., et al., "Numerical Study of the Ideal-MHD Stability Limits on Oblate Spheromaks," *Nucl. Fusion*, **21**, 139 (1981).

Gerdin, G., "Start-up of Advanced Fuel Tokamak," in *Proc. Rev. Mtg. AF Fusion*, C. Choi (ed.), ER-536-SR, EPRI, Palo Alto, California, 1977.

Gibson, A., "Permissible Parameters for Economic Stellarator and Tokamak Reactors," *Proc. British Nuclear Energy Society Nuclear Fusion Reactor Conf.*, Abingdon, England, September 1969, 1969, p. 233.

Gibson, A., R. Hancox, and R.J. Bickerton, "On the Economic Feasibility of Stellarator and Tokamak Fusion Reactors," *Proc. 4th Conf. Plasma Physics and Controlled Nuclear Fusion Research*, June 17–23, 1971, IAEA-CN-28/K-4, v. III, International Atomic Energy Agency, 1971, p. 375.

Gilligan, J.G., et al., "Modularizaton of Advanced-Fuel Plasmoid Reactors," *Eighth IEEE Sym. on Eng. Problems of Fusion Research*, San Francisco, California, November 1979.

Goldenbaum, G., et al., "Formation of a Spheromak Plasma Configuration," *Phys. Rev. Lett.*, **44**, 393 (1980).

Hagenson, R.L., et al., "The Dense Z–Pinch (DZP) as a Fusion Power Reactor: Preliminary Scaling Calculations and Systems Energy Balance," LA-8186-MS, Los Alamos Scientific Laboratory, January 1980.

Hagenson, R.L., and R.A. Krakowski, "A Compact-Torus Fusion Reactor Based upon the Field-Reversed Theta Pinch," *Proc. 4th Topl. Mtg. Technology of Controlled Nuclear Fusion*, King of Prussia, Pennsylvania, October 14–16, 1980, to be published.

Hagenson, R.L., and R.A. Krakowski, "Conceptual Physics Design of a Compact Torus Fusion Reactor (CTOR)," LA-8448-MS, Los Alamos Scientific Laboratory, July 1980.

Hagenson, R.L., and R.A. Krakowski, "The Reversed-Field Pinch Reactor (RFPR) Concept," LA-7973-MS, Los Alamos Scientific Laboratory, August 1979.

Hancox, R., et al., "The Reverse-Field Pinch Reactor," *Nucl. Eng. Des.*, to be published, 1981.

Harris, D.B., and J.H. Pendergrass, *Fusion Technol.*, **8**, 1220 (1985).

Harris, D.B., and J.H. Pendergrass, "KrF Laser Cost/Performance Model for ICF Commercial Applications," *Fusion Technol.*, **8**, 1220 (1985).

Hartman, C.W., "Finite Larmor Radius Stabilized Z–Pinches," UCID–17118, Lawrence Livermore National Laboratory, 1976.

Hartman, C.W., et al., "A Conceptual Fusion Reactor Based on the High-Plasma-Density Z–Pinch," *Nucl. Fusion*, **17**, 909 (1977).

Hartman, C.W., et al., "High-Density Fusion and the Z–Pinch," *Proc. 5th Conf. Plasma Physics and Controlled Nuclear Fusion Research*, Tokyo, November 11–15, 1974, CONF–741105, IAEA–CN–33/H5–2, v. II, International Atomic Energy Agency, 1975, p. 653.

Hedrick, C.L., et al., "A Simple Neoclassical Point Model for Transport and Scaling in EBT," *Nucl. Fusion*, **17**, 1237 (1977).

Hershkowitz, A.N., and J.M. Dawson, "Fusion Reactor with Picket–Fence Walls," *Nucl. Fusion*, **16**, 639 (1976).

Hoffman, A., P. Rose, and L. Steinhauer, "Status of Laser Solenoid Fusion Concept," *Trans. Am. Nucl. Soc.*, **27**, 49 (1977).

Hogan, W.J., and G.L. Kulcinski, "Advances in ICF Power Reactor Design," *Fusion Tech.*, **8**, 717 (1985).

Hogan, W.J., and W.R. Meier, "Economic Requirements for Competitive Laser Fusion Power Production," *Proc. 11th Symposium on Fusion Engineering, Austin, Texas, November 18–22, 1985*, UCRL–92559, Lawrence Livermore National Laboratory, Livermore, California, 1985.

Hugrass, W.N., et al., "Compact Torus Configuration Generated by a Rotating Magnetic Field: The Rotamak," *Phys. Rev. Lett.*, **44**, 1676 (1980); see also I.R. Jones, and W.N. Hugrass, "Steady-State Solutions for the Penetration of a Rotating Magnetic Field into a Plasma Column," *J. Plasma Phys.*, **26**, 441 (1981).

Hyde, R.A., *A Laser Fusion Rocket in Interplanetary Propulsion*, UCRL–88857, Lawrence Livermore National Laboratory, Livermore, California, 1983.

ISX Group, *Proc. 8th Int. Conf. Plasma Physics and Controlled Nuclear Fusion Research*, Brussels, July 1–10, 1980, IAEA–CN–38/A–5, International Atomic Energy Agency, 1980.

Jarboe, T., et al., "Spheromak Studies on CTX," *Proc. 10th Int. Conf. Plasma Physics and Controlled Nuclear Fusion*, London, September 12–19, 1984, IAEA–CN–44/D–III–1, v. 2, International Atomic Energy Agency, Vienna, 1985, p. 501.

Jarboe, T.R., et al., "Motion of a Compact Toroid Inside a Cylindrical Flux Conserver," *Phys. Rev. Lett.*, **45**, 1264 (1980).

Jarboe, T.R., et al., "The Ohmic Heating of a Spheromak to 100 eV," *Phys. Fluids*, 27, 1, 13 (1984).

Jardin, S., "Ideal Magnetohydrodynamic Stability of the Spheromak Configuration," *Nucl. Fusion*, 22, 629 (1982).

Jasshy, D.L.. *Nucl. Fusion*, 17, 373 (1977).

Jones, J.E., et al., "Multimegawatt Space Nuclear Power Concept," in *Proc. 1st Symposium on Space Nuclear Power Systems*, (Albuquerque, New Mexico, January 1984), pp. 249–255.

Katsurai, M., and M. Yamada, "Conceptual Design Study of Spheromak Reactors," PPPL–1614, Princeton Plasma Physics Laboratory, July 1980.

Katsurai, M., and M. Yamada, "Studies of Conceptual Spheromak Fusion Reactors," *Nucl. Fusion*, 22, 1047 (1982).

Kaufmann, M., and W. Köppendörfer, "Fusion Reactor Characteristics in Dependence on Beta and Aspect Ratio," *Proc. 6th European Conference Controlled Fusion and Plasma Physics*, Moscow, July 30 through August 4, 1973, I, 341 (1973).

Kawai, K., and Z.A. Pietrzyk, "Compact Toroid Formation by a Conical θ–Pinch," *Bull. Am. Phys. Soc.*, 26, 905 (1981).

Kidder, R.E., "Laser Compression of Matter: Optical Power and Energy Requirements," *Nuclear Fusion*, 14, 797 (1974).

Kidder, R.E., "Laser-Driven Compression of Hollow Shells: Power Requirements and Stability Limitations," *Nuclear Fusion*, 16, 1 (1976).

Köppendörfer, W., "System Analysis of Magnetically Confined Pulsed Reactors," *Pulsed Fusion Reactors*, EUR–5307e, Euratom, 1974, p. 682.

Kovnizhnykh, L.M., "Transport Phenomena in Toroidal Magnetic Systems," *Soviet Phys. JETP*, 29, 3, 375 (1969).

Krakowski, R.A., "A Survey of Linear Magnetic Fusion Reactors," *Proc. 3rd Topl. Mtg. Technology of Controlled Nuclear Fusion*, San Fe, New Mexico, May 9–11, 1978, CONF.–780508, v. 1, American Nuclear Society, 1978, p. 422.

Krakowski, R.A., et al., "Reactor Systems Studies of Alternative Fusion Concepts," *Proc. 8th Conf. Plasma Physics and Controlled Nuclear Fusion Research*, Brussels, July 1–10, 1980, IAEA–CN–38/V–4, International Atomic Energy Agency, 1980.

Krakowski, R.A., et al., "Systems Studies and Conceptual Reactor Designs of Alternative Fusion Concepts at LASL," *Proc. 7th Conf. Plasma Physics and Controlled Nuclear Fusion Research*, August 1978, IAEA–CN–37/1-2, v. III, International Atomic Energy Agency, 1979, p. 333.

Krakowski, R.A., R.L. Miller, and R.L. Hagenson, "Alternative Concepts for Magnetic Fusion," *Proc. 4th Topl. Mtg. Technology of Controlled Nuclear Fusion*, King of Prussia, Pennsylvania, October 14–17, 1980, to be published.

Krall, N.A., and G.W. Stuart, "Evaluation of Alternative Fusion Concepts," Electric Power Research Institute, to be published, 1981.

Lasche, G.P., *The Feasibility of a Laser or Charged-Particle-Beam Fusion Reactor Concept with Direct Electric Generation by Magnetic Flux Compression*, UCRL–53434, Lawrence Livermore National Laboratory, Livermore, California, 1983.

Lawson, J.D., AERE–GP/R–1807, Atomic Energy Research Establishment, Harwell, 1955.

Leonard, B.R., Jr., *Nucl. Technol.*, 20, 161 (1973).

Lidsky, L.M., *Nucl. Fusion*, 15, 151 (1975).

Lindl, J.D., and J.W–K. Mark, "Recent Livermore Estimates of the Energy Gain of Cryogenic Single-Shell Ion Beam Targets," *Laser and Particle Beams*, 3, 37 (1985).

Logan, B.G., "An Axisymmetric, High Beta Tandem Mirror Reactor," UCRL–83555, Lawrence Livermore National Laboratory, November 1979.

Maisonnier, C., "Plasma Focus and Thermonuclear Fusion," *Pulsed Fusion Reactors*, EUR–5307e, Euratom, 1974, p. 131.

"Major Features of D–T Tokamak Fusion Reactor Systems," 472–1, Electric Power Research Institute, February 1976.

Manheimer, W.M., M. Loumpe, and J.B. Boris, "Effect of a Surrounding Gas on Magnetohydrodynamic Instabilities in Z–Pinch," *Phys. Fluids*, 16, 1126 (1973).

Martin, T.H., *et al.*, "Pulsed Power Accelerators for Particle Beam Fusion," *Conference Record of the 14th Pulse Power Modulator Symposium*, Orlando, Florida, June 1980.

Maya, I., *et al.*, *Final Report: Inertial Confinement Fusion Reaction Chamber and Power Conversion System Study*, GA Report GA–A–17842, GA Technologies Inc., San Diego, California, to be published.

Meeker, D.J., "A High Efficiency ICF Driver Employing Magnetically Confined Plasma Rings," *Fusion Technol.*, 8, 1–2B, 1191 (1985).

Meier, W.R., *et al.*, *Inertial Fusion Power for Space Applications*, UCRL–94138, Lawrence Livermore National Laboratory, Livermore, California, 1986; also in *Proc. 21st IECEC Conference*, (American Chemical Society, Washington, D.C., 1986), pp. 1842–1848.

Meier, W.R., and W.J. Hogan, "ICF Reactor Economics: Identifying the High Leverage Design Features," *Fusion Technol.*, 8, 1820 (1985).

Meier, W.R., W.J. Hogan, and R.O. Bangerter, *Economic Studies for Heavy-Ion-Fusion Electric Power Plants*, UCRL-94335, Lawrence Livermore National Laboratory, Livermore, California, 1986.

Miley, G.H., "Overview of Nonelectrical Applications of Fusion," *2nd Miami Int. Conf. on Alternative Energy Sources*, Miami Beach, Florida, December 1979.

Miley, G.H., et al., "High-Efficiency Advanced-Fuel Fusion Reactors," EPRI ER-581, Electric Power Research Inst., 1977.

Miley, G.H., et al., "High-Efficiency Advanced-Fuel Fusion Reactors," EPRI ER-919, Electric Power Research Inst., California, 1978.

Miller, R.L., and R.A. Krakowski, "Assessment of the Slowly-Imploding Liner (LINUS) Fusion Reactor Concept," *Proc. 4th Topl. Mtg. Technology of Controlled Nuclear Fusion*, King of Prussia, Pennsylvania, October 14-16, 1980, to be published.

Miller, R.L. and R.A. Krakowski, "The Modular Stellarator/Torsatron Fusion Reactor Concept," Los Alamos Scientific Laboratory, to be published, 1980.

Miller, R.L., and R.A. Krakowski, "Thermal Conduction and Alpha-Particle Constraints for the Ignition of a D-T Linear Magnetic Fusion (LMF) Reactor," *Nucl. Fusion*, 18, 1722 (1978).

Miller, R.L., R.A. Krakowski, and C.G. Bathke, "A Parametric Study of the Tormac Fusion Reactor Concept," LA-7935-MS, Los Alamos Scientific Laboratory, August 1979.

Miller, R.L., R.A. Krakowski, and C.G. Bathke, "Tormac Fusion Reactor Design Points," *Trans. Am. Nucl. Soc.*, 33, 98 (1979).

Monsler, M.J., *Laser Cost Scaling*, Memo E&MA 80-106, Lawrence Livermore National Laboratory, Livermore, California, 1980.

Monsler, M.J., et al., "An Overview of Inertial Fusion Reactor Design," *Nucl. Technol./Fusion*, 1, 302 (1981).

Moses, R.W., R.A. Krakowski, and R.L. Miller, "A Conceptual Design of the Fast Liner Reactor (FLR) for Fusion Power," LA-7686-MS, Los Alamos Scientific Laboratory, February 1979.

Motz, H., *The Physics of Laser Fusion*, Academic Press, New York, 1979.

Nagata, M., et al., "Shear Stabilizing Experiment of Gun-Spheromak Plasma," *Proc. 10th Int. Conf. Plasma Physics and Controlled Nuclear Fusion Research*, London, September 12-19, 1984, International Atomic Energy Agency, Vienna, 1985.

Nebel, R.A., et al., "Comparison of Zero-Dimensional and One-Dimensional Thermonuclear Burn Computations for the Reversed-Field Pinch Reactor (RFPR)," LA-8185-MS, Los Alamos Scientific Laboratory, January 1980.

Nuckolls, J., J. Emmet, and L. Wood, "Laser Induced Thermonuclear Fusion," *Physics Today*, 46–53, August 1953.

Orth, C.D., et al., "Interplanetary Propulsion Using Inertial Fusion," *Proc. of 4th Symposium on Space Nuclear Power Systems*, (Albuquerque, New Mexico, January 12–16, 1987), also in *Space Nuclear Power Systems 1987*, (Orbit Book Co., Malabar, Florida, 1987).

Parker, E.N., *Cosmical Magnetic Field*, Clarendon Press, Oxford, 1979.

Persiani, P.J., W.C. Lipinski, and A.J. Hatch, "Survey of Thermonuclear Reactor Parameters," ANL-7807, Argonne National Laboratory, 1972.

Pitts, J.H., "Cascade: A Centrifugal-Action Solid-Breeder Reaction Chamber," *Nucl. Tech. Fusion*, **4** (2), Part 3, 967 (1983).

Pitts, J.H., "Cascade: A High-Efficiency ICF Power Reactor," UCRL-93554, Lawrence Livermore National Laboratory, Livermore California, 1985.

Pitts, J.H., and M.H.L. Jester, "Rankine Cycle Systems Studies for Nuclear Space Power," in *Proc. of the Third IECEC Conference*, (Boulder, Colorado, 1968), pp. 290–298.

Pitts, J.H., and I. Maya, "The Cascade Inertial-Confinement-Fusion Power Plant," *Proc. 11th Symposium on Fusion Engineering, Austin, Texas, November 18–22, 1985*, UCRL-92557, Lawrence Livermore National Laboratory, Livermore, California, 1985.

Pitts, J.H., and C.E. Walter, "Conceptual Design of a 10 MW$_e$ Nuclear Rankine System for Space Power," *J. of Spacecraft and Rockets*, **7** (3), 259–265 (1970).

Politzer, P.A., L.M. Lidsky, and D.B. Montgomery, "Torsatrons and the TOREX Proof of Principle Experiment," PFC-TR-79-2, Massachusetts Institute of Technology, March 1979.

Prestwich, K.R., and M.T. Buttram, "Repetitive Pulsed Power Technology for Inertial Confinement Fusion," *Nucl. Tech./Fusion*, **4**, 945 (1983).

Proc. Symp. Technology of Controlled Thermonuclear Fusion Experiments and the Engineering Aspects of Fusion Reactors, Austin, Texas, November 20–22, 1972, CONF-721111, 1974.

Rioux, E., and C. Jablon, "Losses of a Thermonuclear Plasma Imploded by a High-Velocity Wall," *Nucl. Fusion*, **15**, 425 (1975).

Robson, A.E., "A Conceptual Design for an Imploding-Liner Fusion Reactor," *Megagauss Physics and Technology*, Plenum Publishing Corporation, New York, 1980, p. 425.

Roth, J.R., "Alternate Approaches to Fusion," TM-X-73429, U.S. National Aeronautics and Space Administration, 1976.

Roth, J.R., and H.C. Roland, "Effect of Wall Loading Limitations and Choice of Beta on the Feasibility of Advanced Fuel Fusion Reactors," *Proc. 8th IEEE Sym. on Eng. Problems in Fusion Research*, San Francisco, California, November 1979.

Sethian, J.D., and A.E. Robson, "Use of Relativistic Electron Beams to Create Magnetically Confined Plasma Inside Imploding Liners," *J. Magnetism Magn. Mater.*, 11, 416 (1979).

Shafranov, V.D., "Mixing of Plasma Columns in a Tokamak," *Nucl. Fusion*, 19, 187 (1979).

Shearer, J.W., and W.C. Condit, "Magnetically Driven Liners for Plasma Compression." *Energy Storage, Compression and Switching (1976)*, Plenum Publishing Corporation, New York, 1977, pp. 105–117.

Smith, A.C., Jr., et al., "The Moving Ring Field-Reversed Mirror Reactor," *Proc. 4th Topl. Mtg. Technology of Controlled Nuclear Fusion*, King of Prussia, Pennsylvania, October 14–17, 1980, to be published.

Smith, A.C., Jr., et al., "Use of Coaxial Guns to Startup Field-Reversed-Mirror Reactors," UCRL-52922, University of California, Lawrence Berkeley Laboratory, 1980.

"Standard Mirror Fusion Reactor Design Study," R. Moir (ed.), UCID-17644, Lawrence Livermore National Laboratory, January 1978.

"Status of Tokamak Research," J.M. Rawls (ed.), ER-0034, U.S. Department of Energy, October 1979.

Taylor, J.B., "Relaxation of Toroidal Plasma and Generation of Reverse Magnetic Fields," *Phys. Rev. Lett.*, 33, 1139 (1974).

Tobin, M.T., "The Compact Torus Accelerator — A Driver for ICF," *Fusion Technol.*, 10, 3-2A, 679 (1986).

Todd, A.M.M., et al., "The Spheromak Fusion Reactor," *Proc. 15th Intersociety for Energy Conversion Engineering Conf.*, August 18–22, 1980, 3, 2229 (1980).

Weaver, T., G. Zimmerman, and L. Wood, "Exotic CTR Fuels: Non-Thermal Effects and Laser Fusion Applications," UCRL-74938, Lawrence Livermore Laboratory, 1972.

Wells, D.R., "Dynamic Stability of Closed Plasma Configurations," *J. Plasma Phys.*, 42, 1277 (1970).

Wells, D.R., "Method and Apparatus for Heating and Compressing Plasma," U.S. Patent 4 334 876, June 8, 1981.

Wells, D.R., *et al.*, "Ion Temperatures Inferred from Neutron Yield Measurements," *J. Plasma Phys.*, **31**, 39 (1984).

Wells, D.R., *et al.*, "Ion Temperatures Inferred from Neutron Yield Measurements," *Phys. Rev. Lett.*, **41**, *3*, 169 (1978).

Wells, D.R., and L. Hawkins, "Containment Forces in Low Energy States of Plasmoids," to be published in *J. Plasma Phys.*, 1985.

Werner, C.W., and E.V. George, "Excimer Lasers," *Principles of Laser Plasmas*, G. Bekefi (ed.), (Wiley-Interscience, New York, New York, 1976), pp. 421–456 and references cited therein.

Willenberg, H.J., "TRACT Fusion Reactor Studies," *Proc. 4th Topl. Mtg. Technology of Controlled Nuclear Fusion*, King of Prussia, Pennsylvania, October 14–16, 1980, to be published.

Willenberg, H.J., *et al.*, "TRACT: A Small Fusion Reactor Based on Near-Term Engineering," *Proc. 15th Intersociety of Energy Conversion Engineering Conference*, August 18–21, 1980, **3**, 2214 (1980).

Wong, A.Y., *et al.*, "High-Beta Confinement Experiments in Multipole/Surmac — A Concept for an Advanced Fuel Fusion Reactor," *Proc. 8th Conf. Plasma Physics and Controlled Nuclear Fusion Research*, Brussels, July 1–10, 1980, IAEA–CN–38/AA2, International Atomic Energy Agency, 1980.

Yoder, G.L., and R.L. Graves, "Analysis of Alkali Liquid Metal Rankine Space Power Systems," in *Trans. of 2nd Symposium on Space Nuclear Power Systems*, (Albuquerque, New Mexico, January 1985), pp. EC–4.1 to EC–4.6.